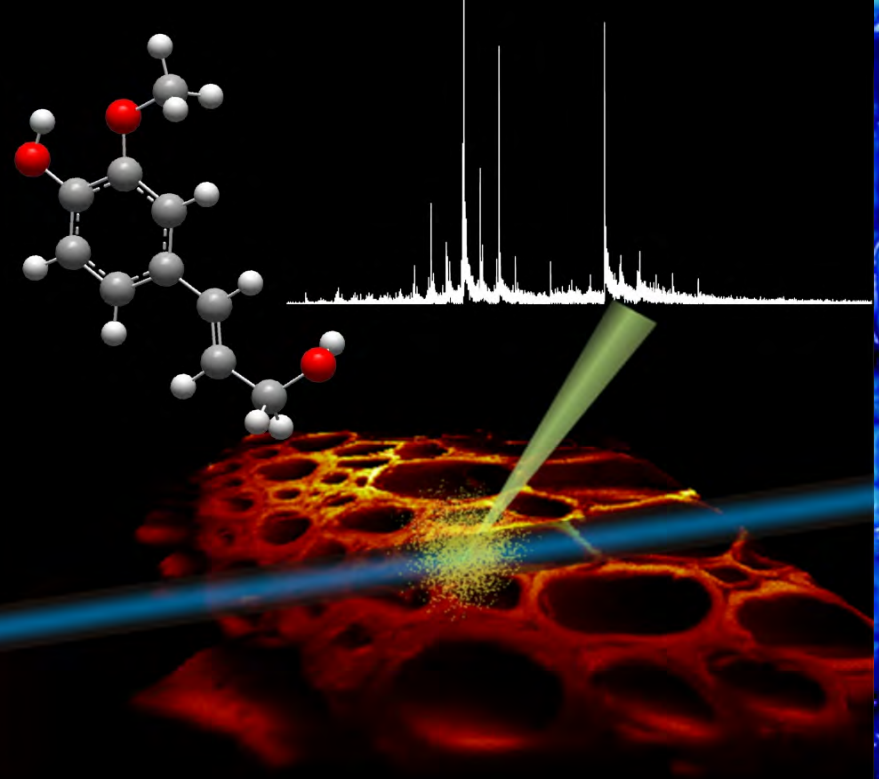

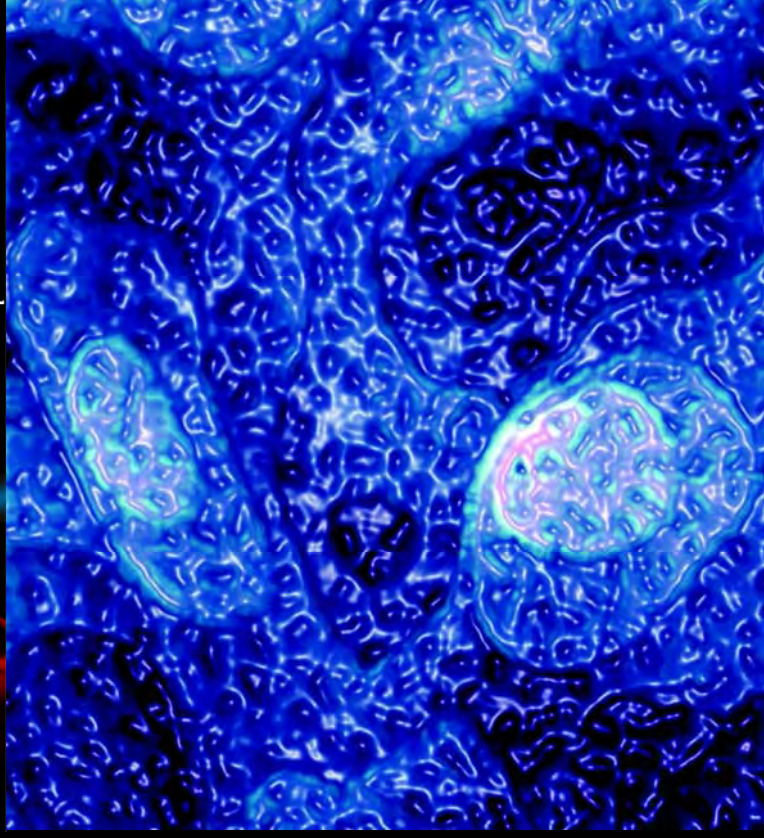

CPIMS 7

Seventh Condensed Phase and Interfacial Molecular Science (CPIMS) Research Meeting

Hyatt Regency, Baltimore, MD
June 12-15, 2011

U.S. DEPARTMENT OF ENERGY | Office of Science

Office of Basic Energy Sciences
Chemical Sciences, Geosciences & Biosciences Division

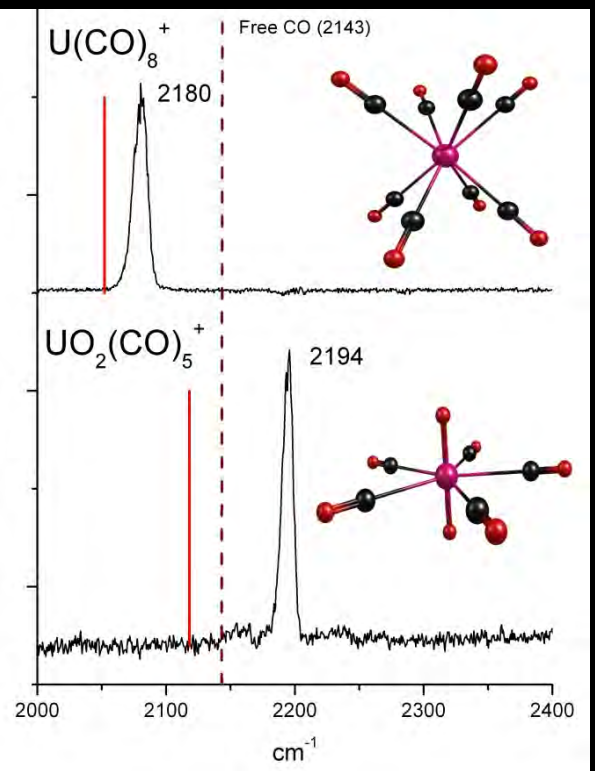

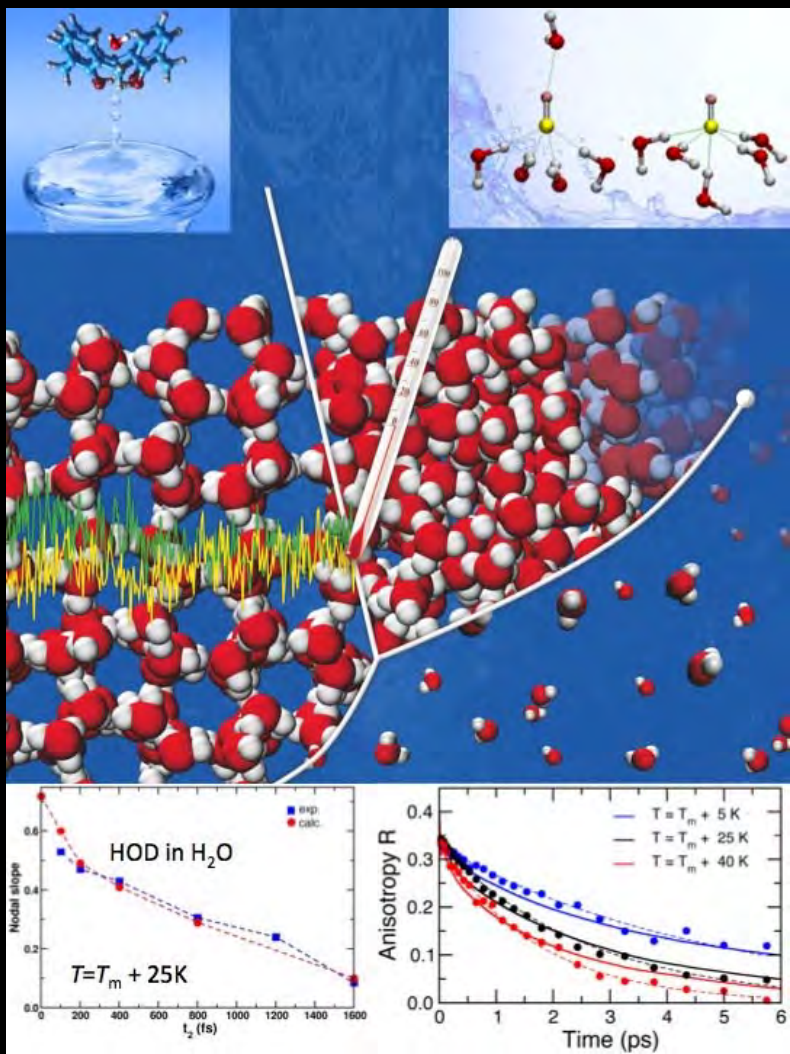

Program and Abstracts for the Seventh Research Meeting of the

Condensed Phase and Interfacial Molecular Science (CPIMS) Program

Hyatt Regency
Baltimore, MD
June 12-15, 2011

Chemical Sciences, Geosciences, and Biosciences Division
Office of Basic Energy Sciences
Office of Science
U.S. Department of Energy

The research grants and contracts described in this document are supported by the U.S. DOE Office of Science, Office of Basic Energy Sciences, Chemical Sciences, Geosciences and Biosciences Division. This document was produced under contract number DE-AC05-06OR23100 between the U.S. Department of Energy and Oak Ridge Associated Universities.

This page is intentionally left blank

A technique to perform chemical imaging on surfaces using a novel mass spectrometry method is being developed. A 349 nm laser photon (shown in green) or a 25 keV Bi cluster ion impinges on the surface. The resulting neutral molecules which are desorbed or sputtered off the surface are interrogated by tunable synchrotron vacuum ultraviolet radiation (shown in blue) and ionized and detected in a reflectron time-of-flight mass spectrometer. Rastering the sample stage and/or ion beam and correlating the mass spectra to position generates a chemical image as shown in the bottom of the figure (secondary ion mass spectrometry total ion image of a section of miscanthus). The structure of coniferyl alcohol, a monomer component of lignin is shown in the figure. The mass spectra on the top right is of laser desorbed lignin, ionized by 10.5 eV synchrotron radiation.

Submitted by Musahid Ahmed (Lawrence Berkeley National Laboratory)

For more information, see abstract on pages 23-26.

False-colored 600 x 600 nm atomic force micrograph of two types of molecules forming a self-assembled monolayer on a gold surface. The self-assembled monolayer is comprised of two species, an alkanethiolate molecule and a partially-fluorinated alkanethiolate molecule with each tail containing 10 carbon atoms. The two components are deposited on the surface as a single disulfide molecule (synthesized by Dong-Chan Lee and Luping Yu at UChicago), which splits at the S-S bond upon adsorption. The advantage of this approach is that it creates a perfectly mixed monolayer of exactly 50-50 composition. We then observe the initial stages of phase separation, driven by the chemical disparity between the two molecular tails. The rippled features in the AFM image are due to nanoscale domains of phase-separated molecules and the associated height difference (~0.2 nm) between the hydrocarbon chain and the fluorocarbon chain arising from the different tilt angles of the immiscible domains. The larger scale terraces in the image are due to atomic steps in the underlying gold surface. Such mixed composition interfaces are of interest for fundamental condensed phase science as well as their potential utilization in many physical and biological applications arising from the ability to precisely tune their surface chemical and physical properties.

Submitted by Steven Sibener (University of Chicago) and Seth Darling (Argonne National Laboratory)

For more information, see abstract on pages 181-184.

CPIMS 7

ABOUT THE COVER GRAPHICS

Uranium and uranium dioxide carbonyl cations produced by laser vaporization are studied with mass-selected ion infrared spectroscopy in the C-O stretching region. Dissociation patterns, spectra and quantum chemical calculations establish that the fully coordinated ions are $U(CO)_8^+$ and $UO_2(CO)_5^+$, with D_{4d} square antiprism and D_{5h} pentagonal bipyramid structures. Backbonding in $U(CO)_8^+$ causes a red-shifted CO stretch but back donation is inefficient for $UO_2(CO)_5^+$, producing a blue-shifted CO stretch characteristic of non-classical carbonyls.

Submitted by Michael Duncan (University of Georgia)

For more information, see abstract on pages 67-70.

High-level electronic structure calculations at the CCSD(T) level are used to quantify intermolecular interactions for large systems and assess the importance of dispersion in recently developed density functionals. These include guest/host interactions controlling the accommodation of various molecules in calix[4]arene cavities [top left; *J. Phys. Chem. A* **114**, 2967 (2010)], the coordination of hydroxide-water clusters [top right; *Chem. Phys. Lett.* **481**, 9 (2009)] and the preliminary description of parts of the phase diagram of liquid water [middle; *J. Chem. Phys.* **130**, 221102 (2009); *ibid.* **134**, 121105 (2011)]. Based on these results we rely on a relative-to-the-melting (T_m) rather than an absolute temperature scale for comparing results obtained with various models with experiment. Preliminary results on that relative scale include the 2-D infrared (IR) spectra [lower left; *J. Phys. Chem. B*, **113**, 13118 (2009)] and the anisotropy of liquid water [lower right; *J. Phys. Chem. Lett.* **1**, 2316 (2010)].

Submitted by Sotiris Xantheas (Pacific Northwest National Laboratory)

For more information, see abstract on pages 221-224.

This page is intentionally left blank

Foreword

This volume summarizes the scientific content of the Seventh Research Meeting on Condensed Phase and Interfacial Molecular Science (CPIMS) sponsored by the U. S. Department of Energy (DOE), Office of Basic Energy Sciences (BES). The research meeting is held each fiscal year for the DOE laboratory and university principal investigators within the BES CPIMS program to facilitate scientific interchange among the PIs and to promote a sense of program identity.

During fiscal year 2009, 95 single investigator and small group research (SISGR) proposals were selected for funding across BES, with five of these new awards being managed as part of the CPIMS program. The Seventh CPIMS meeting includes presentations by principal investigators for two of these projects. Fiscal year 2009 also brought the new Energy Frontier Research Centers (EFRCs) to BES. We have invited one EFRC speaker—Professor Oliver Monti—who will present research that is funded through the EFRC "Center for Interface Science: Solar Electric Materials" at the University of Arizona (see abstract on pages 21–22).

Funding for proposals in a newly initiated program in computational and theoretical chemistry (CTC) resulted in 15 new grants during fiscal year 2009. Efforts supported by the CTC program crosscut the goals of Chemical Sciences, Geosciences and Biosciences Division. CTC investigators seek to develop new levels of sophistication and realism in theories and simultaneously convert these theories into scalable computational tools that are able to more accurately and precisely predict complex chemical and physical processes on multiple temporal and spatial scales. Since its beginning, the program has experienced significant growth. Therefore, five CTC investigators have been invited to speak at the meeting, including three during a session on Monday, June 13, that will be moderated by Mark Pederson, who is the CTC Program Manager. Moreover, a special section of this book contains abstracts from CTC principal investigators (located on pages 1–20).

We are deeply indebted to the members of the scientific community who have contributed valuable time toward the review of proposals and programs. These thorough and thoughtful reviews are central to the continued vitality of the CPIMS program. We appreciate the privilege of serving in the management of this research program. In carrying out these tasks, we learn from the achievements and share the excitement of the research of the many sponsored scientists and students whose work is summarized in the abstracts published on the following pages.

This year's speakers are gratefully acknowledged for their investment of time and for their willingness to share their ideas with the meeting participants. Special thanks are reserved for the staff of the Oak Ridge Institute for Science and Education, in particular, Connie Lansdon, Tim Ledford, and Beth Flick. We also thank Diane Marceau, Robin Felder, and Michaelene Kyler-King in the Chemical Sciences, Biosciences, and Geosciences Division for their indispensable behind-the-scenes efforts in support of the CPIMS program. Finally, we acknowledge Larry Rahn (Program Manager for Separations and Analysis) for his expert advice in assembling this volume.

Gregory J. Fiechtner, Mark R. Pederson, and Michael P. Casassa
Chemical Sciences, Geosciences and Biosciences Division
Office of Basic Energy Sciences

This page is intentionally left blank

Agenda

U. S. Department of Energy
Office of Basic Energy Sciences
Seventh Condensed Phase and Interfacial Molecular Sciences (CPIMS) Research Meeting

Sunday, June 12

3:00-6:00 pm **** Registration (Pisces Dining Room) ****
6:00 pm **** Reception (No host, Pisces Dining Room) ****
7:00 pm **** Dinner (Pisces Dining Room) ****

Monday, June 13

7:30 am **** Breakfast ****

All Sessions held in the Maryland Suite

Introductory Session *Chair:* **Gregory J. Fiechtner**, DOE Basic Energy Sciences

8:30 am **Gregory J. Fiechtner**, DOE Basic Energy Sciences
8:35 am **Eric Rohlfing**, DOE Basic Energy Sciences
9:05 am **Mark R. Pederson**, DOE Basic Energy Sciences

Session I *Chair:* **Alex Harris,** Brookhaven National Laboratory

9:15 am *Probing Photon-Matter and Electron-Matter Interactions at the Molecular Scale*
Mark C. Hersam, Northwestern University
9:45 am *Spectroscopic Imaging toward Space-Time Limit*
Wilson Ho, University of California at Irvine
10:15 am *Single-Molecule Interfacial Electron Transfer*
H. Peter Lu, Bowling Green State University

10:45 am **** Break ****

Session II *Chair:* **Mark R. Pederson,** DOE/Basic Energy Sciences

11:00 am *Coherent Resonance Energy Flow Dynamics in Soft Environments*
Seogjoo Jang, Queens College, City University of New York
11:30 am *Quantum Mechanical Evaluation of New Solar Energy Conversion Materials*
Emily A. Carter, Princeton University
12:00 noon *Multiscale Investigation of Thermal Fluctuations on Solar-Energy Conversion*
Margaret S. Cheung, University of Houston

12:30 pm **** Lunch (Harborview Room) ****

Session II (Continued)

3:30 pm *Theoretical Methods for Describing Passive and Active Plasmon-Enhanced Photochemical Processes*
George C. Schatz, Northwestern University

Session III Chair: **Munira Khalil,** University of Washington

4:00 pm *Structure, Dynamics and Vibrational Spectroscopy of Water at Interfaces*
James L. Skinner, University of Wisconsin

4:30 pm *Water Dynamics and Interactions: Interfaces, Ions, and Confinement*
Michael D. Fayer, Stanford University

5:00 pm *On the Mechanism of Selective Adsorption of Ions to the Liquid Water Surface*
Richard J. Saykally and Phillip L. Geissler,
Lawrence Berkeley National Laboratory

5:45 pm *Molecular Level Understanding of Hydrogen Bonding Environments*
Sotiris S. Xantheas, Pacific Northwest National Laboratory

6:15 pm **** Reception (no host, Pisces Dining Room) ****

6:45 pm **** Dinner (Pisces Dining Room) ****

Tuesday, June 14

7:30 am **** Breakfast ****

Session IV Chair: **Musahid Ahmed,** Lawrence Berkeley National Laboratory

8:30 am *Understanding Water-Mediated Processes through Cluster Ion Photochemistry: Tracking Down Fundamental Intermediates in the Catalytic Activation of CO_2*
Mark A. Johnson, Yale University

9:00 am *Infrared Spectroscopy of Metal Carbonyl and Metal-CO_2 Cluster Ions*
Michael A. Duncan, University of Georgia

9:30 am *Generation, Detection and Characterization of Gas-Phase Transition Metal Containing Molecules*
Timothy C. Steimle, Arizona State University

10:00 am **** Break ****

Session V Chair: **Bruce C. Garrett,** Pacific Northwest National Laboratory

10:30 am *Theory of Dynamics of Complex Systems*
David Chandler, Lawrence Berkeley National Laboratory

11:00 am *Interactions, Phase Equilibria and Self-Assembly in Ionic Systems*
Athanassios Z. Panagiotopoulos, Princeton University

11:30 am *Hydration Mechanisms in Nanoparticle Interaction and Surface Energetics*
Alenka Luzar, Virginia Commonwealth University

12:00 noon **** Lunch (Harborview Room) ****

Session VI Chair: **Ian Carmichael,** Notre Dame Radiation Laboratory

4:00 pm *Development of Statistical Mechanical Techniques for Complex Condensed-Phase Systems*
Gregory K. Schenter, Pacific Northwest National Laboratory

4:30 pm *Ab Initio Approach to Interfacial Processes in Hydrogen Bonded Fluids*
Christopher J. Mundy, Pacific Northwest National Laboratory

5:00 pm *Non-Thermal Reactions at Surfaces and Interfaces*
Greg A. Kimmel, Pacific Northwest National Laboratory

5:30 pm *Structure and Reactivity of Ices, Oxides, and Amorphous Materials*
Bruce D. Kay, Pacific Northwest National Laboratory

6:00 pm **** Reception (No Host, Pisces Dining Room) ****

6:30 pm **** Dinner (Pisces Dining Room) ****

Wednesday, June 15

7:30 am **** Breakfast ****

Session VII Chair: **Steven J. Sibener,** University of Chicago

9:00 am *Theoretical Developments and Applications to Surface Science, Heterogeneous Catalysis, and Intermolecular Interactions*
Mark Gordon, Ames Laboratory

9:30 am *Theory of the Reaction Dynamics of Small Molecules on Metal Surfaces*
Bret E. Jackson, University of Massachusetts Amherst

10:00 am *A Single-Molecule Approach for Understanding and Utilizing Surface and Subsurface Adsorption to Control Chemical Reactivity and Selectivity*
Charles Sykes, Tufts University

10:30 am *Structure and Dynamics at Organic Semiconductor Interfaces*
Oliver L.A. Monti, University of Arizona
(Invited EFRC Presentation, Center for Interface Science: Solar Electric Materials)

11:00 am *Closing Remarks*
Gregory J. Fiechtner, DOE Basic Energy Sciences

11:30 am **** Boxed Lunch (Harborview Room) ****

1:00-3:00 pm *Open Discussion*

This page is intentionally left blank

Table of Contents

Table of Contents

CTC Principal Investigator Abstracts

Quantum Mechanical Evaluation of

New Solar Energy Conversion Materials

Emily A. Carter

Department of Mechanical and Aerospace Engineering, Program in Applied and Computational Mathematics, and Gerhard R. Andlinger Center for Energy and Environment
Princeton University, Princeton, NJ 08544-5263 U.S.A.
eac@princeton.edu
http://carter.princeton.edu

We have launched a major research effort to use quantum mechanics techniques to search for robust, efficient, and inexpensive new materials for photovoltaics (PVs) that convert sunlight to electricity and photo-catalytic electrodes (PCEs) that convert sunlight, carbon dioxide, and water into fuels. Various observables that are key metrics for determining the utility of a given material can be accurately calculated from quantum mechanics; we will discuss our theoretical schemes for each observable and how we validate our approach. The cost-efficiency tradeoff for PV materials based on ultrapure silicon or tandem semiconductor cells motivates a look at new options, and despite periodic media reports to the contrary, no efficient PCEs are available yet. I will discuss why it is so difficult to find effective PCE materials; in particular I will enumerate the very significant constraints beyond those on PVs that they must satisfy to achieve high efficiency. Limiting oneself to abundant elements further constrains the design space. As a result, we are focusing primarily on first row transition metal oxide parent materials, suitably doped or alloyed with other abundant elements. Key material properties, along with some new design principles, will be discussed. The work is revealing which dopants or mixed oxides are most likely to provide solar energy conversion materials that optimize the cost-performance tradeoff.

References

1) P. Liao, M. C. Toroker, and E. A. Carter, "Electron Transport in Pure and Doped Hematite," *Nano Letters*, **11**, 1775 (2011).

2) P. Liao and E. A. Carter, "Testing Variations of the GW Approximation on Strongly Correlated Transition Metal Oxides: Hematite (α-Fe_2O_3) as a Benchmark," submitted (2011).

3) M. C. Toroker, D. K. Kanan, N. Alidoust, L. Y. Isseroff, P. Liao and E. A. Carter, "First Principles Scheme to Evaluate Band Edge Positions in Potential Transition Metal Oxide Photocatalysts and Photoelectrodes," submitted (2011).

This page is intentionally left blank

Multiscale Investigation of Thermal Fluctuations on Solar-Energy Conversion

Margaret S. Cheung
Department of Physics, University of Houston

Abstract:
Solar energy is a desirable source of clean energy that provides a potential solution to global energy crisis. Plants or bacteria have had a magnificent ability in converting and storing solar energy. However, their efficiency has not met the energy need of our modern civilization that has been built on fossil fuels. Recently, inspired by biological light-harvesting species, such as plants and bacteria, a new class of materials that consist of only organic compounds has been created to mimic key reactions in the photosynthetic processes. Triad, a covalently linked carotenoid-porphrin-C_{60} compound that has been synthesized a decade ago, demonstrates an amazing ability to absorb light and to produce excited charge-separation states that can convert solar energy into chemical fuel. One of the challenges has been to improve its efficiency in solar-chemical energy conversion under an ambient condition. Computer simulation such as molecular dynamics has been an excellent tool to provide a quantitative analysis on understanding the effect of solvent at room temperature. However, an atomistic study on triad, particularly regarding its dynamics associated with photo-induced charge-separation in solvent, has been elusive. My research focuses on the distribution of triad's conformation as well as the orientation of water molecules surrounding triad under aqueous condition and in a nano-sized confinement that can drastically alter the hydrogen bonding of water molecules at the solid-liquid interface. The complexity of this problem cannot be understood by using quantum chemistry calculation alone. By using a combined approach of quantum chemistry, statistical physics, and molecular dynamics simulation, we have found that triad is a highly flexible molecule that twists, bends, and wiggles in the presence of solvent. The energy landscape of triad is broad and shallow, indicating that the free energy barriers separating local minima are at the order of kT. Under thermal agitation, a triad conformation can quickly transition from one to another and that can potential impact the efficiency of solar energy conversion. The characteristics of triad's most probable conformation depend on the size of confinement, as well as the orientation of water molecules (1). These findings will further the investigation of the polarization effect from solvent medium on the charge-separation state of triad, which requires interdisciplinary collaboration from quantum chemists and possibly experimentalists.

(1) A Combined Quantum Chemistry and Molecular Dynamics Study on a Light-Harvesting Molecular Triad. Guoxiong Su, Arkadiusz Czader, and Margaret S. Cheung *(to be submitted soon, 2011)*

This page is intentionally left blank

Modeling molecular electron transport for efficient energy conversion schemes

Barry D. Dunietz

Assistant Professor of Chemistry
University of Michigan,
Department of Chemistry
930 North University Avenue
Ann Arbor
Ann Arbor, MI 48109.
Tel: 734-647-4495,
email:bdunietz@umich.edu

1 Project Goal

The goal of the research program is to provide reliable electron transport (ET) modeling and thereby to advance transport control abilities. The resulting insight will be used to design schemes in the area of photovoltaics (PV) and thermoelectric (TE) energy conversions. We aim to provide fundamental understanding of the ET process, to explain experimental measurements and to provide predictions for designing new experiments.

2 Recent Progress

We have achieved progress on the following fronts of modeling electron transport and transfer processes:

We are pursuing several projects that are related to structure-function relationships of molecular bridge used in thermoelectric applications. We have implemented modeling to consider the effect of electron-phonon coupling effects on the figure of merit. We modeled all the related properties that include electrical and thermal conductance and the Seebeck coefficient.[1] See Figure 1 for illustrating the molecular ZT dependence on the molecular structure and electron-phonon coupling.

We have studied electron transport properties of molecular bridges achieved from metal ion ligation by surface coupled pairs of pyridazino derivatives that function as "molecular sockets". The modeling provides predictions to enhance the resulting transport properties using practical device fabrication approaches.[2]

In other molecular transport studies we employed our dynamical electron transport modeling capabilities. Our approach is based on solving the electronic equations of motion as expressed by the Keldysh contour formalism (Kadanoff-Baym equations) using time-dependent (TD) perturbation theory (PT). We used the first order treatment to study bias effects on the electronic spectra of molecular bridges.[3] In another study we used the second order solution to model a molecular photo-induced electron pump.[4]

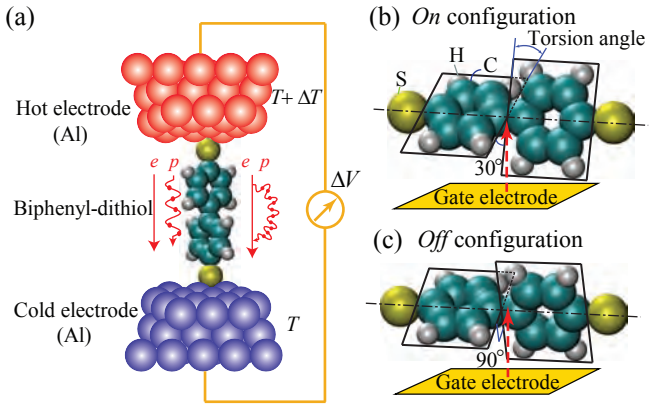

Figure 1: (a) A biphenyl-dithiol molecule bridge between two metal electrodes and the electron and phonon energy carriers and their coupling. The molecular *On* (b) and *Off* (c) states are characterized by the torsion angle (angle between the planes of the phenyl rings) of 30 and 90 degrees respectively. The e-p coupling reduces the transport and the ZT for the *On* state and increases for the *Off* state.[1]

3 Future Plans

We are developing an electron transport modeling approach to treat the non-equilibrium biasing conditions by a dynamical perspective for the steady state description. We will analyze the use of modern functionals for modeling electron transport properties.

In a recently submitted manuscript we report a combined experimental and computational study of a molecular Seebeck coefficient. The molecular bridges include varying numbers of phenyl rings and of the contacting groups that anchor the molecules to the electrodes. We will consider additional molecular scale structure-function relationships of thermoelectric applications:

1. to promote electrical and phononic rectification.
2. to consider quantum interferences and electron-phonon coupling relationships of thermoelectric conversions.
3. to combine TE device functionalities with physical properties to control the transport.

In other studies, we model the photophysics of molecular chromophores attached to octahedral-silsequioxanes (OHSQs). The OHSQs are promoted as molecular building blocks for photovoltaics applications due to their charge transfer signatures in related spectroscopic studies. Our studies implement modern TD-DFT approaches that address properly charge transfer excitations. We will consider photo-induced electron transfer properties of experimentally accessible SQs that are functionalized by a variety of chromophores to promote the control ability of charge separation.

4 Publications

References

[1] N. Sergueev, S. Seungha Shin, M. Kaviany, and B. D. Dunietz. Efficiency of thermoelectric energy conversion in biphenyl-dithiol junction: the effect of electron-phonon interaction. *Phys. Rev. B*, Accepted, 2011.

[2] B. Ding, V. Washington, and B. D. Dunietz. On the conditions for enhanced transport through molecular junctions based on metal centers ligated by pair of pyridazino-derived ligands. *Mol. Phys.*, 108:2591, 2010.

[3] H. Phillips, A. Prociuk, and B. D. Dunietz. Bias effects on the electronic spectrum of a molecular confined and biased bridge. *J. Chem. Phys.*, 134:54708, 2011.

[4] A. Prociuk and B. D. Dunietz. Photo-induced absolute negative current in a symmetric molecular electronic bridge. *Phys. Rev. B*, 82:125449, 2010.

This page is intentionally left blank

Coherent resonance energy flow dynamics in soft environments

Seogjoo Jang

Department of Chemistry and Biochemistry, Queens College of the City University of New York,
65-30 Kissena Boulevard, Flushing, NY 11367

Recent experimental and theoretical studies suggest that Natural photosynthetic complexes utilize the quantum coherence in a positive manner for efficient and robust flow of electronic excitation energy. Clear and quantitative understanding of such suggestion has significant implication in identifying the design principles behind efficient flow of excitons in soft environments, which may be adapted for the design of synthetic soft photovoltaic systems. Addressing these issues requires theoretical means to provide quantitative and reliable description of energy flow dynamics in such soft photovoltaic systems. While the theories by Forster and Dexter have been successful in describing various types of energy transfer processes for many decades, they are often inadequate for describing the energy transfer processes in soft and multichromophoric photovoltaic systems. One of the major issues is that conformational fluctuations and vibrational relaxations need to be treated on the same quantum mechanical footing as the energy transfer dynamics. The other issue is moderate or strong electronic coupling between energy donor and acceptor, which makes the simple rate picture of energy transfer invalid. This talk presents new theories[1-5] addressing these issues and the application of the theories to natural photosynthetic systems[1-2] and organic pi-conjugated systems[6]. These elucidate the sensitivity of quantum coherence on details of how electronic excitations are coupled among themselves and to their environments and suggest ways to utilize them for enhancing the efficiency of energy flow dynamics.

References

1. S. Jang, M. D. Newton, and R. J. Silbey, "Multichromophoric Förster resonance energy transfer," *Phys. Rev. Lett.* **92**, 218301 (2004)
2. S. Jang, M. D. Newton, and R. J. Silbey, "Multichromophoric Förster resonance energy transfer from B800 to B850 in the light harvesting complex 2: Evidence for subtle energetic optimization by purple bacteria," *J. Phys. Chem. B* **111**, 6807 (2007)
3. S. Jang, "Generalization of the Förster resonance energy transfer theory for quantum mechanical modulation of the donor-acceptor coupling," *J. Chem. Phys.* **127**, 174710 (2007)
4. S. Jang, Y.-C. Cheng, D. R. Reichman, and J. D. Eaves, "Theory of coherent resonance energy transfer," *J. Chem. Phys.* **129**, 101104 (2008)
5. S. Jang, "Theory of coherent resonance energy transfer for coherent initial condition," *J. Chem. Phys.* **131**, 164101 (2009)
6. L. Yang, S. Caprasecca, B. Mennucci, and S. Jang, "Theoretical investigation of the mechanism and dynamics of intramolecular coherent resonance energy transfer in soft molecules: A case study of dithia-anthracenophane", *J. Am. Chem. Soc.* **132**, 16911 (2010)

This page is intentionally left blank

Hydration Mechanisms in Nanoparticle Interaction and Surface Energetics

Alenka Luzar and Dusan Bratko
Department of Chemistry,Virginia Commonwealth University,1001 West Main Street, Richmond, VA 23284-2006
aluzar@vcu.edu, dbratko@vcu.edu

Program scope

Emerging nanoparticle technologies require new techniques to control surface properties of the material. Surface thermodynamics and interactions between nanoparticle surfaces are often determined by solvation in electrolyte solutions. The long-term objective of this research is to develop molecular level understanding of energetics, kinetics and hydration in nanoparticle solutions, and ionic solutions in particular. Understanding of basic molecular mechanisms involved in solvation of nanoparticles represents an important step in creating new materials, harvesting energy from nature and storing energy. In nanotechnology, this understanding is essential for effective control of surface interactions and nanocolloid phase behavior. The present focus is on modulating surface free energy and hydration effects in prototypical nanoscale systems through surface functionalization or applied electric field in the presence of conducting (ionic) solution. A further goal concerns molecular mechanisms and the intricate role of salt in surface energy storage in a nanoporous medium controlled by external electric field. The project relies on a combination of theory and simulation techniques using atomistic and coarse-grained models. Theoretical studies of the new effects we anticipate to uncover will likely inspire future experiments. They involve development of optimized algorithms for molecular simulations of nanoscale surface phenomena, focusing on the interplay of applied and ion-induced electric field and hydrogen bond interactions.

Recent progress

***Electrolyte nanodrops under electric field*[1].** In studies in neat water, we demonstrated the importance of molecular events in understanding electrowetting phenomena at the nanoscale. In particular, we highlighted the coupling between interfacial hydrogen bonds and electric field as spontaneous orientations of surface water molecules cooperate, or compete with field alignment. The ensuing dependence on field direction and polarity contrasts with conventional picture in macroscopic systems[2]. Salt ions, themselves orienting adjacent water molecules, affect this coupling. Most applications of electrowetting, occur in the presence of mobile ions, but the role of salt has so far not been addressed at a molecular level. As the first step, we considered wetting by saline nanodrops, a miniature version of the drop-in-capacitor experiment, Bateni *et al*., *J. Coll. Interface Sci.* **283**, 215 (2005). Wetting surface free energy, $\Delta\gamma=\gamma_{sl}-\gamma_{sv}=-\cos\theta_c$ is deduced from contact angle θ_c; γ denotes interfacial free energy and *s*, *l*, and *v* stand for solid, liquid, and vapor, respectively. Using molecular dynamics simulations of sessile nanodroplets, we studied the effect of added salt (NaCl) and applied electric field on the microscopic analogue of contact angle on a hexagonal carbon lattice and compared the results with those in pure water.

In agreement with available experiments, the wetting surface free energy rises upon addition of the salt. The salt effect on the field-induced *reduction* in contact angle is non-monotonic, enhancing the sensitivity to field at 1 mol dm^{-3} salt concentration, but not at the higher concentration 4 mol dm^{-3}. A likely explanation invokes two opposing effects: (a) the adsorption of salt ions in the double layer formed next to the substrate surface due to the applied field, and (b) orientational ordering of water dipoles around the ions that interferes with orientational polarization by the external field. The former effect (a), which reduces the contact angle, is consistent with calculated charge distribution in the drop. The latter effect (b), which weakens the influence of the field on the contact angle, is most prominent within the 1st

hydration layer where the field is particularly strong. From neutron scattering experiments it is well known that the smaller Na^+ cation binds its hydration water more tightly than the Cl^- anion, Mancinelli *et al*., *J.Phys. Chem.* B **111**, 13570 (2007). This is consistent with our structural calculations, showing that *adsorbed* Na^+ ions retain most of their hydration shell, but less so for Cl^- anions. Negative field promotes adsorption of tightly hydrated Na^+ cations, weakening electrowetting. Conversely, in the positive field, the interface is enriched by anions (Cl^-). The looser hydration of Cl^- supports stronger orientational polarization of water in the field, explaining bigger contact angle reduction in the *positive* field. The asymmetry in $\theta_c(E)$ dependence is related to unequal hydration properties of salt cations and anions, and is of different origin than the reported asymmetry in pure water. Both are significant primarily at the nanoscale, where a statistically significant fraction of water molecules reside at the interfaces. The dependences on the field strength and polarity both vary non-monotonically with salt concentration suggesting that moderate concentrations represent the most interesting regime for the electric control of wetting properties.

***Wetting free energy of heterogeneous functionalized surfaces*[3]**. Functionalization by surface groups with desired hydrophilicity provides a promising route to tunable nanomaterials. Using Molecular Dynamics simulations, we have estimated the changes in contact angles of aqueous nanodroplets upon surface functionalization with apolar (methyl) or polar (amino and nitrile) groups at varied compositions. The scaffold surface was a carbon monolayer akin to graphene, with average surface group area close to ~21 A^2. Substitution of methyl coverage by nitrile or amino ones lowered the simulated contact angle and, by implication, the wetting free energy from ~18 mNm^{-1} to ~ -42 mNm^{-1} or -53 mNm^{-1}, respectively.

In mixed systems, observed wetting free energies depart significantly from Cassie-Baxter linear interpolation. For the first time in molecular simulations, we capture and explain *hydrophobic* (higher θ_c) deviations, previously seen only in experiment. Our analysis shows the observed behavior can be traced down to the coupled effect of molecular roughness *and* chemical heterogeneity. The deviations from the linear additivity can be predicted quantitatively by accounting for steric shielding of smaller moieties by the more prominent groups of *different polarity*. For molecularly mixed surfaces comprising apolar and moderately polar groups, the linear interpolation of the mixed surface's wetting free energy is recovered if we use the fractions of solvent accessible surface as the measure of composition. For biomimetic surfaces with increased contrast between the patch polarities, we find a pronounced asymmetry in interface sensitivity to the composition change. The sensitivity is high at "soft" interfaces on a hydrophobic substrate and low on "hard" hydrophilic substrate with compact hydration layer. The trend is accompanied by a strongly asymmetric dependence of the interfacial density fluctuations of water on surface composition. The compressibility varies significantly within the strong-to-moderate hydrophobic regime but becomes less sensitive on hydrophilic surfaces. We find identical trends when we modulate surface wettability by electric field rather than by chemical functionalization.

***Effect of hydrogen bonds and surface ionization on the size-dependence of the wetting free energy of a nanoscale solute*[4]**. In addition to surface chemistry and texture, the particle curvature is an important determinant of nanoparticle wettability. The lengthscale of the crossover between regimes, characterized by solvation free energy scaling with volume at small particle size R, and with area at large size (constant interfacial tension), depends on the range of solute/solvent and solvent/solvent pair potentials. Although the crossover in aqueous medium is well understood, we were particularly interested in extracting the contribution of hydrogen bonds to this transition. In a recent study[4], we have shown that the crossover between the two scaling regimes can be understood in terms of simple geometric considerations, by accounting for the steric restriction imposed by a curved solute surface on hydrogen bonding in its proximity. For a spherical solute and known H-bond coordination and bond length in water, the associated lengthscale is ~ 0.5 nm in agreement with simulations, e.g. Rajamani, Truskett, Garde, *Proc. Natl. Acad. Sci.* **102**, 9475 (2005), and the procedure is easily generalized to estimate the hydrogen bond contribution to the interfacial tension in other geometries.

The presence of surface charges may be expected to favor scaling of solvation free energy with volume. Detailed relations depend critically on the size-dependence of the solute charge. In the case of particle growth at constant surface charge density, like e.g. with association colloids, scaling with volume can be expected for an isolated ionized particle and no electrostatic screening. In experiment, it is often more important to consider a solute comprising a neutral combination of an ionic nanocolloid *and* its counterions at finite concentration. In this scenario, our calculations reveal a very different behavior. In short, as the particle size is increased, the modified free energy effect of dielectric screening in water is matched by ionic screening in the dry state. As both have similar slopes with the size (with nearly identical large-size limit), the *difference* between surface free energies of dry and wetted states (solvation free energy per unit area of the colloid surface) can be virtually insensitive to the curvature. Our molecular simulations for a coarse-grained model solute in extended simple point charge water show this behavior to prevail at unexpectedly small sizes, O(1) nm even at moderate surface charge densities. Solvation free energy of a nanoscale ionic solute, dissolved together with its counterions, can scale in proportion with solute surface area at practically relevant conditions and independently of salt concentration.

Future plans

We will extend the studies of electric control of wetting properties in salt solutions to pore geometries. Here, electrowetting has much stronger effect as it involves migration of solution from external, field-free reservoir *into* the field. We will be considering simultaneous transfer of water *and* ions. Method developments, in particular the implementation of reaction-ensemble simulation involving multi-ion components, will be critical; analogous studies with salt exchange have so far not been reported. Characterization of wetting properties of functionalized surfaces in water will also be broadened to ionic solutions to address the correspondence between electrowetting and chemical surface modulation. Intersurface interactions among nanoparticles with tuned hydrophilicity will be studied as a function of solution conditions, toward control of dispersion stability.

Publications acknowledging DOE support: 2010/2011

[1]C. D. Daub, D. Bratko, A. Luzar, Molecular Dynamics Simulation of Sessile Nanodrops of Salt Solutions, (2011) to be submitted.

[2]C. D. Daub, D. Bratko, A. Luzar, Nanoscale Wetting Under Electric Field from Molecular Simulations in "Multiscale Molecular Methods in Applied Chemistry", *Top. Curr. Chem.*, B. Kirchner and J. Vrabec Eds, Springer 2011, in press.

[3]J. Wang, D. Bratko, A. Luzar, Probing surface tension additivity on chemically heterogeneous surfaces: A molecular approach, *Proc. Natl. Acad. Sci.* **108**, 6374-6379 (2011).

[4]J. Wang, D. Bratko, A. Luzar, Contributions of hydrogen bonds and surface charge on solute size-dependence of hydration free energy, *J. Stat. Phys*. (2011), submitted.

This page is intentionally left blank

INTERACTIONS, PHASE EQUILIBRIA AND SELF-ASSEMBLY IN IONIC SYSTEMS

DE-SC0002128

Principal Investigator: Athanassios Z. Panagiotopoulos

Department of Chemical and Biological Engineering
Princeton University
Princeton, NJ 08544
Tel. 609/258-4591
E-mail: azp@princeton.edu

1 PROGRAM SCOPE

The research project supported by this award focuses on studies of interactions, phase transitions and self-assembly in ionic systems, with special emphasis on the precise determination of free energies and the characterization of phase and conformational transitions. In particular, the main objectives of the proposed work will be (a) to obtain effective interaction potentials that represent accurately activity coefficients in concentrated salt solutions, (b) develop and apply a simulation methodology for Donnan equilibria based on a combination of the reactive canonical and Gibbs Monte Carlo techniques, (c) study forces and structure formation near and between charged surfaces with ionizable groups, (d) investigate micellization in ionic surfactants, (e) model sorption and formation of ionic domains in ionomers and (f) obtain accurate phase diagrams for polyelectrolyte and charged colloidal particle systems, including formation of solid phases. These topics form a logical progression with multiple common themes and synergies in computational methods and models. The project takes advantage of powerful computational techniques developed with prior DOE support, while striving to break new ground both in terms of simulation method development and the selection of physical systems for study.

2 RECENT PROGRESS (SEPT. 2009 – APRIL 2011)

Significant progress has been made in several of the main focus areas described above. In particular, we have obtained ionization curves of weak polyelectrolytes as a function of the charge coupling strength [Publication 1]. In contrast to many earlier studies, this work treats counterions explicitly, thus allowing the investigation of charge correlation effects at strong couplings. For conditions representing typical weak polyelectrolytes in water near room temperature, ionization is suppressed because of interactions between nearby dissociated groups, as also seen in prior work. A novel finding here is that, for stronger couplings, relevant for non-aqueous environments in the absence of added salt, the opposite behavior is observed - ionization is enhanced relative to the behavior of the isolated groups due to ion-counterion correlation effects. The fraction of dissociated groups as a function of position along the chain also behaves non-monotonically. Dissociation is highest near the ends of the chains for aqueous polyelectrolytes and highest at the chain middle segments for non-aqueous environments. At intermediate coupling strengths, dissociable groups appear to behave in a nearly ideal fashion, even though chain

dimensions still show strong expansion effects due to ionization. These findings provide physical insights on the impact of competition between acid/base chemical equilibrium and electrostatic attractions in ionizable systems. We have also completed code development for studies of these ionizable systems as thin films on surfaces.

A second major focus area of the project is to obtain accurate phase diagrams for polyelectrolyte and charged colloidal particle systems, including formation of solid phases. In an initial publication in this area [Publication 2], we present full phase diagrams (including solid phases) of spherical charged colloids, using Monte Carlo sampling and thermodynamic integration of the Helmholtz free energy. We show that added salt stabilizes the fluid phase and shrinks the fluid–solid coexistence region, in agreement with experimental and theoretical results.

In the area of micellization in ionic surfactants, we have used molecular dynamics simulations over microsecond time scales to study the micellization behavior of recently proposed continuum-space, coarse-grained surfactant models [Publication 3]. We obtained the critical micelle concentration (cmc) and equilibrium aggregate size distributions at low surfactant loadings and found that the two coarse grained models significantly underpredict experimental cmc near room temperature for zwitterionic surfactants, but are closer to measured values for nonionic ones. The aggregation numbers for both zwitterionic and nonionic surfactants are near those observed experimentally, but the temperature dependence of the cmc was incorrect in both cases, because of the use of an unstructured solvent. In a subsequent study, we have utilized thermodynamic approaches to quantify the hydrophobic attraction at temperatures ranging from 280 K to 365 K and obtained cmc's and aggregate sizes for various ionic and non-ionic surfactants, specifically sodium dodecyl sulfate, dodecyltrimethylammonium bromide and chloride, and PEG surfactants [Publication 7]. For all systems studied, the model yields cmc and aggregation sizes that are in near-quantitative agreement with experimental results.

The "gold standard" for predictive molecular-based simulations is fully atomistic models with transferrable potentials. We have used molecular dynamics simulations of fully atomistic, explicit-solvent models to obtain the equilibrium critical micelle concentration (cmc) and aggregation numbers for sodium hexyl sulfate, in good agreement to experimental data [Publication 8]. These are the first truly equilibrium simulations of a comparable system close to the cmc and are possible because of the relatively fast time scales of micellization for this system.

We have also initiated a collaboration with the University of Michigan HOOMD project [http://codeblue.umich.edu/hoomd-blue], a "Highly Optimized Object-oriented Many-particle Dynamics" set of codes optimized for Graphics Processing Unit (GPU) processors. In particular, Dr. Steve Barr from our group together with Philipp Mertmann, a visitor from the University of Bochum in Germany, were able to implement the particle-particle particle-mesh long-range electrostatic interaction in HOOMD version 0.9.2, which was released in Oct. 2010.

Several high-visibility papers were completed [Publications 4-6, that include one to *PNAS* and one to *Biophys. J.*], from a collaboration between our group and those of Professors Debenedetti and Kevrekidis at Princeton. This collaboration aims to develop good measures to describe conformational transitions, such as those that occur in polyelectrolyte and protein solutions. While the atomic-level resolution provides unparalleled detail, it can be non-trivial to extract the important motions underlying simulations of complex systems containing many degrees of freedom. The *diffusion map* is a nonlinear dimensionality reduction technique with the capacity to systematically extract the essential dynamical modes of high-dimensional simulation trajectories,

furnishing a kinetically meaningful low-dimensional framework with which to develop insight and understanding of the underlying dynamics and thermodynamics.

A key factor controlling the interactions between surfaces in aqueous solutions is the surface charge density. Surfaces typically become charged though a titration process where surface groups can become ionized based on their dissociation constant and the pH of the solution. We have used a Monte Carlo method to treat this process explicitly in a system with two planar surfaces in a salt solution. We find that the surface charge density changes as the surfaces come close to contact due to interactions between the ionizable groups on each surface. In addition, we observe an attraction between the surfaces above a threshold surface charge, in good agreement with previous theoretical predictions based on uniformly charged surfaces. However, close to contact we find the force is significantly different than the uniformly charged case. A paper on this work is being prepared for submission to a high-impact journal.

3 Future Plans

In the area of micellization of ionic surfactants, we are currently performing fully atomistic, explicit-solvent calculations for sodium octyl sulfate, a system that micellizes more strongly than sodium hexyl sulfate and thus has a lower cmc. Our initial results suggest that existing force fields underestimate the cmc for this system by an order of magnitude. This unexpected finding may be at least partly due to the higher concentration in the simulations relative to the experimental conditions at which the cmc is measured. We plan to investigate these effects and, if necessary, obtain better force field parameters to represent experimental data for these important model systems. In a collaboration with the group of Prof. M. L. Klein of Temple University, we are also pursuing investigations of micellization of a coarse-grained model for sodium dodecyl sulfate, using large-scale simulations with HOOMD. Our implicit-solvent work will also continue, with modeling of double-tailed lipids being the next target.

In the area of surface interactions, we plan to extend studies of electrostatic-dominated forces between surfaces, both flat and curved, in the presence of ionizable chains. An interesting competition can takes place between electrostatic interactions and dispersion interactions can lead to interesting morphologies and to pH- and temperature-responsive surface films.

In the area of polymer electrolyte membranes, we are currently calculating the solubility of water in Nafion fuel cell membranes possessing different nanoscale morphologies. We are using Widom test particle insertions combined with large-scale molecular dynamics calculations and are in the process of developing GPU-based codes for chemical potential and solubility calculations, which will also be incorporated into HOOMD. The results compared to experimental data from the group of our experimental collaborator, Prof. Jay Benziger.

4 Publications

1. A. Z. Panagiotopoulos, “Charge correlation effects on ionization of weak polyelectrolytes,” *J. Phys. Condens. Matter*, **21**, 424113, 7 pp (2009).
2. A.-P. Hynninen and A. Z. Panagiotopoulos, “Phase diagrams of charged colloids from thermodynamic integration,” *J. Phys. Condens. Matter*, **21**, 465104, 7 pp (2009).

3. S. Sanders and A. Z. Panagiotopoulos, “Micellization behavior of coarse grained surfactant models,” *J. Chem. Phys.*, **132**, 114902, 9 pp (2010).

4. A. L. Ferguson, A. Z. Panagiotopoulos, P. G. Debenedetti and I. G. Kevrekidis, “Systematic determination of order parameters for chain dynamics using diffusion maps,” *Proc. Natl. Acad. Sci. USA*, **107**, 13597-602 (2010).

5. A. L. Ferguson, S. Zhang, I. Dikiy, A. Z. Panagiotopoulos, P. G. Debenedetti and A. J. Link, “An Experimental and Computational Investigation of Spontaneous Lasso Formation in Microcin J25,” *Biophys. J.*, **99**, 3056-3065 (2010).

6. A. L. Ferguson, A. Z. Panagiotopoulos, P. G. Debenedetti, and I. G. Kevrekidis, “Integrating diffusion maps with umbrella sampling: Application to alanine dipeptide,” *J. Chem. Phys*., **134**: 135103, 15 pp. (2011).

7. A. Jusufi, S. Sanders, M. L. Klein, and A. Z. Panagiotopoulos, “Implicit-Solvent Models for Micellization: Nonionic Surfactants and Temperature-Dependent Properties,” *J. Phys. Chem. B*, **115**, 990-1001 (2011).

8. M. Sammalkorpi, S. Sanders, A. Z. Panagiotopoulos, M. Karttunen, and M. Haataja, “Simulations of micellization of sodium hexyl sulfate”, *J. Phys. Chem. B* **115**, 1403-1410 (2011).

Theoretical methods for describing passive and active plasmon-enhanced photochemical processes

George C. Schatz and Mark A. Ratner

Northwestern University , Evanston IL 60208-3113

Plasmon excitation in silver and gold nanoparticles has long been of interest for its ability to produce strong electronic extinction and Rayleigh scattering spectra, and there continues to be interest in Surface-Enhanced Raman Scattering (SERS), however a topic that has received less attention, but which is potentially of relevance to energy science involves the use of plasmon excitation to enhance chemistry reactions. This can be accomplished either passively or actively. In the former, plasmon excitation leads to an enhanced electromagnetic field at the position of a nearby photoactive molecule, thus leading to enhancement in the absorption of light by that molecule, and therefore in photochemical reaction. In the latter, plasmon excitation leads to an electron transfer to or from the particle being excited, and this electron ultimately produces a chemical reaction.

In our DOE BES research program, we are developing methods that combine electronic structure theory with electrodynamics to describe both of these processes. A challenge with doing this is that the molecule involved in reaction is often in direct contact with the metal particle surface, so there are important electronic interactions between molecule and surface. In addition, even in the passive case the molecule often experiences a highly anisotropic electromagnetic field that can perturb molecular absorption compared to the same molecule in solution.

The theories we are developing are based on real-time time-dependent density functional theory (RT-TDDFT) wherein the enhanced field from the particle results in a dipole coupling interaction Hamiltonian that is inserted directly into the time-dependent Kohn Sham equations. The talk will present an application to passive plasmon enhanced photoabsorption[1] in which we use the finite-difference time-domain (FDTD) method to determine the enhanced field associated with a silver nanoparticle, and then this is used to drive absorption of a ruthenium-based dye that is important in dye-sensitized solar cells.

In a second application,[2] we show how a constrained version of RT-TDDFT can be used to describe active plasmon-enhanced photochemistry in which an electron is transferred from a silver particle to a silver ion in solution to leading to growth of the silver particle. In this application, the electronic structure of the donor and acceptor is described using a diabatic basis set that is obtained via constrained DFT, and then the dynamics of photoinduced electron transfer (PIET) is described using RT-TDDFT to determine the electron transfer matrix element. Of particular interest here is the comparison of the frequency dependence of PIET and the frequency dependence of photoabsorption, as this shows how plasmon excitation, which is a collective excitation of all conduction electrons, is related to PIET, in which only a single electron uses the photon energy.

1. Hanning Chen, Jeffrey M. McMahon, Mark A. Ratner and George C. Schatz, J. Phys. Chem. C, 114, 14384-392 (2010).
2. Hanning Chen, Mark A. Ratner and George C. Schatz, J. Photochem. Photobiol. A, in press (2011).

This page is intentionally left blank

Invited EFRC Presentation Abstract

Structure and Dynamics at Organic Semiconductor Interfaces

Part of CIS:SEM, Center for Interface Science: Solar Electric Materials, a Department of Energy, Office of Science, Basic Energy Sciences-funded Energy Frontier Research Center under DOE Award DE-SC0001084

Oliver L.A. Monti
Department of Chemistry and Biochemistry
The University of Arizona
Tucson, AZ, 85721
monti@u.arizona.edu

PROGRAM SCOPE: Interest in a molecular-level, first-principles understanding of interfacial structure and dynamics of organic semiconductors has increased dramatically, driven *e.g.* by vigorous efforts to develop efficient systems for solar energy conversion. Interfacial interactions between chemically different molecules or molecules and surfaces alter the molecular electronic structure in important and often subtle ways. A major thrust in this program is to develop a general description of the evolution of electronic structure at organic semiconductor interfaces, at fs time-scales, and its impact on excited-state lifetimes and rates of charge transfer using a range of photoelectron spectroscopies capable of probing both occupied and unoccupied manifolds.

RECENT PROGRESS: Initiated in 2009, the program has focused on several different archetypical combinations of organic semiconductors and surfaces, with particular emphasis on the interface formed at metals and transition metal oxides. We have implemented high-sensitivity angle-resolved photoelectron spectroscopy under highly controlled conditions to investigate the valence- and core-level electronic structure in ultrathin films of perylene derivatives and metal naphthalocyanines. In addition, we have built up the capacity to perform angle-resolved two-photon photoemission (AR-TPPE) in order to investigate molecular excited states, image and conduction bands.

Metal Naphthalocyanines (MNcs): The highly polarizable, dipolar or non-polar, closed- or open-shell MNcs offer a wide range of different molecule-surface interactions while largely maintaining the molecular scaffold. Crucially, their excited-state electronic structure is sensitive to the metal center. This permits isolating systematically the influence of the *molecular* electronic states on the *interfacial* electronic structure and dynamics from the often dominant effects of thin film structure. Our initial efforts in this arena have concentrated on the dipolar vanadyl naphthalocyanine (VONc) on both a weakly (highly oriented pyrolytic graphite, HOPG) and a strongly interacting (Au (111)) surface. The permanent dipole moment of VONc introduces strong long- and short-range electrostatic fields in highly organized thin films, with the result that interfacial dipoles and molecular electronic structure can be altered in a controlled fashion. Indeed, the electric field mediated intermolecular interactions, facilitated by the surface, lead to significant changes to both ground and excited states as probed by ultraviolet (UPS), X-ray (XPS) and two-photon photoemission (TPPE) spectroscopies. In order to capture the key physics at work, we have developed a simple, predictive microelectrostatic model, further supported by full-scale electronic structure calculations. Based on this model we were able to measure for the first time both ground and excited state dipole moment (2.7(4) D) and *zz*-polarizability tensor component ($3.4(11)\cdot10^{-28}$ m^3 and $6.1(6)\cdot10^{-28}$ m^3) directly at an interface; in addition these measurments also allowed an estimate of the exciton radius of 5 Å for this molecule.

Image-derived states near the vacuum-level provide an ideal test-bed for investigating charge-transfer at the organic semiconductor interface, since electrons may be transferred from an image state

to a molecular affinity level. Detailed AR-TPPE investigations of the VONc interface have allowed first steps toward understanding the influence of electrostatic interactions on such charge-transfer dynamics: Depolarization of the affinity level changes the driving force for charge-transfer, while at the same time perturbing the image state sufficiently to influence potentially the coupling between the two states.

Perylene Derivatives: Perylene dyes such as perylene bisimides (PTCDI) and perylene tetracarboxylic dianhydride (PTCDA) are highly versatile, strong electron acceptors commonly used as n-type semiconductors in organic heterojunctions. In an effort to understand charge-transfer at interfaces with transparent inorganic semiconductor surfaces, we have initiated a comprehensive investigation of the electronic structure of perylene derivatives on ZnO. In particular we are pursuing an improved understanding of the role of vacancies, defects and hydroxylation on interfacial electronic structure and charge-transfer dynamics. We have therefore extensively characterized single crystalline ZnO $(10\bar{1}0)$, as well as a range of epitaxial and ALD-grown ZnO films using x-ray diffraction, AFM, UPS and XPS. Upon adsorption of a variety of different perylene derivatives we find evidence for a strong chemisorptive interaction at the ZnO interface, resulting in the formation of a distinct interface state approximately 1.0 eV below E_F. Such states are likely to play a significant role in interfacial charge-transfer processes as well as in determining interface dipoles and energy-level alignment across this hybrid organic / inorganic interface.

FUTURE PLANS: We are currently implementing two-colour fs-time-resolved AR-TPPE in order to investigate the role of electrostatic fields on interfacial charge-transfer more directly. Determining lifetimes of the image states, affinity levels and excitonic states in the case of MNcs will help distinguish different mechanistic contributions to the excited state dynamics. We have also initiated experiments with MNc derivatives with altered molecular periphery in order to control thin film growth and hence electrostatic interactions. In addition, we plan to investigate the excited state electronic structure of perylene derivatives on ZnO using a variety of different spectroscopic tools and characterize growth modes carefully on the single crystalline surface. The molecular-level understanding of large organic semiconductor interfaces provided by these studies is beneficial towards a precise understanding of processes critical for organic electronics including organic semiconductor-based solar energy conversion.

BES-SUPPORTED PUBLICATIONS (SINCE 2010):

Influence of Electrostatic Fields on Molecular Electronic Structure: Insights for Interfacial Charge Transfer, O.L.A. Monti and M.P. Steele, Phys. Chem. Chem. Phys., 12, 12390 (2010) **Invited Perspective**

Image States at the Interface with a Dipolar Organic Semiconductor, M.P. Steele, M.L. Blumenfeld and O.L.A. Monti, J. Chem. Phys., 133, 124701 (2010)

Experimental Determination of Excited State Polarizability and Dipole Moment in a Thin Organic Semiconductor Film, M.P. Steele, M.L. Blumenfeld and O.L.A. Monti, J. Phys. Chem. Lett., 1, 2011 (2010)

Resonance and Localization Effects at a Dipolar Organic Semiconductor Interface, M.P. Steele, N. Ilyas, L.L. Kelly and O.L.A. Monti, submitted (2011)

Interfacial Electronic Structure of the Dipolar Vanadyl Naphthalocyanine on Au (111): The Role of Electrostatic Effects, A. Terjentjevs, M.P. Steele, M.L. Blumenfeld, L.L. Kelly, N. Ilyas, E. Fabiano, O.L.A. Monti and F. Della Sala, submitted (2011)

BES-SUPPORTED PHD-THESES (SINCE 2010):

Interfacial Electronic Structure of Organic Semiconductors, M.P. Steele, August 2011, The University of Arizona

CPIMS
Principal Investigator
Abstracts

"Spectroscopy, Imaging and Analysis of Molecules and Clusters with Vacuum Ultraviolet Radiation"

Musahid Ahmed
MS 6R-2100, 1 Cyclotron road, Chemical Sciences Division
Lawrence Berkeley National Laboratory, Berkeley, CA 94720
mahmed@lbl.gov

A state-of-the-art chemical imaging program to probe biological systems and products from combustion and atmospheric chemistry by mass spectrometry is being developed. Through imaging mass spectrometry, it will be possible to study fundamental processes that contribute to the production and utilization of energy resources and to aid in the discovery of novel mechanisms and methods for enhancing energy utilization and efficiency. By probing a variety of spatial scales ranging from 100 nm to 20 microns with chemical specificity of molecules, this imaging program will reveal new information about mechanisms in chemistry and biology. Fundamental studies of ion sputtering and laser desorption processes, imaging atmospheric aerosols, analysis of combustion products, environmental and geological samples and nanoscale imaging of microbial deconstruction of lignin and cellulose within plant cell walls, are some of the topics that are being explored in this program. In an parallel effort, tunable vacuum ultraviolet (VUV) radiation in conjunction with molecular beams are being used to probe electronic structure and dynamics of hydrogen-bonded and pi stacked systems in biomolecules and water clusters.

Imaging Mass Spectrometry-

In this program a technique to perform chemical imaging on surfaces using a novel mass spectrometry method is being developed, wherein ion-sputtered and/or laser desorbed neutrals are photoionized with high fluxes of tunable synchrotron VUV radiation. Furthermore, it is necessary to perform fundamental photoionization studies of various organic molecules to prepare a knowledge base that is applicable for imaging mass spectrometry. This is performed using two instruments. The first is an imaging mass spectrometer, where ion sputtered and laser or thermally desorbed molecules can be ionized by synchrotron VUV radiation. In the second instrument, supersonically cooled molecular beams of organic molecules are produced by thermal desorption and interrogated in a reflectron TOF with VUV radiation. Using both instruments, fundamental VUV photoionization experiments involving numerous organic molecules were performed. These included DNA bases and amino acids, several compounds important in plant cell walls, and PAH's formed in laboratory generated soot particles. The resulting mass spectra from these experiments are relatively simple and easy to assign, representing a significant improvement over typical secondary ion mass spectrometry (SIMS) mass spectra. The photoionization efficiency (PIE) curves of ion-sputtered neutral thymine and tryptophan in particular show that their corresponding internal energies were similar, each having ~2 eV of excitation from the ion desorption process. This result explains why certain classes of molecules, such as amino acids, often have only characteristic fragments in the VUV photoionization mass spectra.

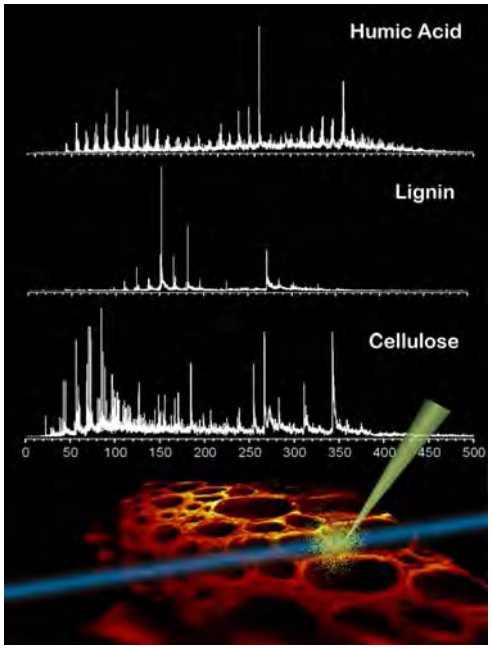

Mass spectra of laser desorbed neutral molecules ionized with 10.5 eV VUV radiation

In the past year, this knowledge was applied to investigate coniferyl and sinapyl alcohol, two monomers of the lignin polymer found in plants. By comparing monolignol mass spectra from SIMS, secondary neutral mass spectrometry

(SNMS) and molecular beams from the beamline, mass peaks arising from dissociative photoionization could be distinguished from fragments arising from the initial desorption event, and characteristic signatures for monitoring monolignols in plant biomass with SNMS could be easily determined. Together, these initial results showcase simplified and easy-to-assign mass spectra, a well-characterized ionization process, and the ability to yield quantitative results. These aspects are of great value when imaging chemically complex systems with mass spectrometry-based techniques.

In addition to the ion-probe, the recent installation of an ultraviolet laser onto the TOF-SIMS apparatus has enabled mass spectral chemical analysis of samples via laser desorption and VUV photoionization (LDPI). LDPI is a complementary imaging technique that is a gentler desorption method compared to ion sputtering, making it ideal for more fragile organic molecules. Unlike matrix assisted laser desorption, which is a common laser-probe analytical technique, laser desorption with VUV photoionization does not require the application of a matrix compound to enhance ionization; thus like SNMS, the chemistry of the native, unmodified samples can be probed. Within the last year, the laser desorption system has received several major improvements, which reduced the laser spot size from ~300 um to ~20 um, and recently using a new set of optics, the spot size has been reduced to 6 um. This smaller spot size has allowed for spatial imaging with laser desorption on bigger length scales. Tandem experiments with laser desorption imaging (LDPI) and ion-probe imaging (SNMS) can thus be envisioned in the future.

The improved LDPI system has already been used to analyze several systems, including lignin polymers, antibiotic-treated biofilms and a modified fullerene. Over lignin polymers, preliminary results have shown that oligomer units of lignin can be detected using laser desorption with VUV photoionization. It may therefore be possible to detect lignin dimers, trimers and tetramers, which will be useful for determining the sequence and structure of lignin polymers. This capability could aid in the optimization of lignin degradation and the separation of lignin from cellulose, which is currently a major problem in the production of biofuels from plant biomass.

LDPI was also used to study extracellular material from biofilms with both vacuum and extreme ultraviolet photons in collaboration with Luke Hanley (UIC). In these studies, LDPI was shown to effectively detect antibiotics and extracellular neutrals from intact bacterial biofilms. Different extracellular material was observed by LDPI-MS in response to rifampicin or trimethoprim antibiotic treatment, illustrating that LDPI can be used to monitor the biofilm's production of metabolites in response to the application of antibiotics.

Concurrent with these real-world applications, we continue to investigate the fundamental mechanisms of laser desorption to gain knowledge on the kinetic and internal energies of laser desorbed neutrals. This is made possible by utilizing the unique wavelength tunability available at the synchrotron and by monitoring the fragment-to-parent peak intensity ratio of laser-desorbed neutrals. These studies are currently being performed as a function of laser desorption power and can be used to determine the optimized conditions for minimizing molecular fragmentation while probing various chemical systems.

There are an extraordinary number of potential scientific problems that can be addressed with imaging mass spectrometry, ranging from combustion science, to materials chemistry, biology, and biogeochemistry. We have a research program that builds on the successes achieved at the beamline coupled with a number of ongoing collaborations. Our major effort is to image plant cells and the chemical changes they undergo after chemical degradation during pyrolysis or pretreatment methods in biofuel production. Fundamental laser desorption studies will be performed on ligno-cellulose molecules to elucidate fragmentation mechanisms. A new project is being initiated to quantify and map organic functional groups and bio-marker molecules in soil organic matter. Exciting new directions in cell biology are being pursued in collaboration with Dr. Hoi-Ying Holman (LBNL) in imaging microbial deconstruction of plant biomass and microbial production of mineral carbonates for CO_2 sequestration efforts. With Dr. Luke Hanley (UIC), we will continue our collaboration in laser desorption and imaging mass spectrometry on bacterial biofilms. With Deidre Olynick (LBNL, molecular foundry), laser assisted lithography studies for high resolution nano-patterning will be performed. With James Davis and Glenn Waychunas (both at LBNL, Earth Sciences Division) we propose to study the effects of

secondary mineral coatings on biogeochemical processes using SIMS and SNMS. Finally, new hardware modifications for single cell analysis, the recent acquisition of a fluorescence microscope for complementary optical imaging and continual improvement of laser desorption capabilities will make the imaging mass spectrometry effort truly state of the art and unique within the chemical imaging community.

Electronic structure and proton transfer in H-bonded and pi stacked systems and water clusters

Fundamental studies of photoionization processes of biomolecules are necessary for their implementation in imaging mass spectrometry. Furthermore determinations of ionization energies and other properties of biomolecules in the gas phase are not trivial, and these experiments provide a platform to generate these data. We have developed a thermal vaporization technique coupled with supersonic molecular beams that provides a gentle way to transport these species into the gas phase. Judicious combination of source gas and temperature allows for formation of dimers and higher clusters of the DNA bases. Extensive theoretical electronic structure and thermodynamic calculations performed in collaboration with Anna Krylov (USC) and co-workers allow for novel insights into these properties of DNA base monomers and dimers. The focus of this particular work is on the effects of noncovalent interactions, i.e., hydrogen bonding, stacking, and electrostatic interactions, on the IEs of the individual nucleobases. The changes in electronic structure upon clustering (i.e., hole localization) induced by these interactions have been discussed and published.

Recently, our studies on methylated uracil and uracil have led to the discovery of a new ionization mediated proton transfer route in stacked systems. We have performed experimental and theoretical characterization of the photoionization dynamics of gas-phase uracil (U) and 1,3-methyluracil (mU) dimers. Our results show that U dimers follow the behavior of other pyrimidine pairs, forming protonated monomers upon ionization. The majority of these pairs are H – bonded systems allowing a barrier-less proton transfer to take place upon ionization. However, mU dimers, cannot form H – bonded structures and yet upon ionization, demonstrate similar proton transfer reactions. To shed light on the mechanism and origin of the transferred proton, an isotopomer of mU was synthesized. In this isotopomer, the hydrogen atoms on the two methyl moieties were replaced by deuterium atoms while the rest of the hydrogens on the ring remained. The results show that the deuterium is transferred in the same fashion as the hydrogen atom, demonstrating the transfer is from the methyl group. Comparison of the experimental results with the theoretical calculations performed by the Krylov group suggests dynamics on the cationic surface helps mediate this proton transfer in stacked systems.

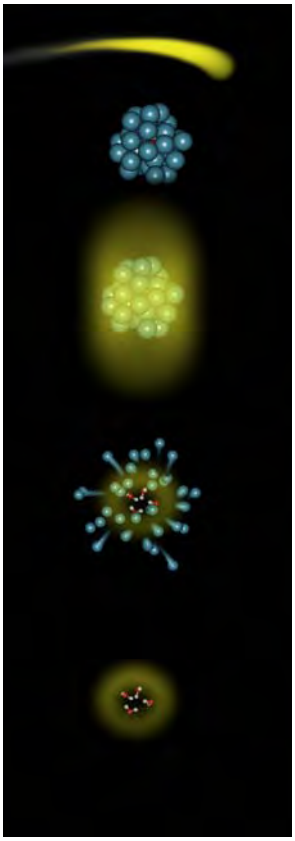

Schematic of intra-cluster Penning ionization of $(H_2O)_4$ by an Ar_{20} cluster.

Typically, photoionization of small water clusters lead to dissociation of the OH group on ultrafast time scales yielding a $(H2O)_nH^+$ type cluster. In order to generate complete (unfragmented) clusters, water doped Ar clusters ($Ar_{n\sim20}$) were produced in a supersonic expansion. Upon ionization with synchrotron VUV, unfragmented water clusters up to n=9 were observed. Analysis of the ionization line shape demonstrated that it is a surface exciton on the Ar cluster which absorbs the photon energy and subsequently, the exciton energy is transferred to the doped water cluster. The resulting water cluster ion is formed intact, since the evaporating Ar atoms remove the excess energy of ionization. This novel method of generating cold water cluster cations will be a valuable tool for probing structure and dynamics using IR and ultrafast spectroscopies in the future.

New experiments are envisioned in studying the organic molecules that are important in bio-fuel development and pyrolysis of biomass. The photoionization dynamics of polyols, sugars, and lignin compounds will be probed with single photon ionization. We are developing 2 color IR-VUV experiments to allow fundamental insight into the structure of molecules being prepared in our various

sources. Towards this end, we are building an IR-OPO system that has a rep-rate up to 25 kHz and will access wavelengths up to 5 μm.

References (DOE sponsored publications 2009-present) –

L.K. Takahashi, J. Zhou, O. Kostko, A. Golan, S. R. Leone and M. Ahmed, "*VUV Photoionization and Mass Spectrometric Characterization of the Lignin Monomers Coniferyl and Sinapyl Alcohol"* J. Phys. Chem. A (2011) (In press)

K. Khistyev, K. B. Bravaya, E. Kamarchik, O. Kostko, M. Ahmed, and A. I. Krylov, "*The effect of microhydration on ionization energies of thymine"* Faraday Disc. (2011) (In press)

G. L. Gasper, L. K. Takahashi, J. Zhou, M. Ahmed, J. F. Moore, and L. Hanley, "*Comparing Vacuum and Extreme Ultraviolet Radiation for Postionization of Laser Desorbed Neutrals from Bacterial Biofilms and Organic Fullerene"* Nuclear Instruments and Methods in Physics Research Section A (2011) (In press)

K. B. Bravaya, O. Kostko, S. Dolgikh, A Landau, M. Ahmed, and A. I. Krylov *"Electronic structure and spectroscopy of nucleic acid bases: Ionization energies, ionization-induced structural changes, and photoelectron spectra"* J. Phys. Chem. A (2010) **114**, 12305

K. R. Wilson, H. Bluhm, M. Ahmed, *Aerosol Photoemission*, in Fundamentals and Applications in Aerosol Spectroscopy, edited by J.P. Reid and R. Signorell, Taylor and Francis, (2010) pp 367-417

G. L. Gasper, L. K. Takahashi, J. Zhou, J. Moore, M. Ahmed, L. Hanley. *"Laser Desorption Postionization Mass Spectrometry of Antibiotic-Treated Bacterial Biofilms using Tunable Vacuum Ultraviolet Radiation"* Anal. Chem. (2010) **82,** 7472

R. I. Kaiser, B. J. Sun, H. M. Lin, A. H. H. Chang, A. Mebel, O. Kostko and M. Ahmed *"An Experimental and Theoretical Study on the Ionization Energies of Polyynes (H-(C≡C)$_n$-H; n = 1 - 9)"* Astrophys. J. (2010) **719** 1884.

O. Kostko, J. Zhou, A. Chang, B. J. Sun, J. S. Lie, A. H. H. Chang, R. I. Kaiser and M. Ahmed "*Determination of ionization energies of C_nN (n=3-12) clusters: Vacuum-ultraviolet (VUV) photoionization experiments and theoretical calculations"* Astrophys. J. (2010) **717**, 674

S. R. Leone, M. Ahmed and K. R. Wilson, "*Chemical Dynamics, Molecular Energetics, and Kinetics at the Synchrotron"* Phys. Chem. Chem. Phys., (2010) **12**, 6564

E. Kamarchika, J. M. Bowman, O. Kostko, M. Ahmed, and A. I. Krylov, "*Spectroscopic signatures of proton transfer dynamics in the water dimer cation".* J. Chem. Phys. (2010) **132,** 194311

J. Zhou, L. Takahashi, K. R. Wilson, S. R. Leone and M. Ahmed, "*Determination of Internal Energies of Ion Desorbed Neutral Organic Molecules with Tunable Vacuum Ultraviolet Photoionization"* Anal. Chem. (2010) **82**, 3905

O. Kostko, K. Bravaya, A. I. Krylov, and M. Ahmed, "*Ionization of cytosine monomer and dimer studied by VUV photoionization and electronic structure calculations."* Phys. Chem. Chem. Phys., (2010), **12**, 2860.

O. Kostko, S. R. Leone, M. A. Duncan and M. Ahmed, "*Determination of ionization energies of small silicon clusters with vacuum-ultraviolet (VUV) photoionization."* J. Phys. Chem. A (2010), **114**, 3176

Bravaya, O. Kostko, M. Ahmed, and A. I. Krylov, "*The effect of pi-stacking, h-bonding, and electrostatic interactions on the ionization energies of nucleic acid bases: adenine-adenine, thymine-thymine and adenine-thymine dimers"* Phys. Chem. Chem. Phys. **12,** (2010) 2261

R. I. Kaiser, A. Mebel, O. Kostko and M. Ahmed, *"On the ionization energies of C_4H_3 Isomers"* Chem. Phys. Lett. **485,** (2010) 281

O. Kostko, S.K. Kim, S.R. Leone, and M. Ahmed, *"Mass-Analyzed Threshold Ionization (MATI) Spectroscopy of Atoms and Molecules using VUV Synchrotron Radiation"* J. Phys. Chem. A **113,** (2009) 14206

J. Zhou, O. Kostko, C. Nicolas, X. Tang, L. Belau, M. S. de Vries, and M. Ahmed, *"The direct observation of guanine tautomers using VUV photoionization"* J. Phys. Chem. A **113,** (2009) 4829

L. Takahashi, J. Zhou, K. R. Wilson, S. R. Leone and M. Ahmed, "*Imaging with Mass Spectrometry: A Secondary Ion and VUV-Photoionization Study of Ion-Sputtered Atoms and Clusters from GaAs and Au"* J. Phys. Chem. A **113,** (2009) 4035

O. Kostko, M. Ahmed, and R. B. Metz, "*A VUV photoionization measurement and ab-initio calculation of the ionization energy of gas phase SiO_2"* J. Phys. Chem. A **113**, (2009) 1225

Model Catalysis by Size-Selected Cluster Deposition

PI: Scott L. Anderson
Chemistry Department, University of Utah
315 S. 1400 E. Rm 2020
Salt Lake City, UT 84112
anderson@chem.utah.edu

Program Scope

The goal of our research is to explore correlations between supported cluster size, electronic and morphological structure, the distributions of reactant binding sites, and catalytic activity, for model catalysts prepared using size-selected metal cluster deposition. The work to date has focused on catalysts with catalytically active metal clusters deposited on metal oxide supports. We also plan a short round of experiments looking at catalysis relating to H_2 splitting and storage in Mg. Finally, with permission of DOE, we are planning to examine electrocatalytic chemistry, initially with size-selected Pt clusters deposited on glassy carbon.

The experimental setup is quite flexible. The main instrument has a mass-selecting ion deposition beamline fed by a 100 Hz laser vaporization source that produces high fluxes at low deposition energies (~10^9 Pd_{10}/sec in a 2 mm diameter spot at 1 eV/atom, for example). Typical samples with ~1.5 x 10^{14} metal atoms/cm^2 deposited in the form of Pd_n^+ can be prepared in 10 – 20 minutes, and our analysis methods are also quite fast. This point is important, because even in UHV these samples are highly efficient at collecting adventitious contaminants, due to substrate-mediated adsorption. Sample morphology is probed by low energy He^+ ion scattering (ISS), electronic structure is probed by x-ray and UV photoelectron spectroscopy and ion neutralization spectroscopy (XPS, UPS, INS), and reactivity is studied using a differentially pumped mass spectrometer surrounded by a cluster of pulsed and cw gas inlets that can be used to dose the sample while various temperature programs are executed.

The main UHV analysis chamber has a port in the bottom, equipped with a gate valve, a triple differential seal, and one of several interchangeable small chambers with their own pumping systems. When the sample is positioned in the lower chamber is it isolated from the main UHV system. This capability allows us to exchange or repair samples without venting the main UHV system, but the lower chamber also allows a variety of procedures, such as growth of oxide or Mg films, to be done without contaminating the main UHV system.

In addition to the main instrument, we recently acquired via donation, an old ESCA spectrometer that we have refitted as a UHV test instrument. This instrument now has functional capabilities for XPS, UPS, temperature-programmed desorption/reaction (TPD/R), as well as for sample introduction and cleaning/annealing. This instrument allows us to test new hardware and experimental protocols (recently, our new UPS, INS and Mg and alumina growth capabilities), and to train new students on UHV methods, without tying up the main instrument.

Recent Progress

Additions to the experimental capabilities needed for the proposed research:

Just at the end of the previous project period, we had demonstrated a one-to-one correlation between the binding energy of the Pd 3d core level, and the activity for CO oxidation. The strong correlation was somewhat surprising in that chemical reactions are expected to depend only to the valence electronic structure, and core levels are only an indirect probe of the valence structure. One component of the current project is to add capabilities for valence level electronic spectroscopy. The original plan was to add a set-up for metastable-impact electron spectroscopy (MIES) which is a surface-sensitive technique in which He^* metastables are collided with the surface, resulting in valence electron spectra by two mechanisms, Auger deexcitation (AD), and Auger neutralization (AN). To assign the contributions from AN and AD, the UPS spectrum is also taken. After discussions with Kempter, who has been a major proponent of MIES, we concluded that for the type of systems we are interested in, ion neutralization spectroscopy (INS) would (also in combination with UPS) give the same information as MIES, but would

be much easier to integrate into our experiment. Accordingly, we have constructed a low energy ion gun and a doubly-differentially pumped capillary discharge lamp for the INS and UPS experiments, respectively. Both have been tested on the UHV test instrument, and we have demonstrated good quality spectra of metal and metal oxide samples in good agreement with literature spectra. Both the lamp and ion gun will be installed on the main instrument the next time we vent the UHV system.

We also have constructed aluminum and magnesium evaporation sources needed for proposed experiments where clusters are deposited on thick aluminum oxide and MgO/Mg substrates. Both sources have been tested and deposition rates vs. temperature calibrated using the XPS capabilities in the test machine. These sources are installed in one of the interchangeable lower chambers that can be attached to the main instrument.

A final addition to the lower chamber experiments is the new *in situ* electrochemistry setup. Microfabrication of the ceramic electrochemical cells has just been completed, and integration into the vacuum system should be done in the next month. For these experiments, the sample (e.g. Pt_n/glassy carbon) will be positioned in the lower chamber, which will be vented with UHP argon. A ~14 microliter ceramic electrochemical cell will then be sealed directly against the face of the glassy carbon electrode/cluster support, then filled with a slowly flowing electrolyte solution, which can be gas-saturated as needed. After electrochemical measurements are completed, the cell will be flushed out, blown dry, and then evacuated, allowing the sample to be retracted into the UHV system for post-reaction analysis. Only the ~2mm diameter spot containing the clusters is exposed to electrolyte, and the sample is never exposed to the laboratory environment. In addition to the electrochemistry experiments, the same cell, minus electrodes, can be used as a high pressure reactor, with on-line mass spectral monitoring of products. While micromachining of the cells was in progress, we built a benchtop mock-up of the experiment, and have demonstrated good CV curves for oxygen reduction on Pt/glassy carbon, confirming that we are preparing clean glassy carbon. Our progress in the electrochemistry area has been greatly aided by help from Prof. Henry White and students at the U of Utah.

Research results:

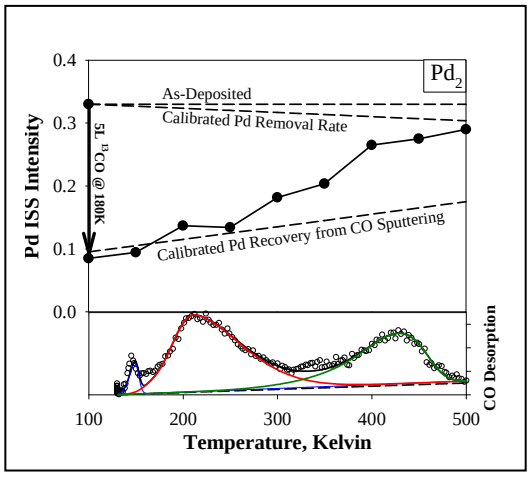

Research in the past year has concentrated on understanding the origins of the interesting size-dependent activity and electronic structure effects observed for CO oxidation over $Pd_n/TiO_2(110)$. We completed a study using a combination of TPD, XPS, and ion scattering to examine the effects of O_2 exposure amount and temperature on the oxidation state of Pd, and the adsorption sites of the O ad-atoms. One of the interesting results of the CO oxidation experiments was that there are two CO adsorption sites associated with the Pd clusters, in addition to CO sites on the TiO_2 surface. There appears to be a correlation between the population of CO in the most stable site, and the CO oxidation activity, thus it is important to understand the nature of the sites. The figure shows a representative experiment, in this case using Pd_2/TiO_2, addressing this question. The lower frame shows the TPD spectrum for CO adsorbed at 180 K on freshly deposited $Pd_2/TiO_2(110)$. Similar results are seen for other cluster sizes and for clusters that were lightly oxidized by O_2 exposure prior to low temperature CO exposure. The lowest temperature feature (T_{peak} ~140 K) is present on clean $TiO_2(110)$ and is consistent with a small amount of CO sticking to the TiO_2 support during the few minutes it takes to cool the sample from 180 K to the TPD starting temperature. The other two features appear for all Pd_n/TiO_2 samples, albeit with significant size-to-size variations in peak temperatures and intensities. The feature desorbing between ~150 and 300 K corresponds to CO in binding sites with desorption energies between ~0.5 and 1 eV. The higher temperature feature between ~350 and 450 K corresponds to CO in sites with $E_{desorption}$ between ~1 and 1.3

eV. The upper frame of the figure summarizes a sequence of ion scattering experiments taken before and after the sample was exposed to 5 L of CO at 180 K (points connected by arrow on the left hand axis). What is plotted is the Pd He^+ ion scattering (ISS) intensity, which is proportional to the fraction of Pd that is exposed in the top-most surface layer. For the as-deposited Pd before CO exposure, the intensity is high because all the Pd atoms are in the surface layer, and therefore accessible to the He^+ beam. After the CO exposure, the Pd ISS intensity drops substantially, demonstrating that in the 5 L CO exposure, the Pd sites are largely saturated, resulting in Pd shadowed or blocked with respect to He^+ scattering, by overlying CO. This result implies that one or both of the CO/Pd sites have CO bound on top of the clusters.

The rest of the ISS data points show the effects of heating the sample to the indicated temperatures. There are two effects. He^+ impacts remove (sputter) CO slowly, and we have measured the rate at which this process exposes underlying Pd by running experiments where the sample is not heated (dashed trend line with positive slope). He^+ also slowly sputters Pd, and the effect of this process on the Pd ISS signal was measured by experiments on CO-free Pd_2 (dashed trend line with negative slope). Note that as the sample is heated to ~300 K, thereby removing all the weakly bound CO, there is essentially no recovery of Pd signal beyond that expected from He^+ sputtering. This behavior indicates that the 0.5 - 1 eV CO binding sites, while associated in some way with Pd, are not on top of the clusters where desorption of CO would expose Pd to the He^+ beam. In contrast, as the sample is heated to remove CO from the more stable Pd binding sites above 350 K, the Pd intensity recovers essentially to the level that would be expected for the initial sample, taking Pd sputter loss into account. Clearly, the higher temperature CO binding site has CO on top of Pd where it attenuates ISS.

The ISS experiments do not reveal any details of the binding geometries. For example, while we know that the higher temperature CO feature is associated with CO on top of the Pd clusters, we cannot clearly distinguish between CO binding in atop, bridge, or hollow sites. Similarly, the lower temperature CO feature, where CO is not shadowing or blocking Pd, could be accounted for by CO bound to TiO_2 at the periphery of the Pd clusters. Alternatively, the CO could be bound to Pd, but at a large angle with respect to the surface normal, where it also would not attenuate He^+ scattering from Pd. Complementary DFT calculations by Ping Liu at BNL suggest that the latter scenario is responsible for the lower temperature CO desorption feature, and that the higher temperature feature corresponds to CO bound in bridge sites on the top of the clusters.

In addition, we have done detailed studies of changes in the morphology of the Pd_n/TiO_2 samples induced by heating, with and without O_2 exposure, and with and without CO exposure. There is evidence that Pd becomes partially encapsulated by TiO_x during heating with CO, or to a lesser extent by simply heating in vacuum. Heating with prior O_2 exposure partially reverses the encapsulation process. Encapsulation is seen directly in ISS, but there are also interesting effects of this process on the intensities of the lower and higher temperature CO binding sites, and on activity for CO oxidation.

Future Plans

We are currently examining hydrocarbon oxidation and partial oxidation on Pd/TiO_2, taking advantage of our detailed understanding of the Pd oxidation kinetics. We will shortly switch to Pt/glassy carbon to try size-selected electrochemistry, but in parallel we will carry out reaction studies on Pt/TiO_2 and Pt/alumina, looking for correlations between activity, morphology, electronic structure, and adsorbate binding properties.

Publications acknowledging DOE support

"Size-dependent oxidation of Pd_n ($n \leq 13$) on alumina/NiAl(110): Correlation with Pd core level binding energies." Tianpin Wu, William E. Kaden, William A. Kunkel, and Scott L. Anderson, Surf. Sci. 603 (2009) 2764-77.

"Electronic Structure Controls Reactivity of Size-Selected Pd Clusters Adsorbed on TiO_2 Surfaces", William E. Kaden, Tianpin Wu, William A. Kunkel, Scott L. Anderson, Science. 326 (2009) 826 - 9.

This page is intentionally left blank

THERMOCHEMISTRY AND REACTIVITY OF TRANSITION METAL CLUSTERS AND THEIR OXIDES

P. B. Armentrout

315 S. 1400 E. Rm 2020, Department of Chemistry, University of Utah,

Salt Lake City, UT 84112; armentrout@chem.utah.edu

Program Scope

The objectives of this project are to obtain quantitative information regarding the thermodynamic properties of transition metal clusters, their binding energies to various ligands, and their reactivities. This is achieved using a metal cluster guided ion beam tandem mass spectrometer (GIBMS) to measure absolute cross sections as a function of kinetic energy for reactions of size-specific transition metal cluster ions with simple molecules. Analysis of the kinetic energy dependent cross sections reveals quantitative thermodynamic information as well as kinetic and dynamic information regarding the reactions under study.

Since 2009, our DOE sponsored work has included studies of the kinetic energy dependences of the size-specific chemistry of Co_n^+ (n = 1 - 18) reacting with CD_4.[1] The latter work can be directly compared to previous studies of Fe_n^+ (n = 2 - 15)[2] and Ni_n^+ (n = 2 - 16)[3] with methane (CD_4). In addition, we have quantitatively examined the collision-induced dissociation of small iron oxide cluster cations, $Fe_mO_n^+$ (m = 1 - 3, n = 1 - 6), with Xe to ascertain their stabilities.[4] These results are discussed further below. Finally, an invited review of our recent work that emphasizes the relationship to bulk phase properties has been published.[5]

Recent Progress

Reactions of Clusters with CD_4. We have studied the kinetic energy dependences of reactions of Fe_n^+ (n = 2 - 16)[2] and Ni_n^+ (n = 2 - 16)[3] with CD_4, and most recently, that for Co_n^+ (n = 2 - 16).[1] Figure 1 shows results typical of most clusters. All observed reactions are endothermic. The lowest energy process for iron and cobalt clusters is generally dehydrogenation, whereas for nickel, double dehydrogenation is efficient enough that the $Ni_nCD_2^+$ species is not observed except for the smallest and largest clusters. These results are qualitatively consistent with observations that carbide formation is an activated process for reactions of hydrocarbons on Fe, Co, and Ni surfaces. Indeed, formation of $Co_nCD_4^+$

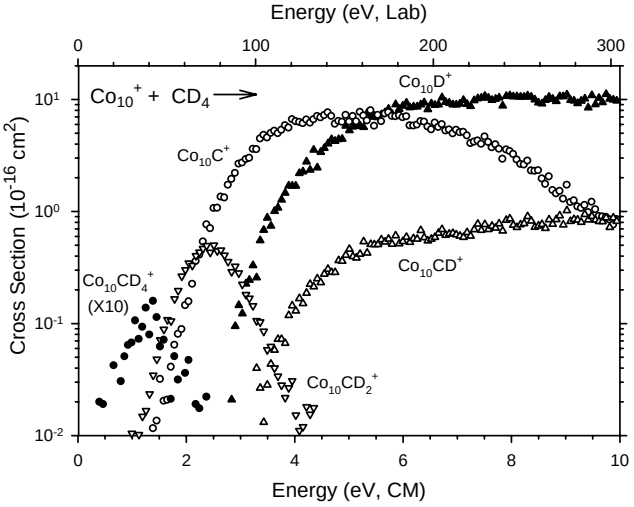

Figure 1. Reaction of Co_{10}^+ with CD_4 to form primary products.

(observed for larger clusters, e.g., Figure 1) has a threshold that directly corresponds to the activation energy for dissociative chemisorption.

Thresholds for the various primary and secondary reactions are analyzed and bond dissociation energies (BDEs) for cluster bonds to C, CD, and CD_2 are determined. Importantly, the accuracy of these BDEs can be assessed because there are usually two independent routes to measure BDEs for each cluster to D, C, CD, and CD_2, e.g., $D_0(Co_{10}^+\text{-D})$ can be measured in the primary reaction of Co_{10}^+ or the secondary reaction of Co_{11}^+ (to form $Co_{10}D^+ + Co + D$). Values obtained from the primary and secondary processes are in good agreement for D (which also agree with the results from D_2 studies),[6-8] C, and CD. For the CD_2 ligand, BDEs obtained from primary reactions are generally low compared to those from secondary reactions, which demonstrates that the initial dehydrogenation reactions have barriers in excess of the endothermicity. For larger clusters, this barrier often corresponds to the initial dissociative chemisorption step.

Figure 2 shows the final BDEs determined in the cobalt study,[1] which vary for small clusters but rapidly reach a relatively constant value at larger cluster sizes. The magnitudes of these bonds are consistent with simple bond order considerations, namely, D (and CD_3) form one covalent bond, CD_2 forms two, and CD and C form three. Previous results indicate that for D and O,[8-11] bond energies for larger clusters (n > 10) closely approach bulk phase values. Therefore, it seems reasonable to conclude that our experimental BDEs for larger clusters should provide reasonable estimates for heats of adsorption to surfaces for these molecular species. As little experimental information is available for *molecular* species binding to surfaces, the thermochemistry derived here for clusters bound to C, CD, and CD_2 provides some of the first experimental thermodynamic information on such species.

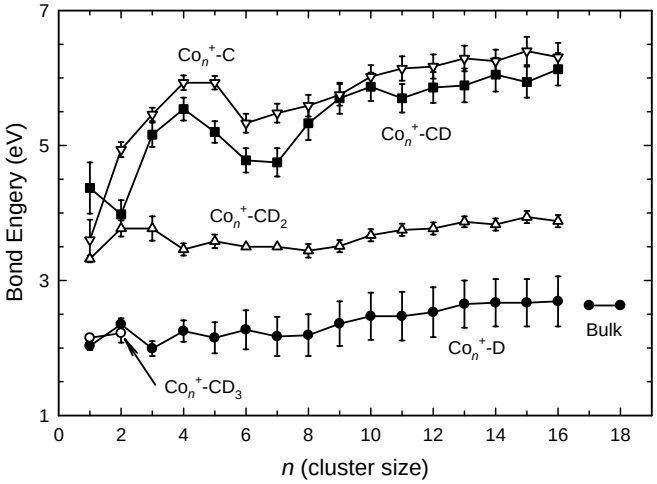

Figure 2. BDEs of D, C, CD, CD_2, and CD_3 to Co_n^+ vs. cluster size.

Iron oxide cluster cations. We have also initiated studies of oxygenated iron clusters, $Fe_nO_m^+$, which might mimic the chemistry of metal oxide surfaces. A broad range of stoichiometries have been produced although larger clusters tend to form clusters containing nearly equal numbers of iron and oxygen atoms. Initially, our studies are focusing on characterizing the thermodynamic stabilities of these clusters by examining their dissociation behavior in collisions with Xe. Some 30 different iron oxide cluster cations (with n = 1 - 10) have been examined, including FeO_m^+ (m = 1 - 5), $Fe_2O_m^+$ (m = 1 - 6), $Fe_3O_m^+$ (m = 2 - 4, 8), $Fe_4O_m^+$ (m = 1 - 6), $Fe_5O_m^+$ (m = 4 - 6), $Fe_6O_m^+$ (m = 5 - 8), $Fe_7O_m^+$ (m = 6 - 8), $Fe_8O_m^+$ (m = 7 - 9), $Fe_9O_m^+$ (m = 8 - 10), and $Fe_{10}O_x^+$ (x = 9 - 11). Not surprisingly, oxygen rich clusters tend to dissociate by losing O, O_2, or FeO_2, whereas iron rich clusters dissociate by losing Fe or FeO, in agreement with the qualitative CID study of Castleman and coworkers.[12] Particularly stable clusters include $Fe_2O_2^+$, $Fe_3O_3^+$, and $Fe_6O_6^+$. For larger clusters, fission is not uncommon, e.g., $Fe_6O_6^+$ dissociates to $Fe_3O_3^+ + Fe_3O_3$ at relatively low energies. The kinetic energy dependent collision-induced dissociation cross sections for the smaller clusters have been analyzed to

obtain both oxygen and iron bond energies for these clusters.[4] Results are shown in Figure 3. As can be seen, the oxygen atom bond energies can be tuned over a broad range by altering the stoichiometry and oxidation state of the cluster, such that specific clusters may prove useful as efficient catalysts for oxidation of species like methane and CO, as previously examined by Castleman and coworkers.[12]

Experimental retrenching. Research over the past year has focused on repairing and upgrading our guided ion beam mass spectrometer and its laser vaporization system. In particular, a new copper vapor laser was purchased and installed last year. We have found that its specifications are sufficiently distinct from the previous laser used that we need to modify our source blocks (where the laser, metal targets, and He gases intersect) in order to efficiently produce metal clusters. We are presently exploring several systematic variations in the block design in order to optimize both clustering efficiency and ion intensity. Figure 4 illustrates some of our recent results for iron clusters, exhibiting good intensity over a broad range of cluster sizes. Further enhancements are anticipated.

Two new students have joined our cluster research efforts (recently conducted primarily by one postdoc) and they are coming up to speed. I am hopeful that the productivity of the instrument coupled with advances by the students will soon allow us to pursue the experimental studies outlined below.

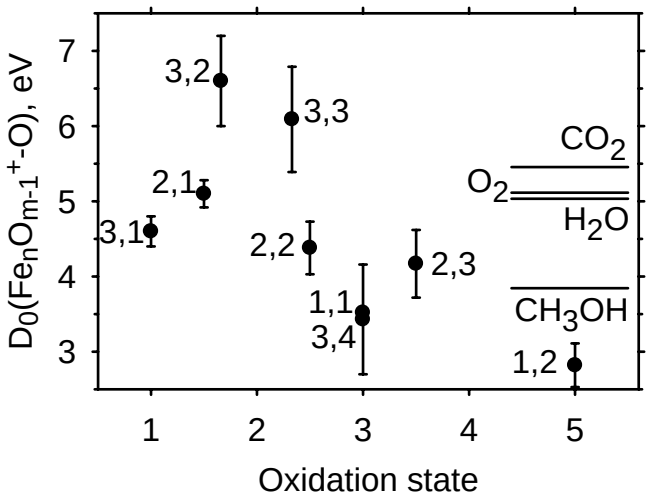

Figure 3. Oxygen atom bond energies to $Fe_nO_{m-1}^+$ clusters indicated by (n,m) versus the average oxidation state of the iron atoms. Similar bond energies for the species on the right are indicated for comparison.

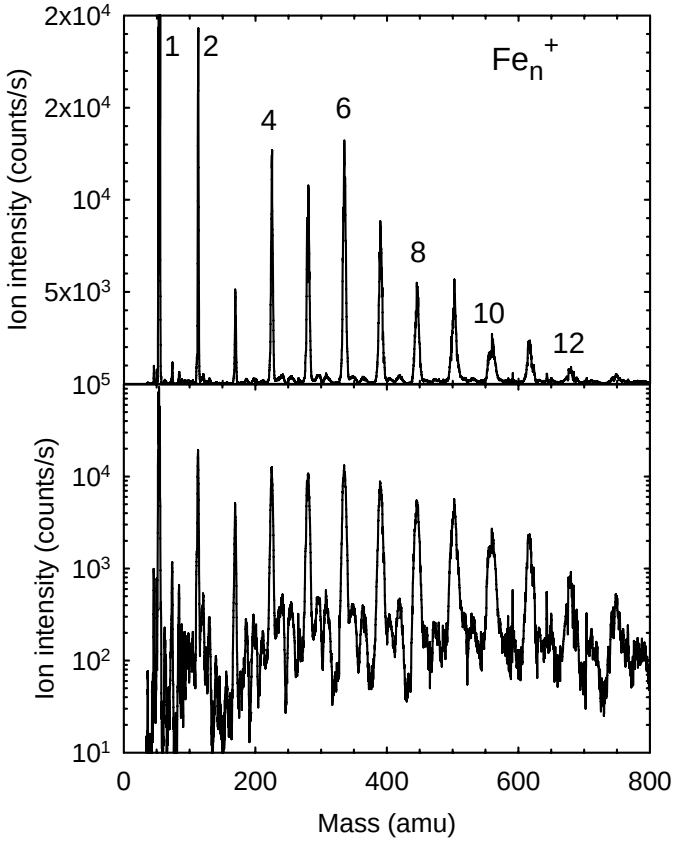

Figure 4. Mass spectrum showing iron cluster intensities on linear and logarithmic scales. Small amounts of monoxides and dioxides of each cluster size can also be seen.

Future studies

Our intent is to extend our previous experimental work in a focused effort to understand the chemistry of several systems related to Fischer-Tropsch and syngas chemistry, including the activation of carbon monoxide and selective

oxidation of methane. Because of the complexity of the data acquisition and data analysis, our work is not amenable to survey studies, which bypass the strength of our approach, the determination of quantitative thermodynamic information. Therefore, we intend to focus our efforts on three metal systems: iron, cobalt, and nickel. These metals are among the most active of the 1st row transition metals in catalytic systems. The mechanisms of iron and cobalt catalysts in Fischer-Tropsch chemistry are similar but have distinct differences that would usefully be elucidated.[13] Further, our recent work indicates that the reactions of iron, cobalt, and nickel clusters show differences in the chemistry with methane, such that examination of the periodic trends in this chemistry should be enlightening. First row metals also give us the most flexibility regarding the range of cluster sizes that can be studied. We already have a broad database of thermodynamic information established for iron, cobalt, and nickel clusters. Additionally, iron and nickel are among the systems that have been studied most thoroughly by theory. Because of the complexity of metal cluster systems, interfacing and comparing with theoretical information is advantageous. Likewise, we anticipate that these results will stimulate further theoretical investigation.

Publications resulting from DOE sponsored research in 2009 – present (1, 4, 5) and References

1. M. Citir, F. Liu, P. B. Armentrout, J. Chem. Phys. **130**, 054309 (2009).
2. R. Liyanage, X.-G. Zhang, P. B. Armentrout, J. Chem. Phys. **115**, 9747 (2001).
3. F. Liu, X.-G. Zhang, R. Liyanage, and P. B. Armentrout, J. Chem. Phys. **121**, 10976 (2004).
4. M. Li, S.-R. Liu, P. B. Armentrout, J. Chem. Phys. **131**, 144310 (2009).
5. Armentrout, P. B. in *Nanoclusters: A Bridge across Disciplines*, Jena, P.; Castleman, W. C.; Eds.; Elsevier, Amsterdam: The Netherlands, 2010, pp. 269-297.
6. J. Conceição, S. K. Loh, L. Lian, P. B. Armentrout, J. Chem. Phys. **104**, 3976 (1996).
7. F. Liu, R. Liyanage, P. B. Armentrout, J. Chem. Phys. **117**, 132 (2002).
8. F. Liu, P. B. Armentrout, J. Chem. Phys. **122**, 194320 (2005).
9. J. B. Griffin, P. B. Armentrout, J. Chem. Phys. **106**, 4448 (1997).
10. D. Vardhan, R. Liyanage, P. B. Armentrout, J. Chem. Phys. **119**, 4166 (2003).
11. F. Liu, F.-X. Li, P. B. Armentrout, P. B. J. Chem. Phys. **123**, 064304 (2005).
12. N. M. Reilly, J. U. Reveles, G. E. Johnson, J. M. del Campo, S. N. Khanna, A. M. Köster, A. W. Castleman, Jr. J. Phys. Chem. C **111**, 19086 (2007).
13. B. H. Davis, Fuel Processing Tech. **71**, 157 (2001).

"Electronic Structure of Transition Metal Clusters and Actinide Complexes and Their Reactivity"
DEFG2-05ER15657 – April 2010-April 2011
K. Balasubramanian,
California State University East Bay, Hayward CA 94542 kris.bala@csueastbay.edu

Program Scope

The focus of our recent work was on electronic structure of actinide complexes and subnano silver-metal clusters. We have made progress in (a) Computing the binding properties of environmentally occurring actinides with carbon nanotubes as possible means of actinide sequestrations (b) electronic structure and spectroscopy of subnano silver particles and alloys of silver and gold particles, which are found to have very interesting fluorescent emissions (c) properties of actinide complexes in aqueous solution. The research work on silver and gold nanocluster was carried out in collaboration with experimentalists. We are providing here only a brief summary of major highlights, in each of the categories.

Computational Studies of Actinide Sequestration with carbon nanotubes and mesoporous materials.

Challenges of nuclear waste disposal and the management of nuclear fuel is attributed to the understanding of actinides behaviors in aqueous systems and the development of novel procedures for successful elemental separation and extraction. In most common forms, actinides in their high oxidation states exist as actinyl ions, like actinyl(V) and actinyl(VII) and the most strictest, but common form is the actinyl(VI) ion, AnO_2^{2+}. Actinyl ions are either found in solutions or in crystals. Moreover, actinide contamination in biological and geological environments is a topic of considerable importance to the United States and many around the world. Bioremediation microbiological, chemical and geological strategies processes, have been investigated experimentally and sometimes combined and/or complemented molecular simulations to measure and elucidate, the sensitive nature of the structural, bonding and energetic characteristics of actinides. However, comprehensive strategies for elimination and remediation of contaminated lands and facilities are still lacking.

Carbon nanotubes (CNTs) have been exploited for many different applications in terms of their chemical, electronic and mechanical properties, as well as their unique tubular structure and large length/diameter ratio. CNTs for gas and biosensing applications have attracted great attention. They possess excellent adsorption ability to form strong interactions with foreign molecules. In addition, their inner cavities and active and topological defective sites on their surfaces can contribute to the high pollutants removal capability of CNTs. The interaction between actinides and CNTs is a subject of intense current interest. Among the actinides, the most extensively studied and characterized by both experiment and theory is uranyl(VI).[45] Uranium exists in aqueous solutions and acidic pH conditions (between 3 and 4) as the actinyl ion UO_2^{2+}. This ion has received considerable interest because of its increased nuclear activity that produces high-level nuclear wastes.

We have carried out computational studies of UO_2^{2+} CNT interactions using high level relativistic computations. The uranyl ion was introduced onto the exterior (EX) and interior (IN) surfaces of a (6, 6) pristine (defect-free, **DF**) and Stone-Wales (**SW**) defect CNT. Topological defects, such as the SW defect in CNTs, were examined as a potential driving force for enhanced binding for foreign atoms and molecules. In addition, to elucidating the magnitude of uranyl binding to the SW, defect we have carried out further calculations on hexagons labeled **6N** (**N=A**, **B**, **C**, **D** and **E**) which neighbor the SW defect. **Fig. 1** shows select DFT/B3LYP-optimized structures of the uranyl ion absorbed on the exterior and interior of the (6, 6) CNT complexes. In order to access the degree of rotational barriers around the curvature of the tube as a function of uranyl's initial orientation, we have considered full optimizations for UO_2^{+2} along the tube axis (*act* -CNT) and perpendicular to the tube's axis (*act*$\perp$-CNT). For the CNT complexes the uranyl

ion bond length (O_x-U-O_y) remained linear with the maximum displacement of ~.05˚ for all complexes. Also, for all act-complexes the average U-O distances ranged from 1.77 Å to 1.80 Å.

Figure 1: Side views selected Stone-Wales (SWD) nanotube complexes with UO_2^{+2}. SWD defect region depicted by carbons highlighted in blue and hexagons rings (A to E) surrounding SWD shown in corresponding orange carbon atoms.

a. *act*-CNTs	***ex***	***en***
***swd*-5A**	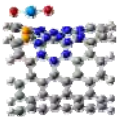	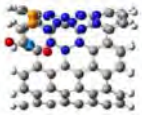
***swd*-6A**	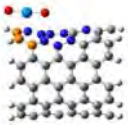	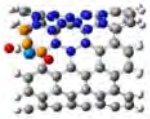
***swd*-6B**	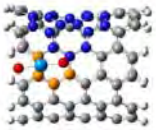	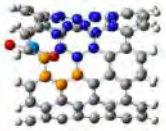
***swd*-6C**	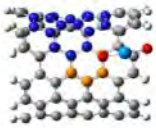	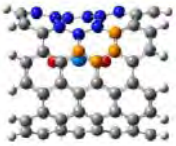
***swd*-6D**	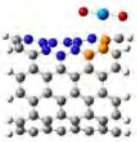	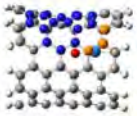
***swd*-6E**	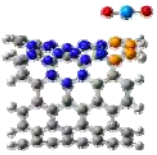	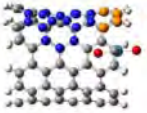
***swd*-5B**	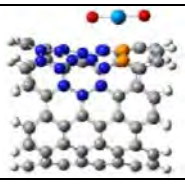	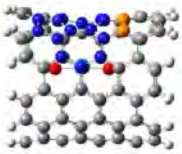

The relative path indexes of the uranyl ion traversing the CNT frameworks were computed and plotted. We have first tried to understand the preferred position of UO_2^{2+} on different pentagonal faces of the SW defect complexes. These computations show the **SW-5A** configurations to be the most favorable compared to **SW-5B** for both **par** and **per** orientations.

For the **par** and **per** complexes, the **SW-5A-EX** binding energies are 133.81 and 158.74 kcal mol^{-1} lower than **SW-5B-EX**. For endohedral complexes, the binding energy differences between **SW-5A-EN** and **SW-5B-EN** are 106.05 and 41.5 kcal mol^{-1}, respectively. This indicates that either the cation-π interaction has an important influence upon the uranyl initially traversing the CNT and/or the π-π framework for **en** complexes contributing significantly to stabilizing UO_2^{2+} compared to their **ex** counterparts. Thus, we now discuss UO_2^{2+} placement on the different hexagonal **6N** (**N**=**A**, **B**, **C**, **D**, **E**) centroids both for the **ex** and **en** subsequently optimized geometries. **Table 1** summarizes the binding energy of the uranyl cation both for **ex** and **en** positions at different hexagonal sites for the CNT. The endohedral positions turns out to be energetically favorable compared to exhohedral, and among all the hexagonal faces the **6A** hexagonal centroid (i.e., with all six carbon atoms in the hexagonal ring) is energetically most stable. In order to ascertain the exhohedral versus endohedral UO_2^{2+} absorption in UO_2^{2+}@CNT, a crucial factor is the local charge depletion that the framework experiences as the ion transverses "outside" and "inside" of the nanotube. That means that even though UO_2^{2+} prefers enegetically endohedral rather than exhohedral positions, a complete understanding is lacking unless and until UO_2^{2+} donation and the CNTs back-donation is assessed. We can deduce the charge contributions (donation) from the Mulliken charge populations of these complexes. In this manner, a slight donation (0.80 e^-) is observed for the **ex** complexes, while higher donation together with predominant back-donation (up to 0.91 e^-) is revealed for **en** systems. More interesting is that such effects also appear for the pristine (defect-free) complexes, where there is a similar amount of (0.85 $|e^-|$) of donation and back-donation. More interesting is that such effects explains why the uranyl ion tends to exhibit enhanced absorption for endhohedral complexes while for similar systems the dopant prefers to deabsorb (exit) the tube.

We have also studied aqueous complexes of Cm (III), U(VI), Np(VI) and Pu(VI) with OH^-.The effects of the aqueous solvent in the configuration preferences of these complexes have been investigated. The free energies of solvation were predicted using a self-consistent reaction-field model and a combined discrete-continuum model. Spectroscopic studies on many of these species are carried out by a fluorescence emission spectroscopy at Berkeley, by Professor Heino Nitsche's group, our experimental collaborators. Extensive *ab initio* calculations have been carried out to study equilibrium structures, vibrational frequencies, and bond characters of hydrated Cm(III) carbonates and hydroxide complexes in aqueous solution and the gas phase. The structures have been further optimized by considering long-range solvent effects as a polarizable continuum dielectric model. Our results reveal that it is necessary to include water molecules bound to the complex for proper treatment of the hydrated complex and the dielectric cavity. Structural reoptimization of the complex in a dielectric cavity seems inevitable to seek subtle structural variations in the solvent and to correlate with the observed spectra. The optimized structure of some of these complexes is not the same in the gaps phase and aqueous solution illustrating the importance of carrying out these computations in solution

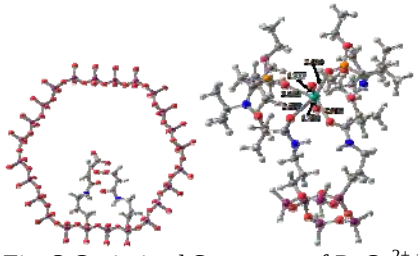

Fig. 3 Optimized Structures of PuO_2^{2+} bound to functionalized mesoporous silica with MAMAGS ligand.

We have carried out computational studies on actinide mesoporous material interactions in collaboration with ongoing experimental studies carried out by Profs Peidong Yang and H. Nitsche at Berkeley. As a representative we have shown our computed structures for plutonyl biding with mesoporous silica in Fig 3.

Electronic Structure & Spectroscopy of Subnano Silver & Gold Clusters.

We have carried out joint experimental-computational studies on gas-phase subnano silver clusters and gold clusters. Stimulated by the recent experimental luminescence spectra of Ag-Au alloy clusters obtained by our experimental collaborators at IIT, Madras, India, we worked on determining the possible structures for $Ag_7Au_6(SR)_9$ and $Ag_7Au_6(SR)_{10}$ theoretically by performing density functional calculations. The lowest energy structure of $Ag_7Au_6(SCH_3)_9$ has a Ag_7Au_6 core with initial symmetry of C_{3v} and the geometries and detailed bond lengths of the two lowest energy structures are shown in Figure 4. The lowest energy structure of $Ag_7Au_6(SCH_3)_{10}$ has a Ag_7Au_6 core with initial symmetry of C_{3v}, and the 2nd lowest energy structure has a Ag_7Au_6 core with initial symmetry of C_2, lying 0.151eV higher on the potential energy surface. The geometries and detailed bond lengths of the two lowest energy structures are shown in Figure 4.

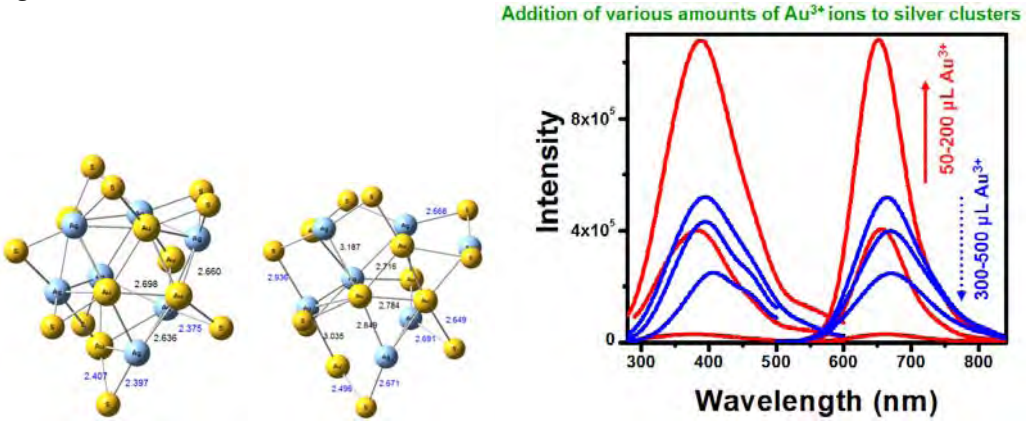

Figure 4: Lowest energy structure of $Ag_7Au_6(SCH_3)_9$ before and after optimization. Luminescence spectra of $Ag_7Au_6(SCH_3)_{10}$

Proposed Plan

We plan to continue our works on environmental actinide complexes and transition metal species. We are investigating Cm(III) and Bk(III) complexes with other ligands such as OH^- and CO_3^{2-} in collaboration with Professor Nitsche and his coworkers who are carrying out EXAFS and time-resolved x-ray fluorescence studies of such curium(III) complexes in solution. We would be continuing our recent exciting experimental-theory collaborations on actinide-nonmaterial interactions. We also propose to continue our work on subnano transition metal clusters with specific focus on spectroscopic properties, geometries, Gibbs Free energies in solutions and potential energy curves.

Select Publications from the DOE BES Grant

1. Z. Cao, Balasubramanian, K., Calvert, M., Nitsche, H., *Inorganic Chemistry* , 48(20):9700-14 (2009).
2. Z. Cao, Balasubramanian, K., J. Chem. Phys. **131**, 164504 (2009)
3. Cao, Z., Balasubramanian, *Journal of Physical Chemistry*, J Phys Chem A. 2009 Nov 12;113(45):12512-24.
4. M. Benavides-Gardia and K. Balasubramanian, "Structural Insights into the Binding of Uranyl with Human Serum Protein Apotransferrin-Structure and Spectra of Protein-Uranyl Interactions", ACS Chem Res Toxicol. (2009) Sep;22(9):1613-21
5. T. Simeon, K. Balasubramanian, and C. Welch, "Computational Studies of Interaction of In and In^{3+} with Stone-Wales Defect Single-Walled Carbon nanotubes", *J. Phys. Chem. Lett.*, 2010, 1 (2), pp 457–46
5. D. M. David Jaba Singh, T. Pradeep, K. Thirumoorthy and K. Balasubramanian, "Closed-cage Tungsten oxide Clusters in the Gas Phase", *J. Phys. Chem. A*, 2010, 114 (17), pp 5445–5452
7. Z. Cao, K. Thiumoorthy, and K. Balasubramanian, "Curium(III) hydroxide Complexes in Aqueous Solution", Submitted.
8. Y. Sun, U. B. Rao T. Pradeep, and K. Balasubramanian, "First principle studies of two luminescent molecular quantum clusters of silver, $Ag_7(H_2MSA)_7$ and $Ag_8(H_2MSA)_8$ based on experimental fluorescence spectra", JPC C(2011)

Influence of medium on radical reactions

David M. Bartels, Ireneusz Janik and Daniel M. Chipman
Notre Dame Radiation Laboratory, University of Notre Dame, Notre Dame, IN 46556
e-mail: bartels.5@nd.edu; ijanik@nd.edu; chipman.1@nd.edu

Program definition

This project pursues the use of radiolysis as a tool in the investigation of solvent effects in chemical reactions, particularly the free radicals derived from solvent which are copiously generated in the radiolysis excitation process. Most recently we have focused on radical reactions in high-temperature water, and some of these results are described below. The project has now evolved toward the particular study of solvent effects on reaction rates in supercritical (sc-)fluids where the fluid density becomes a primary variable. One proposed thrust will be the study of solvated electrons under these conditions. Others will focus on small radicals in supercritical water and CO_2. A theoretical component has also recently been joined with this project, which will be directed to support the analysis and interpretation of experimental results.

An anthropomorphic way to think about near-critical phenomena, is that the fluid is trying to decide whether it is a liquid or a gas. The cohesive forces between molecules that tend to form a liquid are just being balanced by the thermal entropic forces that cause vaporization. The result, on a microscopic scale, is the highly dynamic formation and dissipation of clusters and larger aggregates. The fluid is extremely heterogeneous on the microscopic scale. A solute in a supercritical fluid can be classified as either attractive or repulsive, depending on the potential between the solute and solvent. If the solute-solvent potential is more attractive than the solvent-solvent potential, the solute will tend to form the nucleus of a cluster. When the solute-solvent potential is repulsive, one might expect the solute to remain in a void in the fluid as the solvent molecules cluster together. Extremely large partial molal volumes are known for hydrophobic molecules in near-critical water, indicating an effective phase separation. Such variations in local density around the solute will have implications for various spectroscopies and for reaction rates.

The ultimate goal of our study is the development of a predictive capability for free radical reaction rates, even in the complex microheterogeneous critical regime. Our immediate goal is to determine representative free radical reaction rates in sc-fluid and develop an understanding of the important variables to guide development and use of predictive tools. Electron beam radiolysis of water (and other fluids) is an excellent experimental tool with which to address these questions. The primary free radicals generated by radiolysis of water, $(e^-)_{aq}$, OH, and H, are respectively ionic, dipolar, and hydrophobic in nature. Their recombination and scavenging reactions can be expected to highlight the effects of clustering (i.e. local density enhancements) and solvent microheterogeneity both in terms of relative diffusion and in terms of static or dynamic solvent effects on the reaction rates.

Recent Progress

Work has continued in the past year to carefully characterize properties and reactions of the OH radical in high temperature water. It was previously shown that the major UV absorption spectrum peak used to identify and monitor OH radical in liquid water is largely due to a novel "charge transfer from solvent transition" that occurs when OH is hemibonded to a water molecule. We have now computationally delineated the geometrical regions over which such hemibonding interactions are significant (see Figure 1). These regions are found to lie in a fairly narrow range of azimuthal angles, which adjoin the range in which more stable hydrogen bonding interactions are important, while extending over quite wide regions of O–O separation and tilt angle. In particular, significant hemibonding interactions can occur down to surprisingly short O–O distances, where the oscillator strength for the charge transfer transition becomes very large. These results will be used to design an improved force field for modeling the solvation of OH radical in water over a wide range of temperatures and pressures. This begins a longer range effort to simulate the reactions that radiolytically-produced radicals undergo in water, with a view toward interpreting and complementing current experimental investigations on water radiolysis.

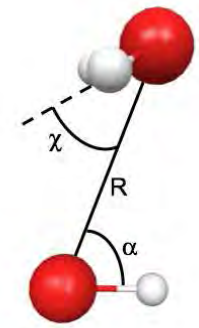

Figure 1. OH radical hemibonded to a water molecule, showing the azimuthal angle χ, the O–O distance R, and the tilt angle α. The hemibonding interaction is maximal at χ of 47°, as shown in the figure, where it is about half as strong as the hydrogen bonding interaction that is maximal at χ of 143°.

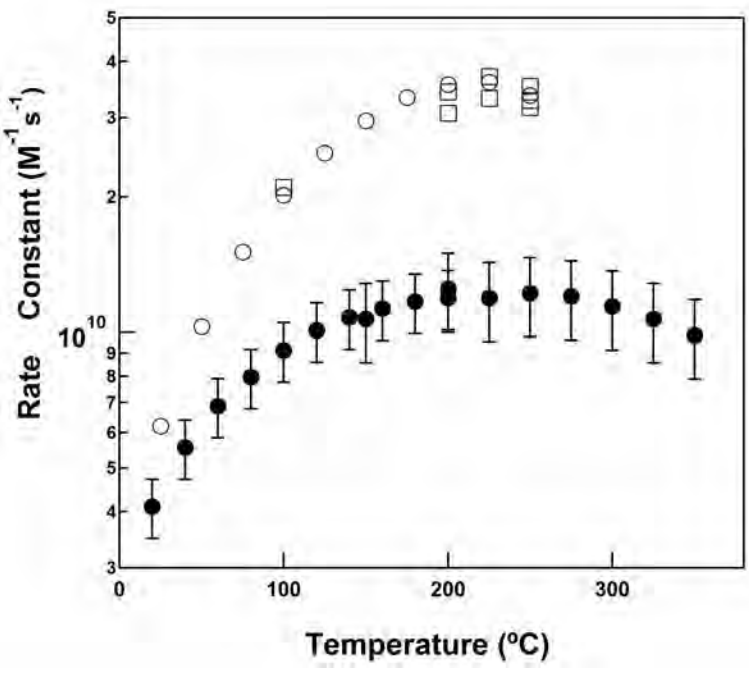

Figure 2: Temperature dependence of second order OH recombination reaction rates. Closed circles, OH + OH; Open circles CO_3- + OH from refit of literature data; Open squares CO_3^- + OH from this work.

The carbonate anion radical $\bullet CO_3^-$ is one of the most extensively studied inorganic radicals due to its ubiquitous nature in the environment, its relatively long lifetime, and its accessible absorption at 600nm. It is inevitably present in high temperature nuclear reactor

cooling loops. For such a well-known radical, the structure, acid/base properties, and recombination mechanism of $\bullet CO_3^-$ have remained controversial for a very long time. A study of the carbonate radical yield in pulse radiolysis of both carbonate and bicarbonate solutions at elevated temperature even suggested several years ago that the radical actually exists in a dimeric form, e.g. $\bullet(CO_3)_2^{3-}$.

The latter claim was based on an incomplete kinetic model. We have reanalyzed the published data and added some high temperature pulse radiolysis/transient absorption experiments of our own. At sufficiently high dose and/or sufficiently low scavenger concentration, the cross reaction (1)

$$\bullet OH + \bullet CO_3^- \rightarrow HOOCO_2^- \qquad (1)$$

cannot be ignored. A plot of rate constant vs. temperature for this reaction and for bimolecular recombination of OH radicals is shown in figure 2. Both reactions reach a limiting value near 200°C. The OH recombination is understood in terms of the entropic barrier or steric effect which limits its rate once diffusion is no longer a factor. It is suggested that a similar entropic barrier limits the rate constant for reaction (1) at high temperature. The results of our study would appear to resolve any remaining controversy over the properties of the $\bullet CO_3^-$ radical.

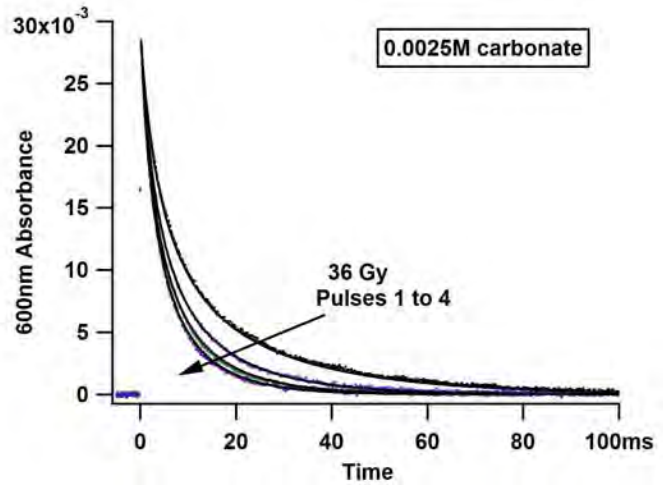

Figure 3. Decay of 600nm $\bullet CO_3^-$ absorbance in room temperature 0.0025M carbonate solution, following four consecutive 36 Gy radiolysis pulses. The effect of H_2O_2 and peroxymonocarbonate product buildup with each pulse is easily seen.

Surprisingly, the complete mechanism of second order self-recombination of $\bullet CO_3^-$ radicals has heretofore not been conclusively demonstrated. A pre-equilibrium between $\bullet CO_3^-$ and a short-lived dimer $C_2O_6^{2-}$ (reactions 2d, -2d) is strongly indicated based on the slightly negative activation energy for the overall recombination found below 300°C.

$$\bullet CO_3^- + \bullet CO_3^- \leftrightarrow C_2O_6^{2-} \qquad (2d, -2d)$$

Existing conductivity data and ab initio calculations we have performed are only consistent with production of CO_2 and CO_4^{2-} (peroxymonocarbonate dianion) from this dimer.

$$C_2O_6^{2-} \rightarrow CO_2 + CO_4^{2-} \qquad (2f)$$

However, there are several reports indicating deviation from pure second order decay, and conflicting reports on the ionic strength effect on recombination of the negatively charged radicals.

Figure 3 shows an experiment which carefully followed the decay of carbonate radical absorbance at 600nm out to 0.1 seconds after a series of 36Gy radiolysis pulses. Successive

radiolysis pulses clearly shorten the decay due to buildup of some product. The effect is too large to be ascribed to hydrogen peroxide, and can only be accounted for in terms of reaction of $\bullet CO_3^-$ with the peroxymonocarbonate HCO_4^- / CO_4^{2-} product . Detailed kinetic analysis allows us to determine the rate constant for this reaction and also to confirm a normal ionic strength effect for all of the species involved. The "almost second order" initial decay of the 600nm absorbance conceals several kinetic processes, which had produced conflicting claims in the literature.

Future Plans

New development of multi-channel transient absorption equipment and high temperature transient EPR coupled to pulse radiolysis is expected to come online within the next year. The EPR will enable the exploration of fundamental hydrogen atom and hydrated electron properties at elevated temperatures for the first time. The transient optical absorption will be applied in particular to record the spectrum of OH radical vs. temperature and density in high temperature water. These spectra will be analyzed using the ab initio tools already described, coupled to a realistic molecular dynamics modeling approach.

As of November 2010, elements of this subtask will be combined with parts of others reported elsewhere in these proceedings (Carmichael, *et al.*; LaVerne, *et al.*) in new initiatives pursuing the basic science underpinning fundamental advances in radiation chemistry and applications to nuclear energy and the biosciences.

Publications, 2008-2011

Bartels, D. M. (2009). "Comment on the possible role of the reaction $H^{\cdot} + H_2O \rightarrow H_2 + OH^{\cdot}$ in the radiolysis of water at high temperatures." Radiation Physics and Chemistry **78**(3): 191-194.

Chipman, D. M. (2011). "Hemibonding between Hydroxyl Radical and Water." Journal of Physical Chemistry A **115**(7): 1161-1171.

Elliot, A. J. and D. M. Bartels (2009). The Reaction Set, Rate Constants and g-Values for the Simulation of the Radiolysis of Light Water over the Range 20° to 350°C Based on Information Available in 2008. Chalk River, Canada, Atomic Energy of Canada, Ltd.

Hare, P. M., E. A. Price and D. M. Bartels (2008). "Hydrated electron extinction coefficient revisited." Journal of Physical Chemistry A **112**(30): 6800-6802.

Hare, P. M., E. A. Price, C. M. Stanisky, I. Janik and D. M. Bartels (2010). "Solvated Electron Extinction Coefficient and Oscillator Strength in High Temperature Water." Journal of Physical Chemistry A **114**(4): 1766-1775.

Haygarth, K. S., T. W. Marin, I. Janik, K. Kanjana, C. M. Stanisky and D. M. Bartels (2010). "Carbonate Radical Formation in Radiolysis of Sodium Carbonate and Bicarbonate Solutions up to 250 degrees C and the Mechanism of its Second Order Decay." Journal of Physical Chemistry A **114**(5): 2142-2150.

Stanisky, C. M., D. M. Bartels and K. Takahashi (2010). "Rate constants for the reaction of hydronium ions with hydrated electrons up to 350 °C." Radiation Physics and Chemistry **79**(1): 64-65.

Surface Chemical Dynamics

N. Camillone III,[a] A.L. Harris,[b] and M. G. White[a]
Brookhaven National Laboratory, Chemistry Department, Building 555, Upton, NY 11973
(nicholas@bnl.gov, alexh@bnl.gov, mgwhite@bnl.gov)

1. Program Scope

This program focuses on fundamental investigations of the dynamics, energetics and morphology-dependence of thermal and photoinduced reactions on planar and nanostructured surfaces that play key roles in energy-related catalysis and photocatalysis. Laser pump-probe methods are used to investigate the dynamics of interfacial charge and energy transfer that lead to adsorbate reaction and/or desorption on metal and metal oxide surfaces. State- and energy-resolved measurements of the gas-phase products are used to infer the dynamics of product formation and desorption. Time-resolved correlation techniques follow surface reactions in real time and are used to infer the dynamics of adsorbate–substrate energy transfer. Measurement of the interfacial electronic structure is used to investigate the impact of adsorbate–surface and interadsorbate interactions on molecular orbital energies. New capabilities to synthesize and investigate the surface chemical dynamics of arrays of supported metal nanoparticles on oxide surfaces include the deposition of size-selected clusters from ion beams as well as solution-phase synthesis and deposition of narrow-size-distribution nanometer-scale particles.

2. Recent Progress

Ultrafast Investigations of Surface Chemical Dynamics. The long-term goal of this aspect of the project is to follow in real time the evolution of surface chemical processes. Of particular interest are the links between substrate electronic excitations and surface reactivity. Recent experiments and theory have begun to show that diabatic processes cannot be ignored even in descriptions of thermal processes, thus it has become increasingly important to understand the role that energy transport due to formal violation of the Born-Oppenheimer approximation plays in surface chemical reactivity.

To understand the dynamics of energy flow, we are working to time-resolve the fundamental steps of surface chemical transformations on the femtosecond timescale and to investigate how the dynamics is impacted by surface morphology and electronic structure. We employ ~100 fs near-IR laser pulses to inject energy into adsorbate–substrate complexes, initiating reactions by substrate-mediated processes such as DIMET (desorption induced by multiple electronic transitions) and heating via electronic friction. Time-resolved monitoring of the complex is achieved by a two-pulse correlation (2PC) method wherein the surface is excited by a “pump” pulse and a time-delayed “probe,” and measurement of the product yield as a function of the delay reports on the energy transfer rate. We have employed this approach to investigate the dynamics of energy transfer in the desorption of both weakly and strongly-chemisorbed species (O_2 and CO) and in a bimolecular reaction ($O + CO \rightarrow CO_2$) on the surface of Pd.

We are currently laying the groundwork for extending this 2PC method to the investigation of desorption and reaction dynamics on small (~1-nm diameter) metal nanoparticles supported on oxide surfaces. These systems will serve as more realistic model catalysts surfaces and provide the opportunity to explore the size-dependence of surface reaction dynamics in the size regime corresponding to the metal to non-metal transition. When supported on a wide band gap metal oxide the nanoparticles are expected to be electronically isolated to some degree, enabling us to address fundamental questions regarding the size-dependence of adsorbate–surface energy transfer and reaction dynamics.

The first step in this direction, nanoparticle synthesis, is well underway. We are developing a protocol involving segregation and reduction of a metal salt [$Pd(OAc)_2$] in the hydrophilic core of inverse micelles of an amphiphilic diblock copolymer [polystyrene-b-poly(4-vinylpyridine)] in an organic solvent

[a] Principal Investigator; [b] Collaborating Investigator

(toluene). The resulting nanoparticles are transferred to a solid support by spin or dip coating. This approach yields high monodispersity and also allows, to some extent, for independent control over nanoparticle size and interparticle distance through control of reaction times and judicious choice of the polymer block lengths. Figure 1 shows a non-contact atomic force microscope (NC-AFM) image of a Pd nanoparticle array supported on rutile TiO_2(110). The particles exhibit a narrow size distribution—the height is 1.15 nm ± 0.25 nm, fwhm—and sit on a pseudo-hexagonal lattice with a narrow distribution of interparticle distances—42 nm ± 5 nm, fwhm.

Significantly, preliminary thermal treatment studies indicate that these arrays are stable with respect to sintering up to at least 670 K. Such thermal stability is critical to planned thermal and photoinduced reaction studies. Surface chemical analysis of these arrays indicates the presence of carbon and palladium oxide, and we are currently working to understand the source of these impurities and eliminate them. These investigations involve multi-technique characterization—NC-AFM, Auger electron spectroscopy, X-ray photoelectron spectroscopy and temperature-programmed desorption—of both bare and Pd-nanoparticle-covered TiO_2(110).

In addition, we have recently completed instrumentation upgrades including installation of a high-pulse-energy (~4 mJ) Ti:Sapphire amplifier and a high-sensitivity quadrupole mass spectrometer. The latter, in particular, will enable detection of ultrafast photoinduced desorption from nanoparticle arrays by enhancing the signal-to-noise ratio to compensate for losses due to reduction in the effective sample area to ~10% or less that in our previous studies of planar bulk surfaces.

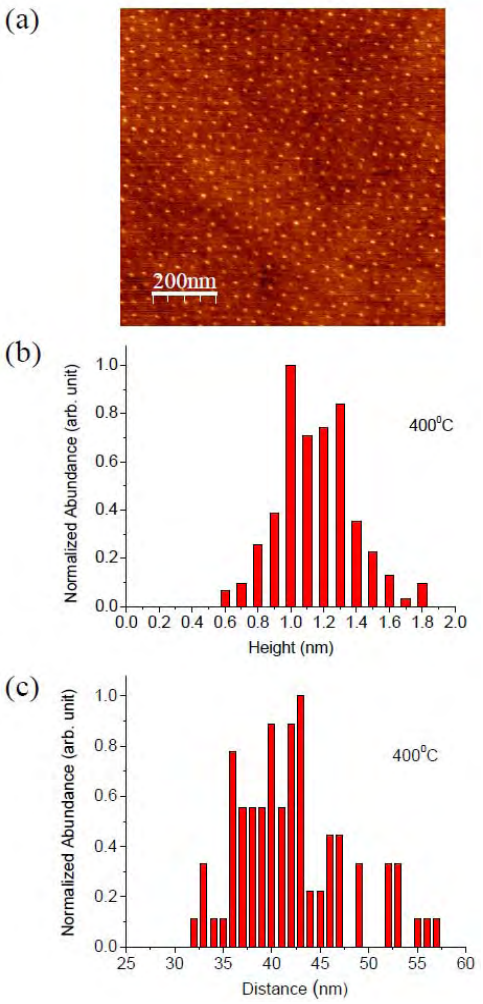

Figure 1. (a) NC-AFM images of Pd nanoparticles on TiO_2(110) after thermal treatment to 670 K. Corresponding height (b) and interparticle distance (c) distributions.

Pump-Probe Studies of Photodesorption and Photooxidation on TiO_2(110) Surfaces. Measurements of the final state properties of gas-phase products are being used as a probe of the mechanism and dynamics of photodesorption and photooxidation on well-characterized TiO_2(110) surfaces. This work is motivated by the widespread use of titania in technological applications where UV photooxidation is used for the degradation of organic materials. Our initial studies on the photodesorption of O_2 on reduced surfaces of TiO_2(110) attempted to address long standing questions about which O_2 binding sites on the reduced TiO_2(110) surface are photoactive, and how these are affected by the presence of surface defects and temperature annealing. Photooxidation studies have focused on the small organic carbonyls, acetaldehyde (CH_3CHO), acetone (CH_3COCH_3), 2-butanone ($CH_3CH_2COCH_3$), and acetophenone ($C_6H_5COCH_3$) adsorbed on a reduced TiO_2(110) surface. Recent work by Henderson (PNNL) showed that small ketones are photochemically inactive in the absence of oxygen, but when co-adsorbed with oxygen form a thermally activated intermediate which is postulated to be a diolate species. The photoactive species (diolate or ketone) decompose via direct ejection of an alkyl radical into the gas phase, *e.g.*, a methyl radical ($CH_3^{\bullet}$) from acetone. Pump-probe measurements in our laboratory show that the velocity distributions for ejection of the methyl radical ($CH_3^{\bullet}$) from all molecules studied consist of a “slow” and

"fast" component suggesting at least two pathways for methyl ejection. The average kinetic energy of the "slow" channel is similar for all the molecules studied and has an overall average of 30 ± 5 meV, which is tentatively assigned to trapping-desorption of methyl radicals on the cold titania surface (105-200 K). The average kinetic energies of the "fast" channels are significantly higher, with values that range from 0.16 eV for acetaldehyde to 0.25 eV for acetophenone. Moreover, the "fast" kinetic energies scale with the mass of remaining surface diolate fragment, e.g., acetate from acetone, suggesting that a simple recoil model can account for observed trend with molecular size. These observations support an assignment of the "fast" channel to prompt fragmentation of the excited diolate following charge transfer to a photoexcited hole. State-resolved measurements of the methyl internal energy distributions (vibration, rotation) using (2+1) REMPI are currently underway to gain more insight into the hole-induced fragmentation dynamics.

Two-Photon Photoemission Studies of Interfacial Electronic Structure. We are currently using a tunable ultrafast laser system for performing two-photon photoemission (2PPE) measurements for probing the electronic structure and hot-electron dynamics of molecules and size-selected clusters deposited on surfaces. The strength of 2PPE is its ability to probe both the occupied and unoccupied resonant states of the adsorbate (cluster) and surface, and explore the time evolution of photoexcited states at the interface. One of our current projects involves the combination of 2PPE with low temperature STM (at BNL's Center for Functional Nanomaterials) to probe the valence band structure and morphology of phenyl isocyanides on a Au(111). Aromatic isocyanides have attracted widespread interest in molecular electronics applications because the N≡C triple bond is expected to act as an effective conductance bridge by connecting pπ orbitals of aromatic molecules with dπ orbitals of the metal contact. Initial studies focused on phenyl diisocyanide (PDI; C≡N–C_6H_4–N≡C) adsorbed on Au(111), which has been the subject of previous theoretical studies and experimental conductance measurements. The key findings of our 2PPE experiments are the observations of a significant decrease in the work function and the appearance of a new photoemission peak when a PDI/Au(111) surface dosed at 90 K is annealed to 300 K. Low temperature STM measurements show that the change in electronic structure is correlated with a change in PDI ordering. As shown in Figure 2, once annealed, the PDI molecules self-assemble into one-dimensional chains extending over the Au(111) terraces. These one-dimensional chains are composed of alternating small and large spots, whose spacing and height are consistent with a recently proposed model in which chains of PDI molecules are held together by Au adatoms released from the surface. The 2PPE spectrum associated with the PDI chains (see Figure 2) exhibits two features corresponding to occupied (HOMO) and unoccupied (LUMO) states with binding energies of 0.87 eV below and above E_F, respectively. The relatively large $|\text{LUMO} - E_F|$ energy gap derived from 2PPE spectra suggests that the PDI/Au system has a relatively high barrier for electron transmission. Further studies using biphenyl diisocyanide (BPDI) are currently underway to understand the possible role of Au adatoms in molecular chain formation.

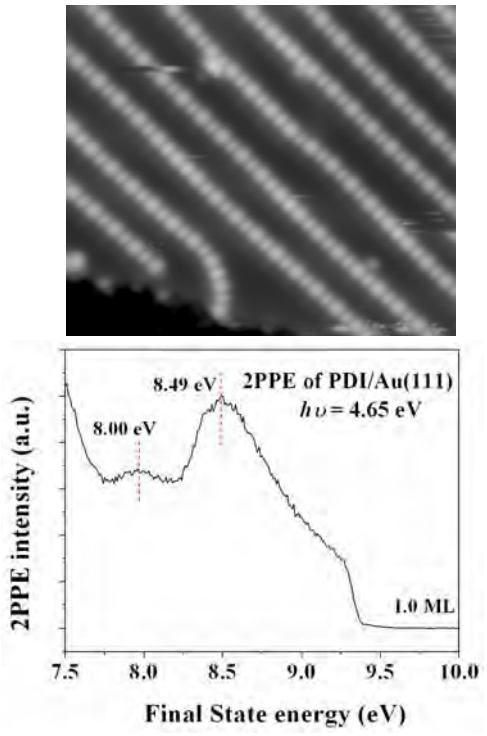

Figure 2. Top: STM image of PDI/Au(111) surface after annealing to RT. Image size 17.5nm× 14.8nm. Bottom: 2PPE spectrum of PDI/Au(111) surface after annealing to RT.

Two-photon photoemission is also being used to study the valence band structure of supported metal compound clusters as a function of size and composition. Current efforts are focused on Mo_xS_y clusters deposited on a Al_2O_3 thin film surface, which we have been studying as model nanocatalysts for desulfurization reactions. Previous experiments and theory have shown that the gas-phase Mo_xS_y clusters (cation and neutral) exhibit HOMO-LUMO "band-gaps" that vary sharply with size and stoichiometry, and we are interested in correlating such information with the structure and reactivity of clusters deposited onto different supports. The clusters are prepared in a gas-phase sputtering source and then mass-selected and deposited at low energy ("soft-landed") onto an Al_2O_3 thin film. Key to these experiments is the ability to limit photoemission from the support by using materials with wide band gaps and high work functions whose valence bands are too deep to ionize using low energy photons. Initial 2PPE results for Mo_xS_y (x/y: 2/6, 4/6, 5/7, 6/8, 7/10) clusters on Al_2O_3/NiAl(110) showed size-dependent local work functions which are sensitive to cluster coverage. Variations of the work function are indicative of charge transfer at the cluster-oxide interface, and were used to derive effective dipole moments for each cluster. Extensions of this work to the TiO_2(110) surface are currently in progress.

3. Future Plans

Our planned work develops three interlinked themes: (i) the chemistry of supported nanoparticles and nanoclusters, (ii) the exploration of chemical dynamics on ultrafast timescales, and (iii) the photoinduced chemistry of molecular adsorbates. The investigations are motivated by the fundamental need to connect chemical reactivity to chemical dynamics in systems of relevance to catalytic processes—in particular metal and metal-compound nanoparticles and nanoclusters supported on oxide substrates. They are also motivated by fundamental questions of physical changes in the electronic and phonon structure of nanoparticles and their coupling to adsorbates and to the nonmetallic support that may alter dynamics associated with energy flow and reactive processes.

Ultrafast photoinduced reaction experiments investigating the dynamics of molecular desorption from and reactions on nanoparticles are aimed at developing a fundamental understanding of the changes in surface reaction dynamics as the size of the metal substrate material is reduced from macroscopic (planar bulk surfaces) to the nanoscale. Size-dependent chemical dynamics will also be the focus of experiments using our cluster beam deposition instrument to prepare a range of supported, size-selected nanoclusters for structure and reactivity studies. Ultrafast 2PPE investigations will provide insight into the electronic structure and dynamics of the nanoclusters and adsorbate resonances involved in chemistry at their surfaces. In addition, future energy- state- and time-resolved pump-probe work will be aimed at elucidating molecular photooxidation mechanisms on titania and other oxide photocatalysts.

DOE-Sponsored Research Publications (2009–2011)

1. Two-Photon Photoemission Study of Thiophene Adsorbed on Au(111), J. Zhou, Y. Yang, N. Camillone and M. G. White, *J. Phys. Chem. B* **114**, 13670-13677 (2010).
2. Fundamental Studies of Methanol Synthesis from CO_2 Hydrogenation on Cu(111), Cu Clusters and Cu/ZnO(0001), Y. Yang, J. Evans, J. A. Rodriguez, M. G. White and P. Liu, *Phys. Chem. Chem. Phys.*, **12**, 9909-9917 (2010).
3. Methanol Synthesis from H_2 and CO_2 on a Mo_6S_8 Cluster: A Density Functional Study, P. Liu, Y. M. Choi, Y. Yang and M. G. White, *J. Phys. Chem. A*, **114**, 3888–3895 (2010).
4. Hydrogenation of Carbon Dioxide by Water: Alkali-Promoted Synthesis of Formate, F. M. Hoffmann, Y. Yang, J. Paul, M. G. White, J. Hrbek, *J. Phys. Chem. Lett.* **1**, 2130-2134 (2010).
5. Dynamics of O_2 Photodesorption from TiO_2(110), D. Sporleder, D. Wilson and R. J. Beuhler and M. G. White, *J. Phys. Chem. C*, **113**, 13180–13191 (2009).

ELECTRON-DRIVEN PROCESSES IN CONDENSED PHASES

PRINCIPAL INVESTIGATORS

I Carmichael (*carmichael.1@nd.edu*)
DM Bartels, DM Chipman, I Janik, JA LaVerne
Notre Dame Radiation Laboratory, University of Notre Dame, Notre Dame, IN 46556

SCOPE

Fundamental physicochemical processes in water radiolysis are probed in an experimental program measuring spur kinetics of key radiolytic transients at elevated temperatures and pressures using a novel laser-based detection system with interpretation supported by computer simulations. Related experimental and computational studies focus on the electronic excitation of liquid water, important aqueous radiolytic species, and the significance and mechanism of dissociative electron attachment in the liquid. Radiolytic decay channels in nonaqueous media are investigated, both experimentally, with product analysis under γ and heavy-ion irradiation and transient identification under pulse radiolysis, and theoretically, via kinetic track modeling and electronic structure calculations.

PROGRESS AND PLANS

Recent experiments at the Synchrotron Radiation Center of University of Wisconsin have revealed a red shift in the peak of the vacuum ultraviolet absorption of liquid water as the density is decreased in the supercritical regime (by decreasing the pressure at fixed temperature) in contrast to previous literature reports. Preliminary results also show a gradual shift to the blue from the monomer spectrum (unchanged at 386°C from that measured at room temperature) concomitant with the formation of dimers, trimers, etc, as the density is increased in accord with theoretical predictions. Further progress requires the design and construction of a customized vacuum monochromator capable of withstanding both the high intensity VUV beam from the synchrotron and the level of vacuum required to minimize light attenuation over the long optical pathlengths. This highly-customized device will enable data collection in supercritical water systems over the crucial wavelength region 120–300 nm. The new optical monochromator design was optimized using the program SHADOW (Nanotech-Wisconsin, University of Wisconsin), a general-purpose ray tracing code specifically designed for synchrotron radiation beamline optics. The program was used to simulate the beam in order to predict the minimum spot size, beam shape, and, in conjunction with theoretical calculations, the possible increases in flux density for a variety of optics settings.

Benchmark calculations have been performed on the H_2O dimer using coupled cluster theory with large basis sets to characterize excited states up to about 10 eV, with a view toward obtaining a better understanding the effects of hydrogen bonding on the ultraviolet absorption spectrum of liquid water. It is found that the two lowest excited states are generally well localized on one monomer or the other, their energy separation depending mainly on where the valence hole is created and only to a lesser degree on perturbation of the excited electron density distribution by the neighboring water molecule. These results suggest that the lowest excitation energies in clusters and liquid water can be associated with broken acceptor hydrogen bonds, which provide energetically favorable locations for formation of a valence hole. Higher valence excited states of the dimer typically involve delocalization of the valence hole and/or delocalization of the excited electron and/or charge transfer (see Figure). Two of the higher valence excited states that involve delocalized valence holes always have particularly large oscillator strengths. Due to the pervasive delocalization and charge transfer, it is suggested that

most condensed phase water valence excitations intimately involve more than one water molecule and, as a consequence, will not be adequately described by models based on perturbation of free water monomer states. The benchmark calculations are further used to evaluate a series of representative semilocal, global hybrid, and range separated hybrid functionals used in efficient time-dependent density functional methods. It is shown that such an evaluation is only meaningful when comparison is made at or near the complete basis set limit of the wave function based reference method. A functional is found that quantitatively describes the two lowest excitations of water dimer and also provides a semiquantitative description of the higher energy valence excited states. This functional will be used in further studies on the absorption spectrum of large water clusters and of condensed phase water.

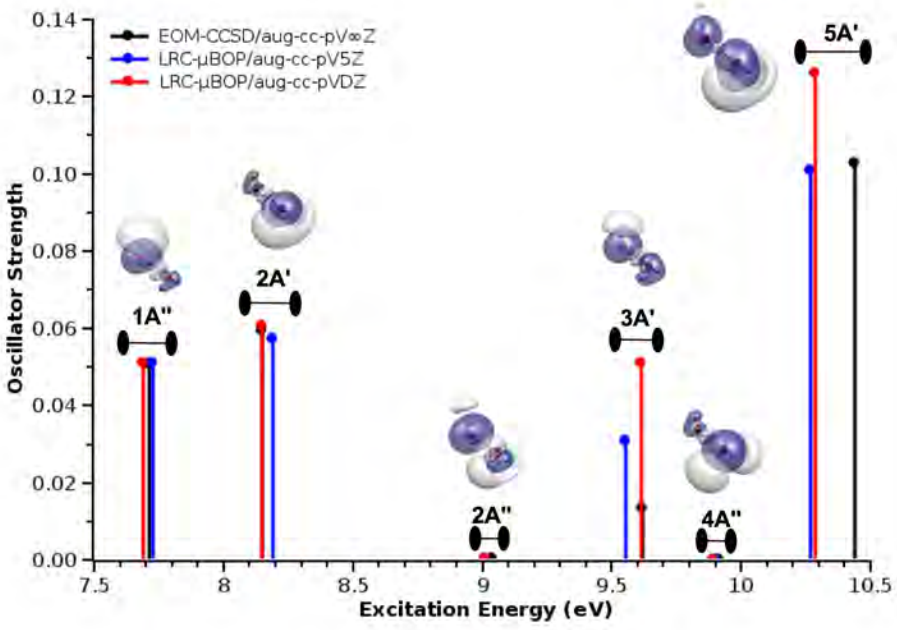

Water dimer excitation energies from CCSD and DFT methods. Plots show the density differences (depletion in blue) induced upon excitation

In previous investigations, low-LET radiolytic yields of hydrated electrons (e^-_{aq}) in supercritical water were determined using the scavenger N_2O, which gives the easily-measured stable product N_2:

$$e^-_{aq} + N_2O \rightarrow N_2 + {}^{\bullet}OH + OH^-_{aq} \qquad (1)$$

Phenol was added to the water to scavenge ${}^{\bullet}H$ atoms, some of which could otherwise convert to solvated electrons (equilibrium 3) and contribute to the observed N_2 yield.

$$PhOH + {}^{\bullet}H \rightarrow {}^{\bullet}HPhOH \qquad (2)$$

$${}^{\bullet}H + OH^-_{aq} \rightleftharpoons e^-_{aq} + H_2O \qquad (3)$$

It was also found that N_2O decomposes to some extent on the hot metal walls of the flow system at 380°C and 400°C. This thermal component could be subtracted out in high-dose-rate accelerator experiments thanks to a short dwell time, but in low-dose-rate nuclear reactor experiments (for neutron radiolysis measurements) the thermal reaction is a serious complication. To overcome this issue we explored the use of SF_6 as a specific scavenger for the hydrated electron. SF_6 is thermally stable at supercritical temperatures, and is known to react with e^-_{aq} and then hydrolyze, producing six fluoride ions for every electron:

$$e^-_{aq} + SF_6 \rightarrow {}^{\bullet}SF_5 + F^-_{aq} \quad (4a)$$

$${}^{\bullet}SF_5 + 4H_2O \rightarrow (HSO^-_3)_{aq} + 6H^+_{aq} + 5F^-_{aq} + {}^{\bullet}OH \quad (4b)$$

The fluoride can be conveniently measured with a fluoride-selective electrode. Acid buildup can be remedied by adding neutralizing base. Phenol is added to quench $^{\bullet}H$ as above.

At room temperature some curvature of the yield vs. dose plot is seen in neutral solutions, due to hydrofluoric acid buildup. Addition of 0.001m KOH recovers a linear plot. In alkaline supercritical water at 380°C, the yield plot appears linear except near zero dose. Numerous experiments were performed to conclude that this curvature represents a chain reduction of the SF_6 by a radical derived from phenol in alkaline solution. Surprisingly, linear results and zero intercepts were obtained in neutral-pH supercritical water. There is no chain reaction and no problem of the hydrofluoric acid buildup. HF is a weak acid at room temperature, and much weaker still in the low-dielectric supercritical water. Also the reaction rate of e^-_{aq} with HF is much slower than with the hydrated proton H^+_{aq}. Neutral-pH SF_6 solutions can thus be confidently used for low-dose neutron radiolysis experiments.

Monte Carlo diffusion kinetic modeling of the hydrogen atom ($^{\bullet}H$) yields in irradiated aqueous formate solutions exhibits marked discrepancies from experimental results. A new channel for $^{\bullet}H$ formation is indicated. One possibility under investigation is the competitive combination of electrons with protonated water molecules formed by reaction of the initial radiolytic hole (H_2O^+). Various parameters related to the precursors of $^{\bullet}H$ are being explored in these simulations to optimize experimental observations and gain sharper insight into the fast processes involving excited states in the radiolysis of water. As with benzene and pyridine, experiments with heavy ions show marked increases in H_2 yields from aniline and toluene with increasing LET. These data suggest that, despite variations of a factor of four at low LET, there is a common high LET liming yield of H_2 for all of these compounds. On the other hand, the dimer yields from these aromatic liquids show no similar LET dependences. The biphenyl and bibenzyl yields from benzene and toluene, respectively, are very nearly independent of LET. In both of these compounds, the molecular radical adds to a medium molecule to give a dimer radical that ultimately decomposes to the dimer by the loss of an H atom. The addition process is unimolecular and LET independent. The yields of dimer products from both aniline and pyridine decreases with increasing LET showing that their precursors to dimer formation are being involved in intratrack reactions. The exact nature of these precursors is still under investigation, but is thought to be a molecule in the triplet excited state. Triplet-triplet annihilation reactions increase in probability with increasing LET, thereby decreasing the amount of precursors available for dimer formation.

Preliminary studies at cryotemperatures using high concentrations of nitrate, an efficient scavenger for both presolvated and hydrated electrons have revealed a remarkable ability to quench specific damage to disulfide bonds in protein crystals during high-dose irradiation with X-rays. For the first time, the radiation chemistry undergone by the protecting nitrate ions is clearly visible in the fitted electron density maps.

As of November 2010, elements of this subtask will be combined with parts of others reported elsewhere in these proceedings (Bartels, *et al.*; LaVerne, *et al.*) in new initiatives pursuing the

basic science underpinning fundamental advances in radiation chemistry and applications to nuclear energy and the biosciences.

DOE SUPPORTED PUBLICATIONS

1. De la Mora E.; Carmichael I.; Garman E.F. *J. Synchrotron Radiat.* **2011**, *18*, in press. Effective scavenging at cryotemperatures: further increasing the dose tolerance of protein crystals.
2. do Couto P.C.; Chipman D.M. *J. Chem. Phys.* **2010**, *132*. Insights into the UV spectrum of liquid water from model calculations.
3. Dziewinska K.M.; Peters A.M.; LaVerne J.A.; Martinez P.; Dziewinski J.J.; Pugmire D.L.; Flores H.G.; Trujillo S.M.; Rajesh P. *IOP Conf. Ser. Mater. Sci. Eng.* **2010**, *9*, 012932. Selection and evaluation of a new Pu density measurement fluid.
4. Haygarth K.; Bartels D.M. *J. Phys. Chem. A* **2010**, *114*, 7479-84. Neutron and β/γ radiolysis of water up to supercritical conditions. II. SF_6 as a scavenger for hydrated electron.
5. Haygarth K.; Janik D.; Janik I.; Bartels D.M. *J. Phys. Chem. A* **2010**, *114*, 5034. Neutron and β/γ radiolysis of water up to supercritical conditions. I. β/γ Yields for H_2,$H^{\bullet}$ atom, and hydrated electron.
6. Hu X.; Zhang W.; Carmichael I.; Serianni A.S. *J. Amer. Chem. Soc.* **2010**, *132*, 4641-52. Amide *cis-trans* isomerization in aqueous solutions of *N*-formyl-D-glucosamine and *N*-acetyl-D-glucosamine: Chemical equilibria and exchange kinetics.
7. Lefticariu L.; Pratt L.M.; LaVerne J.A.; Schimmelmann A. *Earth and Planet. Sci. Lett.* **2010**, *292*, 57-67. Anoxic pyrite oxidation by water radiolysis products - a potential source of biosustaining energy.
8. Schmitt C.; LaVerne J.A.; Robertson D.; Bowers M.; Lu W.; Collon P. *Nucl. Inst. Meth. Phys. Res. A* **2010**, *268*, 1551-7. Equilibrium charge state distributions for boron and carbon ions emerging from carbon and aluminum targets.
9. Atinault E.; De Waele V.; Fattahi M.; LaVerne J.A.; Pimblott S.M.; Mostafavi M. *J. Phys. Chem. A* **2009**, *113*, 949-51. Aqueous solution of UCl_6^{2-} in O_2 saturated acidic medium: An efficient system to scavenge all primary radicals in spurs produced by irradiation.
10. Barker A.I.; Southworth-Davies R.J.; Paithankar K.S.; Carmichael I.; Garman E.F. *J. Synchr. Radiat.* **2009**, *16*, 205-16. Room temperature scavengers for MX: Increased lifetimes and modified dose dependence of the intensity decay.
11. Chipman D.M. *J. Chem. Phys.* **2009**, *131*, 014103. Vertical electronic excitation with a dielectric continuum model of solvation including volume polarization. I. Theory.
12. Chipman D.M. *J. Chem. Phys.* **2009**, *131*, 014104. Vertical electronic excitation with a dielectric continuum model of solvation including volume polarization. II. Implementation and applications.
13. Dziewinska K.M.; Peters A.M.; LaVerne J.A.; Martinez P.; Dziewinski J.J.; Davenhall L.; Rajesh P. *Radiochim. Acta* **2009**, *97*, 213-7. In search for an optimum plutonium density measurement fluid.
14. LaVerne J.A.; Ryan M.R.; Mu T. *Radiat. Phys. Chem.* **2009**, *78*, 1148-52. Hydrogen production in the radiolysis of bromide solutions.
15. Lewandowska A.; Hug G.L.; Hörner G.; Carmichael I.; Kazmierczak F.; Marciniak B. *Chem. Phys. Lett.* **2009**, *473*, 348–53. Chiral discrimination in the hydrogen-atom transfer between tyrosine and benzophenone in rigid peptides.
16. Schmitt C.; LaVerne J.A.; Robertson D.; Bowers M.; Lu W.; Collon P. *Phys. Rev. A* **2009**, *80*, 052711. Equilibrium mean charge states for low Z ions at ≤ 1 MeV/u in carbon.
17. Strzelczak G.; Janeba-Bartoszewicz E.; Carmichael I.; Marciniak B.; Bobrowski K. *Res. Chem. Intermed.* **2009**, *35*, 507–17. Electron paramagnetic resonance (EPR) study of γ-radiation-induced radicals in 1,3,5-trithiane and its derivatives.
18. Tarabek P.; Liu S.; Haygarth K.; Bartels D.M. *Radiat. Phys. Chem.* **2009**, *78*, 168–72. Hydrogen gas yields in irradiated room temperature ionic liquids.
19. Watson C.; Janik I.; Zhuang T.; Charvátová O.; Woods R.J.; Sharp J.S. *Anal. Chem.* **2009**, *81*, 2496-505. Pulsed electron beam water radiolysis for sub-microsecond hydroxyl radical protein footprinting.
20. Yang H.; Wehe D.K.; Bartels D.M. *Nucl. Instru. Methods in Phys. Res. A* **2009**, *598*, 779-87. Spectroscopy of high rate events during active interrogation.

Theory of Dynamics of Complex Systems

David Chandler

Chemical Sciences Division, Lawrence Berkeley National Laboratory
and
Department of Chemistry, University of California, Berkeley CA 94720

chandler@berkeley.edu

DOE funded research in our group concerns the theory of dynamics in systems involving large numbers of correlated particles. Glassy dynamics is a quintessential example. Here, dense molecular packing severely constrains the allowed pathways by which a system can rearrange and relax. The majority of molecular motions that exist in a structural glass former are trivial small amplitude vibrations that couple only weakly to surrounding degrees of freedom. In contrast, motions that produce significant structural relaxation take place in concerted steps involving many particles, and as such, dynamics is characterized by significant heterogeneity in space and time. Our recent contributions to this topic have established that these heterogeneities are precursors to a non-equilibrium phase transition, and that this transition underlies the glass transition observed in laboratory experiments [4,8].[1] We have also shown that relaxation leading up to this transition exhibits a surprising degree of universality [3,9]. Theory on this topic involves complicated esoteric mathematical methods, yet we have been able to produce a review of its essential concepts [7] that should be accessible to a broad audience of chemists and physicists.

Liquid interfacial dynamics is another important example, and here too the Chandler Group has made several new contributions. Much of this latest work is based upon two advances: i. a general and efficient procedure for identifying instantaneous interfaces from molecular coordinates [6], and ii. a generalization of umbrella sampling methods for collecting statistics on rare but important density fluctuations [5,12]. Armed with these techniques, work is underway characterizing pathways of water evaporation (an example of which is illustrated in the top panel of the Figure), the structure and dynamics of water at a Pt surface (lower-right panel), and the structure and dynamics of water at an oily surface (lower-left panel).

An insightful perspective on the nature of hydrophobic effects, created in the Chandler Group's work over the last decade, focuses on the role of interfacial fluctuations in dynamics and forces of assembly. Quantitative detail on this perspective is found in their recent simulation studies [5,11]. These studies were made possible by the developments noted in the previous paragraph. The principal effects of interfacial fluctuations can be captured with coarse-grained modeling, as illustrated in Publications [2] and [11]. The

[1] Numbers in square brackets refer to papers in the list of Recent DOE Supported Research Publications.

fact that this understanding can be used to formulate a quantitatively accurate and computationally convenient theory of solvation and hydrophobic effects is established for the first time in Publication [10]. This paper, which for two months running is the most downloaded paper in the *Journal of Chemical Physics*, provides the tools that we plan to use in the near future to model self assembly dynamics in complex aqueous solutions.

Also for that near future, we will attend to two additional areas of research. In one, we aim to develop transition path sampling algorithms for designing efficient self-assembly systems. In effect, these algorithms will be random walks in the joint space of possible models and trajectories with the purpose of discovering optimized components and conditions for the self-assembly of desired target structures. In the other area, we wish to use molecular dynamics, electronic structure and non-adiabatic dynamics to significantly extend our earlier efforts [1] to understand water and water chemistry at extended metal and semi-conductor surfaces. The ultimate goal will be the creation of theoretical methods capable of treating classes of chemical dynamics catalyzed by nano-scale structures.

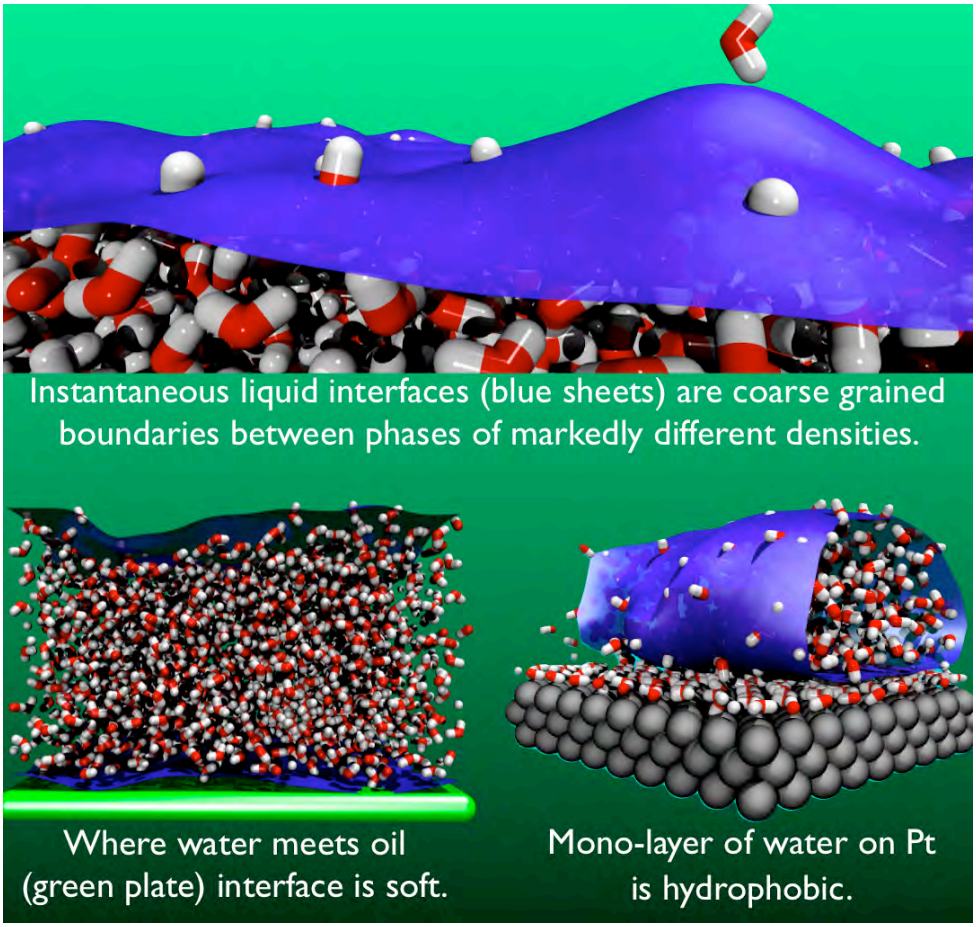

Figure: Snap shots from molecular dynamics trajectories showing some of the systems examined by the Chandler research group in their DOE funded studies of liquid interfaces.

Recent DOE Supported Research Publications

1. Willard, A.P., S.K. Reed, P.A. Madden, and D. Chandler, "Water at an electrochemical interface - a simulation study," *Faraday Discuss.* **141**, 423-441 (2009)

2. Willard, A.P., and D. Chandler, "Coarse Grained Modeling of The Interface Between Water and Heterogeneous Surfaces," *Faraday Discuss.* **141**, 209-220 (2009).

3. Elmatad, Y.S., D. Chandler, and J.P. Garrahan, "Corresponding States of Structural Glass Formers", *J. Phys. Chem. B* **113**, 5563-5567 (2009).

4. Hedges, L. O., R. L. Jack, J. P. Garrahan and D. Chandler, "Dynamic order-disorder in atomistic models of structural glass formers," *Science* **323**, 1309-1313 (2009).

5. Patel, A. J., P. Varilly and D. Chandler, "Fluctuations of water near extended hydrophobic and hydrophilic surfaces," *J. Phys. Chem. B, **114***, 1632–1637 (2010).

6. Willard, A.P. and D. Chandler, "Instantaneous Liquid Interfaces," *J. Phys. Chem. B, **114***, 1954–1958 (2010).

7. Chandler, D. and J.P. Garrahan, "Dynamics on the Way to Forming Glass: Bubbles in Space-time" *Annu. Rev. Phys. Chem*., **61**, 191-217 (2010).

8. Elmatad, Yael S., R.L. Jack, J.P. Garrahan and D. Chandler, "Finite-temperature critical point of a glass transition," *Proc. Natl. Acad. Sci. USA* **107,** 12793-12798 (2010).

9. Elmatad, Y.S., D. Chandler, and J.P. Garrahan, "Corresponding States of Structural Glass Formers II", *J. Phys. Chem. B* **114**, 17113-17119 (2010).

10. Varilly, P., A. J. Patel and D. Chandler, "Improved coarse grained model of solvation and the hydrophobic effect," *J. Chem. Phys.* **134**, 074109.1-15 (2011).

11. Patel, A. J., P. Varilly, S. N. Jamadagni, H. Acharya, S. Garde and D. Chandler, "Hydrophobic effects in interfacial environments," *Proc. Natl. Acad. Sci. USA* submitted (2011).

12. Patel, A. J., P. Varilly, S. Garde and D. Chandler, "Quantifying density fluctuations in volumes of all shapes and sizes using indirect umbrella sampling," *J. Stat. Phys.* submitted (2011).

This page is intentionally left blank

Rapid capture of charges by polyfluorenes in pulse-radiolysis experiments at LEAF

Principal Investigators: Andrew R. Cook and John R. Miller

Department of Chemistry, Brookhaven National Laboratory, Upton, NY, 11973 USA

acook@bnl.gov, jrmiller@bnl.gov

Program Scope: Short electron pulses provide unique tools to investigate questions important in solar energy conversion. This program develops new tools for such investigations, applies them to chemical questions, and makes them available to the research community.

Recent Progress:

"Step" capture of electrons by conjugated polymers: Our group is interested in studies of transport of charges and excitons in conjugated polymers, which are of interest due to their applications in "plastic" electronics and organic photovoltaic devices. Pulse radiolysis is almost unique in its ability to rapidly inject charges into conjugated polymer chains and observe them with optical spectroscopy. But how rapidly can charges be injected? In order to study transport, charges must first be captured; the rate at which they are captured largely determines the time-resolution for charge transport measurements with molecules with pendant trap groups. This paper explores capture of charges in pulse-radiolysis experiments with 5-10 ps electron pulses at short times and high concentrations by conjugated polyfluorene polymers.

Capture of electrons and subsequent electron transport have been studied in THF, where polymer anions can be uniquely produced. In a series of different length and different concentrations of the conjugated polymer polyfluorene, a time resolution limited prompt "step" increase in the transient absorption was observed in the kinetics for electron attachment. Such steps in pulse-radiolysis experiments are the result of capture of electrons before they are fully solvated. At the highest possible concentrations, it was found that ~30% of the electrons formed by pulse radiolysis are captured in the step, producing polymer radical anions. For the 79 unit polymer, this occurs at a concentration of 0.6 mM. The probability (fraction) of electrons captured by smaller molecules in step, or "dry", meaning unsolvated, electron capture, has often been found to follow the form P=(1-exp(-qc)), where q has dimension of inverse concentration. At a concentration 1/q= 2 mM only 1/*e* electrons survive capture.

We now ask whether information in the data presented herein can shed light on the mechanism of the fast, "step" capture process. Efficient step capture at such low polymer concentrations is understood in terms of the large size of the molecules in solution using 2 different possible mechanisms, seen in the figure below:

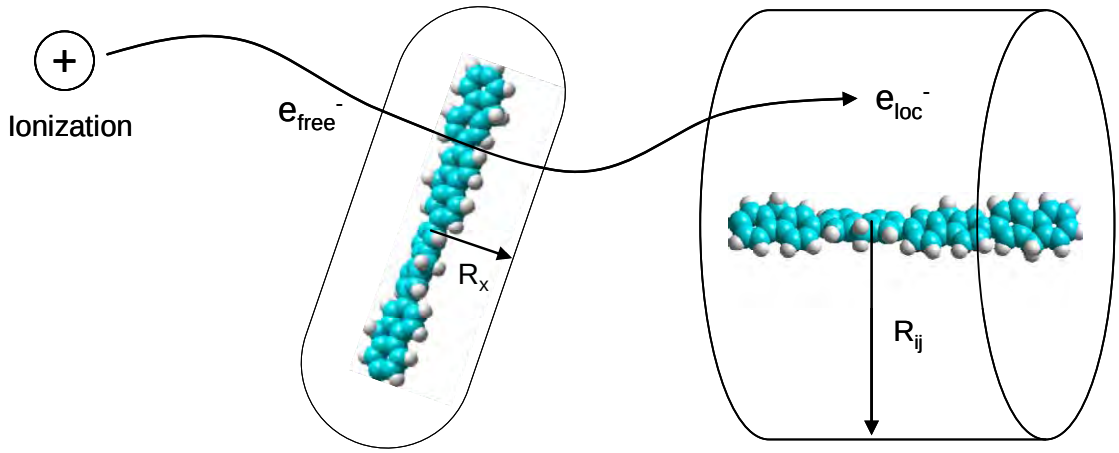

Following ionization of a solvent molecule, the ejected electron looses enough energy to not cause subsequent ionizations, but remains a highly mobile, quasi-free electron, e_{free}^-, and upon thermalization becomes a localized, e_{loc}^-, but not yet solvated electron. Quasi-free electrons may be captured along their trajectory as they pass within some distance, R_x, of a polymer molecule. Localized electrons are only shallowly trapped, having high mobilities and large wavefunctions which may enable them to be captured from a large volume around a polymer molecule, at up to a distance R_{ij}. In both cases, the observed capture implies a capture volume that give physically reasonable values for R_x and R_{ij}. In addition, both models predict an increase in capture which is linear in the length of the molecule. This is consistent with the finding that as the polymer length is increased, the amount of capture per repeat unit was constant, at ~60% of the pre-solvated electron capture efficiency reported for the similar molecule biphenyl in THF. This result is in sharp contrast to the rate constants for diffusion-controlled reactions of solvated electrons with long pF molecules, where each pF unit is only 13% as effective as a single unit. "Step" capture is much more effective per repeat unit than is diffusional reaction for long polymers.

While the data presented cannot uniquely differentiate between capture of these 2 different pre-solvated electron species, the key result of the study is the observation of rapid production of nearly 40% of the total concentration of polyfluorene anions ultimately formed in pulse radiolysis experiments. Pulse radiolysis experiments are unique in their ability to inject electrons into polymer chains and observe them with high time resolution. The time resolution to observe such injected charges has been limited by the need for electrons (or holes), created in the solvent to diffuse to the polymers. The findings here that such a large fraction of electrons are captured at very short times removes that limitation and enables the study of fast subsequent processes on a timescale limited only by the electron pulsewidth (~7ps), such as charge transport along conjugated polymer chains.

Radiation chemistry of chloroform: It is also of interest to study cation or hole transport in conjugated polymers including the same polyfluorenes. Chloroform is an excellent solvent for these materials, usually dissolving them with little aggregation. Electrons in some molecular liquids have mobilities as large as 100 cm^2/Vs, but this is not true for holes, so it is natural to assume that the very fast "step" capture is exclusive to electrons, which are initially mobile and delocalized after they are produced by ionization. Therefore fast injection into conjugated polymer chains, known for electrons, might not be available for holes, greatly limiting time-resolution in subsequent hole transfer experiments. Holes are often studied in chlorinated solvents where they can be uniquely attached. While solubility of polyfluorenes is an issue in many, chloroform was found to allow similar

concentrations as THF. The radiation chemistry of chloroform is not as well known however. In order to understand the yields and nature of holes attached to solute molecules in chloroform, initial experiments have begun to characterize the species produced in pulse radiolysis experiments.

Two absorption bands have been reported in the literature, one at 330 nm and another at 500-550 nm, both with short lifetime. The assignment of these bands is not clear, nor is the lifetime of species able to oxidize solutes. Using a series of solutes with varying ionization potential, it was determined that the 330 nm band belongs to the initially formed solvent radical cation. In deuterated chloroform, this spectrum was found to decay nearly in a nearly single exponential fashion in experiments with a ~200 ps time resolution, with a lifetime of ~25 ns. Decay of this band due in part to recombination with Cl^-, formed by rapid reaction of electrons ejected during ionization and another solvent molecule. The lack of apparent geminate recombination kinetics suggests that most of the recombination occurs on faster timescales. Confirmation of this assignment was found by using large concentrations of hole solutes to scavenge the solvent radical cations before they can recombine, which greatly slows the ultimate recombination kinetics, exposing a large fraction of geminate recombination. The observed ~25 ns decay is thus assigned to recombination of a low yield of solvent radical cations that escape the coloumb attraction to Cl^-, to become free and homogeneous ions in solution.

The rapid, <200 ps, geminate recombination of most solvent radical cations might be expected to greatly reduce the possible yield of polyfluorene radical cations, as they are only soluble to a few milli-molar depending on length. If this occurs, it will make the signals observed small. In addition, because of the ~25ns decay of homogeneous solvent radical cations, lower concentrations of polymer will not be useful, as few holes will be captured.

Step capture of cations by conjugated polymers: Similar to electron capture experiments, different length and different concentration solutions of polyfluorenes were examined. Surprisingly, initial measurements in chloroform find rapid and fascile production polyfluorene radical cations at higher polymer concentration. The figure to the right shows transient absorption of a 1.1 mM solution of a polymer with an average length of 40 repeat units. After correction for other absorbing species, the step shows that more than half of the polyfluorene radical cations are formed within the 15 ps time resolution of the OFSS detection system, seemingly analogous to electron capture in THF. Also contrary to what might have been expected due to the large amount of geminate recombination in chloroform, the data show that a large absolute yield of polyfluorene radical cations was fomed, with G~1 cation/100eV absorbed.

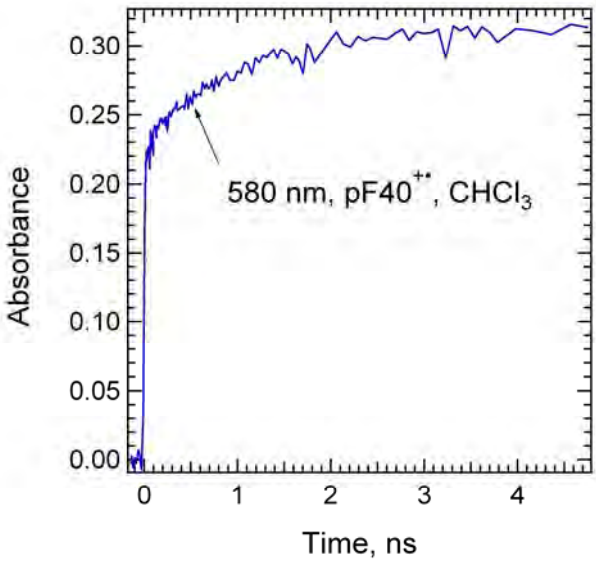

Unlike electrons in THF, it is unlikely that the chloroform radical cation initially travels rapidly through the solution as a molecular ion. Rather, capture mechanisms may involve either initial propagation of the cation electronic wavefunction or capture of the initially larger wavefunction by a solute, within an extended reaction distance.

As noted for electrons, substantial "step" formation of polyfluorene radical cations at the low concentrations possible will create opportunities to investigate their properties and transport at short times. Their natures depend on the still poorly-understood radiation chemistry for hole creation in these solvents. Determinations of transport will require free ions, but a substantial fraction of the holes may be ion-paired with Cl^- counterions.

Optical Fiber Single Shot (OFSS) detection system at LEAF: These experiments were enabled by the ongoing development of a new experimental detection technique that provides electron pulse-width limited single-shot transient absorption spectroscopy. Typical picosecond pulse radiolysis experiments record transient absorption data using a delay line and many thousands of shots. For samples of limited availability or those that cannot be flowed, this results in sample damage that can compromise data. Single-shot experiments provide the ability to avoid these problems, and can also allow for data to be collected more rapidly. The OFSS apparatus allows study of limited availability samples with volumes small as 100 μl without flowing, providing time resolution limited only by the electron pulse-width of 5-10 ps.

This detection system was improved in the last year primarily by the installation of a new fiber bundle. The new bundle provides both smaller time steps (~5 ps) at early times, as well as a many longer fibers to provide data to ~5 ns, which is important for matching to slower-timescale data collected using transient digitizers. In addition, the new bundle produces a smaller image in the sample where it overlaps with the 5 ps electron pulse. This is important as it makes the overlap more uniform, greatly reducing the need for collecting factors to correct for the differences in spatial overlap of the electron pulse with different fibers.

Because of its utility, the improved OFSS system has enabled not only to the work described above, but also utilized in studies of Ionic Liquids (with PI: James Wishart) that are too viscous to flow, and radiolysis in confined environments in solid Controlled Pore Glasses (with PI: Robert Crowell).

Future Plans:

The fast step capture of holes is presently contrary to our intuition. Like those for electron capture the mechanism is not clearly identified. That will be an objective along with mechanisms to observe electrons and holes attached to aggregates and crystallites, that may simulate the behavior of charges in films. We will also be seeking to investigate production of charges in actual films comprised of or containing conjugated polymers.

Publications of DOE sponsored research that have appeared in 2009-present:

(1) Cook, A. R.; Shen, Y. Z. "Optical fiber-based single-shot picosecond transient absorption spectroscopy" *Review of Scientific Instruments* **2009**, *80*.

(2) Sreearunothai, P.; Asaoka, S.; Cook, A. R.; Miller, J. R. "Length and Time-Dependent Rates in Diffusion-Controlled Reactions with Conjugated Polymers" *Journal of Physical Chemistry A* **2009**, *113*, 2786-2795.

(3) Schwerin, A. F.; Johnson, J. C.; Smith, M. B.; Sreearunothai, P.; Popovic, D.; Cerny, J.; Havlas, Z.; Paci, I.; Akdag, A.; MacLeod, M. K.; Chen, X. D.; David, D. E.; Ratner, M. A.; Miller, J. R.; Nozik, A. J.; Michl, J. "Toward Designed Singlet Fission: Electronic States and Photophysics of 1,3-Diphenylisobenzofuran"; *Journal of Physical Chemistry A* **2010**, *114*, 1457-1473.

(4) Shibano, Y.; Imahori, H.; Sreearunothai, P.; Cook, A. R.; Miller, J. R. "Conjugated "Molecular Wire" for Excitons"; *Journal of Physical Chemistry Letters* **2010**, *1*, 1492-1496.

Reactive Intermediates in the Condensed Phase: Radiation and Photochemistry

Robert A. Crowell
Chemistry Department, Brookhaven National Laboratory, P.O. Box 5000, Upton NY, 11973; crowell@bnl.gov

Scope

The scope of this program is to study and gain an understanding of the fundamental processes associated with the interaction of ionizing radiation and energetic photons within bulk liquids, the liquid/solid and solid/solid interface. Specific emphasis is placed upon developing detailed knowledge of the role of the solvent, the interface and nano-confinement on charge recombination, electron transfer and ion-radical chemistry and on making the connection to the fields of radiation chemistry solar energy conversion, energy storage and catalysis. One of the most common sources of chemical reactivity is ionizing radiation. Radiation chemists typically study the rapid, energetic reactions that are initiated by the interaction of ionizing radiation, such as high-energy electrons, with matter. The processes that control these reactions are among the most fundamental events that occur in condensed phase chemistry and related sciences of physics and biology, and are the key steps for efficient energy conversion, catalysis, and energy storage. Understanding of the basic processes that control these reactions impacts many fields including the design of nuclear reactors, radioactive waste management, radiation therapy, polymer processing, and planetary and astrophysics. While much is now understood about radiation chemistry, there is still a significant gap in our knowledge of the many fundamental processes that lead to radiation damage. Detailed mechanisms for these processes are not known and it is commonly accepted that these (and many other) radiation induced processes involve exotic chemistry that occurs on an ultrafast timescale ($<10^{-10}$ s). This work takes advantage of a variety of DOE user facilities, including LEAF, NSLS and the APS.

Recent Progress

To meet the main objectives of our program we are focused on two specific areas: the photochemistry of room temperature ionic liquids and more recently we have begun to study the radiation chemistry of aqueous systems under nano-confinement. In order to achieve our goals we use the techniques of ultrafast pulse radiolysis, ultrafast optical and x-ray spectroscopies.

Photochemistry and Solvation Dynamics of Ionic Liquids In this project we utilize ultrafast optical and x-ray spectroscopies to study the photochemistry and solvation dynamics of bromide based imidazolium room temperature ionic liquids. Due to their unique characteristics, low volatility, low vapor pressures, wide electrochemical windows and remarkable solvent properties, room-temperature ionic liquids (RTILs) have been proposed for use in a wide variety of industrial applications. One class of these compounds, the imidazolium salts, has been shown to be useful in such diverse areas as photocatalysis, dye-sensitized solar cells, separations science and carbon dioxide sequestration. Unfortunately, some common types of imidazolium salts, particularly the halides, have been shown to be susceptible to decomposition under exposure to UV, ionizing radiation and elevated temperatures. In order to design robust RTILs that can fulfill their potential applications it is necessary to understand the fundamental properties that lead to their degradation. Two issues that are common to all of the potential applications of imidazolium based RTILs are the need to understand the fundamental aspects of the initial physico-chemical processes that involve photoinduced electron transfer from the anion to cation and the solvation structure and dynamics of the anion (this is especially important for the use of RTILs in separations and solar cell applications).

In the first part of this effort we focus the photochemistry of the charge transfer (CT) band of the room-temperature ionic liquid 1-hexyl-3-methylimidazolium bromide ($[hmim^+][Br^-]$) using near-IR ultrafast transient absorption (TA) and steady-state UV absorption spectroscopies. This work shows that under

continuous irradiation of the charge transfer (CT) band at 266 nm there is a significant production of dibromide and tribromide species that absorb strongly at 266 nm. The buildup of these species is very rapid when compared to the time of a typical TA measurement. It is shown that these photoproducts, which are apparently very stable, adversely affect ultrafast transient absorption measurements. We have shown that the results of previous ultrafast studies are questionable due to the rapid buildup of stable photo-products that possess a strong absorption cross section (much stronger than the bromide that is solvated by the imidazolium ring) at the pump wavelength (266 nm). When the effects of photo-degradation are eliminated the TA spectrum changes dramatically and absorption features connected to the initial photochemical events in imidazolium based RTILs are revealed. It now becomes possible to begin to understand the initial photochemistry of these interesting and complex systems. Elimination of these effects reveals at least two new transient species that exist within the TA detection window of 100 fs to 3 ns and 850 nm to 1250 nm. One of the components is a short-lived (1.4ps) species that absorbs at 1080 nm. We currently attribute this component to a caged ion pair that is produced during the initial CT event. A second component exhibits a spectrum that is very broad with an absorption maximum below 850 nm and a lifetime of several hundred picoseconds. Although we have not yet been able to resolve the entire spectrum of this component, it is consistent with the formation of triplets. During the recombination process there is sufficient excess energy to produce triplets. The formation of triplets is consistent with recent theoretical studies. Future work will focus on extending our detection window to see if we can confirm the formation of triplets and observe the production radical dication species that are predicted to be produced as a neutral imidazolium ring approaches a positively charged one.

In the second part of this effort we utilize XAS, both static and time resolved (TR) to study the solvation structure and dynamics of the bromide ion. This work was performed at Sector 7 of the APS. We have used static EXAFS in combination with DFT calculations to investigate the equilibrium solvation structure of the bromide ion in a series of imidazolium RTILs. The solvation location of the bromide ion lies primarily above the C2 and H2 entities. The separation between the bromide and the C2 (3.12Å) and nitrogens (3.94Å) is nearly independent of the RTILs that were investigated. In attempt to learn more about the CT process we have performed TR-XAS on ([hmim$^+$][Br$^-$]). Although the time resolution for this technique is currently limited to <500ps, our initial results from the EXAFS (Figure 1A) show that the bromine is slowly diffusing away from the imidazolium ring. An interesting and surprising observation is the lack of a pre-edge feature in the TR-XANES spectrum (Figure 1B). This suggests that on this timescale no bromine atom is formed, but the CT process is accompanied by abstraction of the H2 hydrogen (which is acidic) by the initially formed bromine atom to form HBr. Future work on1,2-dimethyl-3hexyl imidazolium bromide, where the H2 is replaced by a methyl group, should help resolve this mechanism.

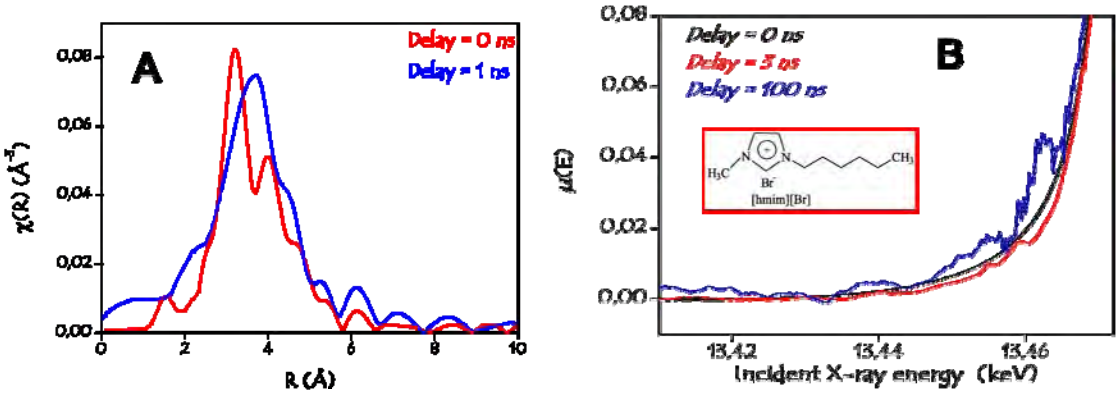

Figure 1. A) TR-EXAFS and B) TR-XANES of ([hmim$^+$][Br$^-$])

The radiation chemistry of nanoconfined water In a new project we have begun to study fundamental radiation induced aqueous reaction in nanoconfined media. It is the goal of this thrust to develop a detailed understating of the role of the interface in radiation induced processes. Currently we are using Brookhaven LEAF facility in its nanosecond mode of operation (>4ns), but soon plan on taking advantage of its piscosecond capability (<10ps). The need to understand the radiolysis of nano-confined/interfacial water in nuclear related fields has become abundantly clear during the recent events at the Fukushima Daiichi nuclear power plant where an explosion occurred that was a result of hydrogen that was produced at the water/zirconia interface. Although the generation of hydrogen was expected, the mechanism and prevention of its formation remains questionable. In this thrust we address the role of heterogeneous boundaries, the inhomogeneous dose distribution and the physical confinement itself which may hinder or promote the formation of spurs, and are believed to strongly influence the radiolytical processes, that are well known in bulk phase. The confining system which we have chosen to investigate water radiolysis is controlled pore glasses (CPGs), a system that exhibits a high porosity, well-defined pore size, excellent mechanical properties, high thermal stability and resistance to acids. CPGs are 50% pores by volume. CPGs of pore diameters 1 nm (330 m^2/gm**)** and 50 nm (40 m^2/gm) were used for this study and the evolution and optical absorption spectrum of the hydrated electron was followed by means of ultrafast pulsed radiolysis. On the nanosecond timescale, little to no difference is exhibited in the absorption spectrum, suggesting that the electrons solvate within the pore, but the confinement of water drastically impacts the reaction kinetics of the aqueous electron. It changes from the bulk value of $5x10^9$/M.s to $1.4x10^{11}$/M.s in the 1nm pore CPG. The initial yield (at 20ns) shows a slight increase with decreasing pore size. Approximately a 30% increase in the yield of solvated electrons in the 1nm pores relative to the yield in bulk water is observed. Formation of the solvated electron most likely occurs by an energy transfer process that occurs at the interface followed by diffusion into the pore. It is believed that in the CPGs a significant quantity of high energy excitons are formed during radiolysis. One possible explanation for the increase in electron yield and decrease in lifetime maybe due to exciton annihilation at the interface.

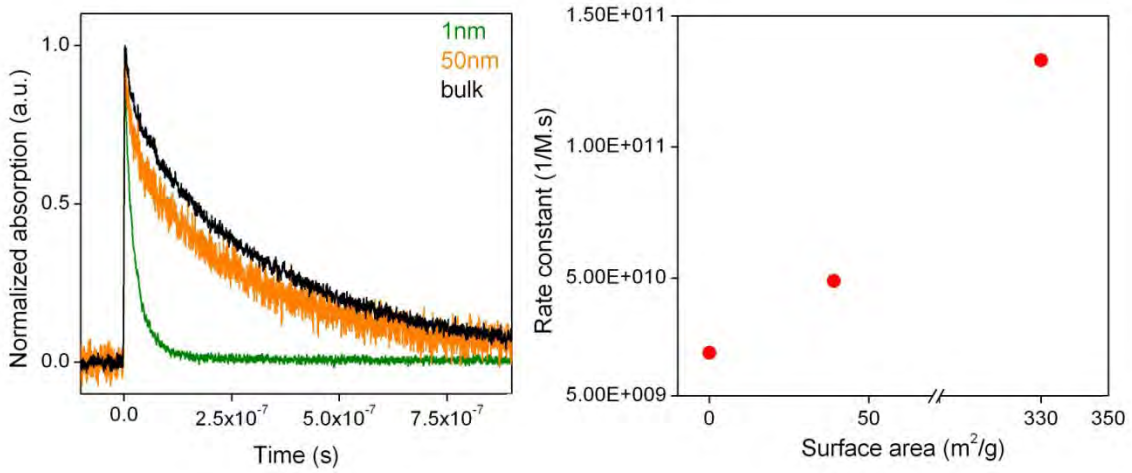

Figure 2.Nanosecond pulse radiolysis of nanoconfined water

Future Plans

Photochemistry and Solvation Dynamics of Ionic Liquids Future work will focus on two main areas of interest. First, we will continue to study both the photochemistry and solvation dynamics of selected room temperature ionic liquids. We are in the process of extending the detection range of our ultrafst

laser system further down into the UV (this will help detect radical dications) as well out into the mid-IR (we can follow structure changes to help complement our TR-XAS work). In order to understand better the hydrogen abstract mechanism (and to verify it) we have begun to use 1,2-dimethyl-3hexyl imidazolium bromide. In this compound the C2 hydrogen, which is the most likely candidate for abstract, is replaced by a methyl group which should shut down this mechanism. Time resolved XAS will be used to verify this.

The radiation chemistry of nanoconfined water To develop of a detailed knowledge of the role of nanoconfinement/interface in radiation and photochemistry we will continue to address the following issues:

1. Develop an accurate description of the properties of nanoconfined/interfacial water and its effect on solvation, particularly at the interface.

2. To study the effect of confinement/interface on reaction kinetics and mechanisms.

3. To understand how nanoconfinement/interface affects ion/radical diffusion and its effect on radiolytic yields.

To accomplish these objectives we will extend our ultrafast laser spectroscopy (both IR and visible), ultrafast pulse radiolysis and our newly developed time resolved XAS technique to studies of the effects of nanoconfinement/interface on basic photochemical and radiation induced reactions. Initial efforts will continue to focus on aqueous systems that have been well characterized in the bulk, e.g. the reaction of solvated electron with protons.

DOE Publications/Manuscripts 2009-present

1. R. Musat, A. R. Cook, J-P Renault, R. A. Crowell, "Nanosecond Pulse Radiolysis of Nanoconfined Water, " to be submitted to J. Phys. Chem. Lett.
2. R Musat, R. A. Crowell, K. Takahashi, D. Polyanskiy, M. Thoas, J. F. Wishart, Y. Katsumura "Ultrafast transient absorption spectrum of the room temperature ionic liquid 1-hexyl-3-methylimidazolium bromide: Confounding effects of photodegredation" to be submitted to J. Phys. Chem. Lett
3. R. Musat, R. A. Crowell, J. F. Wishart, D. Polyanskiy, Y. Li "Solvation structure of bromide based imidazolium ionic liquids, " to be submitted to J. Phys. Chem
4. J. Belloni, R. A. Crowell "Ultrafast Pulse Radiolysis," Recent Trends in Radiation Chemistry Chapter 5 (2010)
5. K. Takahahsi, K. Suda, T. Seto, Y. Katsumura, R. Katoh, R. A. Crowell, J. F. Wishart "Photo-detrapping of solvated electrons in an ionic liquid," Rad. Phys. Chem., 1129, 78 (2009)
6. K. Takahashi, H. Tezuka, T. Sato, Y. Katsumumra, M. Watanabe, R. A. Crowell, J. F. Wishart "Kinetic salt effects on an ionic reaction in ionic liquid/methanol mixtures," Chem. Lett. 38, 236 (2009)
7. C. G. Elles, I. A. Shkrob, R. A. Crowell, D. A. Arms. E. C. Landahl "Transient x-ray absorption spectroscopy hydrated halogen atom," J. Chem. Phys. 128, 061102 (2008)

Computational studies of aqueous and ionic liquids interfaces

Liem X. Dang
Chemical and Materials Sciences Division
Pacific Northwest National Laboratory
Richland, WA 93352
liem.dang@pnl.gov

Background and significance

Ion distributions at aqueous/vapor interfaces have attracted intensive attention due to their fundamental and practical importance. The traditional view is that the liquid/vapor interface is devoid of ions based on interpretations of surface tension measurements due to the Gibbs adsorption isotherm. This argument is challenged from both theoretical and experimental studies, with an enhancement of anion concentrations at the liquid/vapor interface being observed from both molecular dynamics (MD) simulations and spectroscopy. One recent effort on this topic is the work of Sloutskin et al. (*J. Chem. Phys.* **2007**, *126*, 054704), who used x-ray reflectivity techniques to explore the surface structure of concentrated aqueous salt solutions. Their results are a very important contribution to the understanding of liquid/vapor interfaces, and if they can be reliably interpreted, can bring major improvements to the understanding of interfacial ion behavior. Very recently, we have carried out a direct comparison with x-ray reflectivity experiments using molecular dynamics simulations for concentrated $SrCl_2$ aqueous salt interfaces. The ion concentrations were found enhanced at the interfaces, and the calculated structure factor near quantitatively reproduced the experimental one from simulations with polarizable potential models, while the simulations with non-polarizable potential models showed contrasting results.

Another interface that we are investigating is room temperature ionic liquids, RTILs. While RTILs possess some attributes that make them attractive for CO_2 capture technology, greater improvements in their CO_2 sorption and selectivity are being sought. RTILs have been investigated extensively by both computational and experimental methods, and their gas sorption properties have been studied. These previous investigations have provided a significant amount of thermodynamic information and molecular level detail on why RTILs preferentially solvate certain gases over others. Less studied, though, are the interfacial properties of RTILs. For the solvation of any gas, the gas molecule has to first transfer through an interface, and the solvation process heavily depends on this. In addition, gas molecules may adsorb to the surface of an RTIL with a lower free energy than in the bulk, which may be exploited to further optimize gas solvation with the development of nanostructured systems that maximize interfacial area. The interface itself is often a few nanometers in size, making the investigation of gas sorption in this region very difficult experimentally. Molecular simulation is a valuable tool for the investigation of molecular level processes, but requires accurate molecular models to provide confidence in any results obtained.

Details of the anion can significantly influence the interfacial activity. For example, exchanging the borate [BF_4] anion with a hexafluorophosphate [PF_6] anion to make butyl-methylimidazolium hexafluorophosphate [bmim][PF_6] is known to slightly increase the solubility of CO_2 in the RTIL, as the anion has been suggested to be the species in which CO_2 most strongly interacts with. Furthermore, the type of anion is known to affect the interfacial structure of RTILs, and also how the adsorption of other species, such as water, influence its interfacial structure. From these studies, it would be expected that the type of anion would influence the adsorption of gas species to the air-RTIL interface. Recent experimental work by Rivera-Rubero and Baldelli have found that the type of anion has an effect on how H_2O influences RTIL interfacial structure, so it would be expected that anion type would also influence the adsorption of H_2O at the surface of RTILs. To better understand how the type of anion influences gas sorption at the air-RTIL interface, we carried out molecular dynamics (MD) simulations with polarizable potentials to determine how [bmim][BF_4] and [bmim][PF_6] differ in their ability to absorb H_2O and CO_2 at the air-RTIL interface.

Recent Progress and Future Plans

Computational Studies of Aqueous Interfaces of $SrCl_2$ Salt Solutions

We describe our investigation of the distribution of the $SrCl_2$ ions at the aqueous/vapor interfaces using MD simulations. To the best of our knowledge, this work is the first MD calculation of the x-ray reflectivity of the concentrated salt solutions. In addition to the potential models, the divalent cations provided additional changes due to the strong ion-ion interactions. As a consequence, many body effects will be important in these systems. One of our main goals is to make a direct comparison to the measured data, we also discuss the way to improve the agreement between MD and X-ray reflectivity interpretation of the aqueous salt surfaces. We used both polarizable

and non-polarizable potential models and full 3D periodic Ewald summation to investigate the distribution of ions at the aqueous interfaces. Fig.1 shows the calculated $|\Phi(q_z)|^2$ (which is defined as the structure factor which is a measurement of the electron density distribution along the surface normal direction) from simulations with polarizable potentials as well as the experimental results. The experimentally deduced $|\Phi(q_z)|^2$ from X-ray reflectivity measurements shows a single peak at q_z=0.4 Å^{-1}, and large fluctuations in the high frequency region. The calculated $|\Phi(q_z)|^2$ from the simulations with polarizable potentials qualitatively agrees with the experimental curve. The same resonance frequency is observed at q_z=0.4 Å^{-1}, and the trend of the $|\Phi(q_z)|^2$ corresponding to the frequency follows the experiment reasonably well. However, the peak of simulated $|\Phi(q_z)|^2$ is more abrupt than that of experiment and also predicted over-structured spectra (see the green curve). We believe it is possible that a lower interfacial Sr^{2+} concentration at interface than what was found from our simulations would improve the agreement with experiment. Consequently, we demonstrated in Fig. 1 (see the red curve) that by reducing a few percent of the Sr^{2+}-Cl^- interaction (see Fig. 2), a better agreement with the experimental measurement was obtained. Our simulations with polarizable potentials provide a direct comparison with experiment for the interfacial structural properties and providing the mechanistic insight of ion solvation at the molecular level. We propose to refine our current ion-water and ion-ion polarizable potential parameters. To do so, we will calculate the effective ion-ion potentials in water or potentials of mean force, along with the calculation of radial distribution functions, which will then be used to calculate the known osmotic and activity coefficients of the concentrated electrolytes solution. These can be compared with the corresponding experimental osmotic pressure, activity coefficients of electrolyte solution, and x-ray reflectivity of concentrated aqueous salt interfaces values to allow enhanced confidence in simulation results obtained for concentrated solutions. Further efforts on improving the ion-ion and ion-water interactions using electronic structure techniques should be addressed in the future.

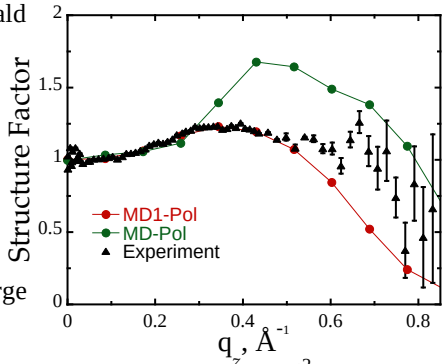

Fig. 1. Simulated $|\Phi(q_z)|^2$ of 2.7 M of $SrCl_2$ salt solution.

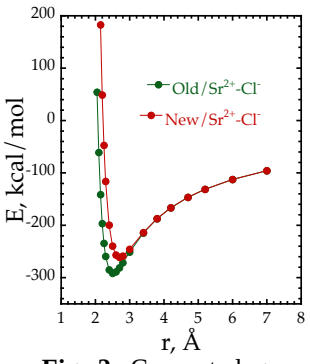

Fig. 2. Computed gas phase interactions between Sr^{2+}-Cl^-.

Anion Effects on Interfacial Absorption of Gases in Ionic Liquids

Molecular dynamics simulations with many-body interactions were carried out to systematically study the effect of anion type, tetrafluoroborate [BF_4] or hexafluorophosphate [PF_6], paired with the cation 1-butyl-3-methylimidazolium [bmim], on the interfacial absorption of gases in room temperature ionic liquids (RTILs). The PMF for H_2O and CO_2 across the air-RTIL interface for the systems investigated at 350K was calculated for this work. A constrained approach was used to calculate the PMF, in which the solute molecules had their center of mass constrained at different *z*-positions, spaced in 1 Å increments. At each position, the average force acting along *z* axis was calculated, and this force was integrated along the *z*-axis to obtain the PMF. The PMFs were calculated to span from 10 Å from the GDS towards the air, in which the interactions with the solute and RTIL were negligible, to 10-15 Å from the GDS towards the center of the RTIL creating 20-25 total points for the PMF. For each point from the GDS towards the air, 2 ns of simulation time was carried out for production, while 4 ns of simulation time was used for each position from the GDS towards the RTIL center, which required greater statistics.

Fig. 3 gives the PMFs for CO_2 across the air-[bmim][BF_4] and air-[bmim][PF_6] interfaces. For these, z = 0 represents the GDS, but due to the large oscillations in the RTILs, the GDS position itself has an uncertainty of around 1 Å. The difference between the gas and average liquid value can be used to estimate the free energy of solvation, and compared with values extracted from experimentally measured Henry's laws coefficients. The value for CO_2 in [bmim][PF_6] is from a temperature at 345K (-0.34 kcal/mol), while the value for [bmim][BF_4] is extrapolated from a plot of free energies versus temperature from experimental values at 283K, 298K, and 323K. The plot had a standard error of 5%, so it would be expected that the estimated value (-0.13 kcal/mol) would be correct within 0.01 kcal/mol. The free energies extracted from the simulations appear to estimate a free energy of solvation (-0.6 kcal/mol for both systems) that is between 0.2 and 0.5 kcal/mol too low, but the uncertainty in the PMFs, calculated from four independent simulation blocks, is around 0.4 kcal/mol, so these values are around the

uncertainty limit of our simulation results. The PMFs get negative a little bit farther out for the [bmim][BF_4] system, but this could be due to the uncertainty in the GDS position as described previously. CO_2 has a free energy minimum at both interfaces of around -1.8 kcal/mol, which has been attributed to the enhanced [bmim] alkyl density in this region. In the region from 2-6 Å from the GDS towards the liquid, there are increases in the free energy for both systems, in the region where the [bmim] ring has its highest density, but it is much more pronounced for the [bmim][BF_4] system. It is known that favorable interactions between CO_2 and fluorinated anions is a reason why CO_2 has reasonably good solubility in RTILs. The [bmim][PF_6] system shows weaker oscillation between [bmim] and its anion than the [bmim][BF_4] system does. Because of this, the CO_2 PMF would be expected to show greater oscillation in [bmim][BF_4] than [bmim][PF_6], as can be observed in Fig. 3. It should also be noted that despite the long simulation times, some of the fine details of the PMF in bulk RTIL may be influenced by the slow movement of the RTILs themselves, causing some oscillation that may disappear with much longer simulation times (on the order of 15-20 ns).

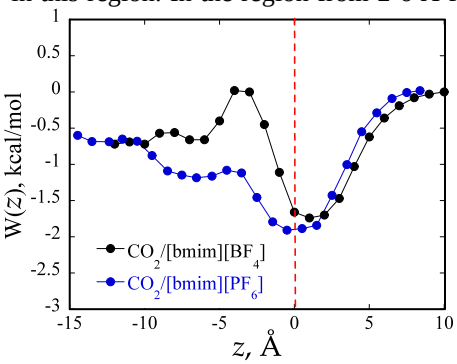

Fig. 3. Calculated PMFs for CO_2 the air-[bmim][BF_4] and air-[bmim][PF_6] interfaces.

The H_2O PMFs were carried out as described in the previous section, using the same system parameters, and the results are given in Fig. 4. Similar as for the CO_2 system, the free energy of solvation for H_2O can be estimated by the difference between the bulk and gas phase free energies in the PMF, which are compared with free energies derived from experimental Henry's Law coefficients. The experimental values for [bmim][BF_4] and [bmim][PF_6] are -5.0 kcal/mol and -3.4 kcal/mol, respectively. They were estimated using the values at lower temperatures for the [omim][BF_4], [omim][PF_6] and [bmim][PF_6] reported by Anthony et al. The values extracted from the simulations are -5.2 kcal/mol and -3.2 kcal/mol for the [bmim][BF_4] and [bmim][PF_6] systems, respectively. The agreement between simulation and experiment is excellent, within the estimated uncertainty of the simulation results of 0.4 kcal/mol. As shown experimentally, the free energy of solvation in [omim][BF_4] is much lower than in [omim][PF_6], which is due to stronger interactions with the [BF_4] anion than with [PF_6]. Despite this, the PMF decreases farther away from the GDS towards the air at the air-[bmim][PF_6] interface than for [bmim][BF_4]. After reaching 5 Å from the GDS of the air-[bmim][PF_6] interface, the free energy decreases only slightly as a H_2O molecules moves towards the bulk. This is unlike what is observed at air-[bmim][BF_4] interface, in which the free energy decreases monotonically and rather sharply from the air until it is around 7.5 Å from the GDS towards the liquid bulk. The quicker flattening of the H_2O PMF at the air-[bmim][PF_6] interface is likely due to the weaker structuring at that interface in comparison with [bmim][BF_4]. The reason for the PMF becoming negative farther away from the air-[bmim][PF_6] interface is discussed later.

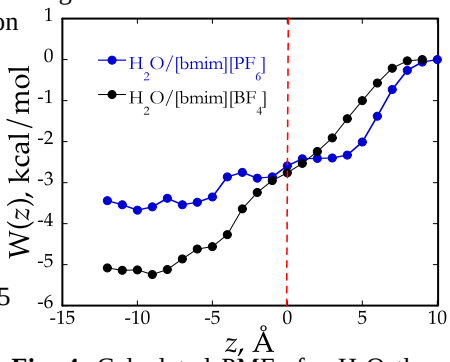

Fig. 4. Calculated PMFs for H_2O the air -[bmim][BF_4] and air-[bmim][PF_6] interfaces.

The PMF results show that it is unlikely to find H_2O at the air-[bmim][BF_4] interface, while there should be a significant amount at the air-[bmim][PF_6] interface. This should lead to a greater influence of H_2O on the interfacial structure of the air-[bmim][PF_6] interface, and would lead to a greater influence of humidity on the interfacial partitioning of CO_2 at the air-[bmim][PF_6] interface than the air-[bmim][BF_4] interface. Previous surface sensitive spectroscopic studies have observed that the presence of H_2O only influences the air-RTIL interfaces of [bmim] with hydrophobic anions (in which the [PF_6] is considered) while little influence on the surface with [BF_4] anions. This is consistent with the simulation results, and is due to the fact that the [BF_4] anion is only present in significant concentration greater than 5 Å from the GDS towards the bulk.

We are expanding the study to look at how the shape and hydrophilic/hydrophobic nature of the anion on the interfacial adsorption of gases in RTILs. We are developing a polarizable potential model for [bmim][Tf_2N], and are examining gas sorption in this system. The preliminary result indicates that the shape of the CO_2-pmf is significantly different from the corresponding pmfs of the CO_2[bmim][[BF_4]/[bmim][[PF_6] systems. The work will be communicated in a future publication.

References to publications of DOE sponsored research (2009-Present)

1. Investigating Hydroxide Anion Interfacial Activity by Classical and Multistate Empirical Valence Bond Molecular Dynamics Simulations. Wick CD and **LXD**, *J. Phys. Chem. A.* 113, 6356 (**2009**).

2. Solvation of Dimethyl Succinate in a Sodium Hydroxide Aqueous Solution. A Computational Study. Sun XQ, Chang TM, Cao Y, **LXD** et al. *J. Phys. Chem. B.* 113, 6473 (**2009**).

3. Computational Studies of Load-Dependent Guest Dynamics and Free Energies of Inclusion for CO_2 in Low-Density p-tert-Butylcalix[4]arene at Loadings up to 2:1. Daschbach JL, Sun XQ, Chang TM, **LXD** et al. *J. Phys. Chem. A.* 113, 3369 (**2009**).

4. Computational studies of aqueous interfaces of RbBr salt solutions. Sun XQ and **LXD**, *J. Chem. Phys.* 130, 124709 (**2009**).

5. Spontaneous Activation of CO_2 and Possible Corrosion Pathways on the Low-Index Iron Surface Fe(100)" Glezakou VA, **LXD** and BP McGrail, *J. Phys. Chem. C*. 113, 3691 (**2009**).

6. Computational Studies of Structures and Dynamics of 1,3-Dimethylimidazolim Salt Liquids and their Interfaces Using Polarizable Potential Models" Chang TM and **LXD**. *J. Phys. Chem.* **A** 113, 2127 **(2009).**

7. Structure, Dynamics and Vibrational Spectrum of Supercritical CO_2/H_2O Mixtures from *ab initio* Molecular Dynamics as a Function of Water Cluster Formation. Glezakou VA, Rousseau R, Dang LX and McGrail BP, *Physical Chemistry Chemical Physics.* 12, 8759-8771 **(2010)**.

8. The Behavior of NaOH at the Air-Water Interface: A Computational Study. Wick CD, Dang LX. *J. Chem. Phys.*, 133, 024705 **(2010)**.

9. Interpreting Vibrational Sum-Frequency Spectra of Sulfur Dioxide at the Air/Water Interface: A Comprehensive Molecular Dynamics Study. Baer M., Mundy CJ, Chang TM, Tao FM, Dang LX. *J. Phys. Chem.* B, 114, 7245-7249 **(2010)**.

10. Grand Canonical Monte Carlo Studies of CO_2 and CH_4 Adsorption in p-tert-Butylcalix[4]Arene. Daschbach JL, Sun XQ, Thallapally PK, McGrail BP and Dang LX, *J. Phys. Chem.* B, 114, 5764-5768, **(2010)**.

11. Computational Investigation of The Influence of Organic-Aqueous Interfaces on Nacl Dissociation Dynamics. Wick CD, Dang LX. *J. Chem. Phys.*, Volume: 132 Issue: 4 Article Number: 044702 **(2010)**.

12. Probing the Hydration Structure of Polarizable Halides: A Multi-Edge XAFS and Molecular Dynamics Study of the Iodide Anion. Fulton, John; Schenter, Gregory; Baer, Marcel; Mundy, Christopher; Dang, Liem; Balasubramanian, Mahalingam. *J. Phys. Chem.* B 114, 12926-12937 **(2010)**.

13. Molecular Mechanism of CO_2 and SO_2 Molecules Binding to the Air/Liquid Interface of 1-Butyl-3-methylimidazolium Tetrafluoroborate Ionic Liquid: A Molecular Dynamics Study with Polarizable Potential Models. Wick, Collin; Chang, Tsun-Mei; Dang, Liem. *J. Phys. Chem*. B 114, 14965-14971 **(2010)**.

14. Computational Study of Ion Distributions at the Air/Liquid Methanol Interface" Sun, Xiuquan; Wick, Collin; Dang, Liem. *J. Phys. Chem*. A **(ASAP, 2011)**.

15. Computational Study of Hydrocarbon Adsorption in Metal–Organic Framework Ni_2(dhtp). Sun XQ, Wick CD, Thallapally PK, Dang, Liem; McGrail, Benard. *J. Phys. Chem*. B, 115, 2842-2849 **(2011)**.

16. Structure and Dynamics of N, N-Diethyl-N-Methyl Ammonium-Triflate Ionic Liquid, Neat and with Water, from Molecular Dynamics Simulations. Chang, Tsun; Dang, Liem; Devanathan, Ram; Dupuis, Michel. *J. Phys. Chem.* B 114, 12764-12774 **(2010)**.

17. Molecular Mechanism of Hydrocarbons Binding to the Metal-Organic Framework. Sun XQ, Wick CD, Thallapally, PK, Dang, Liem; McGrail, Benard; *Chemical Physics Letters*, 501, 455-460 **(2011)**.

Transition Metal-Molecular Interactions Studied with Cluster Ion Infrared Spectroscopy

DE-FG02-96ER14658

Michael A. Duncan

Department of Chemistry, University of Georgia, Athens, GA 30602

maduncan@uga.edu

Program Scope

Our research program investigates gas phase metal clusters and metal cation-molecular complexes as models for heterogeneous catalysis, metal-ligand bonding and metal cation solvation. The clusters studied are molecular sized aggregates of metal or metal oxides. We focus on the bonding exhibited by "physisorption" versus "chemisorption" on cluster surfaces, on metal-ligand interactions with benzene or carbon monoxide, and on solvation interactions exemplified by complexes with water, acetonitrile, etc. These studies investigate the nature of the metal-molecular interactions and how they vary with metal composition and cluster size. To obtain size-specific information, we focus on ionized complexes that can be mass selected. Infrared photodissociation spectroscopy is employed to measure the vibrational spectroscopy of these ionized complexes. The vibrational frequencies measured are compared to those for the corresponding free molecular ligands and with the predictions of theory to reveal the electronic state and geometric structure of the system. Experimental measurements are supplemented with calculations using density functional theory (DFT) with standard functionals such as B3LYP.

Recent Progress

The main focus of our recent work has been infrared spectroscopy of transition metal cation-molecular complexes with carbon monoxide or water, e.g., $M^+(CO)_n$ and $M^+(H_2O)_n$. These species are produced by laser vaporization in a pulsed-nozzle cluster source, size-selected with a specially designed reflectron time-of-flight mass spectrometer and studied with infrared photodissociation spectroscopy using an IR optical parametric oscillator laser system (OPO). In studies on complexes of a variety of transition metals, we examine the shift in the frequency for selected vibrational modes in the adsorbate/ligand/solvent molecule that occur upon binding to the metal. The number and frequencies of IR-active modes reveal the structures of these systems, while sudden changes in spectra or dissociation yields reveal the coordination number for the metal ion. In some systems, new bands are found at a certain complex size corresponding to intra-cluster reaction products. In small complexes with strong bonding, we use the method of rare gas "tagging" with argon or neon to enhance dissociation yields. In all of these systems, we employ a close interaction with theory to investigate the details of the metal-molecular interactions that best explain the spectroscopy. We perform density functional theory (DFT) calculations (using Gaussian 03W or GAMESS) and when higher level methods are required, we collaborate with local theorists (Profs. P.v.R. Schleyer, H.F. Schaefer) or those at other universities (Prof. Laura Gagliardi, Minnesota). Our infrared data on these metal ion-molecule complexes provide many examples of unanticipated structural and dynamical information. A crucial aspect of these studies is the infrared laser system, which is an

infrared optical parametric oscillator/amplifier system OPO/OPA; Laser Vision). This system covers the infrared region of 600-4500 cm^{-1} with a linewidth of about 1.0 cm^{-1}.

$M^+(H_2O)_n$ complexes and those tagged with argon have been studied previously in our lab for the metals iron, nickel, cobalt and vanadium. We have recently extended these studies to titanium, manganese, chromium, scandium, copper, silver, gold and zinc. We have studied the noble metal ions copper, silver and gold with one and two water molecules. The gold system prefers a coordination of two ligands, and its O-H stretches are red shifted much more than those of copper and silver. In the vanadium system, we have studied multiple water complexes. Hydrogen bonding bands appear for the first time for the complex with five water molecules, establishing that four water molecules is the coordination for V^+. Similar measurements establish that the coordination of Zn^+ is three waters. Copper and zinc complexes with a single attached water have unexpected vibrational bands at high frequency above the normal region of the symmetric and asymmetric O-H stretches. With the help of theory by Prof. Anne McKoy (Ohio State), we were able to assign these to combination bands involving the twisting motion of the water. Silver, scandium and chromium complexes were rotationally resolved, providing the H-O-H bond angle in these systems. In new work, we have been able to produce multiply charged transition metal cation-water complexes for chromium, manganese, scandium and niobium systems tagged with multiple argons. IR spectra of these systems have very different intensity patterns and O-H shifts than those for the singly charged systems, and we are able to study the charge dependence of the cation-water interaction.

Transition metal carbonyls provide classic examples of metal-ligand bonding, and carbon monoxide is the classic probe molecule for surface science and catalysis. We have investigated transition metal cation carbonyls to compare these to corresponding neutral carbonyls known to be stable. The stability of these systems is conveniently explained with the 18-electron rule, and this is a guiding principle for our cation work. We studied the $Co^+(CO)_n$ complexes, for which the n=5 species is isoelectronic to neutral $Fe(CO)_5$, and the $Mn^+(CO)_n$ system, for which the n=6 complex is isoelectronic to $Cr(CO)_6$. In both cases, the cation complexes had a filled coordination at the expected n=5 and 6 complexes, respectively, and they had the same structures as the corresponding neutrals (trigonal pyramid and octahedral). However, the frequencies of the CO stretch vibrations, which are strongly red-shifted in the neutrals, were hardly shifted at all for the cations. This trend was attributed to the reduced π back-bonding in the cation systems. We also studied the $Cu^+(CO)_n$ complexes, for which the n=4 species is isoelectronic to neutral $Ni(CO)_4$, and which could also be compared to $Au^+(CO)_n$ complexes we had studied previously. Again, the n=4 complex has a closed coordination, with the expected tetrahedral structure. Unlike the nickel complex, but similar to the gold system, the copper complex has a blue-shifted carbonyl stretch, consistent with the behavior for so-called "non-classical" carbonyls.

A longstanding goal in inorganic chemistry has been to test the limits of the 18-electron rule in situations requiring unusual coordination numbers. Early transition metals with fewer *d* electrons need more carbonyls to achieve a closed-shell configuration. Specifically, the vanadium group cations (d^4) need <u>seven</u> carbonyls. We therefore made and studied the carbonyl cations of V, Nb and Ta. We found that vanadium did not produce the seven-coordinate (7-C) carbonyls, but instead formed a 6-C complex (even though DFT predicted the 7-C complex to be stable). Nb^+ produced both 6-C and 7-C carbonyls, while the tantalum cation formed only the desired 7-C species, providing the first example of a 7-C all-carbonyl complex. Apparently, the size of the ion and its growth mechanism are both important in such a system. Titanium cation, with fewer still *d* electrons, also formed carbonyls with a coordination of only six.

In an unusual example of metal-carbonyl interactions, we studied the uranium system, using a depleted rod sample. Uranium carbonyls were formed easily and found to dissociate efficiently upon infrared excitation. In addition to the $U^+(CO)_n$ species, we also detected $UO_2^+(CO)_n$ complexes. We found that the uranium carbonyls have red-shifted CO stretch vibrations, whereas the oxides have blue-shifted vibrations. The fragmentation behavior and spectral patterns confirmed that the $U^+(CO)_8$ ion is the fully coordinated species, and the spectrum for this ion was consistent with a square antiprism structure predicted by theory. The $UO_2^+(CO)_5$ species was the fully coordinated oxide carbonyl, and its spectrum is consistent with the D_{5h} structure predicted by theory (five equivalent CO's around the UO_2^+ waist). In the course of this work, we also found uranium complexes with multiple oxygens attached. Spectra for UO_4^+ and UO_6^+ showed that each contained a UO_2 core with one η^2 coordinated "superoxide" O_2 ligand. Professor Laura Gagliardi (Univ. of Minnesota) collaborated with us on these uranium systems.

Extending the metal carbonyl work, we examined metal *oxide* carbonyls, i.e., $VO^+(CO)_n$ and $VO_3(CO)_n$. We found that the coordination of VO^+ is five CO's, while that of VO_3^+ is three. The carbonyl stretching frequencies in these systems are less shifted than in the V^+ carbonyl complex. The VO^+ system has a CO stretch that is virtually unshifted with respect to free CO, while the VO_3^+ carbonyl stretches are blue shifted. Increased oxidation apparently leads to reduced available *d* electron density and consequently less back-bonding.

Previous work in our lab had identified intracluster reactions in several metal ion complexes with CO_2, i.e., $M^+(CO_2)_n$ (M=V, Ni, Mg, Al) Vibrational bands in the asymmetric stretch region of CO_2 (near 2350 cm^{-1}) were assigned to coordinated CO_2 in the small clusters (n=1-4) and other bands were assigned to second sphere ligands in the slightly larger clusters (n=5-7). In larger clusters still, however, new bands grew in suggesting that the core ion identity had somehow changed, producing a different environment for some CO_2 ligands. We speculated that the reaction might be the formation of an oxide-carbonyl species, which would have the same mass as the selected $M^+(CO_2)_n$ species, but at that time we could not scan the lower frequency region of the spectrum to investigate this further. Recently, using the new longer wavelength coverage of our IR system, we scanned this region for the $V^+(CO_2)_n$ system. We also intentionally produced the oxide carbonyl species of the form $VO^+(CO)_n$ (see above) to see where the carbonyl and oxide stretches for these systems would come. The lower frequency region of the spectrum also had new bands appearing at the same critical cluster size seen before, but the bands were not those of an oxide carbonyl. Instead, we found that the intracluster reaction had produced an oxalate species in the cluster by coupling two CO_2 molecules in the second sphere (remote from the metal). This new reaction chemistry is presently under further investigation.

Also using the new capability of our infrared laser systems for the lower frequency region, we have examined the metal-benzene and dibenzene complexes of Al^+. We had previously studied the mono-benzene complex using multiphoton dissociation with a free electron laser, but the present experiment using argon tagging and single photon photodissociation has greatly improved signal levels and resolution. The carbon ring stretch (1486 cm^{-1} in isolated benzene) is red shifted to 1467 cm^{-1} in Al^+(benzene), while the out-of-plane C-H bend (673 cm^{-1} in benzene) occurs at 728 cm^{-1} in this complex.

Future Plans

Continuing the work above, we will focus future efforts on doubly charged metal-water complexes, and we will include metal-acetonitrile complexes which might stabilize higher charge states more

effectively. Metal carbonyl work will attempt to extend the atomic complex studies to diatomic and triatomic metal species. Metal-benzene and metal-CO_2 studies will employ the long wavelength laser coverage to examine higher resolution spectroscopy in these systems and to further elucidate the intracluster reaction systems for other metals.

Publications (2009-present) for this Project

1. A. M. Ricks, J. M. Bakker, G. E. Douberly, M. A. Duncan, "IR spectroscopy of $Co^+(CO)_n$ complexes in the gas phase," *J. Phys. Chem. A* **113**, 4701 (2009). **DOI:** 10.1021/jp900239u

2. P. D. Carnegie, A. B. McCoy, M. A. Duncan, "Infrared spectroscopy and theory of $Cu^+(H_2O)Ar_2$ and $Cu^+(D_2O)Ar_2$: Fundamentals and combination bands," *J. Phys. Chem. A* **113**, 4849 (2009). **DOI:** 10.1021/jp901231q

3. A. M. Ricks, Z. D. Reed, M. A. Duncan, "Seven-coordinate homoleptic metal carbonyls in the gas phase," *J. Am. Chem. Soc.* **131**, 9176 (2009). **DOI:** 10.1021/ja903983u (communication)

4. Z. D. Reed, M. A. Duncan, "Infrared spectroscopy and structures of manganese carbonyl cations, $Mn(CO)_n^+$ (n=1-9)," *J. Am. Soc. Mass Spectrom.* **21**, 739 (2010). **DOI:** 10.1016/j.jasms.2010.01.022

5. A. M. Ricks, L. Gagliardi, M. A. Duncan, "Infrared spectroscopy of extreme coordination: The carbonyls of U^+ and UO_2^+," *J. Am. Chem. Soc.* **132**, 15905 (2010). **DOI:** 10.1021/ja1077365 (communication)

6. P. D. Carnegie, B. Bandyopadhyay, M. A. Duncan, "Infrared spectroscopy of $Sc^+(H_2O)$ and $Sc^{2+}(H_2O)$ via argon complex predissociation: The charge dependence of cation hydration," *J. Chem. Phys.* **134**, 014302 (2011). **DOI:** 10.1063/1.3515425

7. M. A. Duncan, "IR spectroscopy of gas phase metal carbonyl cations," *J. Mol. Spec.*, published on-line (invited review). **DOI**:10.1016/j.jms.2011.03.006

Photochemistry at Interfaces

Kenneth B. Eisenthal
Department of Chemistry
Columbia University
New York, NY 10027
kbe1@columbia.edu

Program Scope

The objectives of the program are to advance the development of a molecular level description of the equilibrium and time dependent chemical and physical properties of liquid interfaces using interface selective nonlinear optical spectroscopies.

Recent Progress

A) Femtosecond Time Resolved Vibrational Sum Frequency Generation

a) Solvation Dynamics at the air/water interface

Solvation is important in its impact on molecules in bulk liquids and at liquid interfaces, e.g electronic state energies, acid/base equiilibria, energy relaxation, and chemical reaction dynamics. In the work reported here the solvation dynamics of the organic dye molecule coumarin 314 following femtosecond photoexcitation is monitored by incident visible and IR pulses overlapping in time and space at the interface. The change in the intensity of the SFG signal. as the probe pulses are delayed with respect to the pump pulse yields the solvation dynamics. Based on comparison of the SFG and our separate SHG solvation studies we conclude that the origin of the dynamics is solvation induced shifts in the electronic state energies appearing in the Raman part of the hyperpolarizability, and not to solvation induced shifts in the excited state carbonyl frequency nor to effects on the strength of the vibrational transition moment.

b) Molecular Orientational Motions in 3 Dimensions at the Air/Water Interface

In our previous studies, and those that followed afterwards in other laboratories, the measured orientational relaxation was of a single molecular axis with respect to the interface normal. In order to observe rotational motions in 3-D we have measured the rotational motions about 2 non-collinear axes in a rigid molecule where the angle between the two vibrational transition moments. e.g. the carbonyl and the $-CF_3$ chromophores is known. Knowing the orientation of two axes yields the absolute orientation of the interfacial molecule. From the time dependence of the molecule's absolute orientation we obtain the rotation of the whole molecule. To investigate this approach we have measured the rotational motions of two SFG active vibrational chromophores in C314, namely the carbonyl axis and the fluoromethyl symmetric stretch axis, $-CF_3$, with respect to the interface normal. From separate measurements of the time dependent orientational angles of the two dipoles we obtain the time dependent orientational angle of the normal to the C314 plane, $\mu_{norm} = \mu_{c=o} \times \mu_{CF3}$, and thereby the molecule's rotation in 3 dimensions. We plan to make a movie of the molecule's 3D motion at the air/water interface to visualize this dynamics.

B) Probing the Gold Nanoparticle/ Water Interface with SHG

Studies of metallic nanoparticles with the liquid in which they are suspended are motivated by their unique electronic, optical and chemical properties. Their special properties result from their ultra small dimensions, shapes, composition, and surface plasmon resonances. Up until now investigations of the effects of metal nanoparticles on the photophysical and photochemical properties of molecules in the vicinity of the nanoparticle have been restricted to molecules that are bound to the nanoparticle's surface. What about molecules in the solution that adsorb spontaneously to the interface, what is their interfacial density, and what is the free energy that drives them to the metal nanoparticle/aqueous interface. It was our aim to address this question using SHG. With an aqueous solution containing both 16 nm gold nanoparticles and the organic dye molecules, malachite green, we have measured its adsorption isotherm. This is obtained from measurements of the dependence of the SHG intensity on the bulk solution concentration of the adsorbate.. Our measurements are in good agreement using our modified Langmuir model, from which

we obtain the free energy of adsorption, -15.4 ± 0.4 and the adsorbate interface density of $1.13 \pm 0.04 \times 10^3$.

Future Plans

Carry out femtosecond SHG and SFG measurements of electronic and vibrational spectra of molecules in their ground electronic and in their lowest excited singlet and triplet states.
Using these spectra we plan to investigate how interfacial molecules in excited electronic states redistribute their excess energy, e.g. emission, internal conversion, intersystem crossing, intermolecular energy transfer, structural changes, and chemical reactions.
We also plan to investigate how noble metal nanoparticles affect these competing channels for molecular energy relaxation. Of particular interest are the new channels for energy transformation that are created by these nanoparticles, e.g energy and electron transfer to the nanoparticle.

Publications : 2009 - present

Haber,L.H., Kwok,S,J.J., Semerano,M., Eisenthal,K.B., **Probing the gold nanoparticle/aqueous interface with second harmonic generation,** Chem.Phys.Lett. 2011 - **accepted for publication**

Rao, Yi, Turro,N.J., Eisenthal, K.B., **Solvation dynamics at the air/water interface with time resolved sum frequency generation,** J.Phys.Chem. C 2010, 114, 17703

Sahu,K., McNeill,V.F., Eisenthal, K.B., **Effect of salt on the adsorpton affinity of an aromatic carbonyl molecule to the air/aqueous interface,** J.Phys.Chem. C, 2010, 114, 18258

Piatkowski, L., Eisenthal, K.B., Bakker, H.J., **Ultrafast intermolecular energy transfer in heavy water,** Phys.Chem. Chem.Physics, 2009, 11, 9033

Rao,Yi, Subirm. M., McArthur, E.A., Turro, N.J., Eisenthal, K,B., **Organic ions at the air/water interface,** Chem.Phys.Lett., 2009, 477, 241

Rao, Yi, Turro,N.J., Eisenthal, K.B., **Water structure at air/acetonitrile aqueous solution interfaces, J**.Phys.Chem., 2009, 113, 14384

Kalyanasis, S., Eisenthal, K.B., McNeill, V.F. **Competitive adsorption between coumarin 314 and acetonitrile at the air/water interface: a second harmonic generation study**, J.Phys.Chem. C 2011 - **accepted for publication**

Title: Time Resolved Optical Studies on The Plasmonic Field Enhancement of Bacteriorhodopsin Proton Photo-current.

INVESTIGATOR: MOSTAFA EL-SAYED
School of Chemistry and Biochemistry, Georgia Institute of Technology
Atlanta, GA 30332
email: melsayed@gatech.edu

Program Scope:

Studying and developing systems that could potentially used in the conversion of solar energy into either current or hydrogen. Two systems are now being examined, Bacterio-rhodopsin and TiO_2 .At this meeting we report on our progress of using plasmonic field enhancement of the photocurrent extracted from the photo-cycle of the other natural photosynthetic system of bacteriorhodopsin.

Bacteriorhodopsin (bR) is the other photosynthetic system in nature. The proton pump function of bR determines its efficiency in converting solar energy into electric then chemical energy (ATP formation). Understanding it and attempting to increase its rate is thus very important direction in order to understand how nature works. The program is aimed at examining the plasmonic field effect on the kinetics of bR photo-cycle and the rate of its proton pump. The program that has started last year and aimed at developing an electrochemical cell based on the plasmonically enhanced proton pump photo-cycle of Bacteriorhodopsin is continuing in order to further enhance the current we observed last year.

Plasmonic Field Enhancement of the Electric Current Produced During the Proton Pump Cycle of Bacterio-Rhodopsin (bR):

Introduction

Researchers have been actively trying to convert solar energy into afuel for the last 40 years without a profound success, despite the fact that nature has already been doing so for millions of years through photosynthesis. There are two distinct photosynthetic systems in nature: chlorophyll (using electron pump system) and bacteriorhodopsin (using proton pump system). Bacteriorhodopsin (bR), a natural light activated protein, is found in the purple membrane of Halobacterium salinarum. The exceptional stability of bR makes it a potential biomaterial for various applications. bR can absorb sun light and transform it into electricity, which makes it promising for a plethora of applications especially those related to solar energy conversion. However, the photocurrent of bR-based photovoltaic cells is still limited to the pico-ampere range (approximately 0.2-40 pA cm^{-2} $monolayer^{-1}$ in thin film systems). In our recent research of

the DOE program , we began to use plasmonic field enhancements to try to enhance the observed photo-current from the proton-pump system.

Experimental Results

To successfully enhance the bR photocurrent , we used two strategies to achieve it:

1.The new bR electrochemical cell

We want to replace the thin film technology that has been used so far. Charge trapping in the film greatly reduce the observed current and requires the use of external bias to measure the very weak current producesd. In our last year report, we indicated that our group was able to build a solution-based electrochemical cell.[1] A simple design of cell by constructing commercially-available indium tin oxide (ITO) glasses as the optical windows and electrodes and small amounts of bR solutions as the photovoltaic medium to generate the proton gradient between two half-cells separated by a molecular porous membrane. Our easily-built electrochemical cell offers an appropriate tool for biomolecule-based photovoltaic devices and is proposed as a candidate for the conversion of solar to electrical energy, without the need for manufacturing of film-based photovoltaic devices and external bias.

2.Using the plasmonic field to Enhance the blue light Effect on The Proton Pump Rate:

We used the plasmonic fields of silver nanoparticles to modify the photocycle of bR and thus increase the duty cycle of proton production.[2] Surface plasmon resonance (SPR) is an interesting optical phenomenon induced by the coupling of the incident electromagnetic wave of light of resonant frequencies with the conduction band electrons of Au or Ag nanoparticles. We have previously reported the plasmonic fields of metal nanoparticles can perturb the photocycle of bR. We showed that both the retinal photoisomerization in the primary step and the proton pump process of the bR were both perturbed by plasmonic fields of gold nanoparticles. [3,4]

The conventional photocycle of bR takes 15 ms to complete during which a proton is pumped into the solution . However, by exposing the excited bR to blue light. a short-cut of the photocycle, takes place which makes it complete in only 70 micro-seconds (blue light effect).This is carried out by exciting the M intermediate in the photo-cycle with the blue light which is converted directly into the parent molecules(bR) , avoiding going back to it via the long thermal route. As a result the rate of the proton production increases

Upon the addition of silver nanoparticles (with a resonance peak in the blue light region), the plasmonic field of the silver nanoparticles is significantly enhanced resulting in large enhancement of the intensity of the blue light. This in turn leads to a large enhancement of the generated photocurrent density up to 25 nA/cm^3 (Figure 1). This is 15 times higher than that of pure bR and also orders of magnitude higher than the previously reported currents from the thin films. A possible mechanism is proposed which is in agreement with spectroscopic and kinetic studies.[5] However time resolved dynamic studies is needed and hope to be carried out soon.

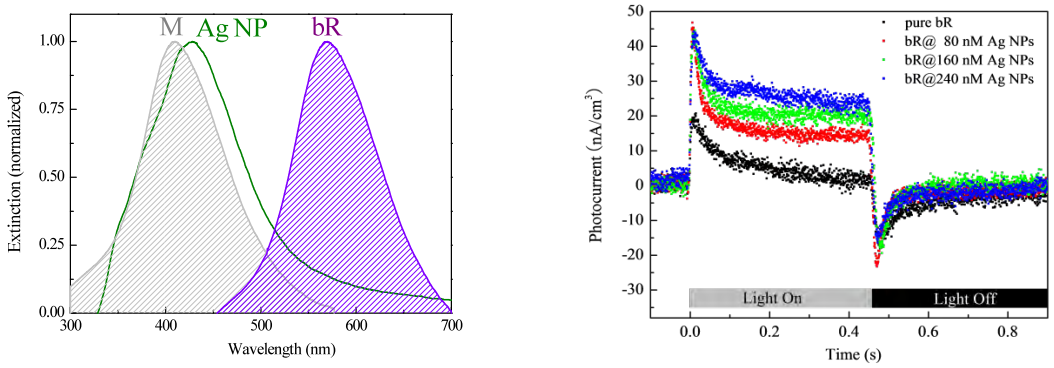

Figure 1 (Left) Normalized surface Plasmon resonance spectra of 40 nm (green) Ag NPs. The absorption contours of M and bR species are represented by gray and purple. (Right) The photocurrent density of bR observed by mixing silver nanoparticles: The value of the stationary photocurrent density was 25 nA/cm^3 when bR was mixed with 1.2 nM of Ag NPs (shown in blue), and it was 15 times higher than that of pure bR (shown in black).

.

References

1. Chu, L.-K.; Yen, C. W.; El-Sayed, M. A. *Biosesn. Bioelectron.* **2010**, *26*, 620. 2. Yen, C. W.; Chu, L.-K.; El-Sayed, M. A. *J. Am. Chem. Soc.* **2010**, *132*, 7250. 3. Biesso, A.; Qian, W.; El-Sayed, M. A. *J. Am. Chem. Soc.* **2008**, *130*, 3258. 4. Biesso, A.; Qian, W.; Huang, X.; El-Sayed, M. A. *J. Am. Chem. Soc.* **2009**, *131*, 2442. 5. Chu, L.-K.; Yen, C. W.; El-Sayed, M. A. *J. Phys. Chem. C* **2010**, *114*, 15358.

III. Future studies:

I. Further Enhancement of the Proton Pump Current of bR:

In fig 1 (Right), the initial current seems to be larger than the steady state value.
. This is due to the decrease of the initial polarization due to the mixing of the ions initially formed at the two electrodes. A molecular porous membrane is used to separate the two half cells of the bR solutions of the electrochemical cell. The proton transport efficiency is not the best by using porous membrane. Nafion membrane, a sulfonated tetrafluoroethylene based fluropolymet-copolyer is frequently used as a proton conductor for proton exchange membrane fuel cells. Its excellent cation selectivity can effectively accelerate proton transfer efficiency of our designed cell. However, the super-acidic characteristic of Nafion may cause the aggregation of the silver nanoparticles. The substitution of capping molecules of silver nanoparticles is required. Moreover, previous published results were all based on the same shape of metal nanoparticles (sphere). Different shapes of nanoaprticles may provide another possibility of further photocurrent enhancement. When those factors are all met, we firmly believe that the generated photocurrent may be increard to another level.

Publications during the past period.

1.Yen, C.-W.; Chu, L.-K.; El-Sayed, M.A., Plasmonic Field Enhancement of the Bacteriorhodopsin Photocurrent during its Proton Pump Photocycle. Journal of the American Chemical Society, 132 (21), 7250 – 7251 (2010).
2.Chu, L.-K.; Yen, C.-W.; El-Sayed, M.A., Bacteriorhodopsin-based photoelectrochemical cell. Biosensors and Bioelectronics, 26 (2), 620-626 (2010).
3.Chu, L.-K.; Yen, C.-W.; El-Sayed, M.A., On the Mechanism of the Plasmonic Field Enhancement of the Photocurrent from the Proton Pump Photocycle of Bacteriorhodopsin: Kinetic and Spectroscopic Study. The Journal of Physical Chemistry C 114, 15358-15363 (2010).
4.Chu, L.-K.; El-Sayed, M.A., Bacteriorhodopsin O-state photocycle kinetics: A surfactant study. Photochemistry and Photobiology, 86, 70 (2010). (Featured by American Society for Photobiology)
5.Chu, L.-K.; El-Sayed, M.A., Kinetics of the M intermediate in the photocycle of bacteriorhodopsin upon chemical modification with surfactants. Photochemistry and Photobiology, 86, 316 (2010).
6.Hayden, S.C.; Allam, N.K.; El-Sayed, M.A., TiO2 Nanotube/CdS Hybrid Electrodes: Extraordinary Enhancement in the Inactivation of Escherichia coli. Journal of the American Chemical Society Communication, 132(41), 14406-14408 (2010).
7.Allam, N.K.; El-Sayed, M.A., Photoelectrochemical Water Oxidation Characteristics of Anodically Fabricated TiO2 Nanotube Arrays: Structural and Optical Properties. Journal of Physical Chemistry C, 114(27), 12024-12029 (2010).
8..Allam, N.K.; Alamgir, F.; El-Sayed, M.A. Enhanced photoassisted water electrolysis using vertically oriented anodically fabricated Ti-Nb-Zr-O mixed oxide nanotube arrays. ACS Nano, 4(10), 5819-5826 (2010).

Statistical Mechanical and Multiscale Modeling of Surface Reaction Processes

Jim Evans (PI) and Da-Jiang Liu
Ames Laboratory – USDOE and Department of Mathematics,
Iowa State University, Ames, IA 50011
evans@ameslab.gov

PROGRAM SCOPE:

The Chemical Physics and Computational & Theoretical Chemistry projects at Ames Laboratory pursue the modeling of **heterogeneous catalysis and other complex reaction phenomena** at surfaces and in mesoporous materials. This effort integrates ***electronic structure analysis, non-equilibrium statistical mechanics, and coarse-graining or multi-scale modeling***. The *electronic structure* component includes DFT-VASP analysis of chemisorption and reaction energetics on metal surfaces, as well as application of QM/MM methods in collaboration with Mark Gordon (PI). The *non-equilibrium statistical mechanical and related studies* of reaction-diffusion phenomena include Kinetic Monte Carlo (KMC) simulation of atomistic models, coarse-graining, and heterogeneous multi-scale formulations. Topics of interest include: (i) chemisorption and heterogeneous catalysis on metal surfaces, including both reactions on extended crystalline surfaces (connecting atomistic to mesoscale behavior) and nanoscale catalyst systems (exploring the role of fluctuations); (ii) anomalous transport and catalytic reaction in functionalized mesoporous materials; (iii) diffusion, self-organization, and reaction on non-conducting surfaces; (iv) general statistical mechanical models for reaction-diffusion processes exhibiting non-equilibrium phase transitions, metastability, critical phenomena, etc..

RECENT PROGRESS:

CHEMISORPTION AND HETEROGENEOUS CATALYSIS ON METAL SURFACES

(i) Chemisorption on metal surfaces. Reliable description of chemisorption is key for modeling of catalytic reactions, e.g., to describe ordering in reactant adlayers, and possible restructuring and dynamics of the metal surface induced by chemisorbed reactants or other impurities. One recent study [14] explored the unusual interaction energetics of O/Pt(110) explaining the occurrence of striped (nx1)-O ordering observed both in O-chemisorption studies, and also during reaction with CO. The striped ordering derives from a strong anisotropy in the interactions between O adsorbed on neighboring pairs of bridge sites, with a much stronger repulsion for sites separated by a Pt atom vs. a hollow site. Sulfur (S) can act as a poison or promoter in catalysis, but also can induce metal substrate dynamics. Following our previous analysis of self-organized row-dot formation for S/Ag(111) [2,3,16], we have analyzed the diffusion and clustering of H_2S on Ag(111) as observed by low-T STM studies [15]. We have also used DFT to analyze chemisorption and metal-S complex formation for S/Ag(100) [20]. For both S on Ag (111) and (100), we propose that enhanced destabilization of metal nanostructures is induced by metal-S complex formation. We are modeling kinetics of these processes.

(iii) Multi-site lattice-gas modeling of CO-oxidation. A long-standing goal for surface science has been to develop realistic atomistic models for "complete" catalytic reaction processes on metal surfaces. We have continued development and application of realistic multi-site lattice-gas (LG) models and efficient KMC simulation algorithms [1] to describe CO-oxidation on unreconstructed metal surfaces. The current focus is on better estimating adspecies energetics, and on a more realistic treatment of diffusion, adsorption-desorption, and LH reaction kinetics.

(i) Tuning the reactivity of metal nanostructures on surfaces. A potential exists to tune the electronic structure and thus catalytic reactivity or selectivity of metal nanostructures exploiting "quantum size effects (QSE)" of confined electrons. We have considered the utility of a general, simple and versatile Free Electron Gas Model in predicting various aspects of QSE for metal nanostructures [7,12]. DFT analysis of QSE on key energies was also performed [13].

CATALYTIC REACTIONS IN FUNCTIONALIZED MESOPOROUS MATERIALS

We performed KMC analysis of our lattice model describing single-file diffusion-mediated polymerization ($A+A_n \rightarrow A_{n+1}$) within mesopores, where reaction occurs at catalytic sites inside the pores [6]. The modeling elucidated "pore clogging" observed in the formation of PPB in Cu^{2+}-functionalized MCM-41 silica. We also found unusual growth kinetics of the mean length of polymer, as well as scaling of the spatial and length distributions, which we explained within a non-Markovian Continuous-Time-Random-Walk formalism [18]. This analysis is being extended to describe the A+B Sonagashira cross-coupling polymerization reaction mechanism.

We have also analyzed a lattice model for a basic conversion reaction $A \rightarrow B$ occurring inside linear nanopores where reactants and products are subject to single-file diffusion [21]. Previous studies utilized mean-field treatments of diffusion, but we find that these fail to describe both the scaling of reactivity with basic parameters, and also the evolution of concentration profiles towards the steady-state. An alternative more effective hydrodynamic treatment was developed.

DIFFUSION, SELF-ORGANIZATION, REACTION ON NON-CONDUCTING SURFACES

We continued analysis of the self-organization of atomic rows via a "surface-polymerization reaction" during deposition of Group III metals on Si(100) [9,10]. We utilized both Gordon's QM/MM analysis of adatom binding and diffusion, and KMC simulation of atomistic lattice-gas models. In addition, we further analyzed the complex competitive etching & oxidation of stepped Si(100) surfaces [8,11]. A related general challenge is to develop efficient approaches to treat processes involving interplay between non-linear reaction kinetics and complex morphological evolution of a dynamic surface. See Ref.[19] for new coarse-grained step dynamics approach.

FUNDAMENTAL PHENOMENA IN FAR-FROM-EQUILIBRIUM REACTION SYSTEMS

Understanding non-equilibrium phase transitions and associated metastability and critical phenomena at a level comparable to that for equilibrium systems is a goal of the ***BESAC Science Grand Challenges*** report under the heading ***Cardinal Principles of Behavior beyond Equilibrium.*** This requires advancing from traditional mean-field kinetics models of reactions to atomistic statistical mechanical modeling which we have performed for a version of Schloegl's second model for autocatalysis. This model display a discontinuous non-equilibrium "catalytic poisoning transition" between reactive and poisoned states, and "generic two-phase coexistence" between these states for a finite range of control parameter. We have analyzed nucleation of the poisoned state from the metastable reactive state utilizing, e.g., KPZ theory for non-equilibrium interfaces [4,17]. We have also analyzed non-equilibrium critical behavior in this model [5].

FUTURE PLANS:

CHEMISORPTION AND HETEROGENEOUS CATALYSIS ON METAL SURFACES

(i) Catalytic reactions on metal surfaces: higher pressures, nanoscale effects, etc. Realistic multi-site atomistic LG models will be developed for KMC simulation of catalytic reactions on various metal (111) and (100) surfaces [1]. Such models can elucidate: (i) fluctuation-mediated

behavior in nanoscale systems (e.g., supported clusters); (ii) higher-coverage reactant phases at moderate pressures; (iii) mass-transport limited behavior at higher pressures (coupling CFD and non-isothermal effects to the atomistic model), and noting evidence that oxide formation does not always control high-P behavior. We will incorporate input from electronic structure studies.

(ii) Chemisorbed adlayer dynamics; interplay of steps with chemisorption and reaction. We plan to explore ordering and dynamics in chemisorbed layers on metal surfaces which is observed by in-situ STM and PEEM: chalcogens on coinage metals (with Thiel); CO-clusters for CO+H/Pd(111) (with Salmeron); and diffusion in high-density O adlayers on Pt(111) (with Imbihl). We will also explore the interplay of steps with chemisorbed adlayers and with reaction processes. Experiments reveal a strong effect of chemisorbed structures on step fluctuations, and in-situ LEEM indicates that steps on Pt(111) are also strongly modified during NO reduction. Suitable models must couple chemisorbed layer dynamics/reaction kinetics to step dynamics.

(ii) Heterogeneous Coupled Lattice-Gas modeling of spatiotemporal behavior in reactions. Our HCLG heterogeneous multiscale modeling (HMM) approach [1] uses continuous-time parallel KMC simulation to provide a realistic atomistic-level description of the reaction process at distinct macroscopic points distributed across a surface. These simulations are coupled accounting for mass transport between points, but this requires accurate description of chemical diffusion in mixed interacting reactant adlayers. Further HCLG development will be pursued.

CATALYTIC REACTIONS IN FUNCTIONALIZED MESOPOROUS MATERIALS

We plan to perform detail studies of conversion reactions in mesoporous silica (MSN), in particular elucidating the observed dependence of reactivity on pore diameter for PNB conversion to an aldol compound (by Slowing, Pruski, et al.). This requires detailed analysis of the passing propensity for reactants and products inside narrow pores, and incorporation of this behavior into coarse-grained models describing the interplay of inhibited transport and reaction. In addition, further theoretical development is needed for these systems, e.g., to describe fluctuation effects which control steady-state reactivity near pore openings, effects of differing reactant/product mobilities, etc. Detailed studies are also planned for the Sonogashira cross-coupling polymerization reaction studied in Pd-MSN (with Pruski, Lin, et al).

In addition, we are implementing a bond-switching MC algorithm for a Continuous Random Network (CRN) model to provide an atomistic-level description of amorphous catalyst materials.

DIFFUSION AND REACTION ON NON-CONDUCTING SURFACES

We plan to continue and integrate high-level QM/MM analysis (with Gordon), atomistic KMC modeling, and potentially also computationally efficient and versatile coarse-grained step dynamics modeling of etching, oxidation, and other reactions on dynamic stepped surfaces. QM/MM can help address the limitations of DFT-based analysis of energetics in these systems.

FUNDAMENTAL PHENOMENA IN FAR-FROM-EQUILIBRIUM REACTION SYSTEMS

Analysis will continue of non-equilibrium phase transitions in a variety of statistical mechanical reaction-diffusion models. Issues of metastability and nucleation, and well as critical phenomena, are of fundamental interest for these non-equilibrium systems where the standard thermodynamic framework (i.e., involving a free energy) cannot be applied. We are extending these analyses to various ZGB-type surface reaction models, which although too simplistic to describe standard low-pressure reaction behavior, should provide a valuable paradigm for higher-pressure (and coverage) low-effective-surface-mobility fluctuation-dominated reaction systems.

PUBLICATIONS SUPPORTED BY USDOE CHEM. SCIENCES FOR 2009-PRESENT:

[1] *Atomistic &Multiscale Modeling of CO-Oxidation on Pd(100) &Rh(100): From Nanoscale Fluctuations to Mesoscale Reaction Fronts,* D.-J. Liu, J.W. Evans, Surf. Sci. (Ertl Nobel Issue) 603, 1706 (2009).

[2] *Accelerated Coarsening of Ag… Islands on Ag(111) due to Trace Amounts of S: Mass Transport mediated by Ag-S Complexes,* M.M. Shen, D.-J. Liu, C.J. Jenks, et al. J. Chem. Phys. 130, 094701 (2009).

[3] *Coarsening of Two-dimensional Nanoclusters on Metal Surfaces,* P.A. Thiel, M. Shen, D.-J. Liu, et al. J. Phys. Chem. C (Invited Centennial Feature Article), 113, 5047-5067 (2009).

[4] *Schloegl's Second Model for Autocatalysis with Particle Diffusion: Lattice-Gas Realization exhibiting Generic Two-Phase Coexistence,* X. Guo, D.-J. Liu, J.W. Evans, J. Chem. Phys., 130, 074106 (2009).

[5] *Generic Two-phase Coexistence and Non-equilibrium Criticality in a Lattice Version of Schloegl's Second Model for Autocatalysis,* D.-J. Liu, J. Stat. Phys., 135, 77 (2009).

[6] *Statistical mechanical modeling of catalytic polymerization within surface functionalized mesoporous materials,* D.-J. Liu, H.-T. Chen, V.S.-Y. Lin, J.W. Evans, Phys. Rev. E 80, 011801 (2009).

[7] *Quantum Size Effects in Metal Nanofilms: Comparison of an Electron-Gas Model and Density Functional Theory Calculations,* Y. Han, D.-J. Liu, Phys. Rev. B 80, 155404 (2009).

[8] *KMC Simulation Atomistic Models for Oxide Island Formation and Step Pinning during Etching by Oxygen of Vicinal Si(100),* M. Albao, F.-C. Chuang, J.W. Evans, Thin Solid Films, 517, 1949 (2009).

[9] *Binding and Diffusion of Al Adatoms… on the Si(100)-2x1 Surface: A Hybrid QM/MM embedded Cluster Study,* D. Zorn, M. Albao, J.W. Evans, M.S. Gordon, J. Phys. Chem. C 113, 7277-7289 (2009).

[10] *Kinetic Monte Carlo Study on the Role of Defects and Detachment of Formation and Growth of In Chains on Si(100),* M. Albao, J.W. Evans, F.-C. Chuang, J. Phys.: Cond. Matter, 21, 405002 (2009).

[11] *Diffusion of Atomic Oxygen on the Si(100) Surface,* P. Arora, W. Li, P. Piecuch, J.W. Evans, M. Albao, M.S. Gordon, J. Phys. Chem. C, 114, 12649 (2010).

[12] *Shell structure and phase relations in electronic properties of metal nanowires from an electron-gas model,* Y. Han, D.-J. Liu, Phys. Rev. B, 82, 125420 (2010).

[13] *Density functional analysis of key energetics in metal homoepitaxy: Quantum size effects in periodic slab calculations,* D.-J. Liu, Phys. Rev. B, 81, 035415 (2010).

[14] *Interactions between Oxygen Atoms on Pt(100): Implications for Ordering during Chemisorption and Catalysis,* D.-J. Liu, J.W. Evans, ChemPhysChem, 11, 2174 (2010).

[15] *Low-temperature adsorption of H_2S on Ag(111),* S.M. Russell, D.-J. Liu, M. Kawai, Y. Kim, P.A. Thiel, J. Chem. Phys., 133, 124705 (2010).

[16] *Adsorbate-enhanced transport of metals on metal surfaces: Oxygen and sulfur on coinage metals,* P.A. Thiel, M.M. Shen, D.-J. Liu, et al., J. Vac. Sci. Technol. A. 28 1285-1298 (2010) (JVSTA Cover)

[17] *Metastability in Schloegl's second model for autocatalysis: Lattice-gas realization with particle diffusion,* X.F. Guo, Y. De Decker, J.W. Evans, Phys. Rev. E, 82, 021121 (2010).

[18] *Polymer length distributions for catalytic polymerization within mesoporous materials: Non-Markovian behavior associated with partial extrusion,* D.-J. Liu, H.T. Chen, V.S.Y. Lin, J.W. Evans, J. Chem. Phys. 132, 154102 (2010).

[19] *Boundary conditions for Burton-Cabrera-Frank type step-flow models: coarse-graining of discrete deposition-diffusion equations,* D.M. Ackerman, J.W. Evans, SIAM Multiscale Model. Sim. 9, 59 (2011)

[20] *Adsorption of sulfur on Ag(100),* S.M. Russell, M.M. Shen, D.J. Liu, et al., Surf. Sci. 605, 520 (2011).

[21] *Catalytic conversion reactions mediated by single-file diffusion in linear nanopores..,* D. Ackerman, J. Wang, J.H. Wendel, D.-J. Liu, M. Pruski, J.W. Evans, J. Chem. Phys. 134, 114107 (2011).

Confinement, Interfaces, and Ions: Dynamics and Interactions in Water, Proton Transfer, and Room Temperature Ionic Liquid Systems (DE-FG03-84ER13251)

Michael D. Fayer
Department of Chemistry, Stanford University, Stanford, CA 94305
fayer@stanford.edu

Water exists in confined environments and at interfaces in a wide variety of important systems in chemistry, materials science, biology, geology, and technological applications. In chemistry, water plays an important role as a polar solvent often in contact with interfaces, for example, in ion exchange resin systems and chromatographic surfaces. Water in the nanoscopic channels of polyelectrolyte membranes is central to the operation of hydrogen and other fuel cells. In biology, water is found in crowded environments, such as cells, where it hydrates membranes and large biomolecules, as well as in pockets in proteins. In geology, interfacial water molecules can control ion adsorption and mineral dissolution. Embedded water molecules can change the structure of zeolites used as catalysts.

Water's unique properties can be traced to its formation of an extended hydrogen bonding network. Water molecules can make up to four hydrogen bonds in an approximately tetrahedral arrangement. However, the hydrogen bonded network is not static. The network evolves constantly on a picosecond time scale by the concerted dissociation and formation of hydrogen bonds. This rapid evolution of water's hydrogen bond network enables processes ranging from proton diffusion to protein folding. While a great deal is known about the dynamics of bulk water, much less is known about the dynamics of water in nanoconfinement, at interfaces and when it is interacting with ionic species. The dynamics of water are changed a great deal when water is in nanoscopic environments, interacting with interfaces or ions. In addition, important processes such as proton transport, which is necessary in fuel cells, are dramatically changed when they do not occur in bulk pure water.

A variety of nanoconfined water systems and interfaces, such as reverse micelles, lamellar structures, polyelectrolyte fuel cell membranes, and sol-gel glasses are being investigated using ultrafast two dimensional infrared (2D IR) vibrational echo techniques, and polarization and wavelength selective IR pump-probe experiments. These methods permit molecular dynamics and intermolecular interactions to be studied in unprecedented detail. The 2D IR vibrational echo techniques are akin to 2D NMR, but they operate on time scales that are many orders of magnitude shorter than NMR. Recently we have performed the first 2D IR vibrational echo experiments on the nanoscopic water pools of very small reverse micelles in different organic phase solvents. Water dynamics as reflected by the spectral diffusion of the OD hydroxyl stretch of 5% HOD in H_2O were measured in w_0=2 (1.7nm diameter) AOT/water reverse micelles in carbon tetrachloride and in isooctane solvents. Orientational relaxation and population relaxation are observed for w_0=2, 4, and 7.5 in both solvents using IR pump-probe measurements. w_0 is the number of water molecules per AOT surfactant molecule. It is found that the pump-probe observables (orientational relaxation that is controlled by hydrogen bond dynamics) are sensitive to w_0 but not to the solvent. However, initial analysis of the vibrational echo data from the water nanopool in the reverse micelles in the isooctane solvent seemed to yield different dynamics than the CCl_4 system in spite of the fact that the spectra, vibrational lifetimes, and orientational relaxation are the same in the two systems. It was found that there are beat patterns in the 2D IR vibrational echo interferograms with isooctane as the solvent. The beats are observed from a signal generated by the AOT/isooctane system even when there is no water or with H_2O but without the OD chromophore. A beat subtraction data processing procedure was developed. It does a reasonable job of removing the distortions in the isooctane data, showing that the reverse micelle dynamics are the same within experimental error regardless of whether isooctane or carbon tetrachloride is used as the organic phase.

Two time scales are observed in the vibrational echo data, ~1 ps and ~10 ps. The slower component contains a significant amount of the total inhomogeneous broadening. Physical arguments indicate that there is a much slower component of spectral diffusion that is too slow to observe within the experimental time window, which is limited by the OD stretch vibrational lifetime. Orientational relaxation measurements (pump-probe) for $w_0 = 2$ show extremely slow reorientation, >100 ps. Therefore, the 2D IR spectroscopy is sensitive to dynamics that are not manifested as orientational relaxation. It is possible that these dynamics are associated with the influence of the interface's topography fluctuations that drive structural changes of the water nanopool. Experiments and analysis using 2D IR vibrational echoes on a range of larger water nanopool sizes are in progress. As the size of the reverse micelles increase to $w_0 = 4$, 7.5, and larger, the spectral diffusion dynamics become faster. There is a fundamental difference between very small reverse micelles, ($w_0 = 2$ and 4) and large reverse micelles, $w_0 > 12$. The small reverse micelles do not have a bulk-like water core. They are so small that virtually all of the water molecules are directly influenced by the interface. Large reverse micelles have a bulk water core. In the large systems, water at the interface is interacting with bulk water. The sizes of $w_0 = \sim 7.5$ to ~10, are intermediate. They have a core of water molecules not directly interacting with the interface, but these core water molecules are not bulk-like because of indirect influence of the interface. A theoretical method is being developed to separate the contribution of spectral diffusion of water at the interface from that of the bulk-like water in the reverse micelle core. This procedure, while theoretically more complex, is similar in spirit to the method we developed to separate interfacial orientational relaxation from that of bulk water in reverse micelles and other systems.

Room temperature ionic liquids (RTIL) have been the object of extensive study in the past decade due to their unique properties including very low vapor pressure and non-flammability under ambient conditions, selective reaction medium, etc. One particular area of interest is the possible use of ionic liquids as alternative solvents in lithium ion batteries. The current generation of such batteries uses organic compounds as solvents. These solvents present safety issues due to properties such as volatility and high flammability. Thus RTILs could become greener and safer alternative.

The addition of lithium salts to ionic liquids causes an increase in viscosity and decrease in ionic mobility that hinders their possible application as alternative solvent in lithium ion batteries. Optically heterodyne-detected optical Kerr effect (OHD-OKE) spectroscopy was used to study the change in dynamics, principally orientational relaxation, caused by the addition of lithium bis(trifluoromethylsulfonyl)imide to the ionic liquid 1-butyl 3-methylimidazolium bis(trifluoromethylsulfonyl)imide. Thus, the lithium cation could be added without changing the anion of the pure liquid. The experiments on the pure ionic liquid were conducted over a wide range of temperatures. Over the time scales studied (1 ps to 16 ns) for the pure ionic liquid, two temperature independent power laws were observed, the intermediate power law (1 ps to ~1 ns) followed by the von Schweidler power law. The von Schweidler power law is followed by the final complete exponential relaxation, which is highly sensitive to temperature. A mode coupling theory (MCT) schematic model was also used to fit the data for both the pure ionic liquid and the different salt concentration mixtures. Detailed comparisons of the temperature dependent data to the scaling prediction of MCT were performed. It was found that dynamics in the pure liquid and the liquids with lithium cations are described very well by MCT. Therefore, changes in the MCT parameters extracted from the data could be used to examine the influence of the addition of lithium cations.

The lithium salt concentration was found to affect both power laws and a discontinuity could be found in the trend observed for the intermediate power law when the concentration (mole fraction) of lithium salt is close to $\chi(LiTf_2N) = 0.2$. The exponential relaxation, which reflects the complete structural randomization in the liquids, was found to display a non-

hydrodynamic behavior with increasing lithium salt concentration, which increases the viscosity. The non-hydrodynamic behavior is manifested by a non-constant value of the product of the orientational relaxation diffusion constant and the viscosity. The nature of the deviation reverses direction at the lithium salt mole fraction of $\chi(LiTf_2N) = 0.2$. The observed breaks in this and the other dynamical observables at $\chi(LiTf_2N) = \sim 0.2$ indicate that the dynamics are influenced by structural changes in the liquid that have been observed by MD simulations. The changes in dynamics may be associated with a change from a coordination of anions per lithiuj cation. At low lithium mole fraction, two anions coordinate a lithium cation. At $\chi(LiTf_2N) = 0.2$ and above, the structure changes to four anions coordinating a lithium cation.

We are currently broadening our studies of water in nanoscopic structures to systems such as sol-gel glasses, and various polyelectrolyte fuel cell membranes. We will combine the IR studies of water dynamics with time dependent UV/Vis spectroscopy using photoacids to study proton transfer dynamics in the same systems. The studies are extensions of our successful investigations of Nafion fuel cell membranes using these methods. In Nafion we found that water dynamics and proton transfer are vastly different from those observed in bulk water. Nafion, like AOT reverse micelles that we are studying, have charged sulfonate head groups at the water interface. Sol-gel classes provide a system in which we can control the size of water nanopores and study water dynamics and proton transfer with a neutral interface. It is also possible to functionalize the sol-gel interfaces to vary the interfacial properties. These studies will be a counter point to the studies in fuel cell membranes to separate the influences on water dynamics and proton transfer of the nanoconfinement and interfacial properties.

Publication from DOE Sponsored Research 2009 – present

(1) "Ion-Water Hydrogen Bond Switching Observed with 2D IR Vibrational Echo Chemical Exchange Spectroscopy," David E. Moilanen, Daryl Wong, Daniel E. Rosenfeld, Emily E. Fenn, and M. D. Fayer Proc. Nat. Acad. Sci. U.S.A. 106, 375-380 (2009).

(2) "Water Dynamics and Interactions in Water-Polyether Binary Mixtures," Emily E. Fenn, David E. Moilanen, Nancy E. Levinger, and Michael D. Fayer J. Am. Chem. Soc. 131, 5530-5539 (2009).

(3) "Water Dynamics at the Interface in AOT Reverse Micelles," David E. Moilanen, Emily E. Fenn, Daryl Wong and M.D. Fayer J. Phys. Chem. B 113, 8560–8568 (2009).

(4) "Geometry and Nanolength Scales vs. Interface Interactions: Water Dynamics in AOT Lamellar Structures and Reverse Micelles," David E. Moilanen, Emily E. Fenn, Daryl Wong, and M.D. Fayer J. Am. Chem. Soc. 131, 8318-8328 (2009).

(5) "Water Dynamics in Salt Solutions Studied with Ultrafast 2D IR Vibrational Echo Spectroscopy," M. D. Fayer, David E. Moilanen, Daryl Wong, Daniel E. Rosenfeld, Emily E. Fenn, and Sungnam Park Acc. of Chem. Res. 42, 1210-1219 (2009).

(6) "Water Dynamics in Large and Small Reverse Micelles: From Two Ensembles to Collective Behavior," David E. Moilanen, Emily E. Fenn, Daryl Wong, and Michael D. Fayer J. Chem. Phys. 131, 014704 (2009).

(7) "Water Dynamics at Neutral and Ionic Interfaces in Reverse Micelles," Emily E. Fenn, Daryl B. Wong, and M.D. Fayer Proc. Nat. Acad. Sci. U.S.A. 106, 15243-15248 (2009).

(8) "Solvent Control of the Soft Angular Potential in Hydroxyl-π Hydrogen Bonds: Inertial Orientational Dynamics," Daniel E. Rosenfeld, Zsolt Gengeliczki, and M. D. Fayer J. Phys. Chem. B 113, 13300-13307 (2009).

(9) "Proton Transfer and Proton Concentrations in Protonated Nafion Fuel Cell Membranes," D. B. Spry and M. D. Fayer J. Chem. Phys. B 113, 10210-10221 (2009).

(10) "Analysis of Water in Confined Geometries and at Interfaces," M. D. Fayer and Nancy E. Levinger Ann. Rev. Analytical Chem. 3, 89-107 (2010).

(11) “Room Temperature Ionic Liquids–Lithium Salts Mixtures: Optical Kerr Effect Dynamical Measurements,” Bruno G. Nicolau, Adam Sturlaugson, Kendall Fruchey, Mauro C. C. Ribeiro, and M. D. Fayer J. Phys. Chem. B 114, 8350-8356 (2010).
(12) “Water Dynamics in Small AOT Reverse Micelles in Two Solvents: 2D IR Vibrational Echoes with 2D Background Subtraction,” Emily E. Fenn, Daryl B. Wong, and M.D. Fayer J. Chem. Phys. 134, 054512 (2011).
(13) “Dynamics of Water Interacting with Interfaces, Molecules, and Ions,” M. D. Fayer Acc. of Chem. Res. ASAP (2011).

Chemical Kinetics and Dynamics at Interfaces

Fundamentals of Solvation under Extreme Conditions

John L. Fulton

Chemical and Materials Sciences Division
Pacific Northwest National Laboratory
902 Battelle Blvd., Mail Stop K2-57
Richland, WA 99354
john.fulton@pnl.gov

Collaborators: M. Baer, M. Balasubramanian, E. J. Bylaska, L. X. Dang, S. M. Kathmann, C. J. Mundy, T. Pham, G. K. Schenter, J. H. Weare

Program Scope

The primary objective of this project is to describe, on a molecular level, the solvent/solute structure and dynamics in fluids such as water under extremely non-ideal conditions. The scope of studies includes solute–solvent interactions, clustering, ion-pair formation, and hydrogen bonding occurring under extremes of temperature, concentration and pH. The effort entails the use of spectroscopic techniques such as x-ray absorption fine structure (XAFS) spectroscopy, coupled with theoretical methods such as molecular dynamics (MD-XAFS), and electronic structure calculations in order to test and refine structural models of these systems. In total, these methods allow for a comprehensive assessment of solvation and the chemical state of an ion or solute under any condition. The research is answering major scientific questions in areas related to energy-efficient separations, hydrogen storage and sustainable nuclear energy (aqueous ion chemistry and corrosion). This program provides the structural information that is the scientific basis for the chemical thermodynamic data and models in these systems under non-ideal conditions.

Recent Progress

The hydration of ions and the formation of contact ion pairs underlie processes in a large number of aqueous systems. Direct experimental measurement of ion-ion interactions decoupled from those of ion-water are limited. X-ray absorption fine structure (XAFS) spectroscopy, coupled with molecular dynamics (MD-XAFS) are being used to test and refine structural models of these systems.

Hydronium Ion (H_3O^+) Pairing with Chloride (Cl^-) . Experimental measurements of the structure of hydronium ion in water are scarce even though it is prevalent in a large number of biological, chemical, and geochemical systems. This difficulty is highlighted by a recent effort using neutron diffraction (NDIS) that returned only limited results. In this case, the various pair distribution functions could not be fully resolved, mandating a reliance on a Monte Carlo interpretation with only partially satisfactory results. Whereas the NDIS method attempts to decouple about 12 different pair distribution function, the advantage of XAFS is that it probes only the structure of the first peak in Cl-O pair distribution function comprising contributions from only Cl^-/H_2O and Cl^-/H_3O^+ interactions.

These new XAFS measurements [6] reveal that the structure of the Cl^-/H_3O^+ contact ion pair, as depicted in Fig. 1, is distinctly different from that of the H_2O structure about Cl^-. The Cl-O bond length (2.98 Å) for Cl^-/H_3O^+ is approximately 0.16 Å shorter than the Cl^-/H_2O bond. The bridging proton resides at an intermediate position between Cl and O at 1.60 Å from the Cl^- and

approximately 1.37 Å from the O of the H_3O^+. The bridging-proton structure of this contact ion pair, (Cl-H-OH_2), is similar to the structure of the water Zundel ion, (H_2O-H-OH_2^+). In both cases there is a shortened Cl-O or O-O bond, and the intervening proton bond distances are substantially longer than for the covalent bonds of either HCl or H_2O. This XAFS study shows that, at the lower concentrations (6 m HCl), the Cl^-/H_3O^+ ion pair is starting to form in appreciable amounts up to the point in the concentrated acid (16 m HCl) where all of the H_3O^+ species are paired with a Cl^-.

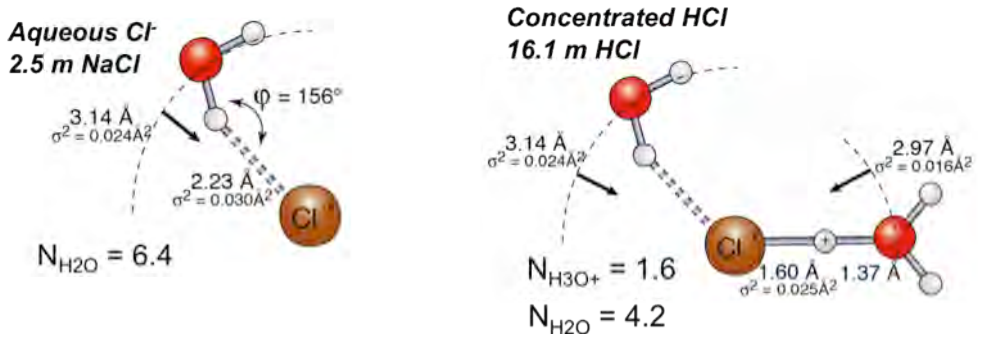

Figure 1. XAFS structural characterization of aqueous Cl- and the H_3O^+/Cl^- ion pair.

The highest level of ab initio theory for small clusters with up to six water molecules provides good agreement with most of the experimentally observed structures. On the other hand ab initio-based molecular dynamics simulations capture some but not all of the measured local structure. Finally the Cl^-/H_3O^+ ion pair structure is difficult to reproduce using classical intermolecular potentials or models that rely on these potentials. Overall the XAFS results provide important new insights into this bulk aqueous structure.

Hydration Structure of Zn^{2+} and other First-row Transition Metals: XAFS and ab initio MD Simulations. We explored a series of first-row transition metal ions starting with an initial study of Zn^{2+}. [3] The Zn^{2+} involves a well-ordered octahedral water structure that gives rise to a series of strong XAFS multiple scattering signals from the various scattering geometries. We found that a DFT-MD simulation (QM/MM Zn^{2+} + $6H_2O$ / 58 H_2O, CPMD PBE96 , MM SPC/E) *quantitatively* reproduces the XAFS data. For instance, the simulation faithfully reproduces the shape of the first peak in the Zn-O radial distribution function. In the photoelectron multiple scattering region from 2 to 5.4 Å, the level of agreement is exceptional. The signal in this region is directly related to the photoelectron multiple scattering processes associated with both collinear 180° and triangular 90° O–Zn–O paths. In order to achieve this level of agreement, the simulation must accurately predict the local pair distribution functions and angular distribution functions for these specific sets of O–Zn–O atoms in the first shell structures. To our knowledge, this is the first time that any simulation has quantitatively modeled this series of multiple scattering features.

The success with Zn^{2+} led immediately to an examination of a series of transition metals. For many of the transition metals, e.g. Cr^{3+} and Fe^{3+}, the agreement between simulation (CPMD QM/MM PBE0 (with exact exchange)) and experiment is even better than for Zn^{2+}. This evaluation of a series of transition metals led to several important discoveries. We found that

the default DFT pseudopotentials that are commonly used in electronic structure codes lead to metal-water distance errors of about 0.1 to 0.15Å. For the trivalent ions such as Cr^{3+} and Fe^{3+} this amounts to an error in the hydration enthalpy of about 400 kJ/mole from just the coulombic contribution alone. This distance error was corrected by adjusting the metal pseudopotential to include a smaller set of the core electrons, and thereby increasing the number of valence orbitals in the DFT calculation to include the 3s and 3p orbitals. Although these orbitals are not directly involved in bonding to the water, they are polarized by changes in the 3d bonding orbitals. Further we found that there is a minor improvement in the metal-water distance by including exact exchange (PBE0).

The implications of these finding have far reaching consequences on how DFT-MD is deployed in describing aqueous ions in chemistry, interfaces and separations (e.g. lanthanide and actinides). Further this dramatic improvement in the simulation fidelity opens up the opportunity to quantitatively evaluate the XAFS higher order scattering features (> 4Å) that have mostly been ignored up to this point.

Future Plans

Cation-anion interactions in concentrated aqueous phase. The interaction of anions with cations in aqueous solutions underlies broad areas of biochemistry, geochemistry and atmospheric chemistry. To this day, there is an incomplete understanding of the interaction of simple salts such as Na^+ with Cl^- or of Li^+ with Cl^- dissolved in water. The electrostatic attractive interactions between counter ions are modulated by a delicate balance of different aqueous hydration effects that are not yet fully understood. In a preliminary study, an XAFS measurement was made of a concentrated, 15 m LiCl solution. In contrast to expectations, almost no ion pairing was detected at 15 m LiCl. The experimentally determined degree of ion pairing (0 ion pairs at 6 m LiCl and 0.32 at 15m LiCl) was far below recently published values derived from molecular dynamics (MD) simulations using the classical intermolecular potentials. So far the cause of this discrepancy is unclear. Is this due to incorrect ion polarizability or due to an incorrect description of the cation-anion interaction potential? What is the relationship between the cation charge/size and the degree of chloride-cation interaction? We intend to explore this area with joint XAFS and MD analysis of these system using both classical and DFT molecular dynamics methods. We intend to expand this area of study to explore the interaction of chloride with a series of monovalent and divalent cations in concentrated aqueous solutions. The interaction of chloride (Cl-) with cations from the Group IA (Li^+, Na^+, K^+, Rb^+) and IIA (Be^{2+}, Mg^{2+}, Ca^{2+}, Sr^{2+}) elements is one of the primary interests since there are very few studies of these structures. The proposed study involves XAFS spectroscopy at the Cl K-edge using a new, low-Z cell that incorporates 200 nm thick Si_3N_4 windows (3 x 3 mm) attached to a small stepper motor drive that will allow for adjusting the pathlength between 25 to 500 μm while the sample is in the beam. This allows for rapid optimization of the edge step height and quick screening of a large series of samples.

Solvent-Separated Ion Pair Structure via High Energy X-ray Diffraction. Two types of ion-pair species are believed to exist. There is the contact ion pair wherein the anion directly adjoins the cation. There is also the solvent-separated ion pair wherein the cation and the anion are bridged by a single solvent molecule. This type of species has been predicted from theory under certain conditions however a comprehensive characterization of these structures has not been reported. Simulations suggest that both types of ion pairs co-exit for Na^+Cl^- solutions at

high concentrations or at high temperatures. Further, the solvent-separated ion pair is believed to have a profound effect on chemistry and nucleation in atmospheric aerosols.

One strategy is to induce the cation-to-anion association at elevated temperatures without changing the chemical composition of the systems. Near- or above the critical point of water (T_c = 375°C), ion pairs form when the hydrogen bonding network is largely destroyed leading to strong electrostatic interactions between ions. The hypothesis is that most monovalent salts exist as a preponderance of solvent-separated ion pairs at elevated temperatures. A limitation of XAFS is that it is not capable of detecting the solvent-separated ion pair since the ion-ion distances are beyond the detection limits in aqueous systems. The use of high energy x-ray diffraction will provide important insights into the structure of these systems.

References to publications of DOE sponsored research (CY 2009-present)

1. R. Rousseau, G.K. Schenter, J.L. Fulton, J.C. Linehan, M.H. Engelhard, T. Autrey. "Defining the Active Catalyst Structure and Reaction Pathways from *Ab inito* Molecular Dynamics and *Operando* XAFS: Dehydrogenation of Dimethylaminoborane by Rhodium Clusters" **J. Am. Chem. Soc**., 131 (30), 10516–10524, (2009)
2. J. L. Fulton, S. M. Kathmann, G. K. Schenter and M. Balasubramanian, "Hydrated Structure of Ag(I) Ion from Symmetry-Dependent, K- and L-Edge XAFS Multiple Scattering and Molecular Dynamics Simulations." **J. Phys. Chem. A** 113 (50), 13976-13984 (2009).
3. E. Cauet, S. Bogatko, J. H. Weare, J. L. Fulton, G. K. Schenter and E. J. Bylaska, "Structure and dynamics of the hydration shells of the Zn2+ ion from ab initio molecular dynamics and combined ab initio and classical molecular dynamics simulations." **J. Chem. Phys.** 132 (1), 194502 (2010).
4. G. S. Li, D. M. Camaioni, J. E. Amonette, Z. C. Zhang, T. J. Johnson and J. L. Fulton, "[CuCln](2-n) Ion-Pair Species in 1-Ethyl-3-methylimidazolium Chloride Ionic Liquid-Water Mixtures: Ultraviolet-Visible, X-ray Absorption Fine Structure, and Density Functional Theory Characterization." **J. Phys. Chem. B** 114 (39), 12614-12622 (2010).
5. J. L. Fulton, G. K. Schenter, M. D. Baer, C. J. Mundy, L. X. Dang and M. Balasubramanian, "Probing the Hydration Structure of Polarizable Halides: A Multiedge XAFS and Molecular Dynamics Study of the Iodide Anion." **J. Phys. Chem. B** 114 (40), 12926-12937 (2010).
6. J. L. Fulton and M. Balasubramanian, "Structure of Hydronium (H3O+)/Chloride (Cl-) Contact Ion Pairs in Aqueous Hydrochloric Acid Solution: A Zundel-like Local Configuration." **J. Am. Chem. Soc.** 132 (36), 12597-12604 (2010).

Ion Solvation in Nonuniform Aqueous Environments

Principal Investigator
Phillip L. Geissler
Faculty Scientist, Chemical Sciences, Physical Biosciences, and Materials Sciences Divisions

Mailing address of PI:
Lawrence Berkeley National Laboratory
1 Cyclotron Road
Mailstop: HILDEBRAND
Berkeley, CA 94720

Email: plgeissler@lbl.gov

Program Scope

Research in this program applies computational and theoretical tools to determine structural and dynamical features of aqueous salt solutions. It focuses specifically on heterogeneous environments, such as liquid-substrate interfaces and crystalline lattices, that figure prominently in the chemistry of energy conversion. In these situations conventional pictures of ion solvation, though quite accurate for predicting bulk behavior, appear to fail dramatically, e.g., for predicting the spatial distribution of ions near interfaces. We develop, simulate, and analyze reduced models to clarify the chemical physics underlying these anomalies. We also scrutinize the statistical mechanics of intramolecular vibrations in nonuniform aqueous systems, in order to draw concrete connections between spectroscopic observables and evolving intermolecular structure. Together with experimental collaborators we aim to make infrared and Raman spectroscopy a quantitative tool for probing molecular arrangements in these solutions.

Recent Progress

Computer simulations of atomistically detailed models for aqueous solutions suggest that certain small ions adsorb to air-water interfaces. A variety of experimental data support this notion, and there has been considerable speculation on its relationship to more complex issues (e.g., the role of dissolved salts in protein solubility). Such behavior defies expectations from dielectric theories of solvation, which have proved remarkably accurate for bulk liquids. Put simply, the enormously favorable enthalpy of introducing an ion into highly polarizable environments would seem to be sacrificed in the interfacial region; ion concentrations at the liquid surface should be correspondingly suppressed. Weighing against this expected energetic cost of ion adsorption, the entropy sacrificed upon creating a cavity in solvent to accommodate the ion should be recovered in the interfacial region. From our understanding of solvation in bulk, however, this expected entropic drive towards the surface should be considerably weaker than the energetic repulsion.

During the last year we have used Monte Carlo simulations to quantify such thermodynamic changes accompanying adsorption of small ions at the air-water interface. In accord with recent measurements by Saykally's lab, we find a counterintuitively favorable energy of association between charged solutes and the liquid's boundary, as well as a counterintuitively unfavorable entropy of adsorption. Similar behavior in a schematic model polar liquid (the Stockmayer fluid) and for a variety of ion charges suggests these trends to be general and closely connected to microscopic mechanisms of adsorption. Generic to all these scenarios is partial desolvation of ions (or, viewed another way, changes in the interfacial density profile) accompanying the reduction in energy as an ion approaches the liquid's boundary. It is not yet clear why removal of a few coordinating solvent molecules should be favorable (by tens of kJ/mol), while full desolvation is greatly unfavorable (by hundreds of kJ/mol). The coupling between local solvation structure and longer wavelength interfacial deformations appears to be key.

We have also made progress towards an analytical theory for ion adsorption by establishing a Green's function for dielectric response at extended interfaces. Armed with this result we can begin to explore how changes in dielectric boundary conditions, as the air-water interface fluctuates and deforms, influence ions' spatial distributions.

Finally, we have resolved a significant issue that had hindered theoretical predictions for nonlinear spectroscopic signals specific to interfacial structure. Computer simulations of liquid-vapor interfaces typically involve a periodically replicated slab of liquid, bounded by two opposing interfaces. Obtaining a nonzero prediction of dipole-order susceptibilities requires breaking this symmetry, typically by assigning each molecule to the nearest interface. Because water molecules have internal structure, this designation suffers from an unavoidable ambiguity for molecules that straddle the slab's midplane. Different, and equally reasonable, protocols for this dissection lead to qualitatively different calculated spectroscopic responses.

We have resolved this issue by considering quadrupole-order contributions to pertinent response functions. These contributions suffer from their own ambiguity, namely, in defining the origin of a molecular coordinate system. When molecules bear a net dipole, quadrupole values are not invariant to translation of this origin. We have proved that the two ambiguities are in fact one and the same. Most importantly, we have shown that any choice of molecular coordinate system, when applied consistently to dipole- and quadrupole-order responses, yields the same result. Strictly dipole-order response (the focus of many previous simulation studies) is thus not a well-defined, observable quantity, but is instead inseparable from certain quadrupole-order effects. We have developed approximations that direct a choice of coordinate system minimizing such quadrupole effects.

Future plans

Our recent calculations, together with Saykally's experiments, raise intriguing questions about the connection between solvation structure and the thermodynamics of ion

adsorption. It is not clear why the enormously favorable energy of solvating small ions is not sacrificed but instead enhanced by partial removal from solution. Future calculations will isolate contributions from local coordination geometry, interfacial fluctuations, and long-range polarization, both in water and in the Stockmayer fluid. These studies will similarly clarify the origin of reduced entropy when ions approach the liquid's boundary.

Ongoing analytical calculations will determine dielectric solvation energies at non-planar interfaces. Our approach builds on bulk solvation theories that account for the dependence of solvent polarization modes on volume-excluding shape and size of dissolved molecules. The reference system in our case is not a bulk liquid but instead a flat solvent-air interface; a similar formalism nonetheless applies for the dependence of dielectric susceptibility on interfacial deformations. Combined with a lattice gas representation of density fluctuations, this advance will enable the first proper accounting of the influence of interfacial shape variation on ions' spatial distributions.

Finally, we will begin extending our work on time-independent statistics of ions at the air-water interface to address their impact on dynamics of evaporation. Results from Chandler's and Saykally's groups indicate that transition states for evaporation involve substantial local distortions of the liquid's boundary. Our finding that small ions reshape the natural spectrum of interfacial fluctuations suggests fruitful connections among these efforts.

Articles supported by DOE funding, 2005-2010

1. Geissler, P.L. "Temperature dependence of inhomogeneous broadening: On the meaning of isosbestic points," *J. Am. Chem. Soc.* **2005**, *127*, 13019.

2. Eaves, J.D.; Tokamkoff, A.; Geissler, P.L. "Electric field fluctuations drive vibrational dephasing in water," *J. Chem. Phys. B* **2005**, *109*, 9424.

3. Smith, J.D.; Cappa, C.D.; Wilson, K.R.; Cohen, R.C.; Geissler, P.L.; Saykally, R.J. "Unified description of temperature-dependent hydrogen bond rearrangements in liquid water," *Proc. Natl. Acad. Sci. U.S.A.* **2005**, *102*, 14171.

4. Smith, J.D.; Saykally, R.; Geissler, P.L. "The effects of dissolved halide ions on hydrogen bonding in liquid water," *J. Am. Chem. Soc.* **2007**, *129*, 13847.

5. Noah-Vanhoucke, J.; Smith, J.D.; Geissler, P.L. "Statistical mechanics of sum frequency generation spectroscopy for the liquid-vapor interface of dilute aqueous salt solutions," *Chem. Phys. Lett.* **2009**, *470*, 21.

6. Noah-Vanhoucke, J.; Smith, J.D.; Geissler, P.L. "Toward a simple molecular understanding of sum frequency generation at air-water interfaces," *J. Chem. Phys. B* **2009**, *113*, 4065.

7. Noah-Vanhoucke, J.; Geissler, P.L. “On the fluctuations that drive small ions toward, and away from, interfaces between polar liquids and their vapors,” *Proc. Natl. Acad. Sci. U.S.A.* **2009**, *106*, 15125.

8. Pasqua, A.; Maibaum, L.; Oster, G.; Fletcher, D.A.; Geissler, P.L. "Large-scale simulations of fluctuating biological membranes," *J. Chem. Phys.* **2010**, *132*, 154107.

Program Title: Theoretical Developments and Applications to Surface Science, Heterogeneous Catalysis, and Intermolecular Interactions

Principal Investigator: Mark S. Gordon, 201 Spedding Hall, Iowa Sate University and Ames Laboratory, Ames, IA 50011; mark@si.msg.chem.iastate.edu

Program Scope. Our research effort combines new theory and code developments with applications to a variety of problems in surface science and heterogeneous catalysis, as well as the investigation of intermolecular interactions, including solvent effects in ground and excited electronic states and the liquid-surface interface. Many of the surface science studies are in collaboration with Dr. James Evans. Much of the catalysis effort is in collaboration with Drs. Marek Pruski, and James Evans.

Recent Progress. Chemical processes on and with the Si(100) surface have been one focus of recent efforts. The diffusion of Al on Si(100) was studied using an embedded cluster model and multi-reference electronic structure methods, including CASSCF explorations of the doublet and quartet potential energy surfaces and improved energies with multi-reference perturbation theory. The details of the potential energy surfaces (i.e., the identity of minima and transition states) depend critically on the presence of the bulk that is represented by molecular mechanics (MM). It appears that only when edge effects are minimized by embedding the quantum mechanics (QM) region in a much larger MM region does a consistently realistic picture emerge. Similar results are obtained in the more recent study of Ga diffusion on Si(100). It appears that both Al and Ga can form metal wires on the Si(100) surface. The etching and diffusion of O atoms on the Si(100) surface was also studied with the QM/MM model and both multi-reference methods and the new cluster-in-molecule (CIM) CR-CC(2,3) coupled cluster method. The latter method is very exciting because it combines a coupled cluster method, CR-CC(2,3), that is able break single bonds and account for the diradical character that is inherent in the Si(100) surface) with a novel method (CIM) for greatly speeding up accurate coupled cluster calculations. The CIM method enables the calculation of large clusters that can diminish the importance of the MM part of the embedding scheme. Two complementary approaches for increasing the size s of clusters that can be studied with accurate QM methods are the occupation restricted multiple active space (ORMAS) and the fragment molecular orbital (FMO) methods. The ORMAS method divides a large, intractable active space into chemically sensible subspaces, thereby making a very diffiult calculation feasible. The utility of the ORMAS method has been demonstrated with Si(100) clusters of increasing size. We have now developed a second order perturbation theory method that is built upon ORMAS so that dynamic correlation can be included. The FMO method divides a large species into fragments to facilitate accurate QM calculations on very large systems. A fully analytic FMO gradient has now been derived and implemented in GAMESS (General Atomic and Molecular Electronic Structure System), to enable geometry optimizations and molecular dynamics simulations. The mesoporous silica nanoparticles (MSN) that were in large part designed by the late Victor Lin have received increasing attention due to their catalytic capabilities. Because the MSN species are very complex, we have implemented the ReaxFF force field into

GAMESS and are currently exploring the possibility of using this method to study catalytic processes in MSN species.

The effective fragment potential (EFP) method that is designed to be a sophisticated model potential designed to accurately describe intermolecular interactions has been interfaced with the FMO method, so that low-cost explicit solvent effects can be incorporated into FMO studies. Both FMO-EFP energies and analytic gradients are now available. EFP interfaces have also been derived and implemented for configuration interaction with single excitations (CIS), multi-reference, multi-state perturbation theory, and equations-of-motion (EOM) coupled cluster theory. These interfaces provide an array of tools that are available to study solvent effects on electronic spectra and photochemistry. Initial studies have addressed the aqueous solvation of the n-π^* and π–π^* excitations in uracil. These are by far the most accurate calculations on this topic. The MCSCF-EFP method was used to study solvent relaxation in the low-lying excited states of coumarin. The EFP method was also applied to the study of aqueous solvation of several anions, including bihalide ions and the nitrate ion. The latter study was particularly important, because it demonstrated that, contrary to predictions from simulations with (mostly inadequate) simple model potentials, only a modest number of water molecules are needed to force the anion to the interior. New advances in the EFP method include the development of a general approach to damping the various contributions to the potential and the development and implementation of the QM-EFP exchange repulsion.

Time-dependent density functional theory (TDDFT) is in principle a good compromise between accuracy and computational cost for studying electronic excited states. However, because DFT, and therefore TDDFT, is at it core a single determinant method, there are some phenomena that are very difficult to address with TDDFT. One very important phenomenon is the conical intersections that occur when two or more potential energy surfaces cross. Conical intersections are ubiquitous, and therefore very important, in photochemistry and photobiology. We have implemented the Krylov spin-flip approach with TDDFT and have demonstrated for ethylene, and most recently stilbene, that the new combined method can correctly describe conical intersections and the associated detailed structural information.

Advances have also been made in high performance computational chemistry. We are in the process of systematically developing features of GAMESS for graphical processing unit (GPU) architecture. The first step was to develop GPU code for general two-electron integrals for arbitrary angular momenta, since previous developments had only addressed s and p integrals. The GPU Hartree-Fock code is already available for web download, and the MP2 code has been completed and is being tested. An INCITE grant has enabled us to have access to the BlueGene /P at Argonne, where we have demonstrated that the FMO method allows essentially perfect scaling to the petascale.

Future Plans. The development of the ORMAS-PT2, FMO, and CIM-CR-CC(2,3) methods will allow us to explore fully quantum studies of heterogeneous catalysis, in which we can still minimize edge effects. This can be accomplished because these

methods will allow us to expand the size of the QM region in a computationally efficient manner. The ORMAS-PT2 and CIM-CR-C(2,3) methods will initially be applied to studies of phenomena on the Si(100) surface, such as more extensive studies of diffusion on metals. We will also explore the use of ORMAS-PT2 for the adsorption of substrates on conducting metals, since QM/MM embedded cluster methods are not appropriate for such problems. Preliminary FMO studies have been performed on model MSN species at the Hartree-Fock level of theory with a minimal basis set. The agreement with the fully ab initio method is excellent, so we will now apply FMO with higher levels of theory and reliable basis sets. These calculations will include EFP solvents. The EFP-QM exchange repulsion analytic gradients have been derived, and these will now be implemented so that any solvent can be studied. Related to this, we will work with the ReaxFF developers to obtain improved parameters for silica and silica-X, where X represents atoms in the important substrates. This will improve the ReaxFF capability to address heterogeneous catalysis on MSN species. Many of the catalysis studies will be performed in collaboration with the Pruski and Evans groups.

The spin-flip TDDFT method will be interfaced with the EFP method, so that one can explore photochemistry and photobiology, including conical intersections, in the presence of solvent. The SF-TDDFT method will also be interfaced with our non-adiabatic (vibronic) coupling matrix element code, so that one can study non-adiabatic interactions in solution.

Our GPU developments will continue with the implementation of the various coupled cluster levels of theory that are available in GAMESS, DFT, and TDDFT, as well as analytic HF, DFT, and MP2 gradients. Many of the GPU developments are accomplished in collaboration with Professor Theresa Windus.

References to publications of DOE sponsored research 2009-present

1. L. V. Slipchenko and M.S. Gordon, "Water-benzene interactions: An effective fragment potential and correlated quantum chemistry study", J. Phys. Chem A., 113, 2092 (2009).
2. L. Slipchenko and M.S. Gordon, "Damping functions in the effective fragment potential method", Mol. Phys., 107, 999 (2009).
3. D. Kina, P. Arora, A. Nakayama, T. Noro, M.S. Gordon, and T. Taketsugu, "QM/MM excited-state molecular dynamics study of coumarin 151 in water solution", Int. J. Quantum Chem., 109, 2308 (2009).
4. M.S. Gordon, J.M. Mullin, S.R. Pruitt, L.B. Roskop, L.V. Slipchenko and J.A. Boatz, "Accurate Methods for Large Molecular Systems", J. Phys. Chem. B (Invited Centennial Feature Article), 113, 9646 (2009).
5. T. Nagata, D. Fedorov, K. Kitaura, and M.S. Gordon, "A Combined Effective Fragment Potential - Fragment Molecular Orbital Method. I. The Energy Expression and Initial Applications", J. Chem. Phys., 131, 024101 (2009)
6. D.D. Zorn, M.A. Albao, J.W. Evans, and M.S. Gordon, "Binding and Diffusion of Al Adatoms and Dimers on the Si(100)-2x1 Reconstructed Surface: A Hybrid QM/MM Embedded Cluster Study", J. Phys. Chem. C, 113, 7277 (2009).

7. Y. Miller, J. Thomas, D.D. Kemp, B. Finlayson-Pitts, M.S. Gordon, D. Tobias, and R.B. Gerber, "Structure of Large Nitrate-Water Clusters at Ambient Temparatures: Simulations with Effective Fragment Potentials and Force Fields with Implications for Atmospheic Chemistry", J. Phys. Chem. A, 113, 12805 (2009).
8. N. Minezawa and M.S. Gordon, "Optimizing Conical Intersections by Spin-Flip Density Functional Theory: Application to Ethylene", J. Phys. Chem. A, 113, 12789 (2009).
9. D.D. Kemp and M.S. Gordon, "Aqueous Solvation of Bihalide Ions", J. Phys. Chem. A, 114, 1298 (2010).
10. D.D. Kemp, J. Rintelman, M.S. Gordon, and J.H. Jensen, "Exchange Repulsion between Effective Fragment Potentials and *Ab Initio* Molecules", Theor. Chem. Accts., 125, 481 (2010).
11. Y. Ge, M.S. Gordon, F. Battaglia, and R.O. Fox, "Theoretical Study of the Pyrolysis of Methyltrichlorosilane in the Gas Phase. 3. Reaction Rate Constants", J. Phys. Chem. A, 114, 2384 (2010).
12. A. Asadchev, V. Allada, J. Felder, B.M. Bode, T.L. Windus, and M.S. Gordon, "Uncontracted Rys Quadrature Implementation of up to g Functions on Graphical Processing Units", J. Comp. Theor. Chem., 6, 696 (2010).
13. P. Arora, L.V. Slipchenko, S.P. Webb, A. DeFusco, and M.S. Gordon, "Solvent-Induced Frequency Shifts: Configuration Interaction Singles combined with the Effective Fragment Potential Method, J. Phys. Chem. A, 114, 6742 (2010).
14. P. Arora, W. Li, P. Piecuch, J.W. Evans, M. Albao, and M.S. Gordon, "Diffusion of atomic oxygen on the Si(100) surface", J. Phys. Chem. C, 114, 12649 (2010).
15. D. Ghosh, D. Kosenko, V. Vanovschi, C.F. Williams, J.M. Herbert, M.S. Gordon, M.W. Schmidt, L.V. Slipchenko, and A.I. Krylov, "Non-covalent interactions in extended systems described by the Effective Fragment Potential method: Theory and application to nucleobase oligomers", J. Phys. Chem. A, 114, 12739 (2010).
16. T Nagata, D.G. Fedorov, K. Kitaura, and M.S. Gordon, "A combined effective fragment potential-fragment molecular orbital method. II. Analytic gradient and application to the geometry optimization of solvated tetraglycine and chignolin", J. Chem. Phys., 134, 034110 (2011).
17. T. Nagata, K. Brorsen, D.G. Fedorov, K. Kitaura, and M.S. Gordon, "Analytic energy gradient in the fragment molecular orbital method", J. Chem. Phys., 134, 124115 (2011).
18. A. DeFusco and M.S. Gordon, "Solvent-Induced Shifts in the Electronic Spectra of Uracil", J. Phys. Chem., in press.

Fluctuations in Macromolecules Studied Using Time-Resolved, Multi-spectral Single Molecule Imaging

Carl Hayden
Sandia National Laboratories
P. O. Box 969, MS 9055
Livermore, CA 94551-0969
cchayde@sandia.gov

Haw Yang
Department of Chemistry
Princeton University
Princeton NJ 08544
hawyang@princeton.edu

Program Scope

In this research program we study local chemical environments and their fluctuations in systems including single macromolecules and larger molecular assemblies. Much of our recent work has been directed toward extending our studies to proteins bound on lipid membranes and attempting to directly relate molecular scale processes to macroscopic phenomena. For our research we use a variety of imaging techniques including multi-parameter confocal, widefield and total internal reflection microscopies. We focus on simultaneous measurement of multiple fluorescence properties in an effort to fully characterize local molecular environments. A unique instrument in our laboratory is a time-resolved multispectral confocal microscope that simultaneously measures fluorescence spectra and lifetimes with single-molecule sensitivity.[1] This instrument is designed to extract the maximum information from fluorescent probes. It records the wavelength (λ), and emission time relative to excitation (τ) for each detected fluorescence photon along with its absolute detection time (Δ) so that correlations among all the fluorescence properties are maintained. Fully correlated photon records of λ, p, τ, and Δ improve the capability of fluorescence measurements to characterize local chemical environments. The record of fluorescence photon emission provides detailed information on chemical processes, including energy transfer and conformational changes, on time scales from picoseconds to minutes. These experimental capabilities are combined with the development of rigorous analysis based on maximum information methods to allow us to more clearly resolve the fluctuations of macromolecules and the chemical environments around them.

Recent Progress:

Structural distributions of poly-L-proline peptides

We have had a long term effort to study the structure of poly-L-proline peptides using Förster-type resonance energy transfer (FRET) measurements.[2,3] An extensive experimental and molecular modeling study we recently completed examined how the structural distribution could be determined and used as an effective means for extracting molecular mechanical properties.[4] End-to-end distance distributions for a series of short poly-l-proline peptides with the sequence P_nCG_3K-biotin (n = 8, 12, 15 and 24) were used to experimentally illustrate this new approach. High-resolution single-molecule FRET experiments were carried out and the conformation-resolving power was characterized and compared to the conventional constant-time binning

procedure for FRET data analysis. It was shown that commonly adopted theoretical polymer models including the worm-like chain, the freely jointed chain, and the self-avoiding chain, could all predict and thus not be distinguished by the averaged end-to-end distances. However, all failed to model the molecular details gained by conformational distribution analysis. Specifically, by fitting the molecular conformational distribution to a semi-flexible polymer model, the effective persistence lengths for the series of short poly-l-proline peptides were found to be size-dependent with values of ~190 Å, ~67 Å, ~51 Å, and ~76 Å for n = 8, 12, 15, and 24, respectively—the first experimental evidence of such behavior on the molecular level. Comprehensive computational modeling was carried out to gain further insights for this surprising discovery. It was found that P_8 exists as the extended all-*trans* isomer whereas P_{12} and P_{15} predominantly contained one proline residue in the *cis* conformation. P_{24} exists as a mixture of one-*cis* (75%) and two-*cis* (25%) isomers where each isomer contributes to an experimentally resolvable conformational mode. This work demonstrates the resolving power of the distribution-based approach, and the capacity of integrating high-resolution single-molecule FRET experiments with molecular modeling to reveal detailed structural information about the conformation of molecules on the length scales relevant to the study of biological molecules.

Protein-lipid membrane interactions

The interactions of proteins and lipid membranes are crucial for energy production, storage and transduction in biological systems. Studies of these interactions are challenging because of the varied local environments, from hydrophobic to hydrophilic, experienced by the proteins, and the difficulty of placing active membrane associated proteins into artificial model membranes. Our multi-parameter fluorescence techniques are well suited to investigating proteins in membrane environments. We have been working to create a variety of lipid membrane surfaces and vesicles that can bind and incorporate proteins and exhibit properties of natural membranes. We have developed several lipid membrane systems that effectively bind proteins.[5] Our current studies focus on proteins that create curvature and hence membrane structures. They also explore the role of lipid membranes' composition and phase on their interactions with proteins.

Tubulation of vesicles by steric confinement of proteins

Deformation of lipid membranes into curved structures such as buds and tubules is essential to many cellular structures. Binding of specific proteins to lipid membranes has been shown to promote membrane bending during endocytosis and transport vesicles formation. Additionally, specific lipid species are found to co-localize with many curved membrane structures, inspiring ongoing exploration of a variety of roles for lipid domains in membrane bending. However, the specific mechanisms by which lipids and proteins collaborate to induce curvature remain unknown. Using artificial giant unilamellar vesicles (GUVs) that contain domains with metal-chelating lipids designed for high affinity to his-tagged proteins, we show that crowding on lipid domain surfaces, even of proteins such as GFP not normally associated with membrane bending, spontaneously bends the domain into stable buds and tubules.[6] Our results suggest that confining structures, such as lipid

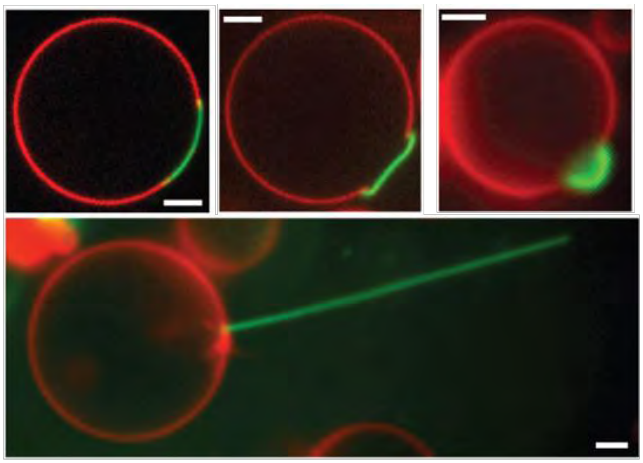

Figure1. Protein (green) is confined to a domain on a lipid vesicle. Crowding of the protein causes domain distortion that often leads to tubule formation

domains and protein lattices, can amplify membrane bending by concentrating the steric interactions between bound proteins. This observation highlights a fundamental physical mechanism for membrane bending that may help explain how lipids and proteins collaborate to create the highly curved structures observed *in vivo*. The protein binding lipids used in these experiments form a gel-phase domain in a fluid vesicle. Tubule formation is found to depend upon the nature of the fluid-phase lipids and using fluorescence correlation spectroscopy we have demonstrated that these lipids enter and partially fluidize the otherwise gel-phase domain.

Targeting proteins to lipid domains of controlled phase

In the presence of sterols, such as cholesterol, membranes of lipid mixtures can separate into fluid liquid-disordered phases and liquid-ordered (Lo) phases of varied fluidity. These phases influence the function of membrane proteins and have been postulated to lead to protein sorting and clustering. Therefore, for our studies of protein membrane interactions we need control over lipid phase and especially protein binding to specific phases. A new metal-chelating lipid-like molecule, DPIDA, was designed by collaborator Dr. Darryl Sasaki, to partition into Lo phases. Studies performed on GUVs with varying mole fractions of dipalymitoylphosphatidylcholine (DPPC), cholesterol, and diphytanoylphosphatidyl choline (DPhPC), showed DPIDA selectively partitioned into either gel or liquid-ordered phases depending on membrane composition. Fluorescence imaging established the phase behavior of the resulting quaternary lipid system. Fluorescence correlation spectroscopy confirmed the fluidity of the Lo phase containing DPIDA. The iminodiacetic acid (IDA) headgroup of DPIDA can form the Cu(II)-IDA complex that exhibits a high affinity for histidine residues. His-tagged proteins were bound specifically to domains enriched in DPIDA, demonstrating the capacity to target protein binding selectively to both gel and Lo phases. Pressure from the crowding of surface-bound proteins transformed the domains into tubules with persistence lengths that depended on the phase state of the lipid domains. We now have the capability to produce and bind proteins to domains of any lipid phase in GUVs.

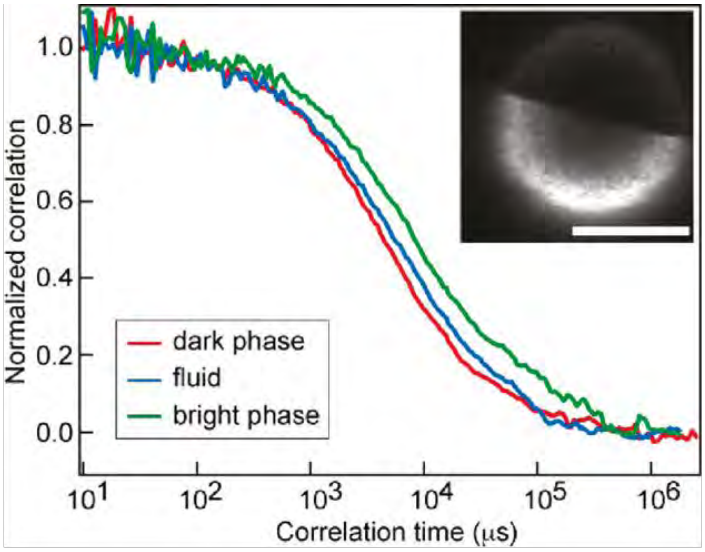

Figure2. Fluorescence correlation spectroscopy shows coexistence of liquid ordered(dark) and disordered(bright) phases with mobility of a fluid membrane. Vesicle is composed of roughly equal amounts of DPhPC, DPIDA, cholesterol and DPPC.

Ongoing Work and Future Plans:

Epsin1 bends membranes by molecular crowding

We are currently incorporating natural protein binding lipids into GUVs to investigate how the binding mechanism influences the protein membrane interaction. Epsin1 is a natural membrane bending protein that binds to membrane surfaces by recognizing the lipid phosphatidylinositol-4,5-bisphosphate (PI(4,5)P2) and inserting an amphipathic peptide helix. We have developed artificial GUVs containing (PI(4,5)P2) that effectively bind the Epsin1 (ENTH domain). Using fluorescence lifetime imaging to detect density dependent FRET of

labeled Epsin1 ENTH we find that a surface coverage of greater than 20% is required to bend membranes in these GUVs. A simple mechanical model suggests that this high protein density could lead to membrane bending simply through steric interactions between tightly-bound diffusing proteins, regardless of how the proteins are attached to the membrane. To test this idea, we replaced ENTH's helix with a hexa-histidine tag, which strongly binds metal chelating lipids, measured the protein surface coverage required to induce bending, and found a similar threshold of approximately 20%. Our results demonstrate that Epsin1 can bend membranes through molecular crowding. Contrary to the mechanisms previously proposed, these findings suggest that the amphipathic anchoring motifs found frequently in membrane bending proteins may function to enable crowding by increasing protein-membrane affinity, rather than directly bending membranes via insertion.

Voltage gated ion channels

Ion channels and pumps are important in energy storage, transduction and ion transport in all biological systems. We are beginning studies of the proteins that comprise voltage gated ion channels. Many ion channels are comprised of multiple subunits, commonly as a tetramer. Our first studies will investigate the formation of functioning channels from monomer subunits in artificial membranes. Initial studies will involve peptides, such as alamethicin, that self-assemble into ion channels.

References:

1. Luong, A.K.; Gradinaru, C.C.; Chandler, D.W. and Hayden, C.C. *J. Phys. Chem. B*, **2005,** *109***,** 15691.
2. Watkins, L. P.; Yang, H. *Biophysical Journal* **2004**, *86*, 4015-4029.
3. Hanson, J. A.; Duderstadt, K.; Watkins, L. P.; Bhattacharyya, S.; Yang, H. *Proc. Natl. Acad. Sci. U.S.A.* **2007**, *104*, 18055-18060.
4. Hanson, J.A.; Brokaw, J.; Hayden, C.C.; Chu, J.-W. and Yang, H. *Chem. Phys., submitted.*.
5. Hayden, C.C.; Hwang, J.S.; Abate, E.A.; Kent, M.S. and Sasaki, D.Y. *J. Am. Chem. Soc.,* **2009**, *131*, 8728.
6. Stachowiak, J. C.; Hayden, C.C. and Sasaki, D.Y. *PNAS*, **2010**, *107*, 7781.
7. Stachowiak, J. C.; Hayden, C.C.; Sanchez, M.A.A.; Wang, J.; Bunker, B.C.; Voigt, J.A. and Sasaki, D.Y. *Langmuir* **2011,** *27*, 1457-1462.

DOE sponsored publications, 2008-2011

1. C. S. Xu, H. Kim, C. C. Hayden and H. Yang, "Joint Statistical Analysis of Multi-Channel Time Series from Single Quantum Dot-$(Cy5)_n$ Constructs," *J. Phys. Chem. B,* **112** (19), 5917-5923, 2008.
2. H. Liu, G. D. Bachand, H. Kim, C. C. Hayden, E. A. Abate, and D. Y. Sasaki, "Lipid Nanotube Formation from Streptavidin-Membrane Binding," *Langmuir,* **24** (8), 3686 -3689, 2008.
3. C. C. Hayden, J. S. Hwang, E. A. Abate, M. S. Kent and D. Y. Sasaki, "Directed Formation of Lipid Membrane Microdomains as High Affinity Sites for His-Tagged Proteins," *J. Am. Chem. Soc.,* **131** (25), 8728–8729, 2009.
4. J. C. Stachowiak, C. C Hayden and D.Y. Sasaki, "Steric Confinement of Proteins on Lipid Membranes Can Drive Curvature and Tubulation," *PNAS*, **107**, 7781, 2010.
5. J. C. Stachowiak, C. C. Hayden, M. A. A. Sanchez, J. Wang, B. C. Bunker, J. A. Voigt and D. Y. Sasaki, "Targeting Proteins to Liquid-Ordered Domains in Lipid Membranes," *Langmuir*, **27**, 1457-1462, 2011.
6. J. A. Hanson, J. Brokaw, C. C. Hayden, J.-W. Chu and H. Yang, "Structural Distributions from Single-Molecule Measurements as a Tool for Molecular Mechanics," *Chem. Phys.*, submitted.

Program Title: "SISGR: Single Molecule Chemical Imaging at Femtosecond Time Scales" (DOE Grant Number: DE-SC0001785)

PI: Mark C. Hersam, Professor of Materials Science and Engineering, Chemistry, and Medicine; Northwestern University, 2220 Campus Drive, Evanston, IL 60208-3108;
Phone: 847-491-2696; Fax: 847-491-7820; E-mail: m-hersam@northwestern.edu;
WWW: http://www.hersam-group.northwestern.edu/

Co-PIs: Matthias Bode (Argonne National Lab), Jeffrey R. Guest (Argonne National Lab), Nathan P. Guisinger (Argonne National Lab), George C. Schatz (Northwestern University), Tamar Seideman (Northwestern University), Richard P. Van Duyne (Northwestern University)

1. Program Overview

Imaging molecular functionality with atomic spatial resolution and femtosecond temporal resolution will enable improved understanding of light-matter interactions and thus has the potential to impact the design of photovoltaic, photosynthetic, and photocatalytic materials and devices. While ultra-high vacuum (UHV) scanning tunneling microscopy (STM) can image and manipulate single molecules with atomic precision on surfaces, its temporal resolution is typically limited to the millisecond bandwidth of current preamplifiers. Furthermore, scanning tunneling spectroscopy (STS) only provides indirect chemical identification via measurements of the electronic density of states. On the other hand, pump-probe spectroscopy with ultrafast lasers can routinely achieve femtosecond temporal resolution. In addition, chemical fingerprinting can be achieved with vibrational spectroscopies such as surface-enhanced Raman spectroscopy (SERS). However, these optical techniques struggle to overcome the diffraction limit, which often implies spatial resolution at the micron scale. This SISGR program seeks to overcome the respective limitations of UHV STM and laser spectroscopy by integrating these techniques into one experimental platform. This interdisciplinary challenge is being pursued by a multidisciplinary and multi-institutional team with expertise in UHV STM, STS, SERS, femtosecond pump-probe laser spectroscopy, and innovative theoretical and computational modeling techniques. Ongoing work is addressing fundamental light-matter interactions at the single molecule limit including nonequilibrium electron transfer, energy transfer, reversible photochemistry (e.g., photoisomerization), and irreversible photochemistry (e.g., light-driven desorption, dissocation, and polymerization). Since the systems and substrates to be studied are directly applicable to dye-sensitized solar cells, organic photovoltaics, and photocatalysis, this research program will inform efforts to improve alternative energy technologies in addition to impacting the fundamental scientific goals outlined in the DOE Grand Challenges.

2. Recent Progress and Future Plans

2.1. Ultrafast Single-Molecule Raman Spectroscopy

A primary goal of this SISGR program is the development of tools and techniques that will enable ultrafast Raman spectroscopy with single molecule sensitivity. Toward this end, progress has been made in several areas:

(1) *Single molecule surface-enhanced Raman spectroscopy (SMSERS)*: The isotopologue proof of SMSERS has recently been extended to crystal violet [1].

(2) *Surface-enhanced femtosecond stimulated Raman spectroscopy (SE-FSRS)*: FSRS is a state-of-the-art, coherent and stimulated Raman technique that can simultaneously achieve a spectral and temporal resolution below the limit dictated by the time-energy uncertainty

principle. With this ultrafast technique, the vibrational structure of molecules bound to metal nanoparticles has been probed for the first time [2]. Time-resolved and single-molecule SE-FSRS experiments are in progress.

(3) *UHV tip-enhanced Raman spectroscopy (TERS)*: UHV-TERS is a route toward site-specific, single-molecule spectroscopy from a surface imaged with atomic resolution. Achievement of this goal requires the fabrication of plasmonic tips capable of both efficient Raman enhancement and high resolution STM imaging under laser irradiation. Electrochemical etching techniques to fabricate Ag and Au STM tips have been developed. In addition, tungsten tips with electron-beam evaporated silver coatings have been fabricated. Using these plasmonic tips, sub-molecular resolution STM images of copper phthalocyanine (CuPc) on Si(100) have been achieved with 1 mW of 633 nm laser light focused on the tip apex. Furthermore, UHV-TERS spectra of Malachite Green on an evaporated silver film on glass have been successfully obtained with a Ag tip. Progress has also been made toward single-molecule sensitivity in ambient TERS using an isotopologue approach that will be extended to UHV-TERS experiments in future work.

(4) *Modeling the electrodynamics of plasmonic tip structures*: This work on modeling tip structures was initially directed at understanding nonlocal electrodynamic effects, and how this reduces the intensity of fields at metal tips and other locations [3,4]. However, standard local electrodynamics methods were found to give results that are correct except for tips with extremely sharp points that are not likely to be realistic experimentally. Consequently, more recent efforts have switched to using local electrodynamics with the goal of determining the tip structures and wavelength ranges of most interest in TERS [5]. In particular, the variation of hot spot behavior with tip structure for wedge-shaped tips is being studied using a quasistatic approach that gives nearly analytical results for these tips. Also, the FDTD method is being employed to calibrate and provide higher accuracy to the quasistatic results.

(5) *Coupling quantum and electrodynamics for surface-enhanced optical phenomena*: Efforts to couple quantum mechanics to classical electrodynamics have considered both time domain and frequency domain theories. In the time domain, a real-time TDDFT method is being developed that determines induced polarization and then Raman intensities by adding a light pulse into the Kohn-Sham equations. Current work is designed to extend this method to consider the nonlinear optical response, which is especially important in stimulated Raman scattering. In the frequency domain, a code based on the NWCHEM program has been developed to calculate resonant frequency-dependent polarizability derivatives. Benchmark results for pyridine/silver nanoparticles have determined Raman intensities that are similar to the time-domain results but are calculated in a more efficient manner [6]. This approach provides a straightforward perturbation approach to the determination of nonlinear optical response.

(6) *Ultrafast molecular nanoplasmonics*: Theoretical calculations have illustrated the possibility and implications of molecular focusing and alignment in the spatially and orientationally inhomogeneous fields generated by nanoparticles [7,8] and introduced a rigorous formalism of oblique incidence from disperse media with implications for plasmon focusing [9].

2.2. Molecular-Resolution Characterization and Manipulation of Surface Chemistry

This SISGR program is actively exploring UHV STM methods for characterizing and manipulating chemical reactions at the molecular scale. For example, electron-driven and photon-driven chemistries are being studied on the surfaces of electronic materials such as silicon and graphene. The band gap of silicon presents unique opportunities to drive chemical

reactions with reduced screening (compared to metal surfaces), while graphene is a transparent conductive material with emerging applications in photovoltaics. Specific efforts include:

(1) *Directed assembly of one-dimensional organosilicon nanostructures*: One-dimensional self-assembly of *o*-phthaldialdehyde, phenylacetylene, and styrene has been templated with atomic-scale precision using feedback-controlled lithography (FCL) on Si(100)-2x1:H surfaces [10,11]. Of particular interest are heteromolecular one-dimensional nanostructures of phenylacetylene and styrene since they enable direct studies of the influence of the level π-conjugation on the electronic properties of organosilicon nanostructures [11].

(2) *Theory and experiment for STM-driven organic molecule desorption from silicon*: Desorption of saturated hydrocarbons (e.g., cyclopentene covalently bound to silicon) has been quantified using FCL and understood using inelastic tunneling theory [12]. In particular, theory accounts for nonequilibrium dynamics, open boundary conditions, strong vibronic interactions, and dissipation by substrate phonon and electron-hole pair excitation [13,14].

(3) *Characterization and manipulation of organic molecules on graphene*: Organic adlayers of 3,4,9,10-perylene-tetracarboxylic acid dianhydride (PTCDA), N,N′-dioctyl-3,4,9,10-perylenedicarboximide (PTCDI-C8), 10,12 pentacosadiynoic acid (PCA), and 4-nitrophenyl diazonium (4-NPD) tetrafluoroborate have been assembled and characterized at the molecular scale with UHV STM and STS on epitaxial graphene on SiC(0001) [15,16]. Furthermore, FCL has been employed to form heteromolecular nanostructures of PTCDA and PTCDI-C8, while graphene nanoribbons have been nanopatterned by FCL on 4-NPD functionalized surfaces. Ongoing work is exploring ultraviolet photopolymerization of PCA on graphene.

(4) *Characterization and manipulation of inorganic atomic adsorbates on graphene*: In this work, graphene is grown via chemical vapor deposition on copper [17-19]. STM studies have revealed the first atomic-scale structural information of graphene on polycrystalline Cu. In addition, reversible and local modification of the electronic properties of graphene by hydrogen passivation and subsequent STM-driven electron-stimulated desorption has been demonstrated. Future work will explore alternative inorganic atomic adsorbates (e.g., oxygen and fluorine).

2.3. Reversible Rectification in Sub-Monolayer Molecular *p-n* Junctions

The interfaces in bulk heterojunction organic photovoltaics are critical to their functioning; however, characterization of these interfaces is non-trivial since they are buried in device-scale structures. In order to gain insight into correlations between structure and function, model *p-n* junctions with a prototypical acceptor-donor system – C_{60} and pentacene – have been fabricated in UHV and characterized with STM and STS. STM reveals that submonolayer structures of pentacene on close-packed C_{60} (on Cu(111)) form an upright close-packed arrangement. STS spectra obtained on this heterojunction show rectification of the current between the tip and substrate in the direction expected for this donor-acceptor orientation. In the opposite orientation (i.e., C_{60} on pentacene), the direction of rectification reverses as expected. A rate equation-based model reproduces the qualitative behavior observed in these studies.

In order to correlate photophysical function with structure, these measurements should ideally be performed under laser excitation. The challenge in this case rests with extracting the weak photoresponse of these structures from current changes due to laser heating of the tip-sample junction. Consequently, a laser-STM has been developed with integrated high-numerical-aperture optics behind the sample to provide a small (~1.5 μm) and stable laser spot. This small spot provides large optical intensities with minimal laser power, thus minimizing tip-sample heating. Ongoing work is exploring TERS in this geometry, including the observation of the G and 2D peaks in graphene when a plasmonic Au STM tip is in tunneling range.

3. Publications

[1] S. L. Kleinman, E. Ringe, N. Valley, K. L. Wustholz, E. Phillips, K. A. Scheidt, G. C. Schatz, and R. P. Van Duyne, "Single-molecule surface-enhanced Raman spectroscopy of crystal violet isotopologues: Theory and experiment," *J. Am. Chem. Soc.*, **133**, 4114 (2011).

[2] R. R. Frontiera, A.-I. Henry, N. L. Gruenke, and R. P. Van Duyne, "Surface enhanced-femtosecond stimulated Raman spectroscopy," *J. Phys. Chem. Lett.*, submitted, 2011.

[3] J. M. McMahon, S. K. Gray, and G. C. Schatz, "Nonlocal dielectric effects in core-shell nanowires," *J. Phys. Chem. C*, **114**, 15903 (2010).

[4] N. Harris, L. K. Ausman, J. M. McMahon, D. J. Masiello, and G. C. Schatz, "Computational electrodynamics methods," in *Computational Nanoscience*; E. Bichoutskaia, Ed.; RSC theoretical and computational chemistry series, **4**, 148 (2011).

[5] M. Sukharev and T. Seideman, "Optical properties of metal tips for tip-enhanced spectroscopies," *J. Phys. Chem.*, **113**, 7508 (2009).

[6] J. M. Mullin and G. C. Schatz, Survey of density functional approximations for surface enhanced Raman (SERS) spectroscopy, *Comput. Theor. Chem.*, submitted, 2011.

[7] M. Artamonov and T. Seideman, "Molecular focusing and alignment with plasmon fields," *Nano Lett.*, **10**, 4908 (2010).

[8] M. Sukharev, P. R. Sievert, L. Luan, T. Seideman, and J. B. Ketterson, "Perfect coupling of light to surface plasmons with ultranarrow linewidths," *J. Chem. Phys.*, **131**, 034708 (2009).

[9] L. Zhang and T. Seideman, "Rigorous formulation of oblique incidence scattering from dispersive media," *Phys. Rev. B*, **82**, 155117 (2010).

[10] M. A. Walsh and M. C. Hersam, "STM study of one-dimensional *o*-phthalaldehyde chain reactions on the Si(100)-2x1:H surface," *Chem. Comm.*, **46**, 1153 (2010).

[11] M. A. Walsh, S. R. Walter, K. H. Bevan, F. M. Geiger, and M. C. Hersam, "Phenylacetylene one-dimensional nanostructures on the Si(100)-2x1:H surface," *J. Am. Chem. Soc.*, **132**, 3013 (2010).

[12] N. L. Yoder, R. Jorn, C.-C. Kaun, T. Seideman, and M. C. Hersam, "Current-driven desorption at the organic molecule-semiconductor interface: Cyclopentene on Si(100)," *Current-Driven Phenomena in Nanoelectronics*, T. Seideman, Ed.; World Scientific (2011).

[13] R. Jorn and T. Seideman, "Implications and applications of current induced dynamics in molecular junctions," *Acc. Chem. Res.*, **43**, 1186 (2010).

[14] R. Jorn and T. Seideman, "Competition between current-induced excitation and bath-induced decoherence in molecular junctions," *J. Chem. Phys.*, **131**, 244114 (2009).

[15] Md. Z. Hossain, M. A. Walsh, and M. C. Hersam, "Scanning tunneling microscopy, spectroscopy, and nanolithography of epitaxial graphene chemically modified with aryl moieties," *J. Am. Chem. Soc.*, **132**, 15399 (2010).

[16] Q. H. Wang and M. C. Hersam, "Nanofabrication of heteromolecular organic nanostructures on epitaxial graphene via room temperature feedback-controlled lithography," *Nano Lett.*, **11**, 589 (2011).

[17] L. Gao, J. R. Guest, and N. P. Guisinger, "Epitaxial graphene on Cu(111)," *Nano Lett.*, **10**, 3512 (2010).

[18] Q. Yu, *et al.*, "Control and characterization of individual grains and grain boundaries in graphene grown by chemical vapour deposition," *Nature Materials*, in press, 2011.

[19] J. Cho, L. Gao, J. Tian, H. Cao, W. Wu, Q. Yu, J. R. Guest, Y. P. Chen, and N. P. Guisinger, "Atomic-scale investigation of graphene grown on Cu foil and the effects of thermal annealing," *ACS Nano*, in press, 2011.

Chemical Kinetics and Dynamics at Interfaces

Laser induced reactions in solids and at surfaces

Wayne P. Hess (PI), Alan G. Joly and Kenneth M. Beck

Chemical and Materials Sciences Division
Pacific Northwest National Laboratory
P.O. Box 999, Mail Stop K8-88,
Richland, WA 99352, USA
wayne.hess@pnl.gov

Additional collaborators include A.L. Shluger, P.V. Sushko, N. Govind, K. Kowaslki
J.T. Dickinson, and O. Diwald

Program Scope

The chemistry and physics of electronically excited solids and surfaces is relevant to the fields of photocatalysis, radiation chemistry, and solar energy conversion. Irradiation of solid surfaces by UV, or higher energy photons, produces energetic species such as core holes and free electrons, that relax to form electron-hole pairs, excitons, and other transient species capable of driving surface and bulk reactions. These less energetic secondary products induce the transformations commonly regarded as radiation damage. The interaction between light and nanoscale oxide materials is fundamentally important in catalysis, microelectronics, sensor technology, and materials processing. Photo-stimulated desorption, of atoms or molecules, provides a direct window into these important processes and is particularly indicative of electronic excited state dynamics. Excited state chemistry in solids is inherently complex and greater understanding is gained using a combined experiment/theory approach. We therefore collaborate with leading solid-state theorists who use *ab initio* calculations to model results from our laser desorption and photoemission experiments.

Approach:

Photon energies are chosen to excite specific surface structural features that lead to particular desorption reactions. The photon energy selective approach takes advantage of energetic differences between surface and bulk exciton states and probes the surface exciton directly. We measure velocities and state distributions of desorbed atoms or molecules from ionic crystals using resonance enhanced multiphoton ionization and time-of-flight mass spectrometry. Application of this approach to controlling the yield and state distributions of desorbed species requires detailed knowledge of the atomic structure, optical properties, and electronic structure. To date we have thoroughly demonstrated surface-selective excitation and reaction on alkali halides. However, technological applications of alkali halides are limited compared to oxide materials. Oxides serve as dielectrics in microelectronics and form the basis for exotic semi- and super-conducting materials. Although the electronic structure of oxides differs considerably from alkali halides, it now appears possible to generalize the exciton model for laser surface reactions to these interesting new materials. Our recent studies have explored nanostructured samples grown by chemical vapor deposition or thin films grown by reactive ballistic deposition (RBD) in addition to cleaved single-crystal surfaces. We have demonstrated that desorbed atom product states can be selected by careful choice of laser wavelength, pulse duration, and delay between laser pulses. Recently, we have applied the technique of photoemission electron microscopy

(PEEM) to these efforts. In particular, we are developing a combined PEEM two-photon photoemission approach to probe spatially-resolved excited electronic state dynamics in nanostructured materials.

Recent Progress

Calculations indicate that it is possible to excite preferentially either the surface or bulk of ionic materials (crystals) and induce surface or bulk specific reactions. We have excited low-coordinated surface sites (e.g. corners, steps and terraces) using sub-bandgap photons and induced hyperthermal neutral atom emission. In parallel experiments we excited bulk transitions using above bandgap photon energies and induce only thermal neutral atom emission. The kinetic energy distributions provide a signature for the surface or bulk origin of the desorption mechanism. In the particular case of rough CaO films, we irradiate nanostructured CaO samples using tunable UV laser pulses and observe hyperthermal O-atom emission indicative of a surface excited-state desorption mechanism. The O-atom yield increases dramatically with photon energy, between 3.75 and 5.4 eV, well below the bulk absorption threshold. The peak of the kinetic energy distribution does not increase with photon energy in this energy range. When the data are analyzed, in the context of a laser desorption model developed previously for nanostructured MgO samples, the results are consistent with desorption induced by exciton localization at corner-hole trapped surface sites following electronic energy transfer from higher coordinated surface sites.

Since hyperthermal desorption is typically observed following surface excitation, we surmise that the hyperthermal O-atom desorption, from metal oxides, is due to electronic state dynamics induced by *surface specific* excitation. In contrast, *bulk* excitation of these oxides at higher photon energies (7.9 eV) has always led to lower kinetic energy (thermal) O-atom emission. Similar results were obtained in irradiation studies of alkali halides. Recently we observed a new highly-hyperthermal (HHT) O-atom desorption from nanostructured CaO using 6.4 eV photons, which strongly excite the bulk material. The resulting O-atom kinetic energy distribution peaks near 0.7 eV, more than four times that observed previously for either CaO or MgO following surface specific excitation. Irradiation of a nanostructured CaO sample with 6.4 eV photons charges the surface and creates surface hole species. Further absorption of 6.4 eV photons in the bulk induces indirect $\Gamma - X$ transitions and produces bulk excitons, in which the electrons occupy 3*d* states of Ca ions. These bulk excitons can diffuse at room temperature towards the surface and subsequently tunnel to the surface layer or undergo Förster resonance energy transfer to surface trapped hole sites to form a trapped hole + exciton complex. We suggest that some amount of this excess exciton energy is transferred into the kinetic energy of desorbing O-atoms making them highly-hyperthermal.

Very intense photoelectron emission has been observed from localized points on nanostructured metal surfaces following UV femtosecond (fs) laser excitation. The regions of intense emission, dubbed ‘hot spots’, are due to collective charge oscillations, termed localized surface plasmons (LSPs). The intensity of the incident electric field can be amplified several orders of magnitude when resonantly coupled with the LSP mode of the nanostructure. The electromagnetic (EM) field amplification is largely responsible for non-linear phenomena such as surface enhanced Raman scattering (SERS) although SERS intensities are a convolution of both electronic and chemical Raman enhancement factors. While the EM contribution is believed to dominate the overall SERS signal, obtaining a quantitative measure of individual chemical and EM contributions, from a single molecule or hot spot, has proved challenging.

It is possible to measure the field enhancement due to a nanoparticle LSP using photoemission

electron Microscopy (PEEM). By applying a two-photon excitation scheme, using fs laser pulses, isolated EM enhancements can be examined and photoemission yields can be correlated with detailed structural images from complementary microscopic techniques such as scanning electron microscopy (SEM). Polystyrene spherical nanoparticles (average diameter ~ 465 nm) were deposited on an atomically flat mica substrate and covered with a 50 nm Ag thin film. This sample geometry provides a clear distinction between two fundamental shapes, *i.e.* a flat surface and a semi-shell nanoparticle. Since both particle and substrate are coated with the same 50 nm thick Ag film, intense nanoparticle photoemission can be attributed to field enhancement derived from the LSP. We determined the EM enhancements for a collection of 95 individual nanoparticles. The distribution is asymmetric with a median value of roughly 16 but with some particles yielding values between 100 and 375. We then correlated the photoemission yields with detailed structures of the individual particles and were able to associate particular anomalous structures with the most intense electron emission.

Future Directions

Since it is possible to selectively excite terrace, step, or corner surface sites, we have explored various sample preparation techniques that produce high concentrations of low-coordinated surface sites such as 4-coordinated steps and 3-coordinated corner or kink sites. In particular, we have employed reactive ballistic deposition (a technique developed in Bruce Kay's lab) to grow very high surface area MgO and CaO thin films. These films have been thoroughly characterized using XPS, SEM, TEM, and XRD techniques. Similarly, we have also studied laser desorption of MgO and CaO nano-powders grown by a chemical vapor deposition technique (in collaboration with Oliver Diwald of the Technical University of Vienna). The MgO nano-powders show cubic structure and edge lengths ranging between 3 and 10 nm (through TEM analysis).

If exciton-based desorption can be generalized from alkali halides to metal oxides then selective excitation of specific surface sites could lead to controllable surface modification, on an atomic scale, for a general class of technologically important materials. While exciton-based desorption is plausible for MgO and CaO, we note that the higher valence requires a more complex mechanism. With the aid of DFT calculations we have developed such a hyperthermal desorption mechanism that relies on the combination of a surface exciton with a three-coordinated surface-trapped hole, a so-called "hole plus exciton" mechanism. In every instance we have studied, a hyperthermal O-atom KE distribution can be linked to an electronic surface excited state desorption mechanism. In contrast, a thermal O-atom KE distribution clearly indicates a bulk derived origin for desorption. In analogy to alkali halide thermal desorption, we have considered a bulk-based thermal desorption mechanism involving trapping of two holes at a three-coordinated site (a "two-hole localization" mechanism). Our calculations, however, do not indicate that two-hole localization is likely without invoking a dynamical trapping process. The details of these mechanisms need to be further delineated and confirmed by demonstrating control of the various desorption processes. We plan to grow and study several other oxide surfaces in the near term including ZrO_2, BaO, and ZnO.

Future plans include femtosecond PEEM to study plasmon resonant photoemission from noble metal nanostructures and pulse-pair PEEM to probe dynamics of oxide nanostructures on surfaces. We will interrogate such metal-insulator systems using a variety of advanced techniques including: x-ray and ultraviolet photoelectron spectroscopy (XPS, UPS) femtosecond 2PPE, PEEM, atomic force microscopy (AFM) and laser desorption. Femtosecond time-resolved PEEM can reveal spatially resolved ultrafast dynamics and is a powerful tool for studying the near-surface electronic states of nanostructures or plasmonic devices. We will explore the formation of interfacial polarons on a sample of nanoscale NaCl islands on Cu (111). Our goal is to resolve the

temporal and spatial evolution of electron emission and the dynamics of small interfacial polarons using the combined PEEM and 2PPE approach. We are also presently developing capabilities to perform energy-resolved two-photon photoemission using a hemispherical analyzer XPS instrument. In combination we expect these two techniques will provide *spatially-resolved* electronic state dynamics of nanostructured oxide materials.

References to publications of DOE BES sponsored research (2009 to present)

1. P.E. Trevisanutto, P.V. Sushko, A.L. Shluger, K.M. Beck, A.G. Joly, and W.P. Hess, "Excitation, ionization, and desorption: how sub-band-gap photons modify the electronic properties and atomic structure of oxide nanoparticles," J. Phys. Chem. C **113**, 1274 (2009).

2. E.H. Khan, S.C. Langford, J.T. Dickinson, L.A. Boatner, and W.P. Hess, "Photoinduced Formation of Zinc Nanoparticles by UV Laser Irradiation of ZnO," Langmuir, **25**, 1930 (2009).

3. Govind, P. V. Sushko W. P. Hess, M. Valiev, K. Kowalski, "Excitons in insulators: a study using embedded time-dependent density functional theory and equation-of-motion coupled cluster methods," Chem. Phys. Lett. **470**, 353 (2009).

4. KM Beck, AG Joly, and WP Hess, "Two-color laser desorption of nanostructured MgO thin films," Appl. Surf. Sci. **255**, 9562 (2009).

5. AG Joly, KM Beck, and WP Hess, "Photodesorption of excited iodine atoms from KI (100)," J. Chem. Phys. **131**, 144509 (2009)

6. KM Beck, AG Joly, and WP Hess, "Effect of Surface Charge on Laser-induced Neutral Atom Desorption." Appl. Phys. A, **101**, 61 (2010).

7. G Xiong, R Shao, SJ Peppernick, AG Joly, KM Beck, WP Hess, M Cai, J Duchene, JY Wang W. D. Wei "Materials Applications of Photoelectron Emission Microscopy," J. Metals, **62**, 90 (2010).

8. SJ Peppernick, AG Joly, KM Beck, WP Hess "Plasmonic Field Enhancement of Individual Nanoparticles by Correlated Scanning and Photoemission Electron Microscopy" J. Chem. Phys. **134**, 034507 (2011).

9. PV Sushko, AL Shluger AG Joly, KM Beck, and WP Hess, "Exciton-driven highly-hyperthermal O-atom desorption from nanostructured CaO" J. Phys. Chem. C. **115**, 692 (2011) Cover.

Spectroscopic Imaging Toward Space-Time Limit

Wilson Ho

Department of Physics & Astronomy and Department of Chemistry
University of California, Irvine
Irvine, CA 92697-4575 USA

wilsonho@uci.edu

Program Scope:

This project is concerned with the experimental challenge of reaching single molecule sensitivity with sub-molecular spatial resolution in optical spectroscopy and photochemistry. These experiments would lead to an understanding of the inner machinery of single molecules that are not possible with other approaches. Results from these studies will provide the scientific basis for understanding the unusual properties, processes, and phenomena in chemical and physical systems at the nanoscale. The experiments rely on the combination of the unique properties of lasers and scanning tunneling microscopes (STM). By using a low temperature scanning tunneling microscope (STM) and coupling light to the nano-junction, it has become possible to probe optical phenomena with sub-atomic resolution. Specific examples of such capabilities include the spatial dependence of single molecule fluorescence and the primary steps of electron transfer to a single molecule. In the conversion of sun light to energy and in optoelectronics, a promising scheme involves the use of nanoscale objects as the active media. The investigation of the fundamental mechanisms of how light can be efficiently coupled to molecules and nanostructures not only can lead to new scientific phenomena but also form the basis for new technology.

Recent Progress:

Optical imaging of the interior of a single molecule has been achieved, for the first time, with Ångstrom resolution [1]. Up to now fluorescence imaging has not been able to resolve the internal structure of individual chromophores, and instead each chromophore is seen only as a bright feature. Using a scanning tunneling microscope, we have achieved spatial resolution down to the atomic scale in optical imaging and revealed the intensity distribution of the emitted light from different parts within a single molecule (Figure 1). The Ångström-scale spatial resolution is obtained by exciting the molecule with tunneling electrons although light is collected in the far field. The intensity reflects the probability of tunneling that is related to the spatially resolved local density of states, i.e. the spatial distribution of the molecular orbital wavefunction. The emitted light is also spectrally resolved so that the optical images correspond to the spatial distribution of selected single vibrational mode, i.e. at the limit of resolution in both space and energy. The experimental results were further understood from theoretical analysis, leading to a new mechanism for light emission from a single molecule in a nanoscale cavity. The subject matter is of broad interest due to its implications for photoinduced processes in solar energy conversion, photochemistry, and the general decay pathways of light induced excited states.

This work demonstrated a new method of optical imaging of single molecules at the limit of spatial and energetic resolutions.

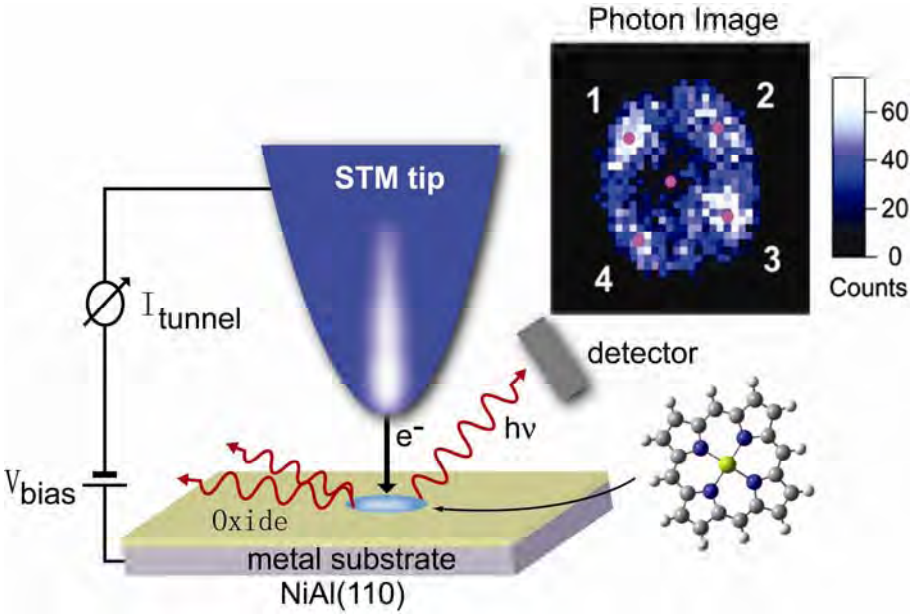

Figure 1. Schematic shows the STM geometry for the excitation by tunneling electrons and detection of the fluorescent signals of a single Mg-porphine molecule (the chromophore in chlorophyll). The photon image displays the spatial distribution of fluorescence inside a single Mg-porphine molecule.

The combination of lasers with the Scanning Tunneling Microscope (STM) would lead to new opportunities by tapping into the unique capabilities of both tools, including spectral and temporal resolutions from lasers and spatial resolution from the STM. The irradiation of femtosecond laser pulses in the tunneling junction of a STM leads to the possibility of probing the electronic and nuclear dynamics on a surface with atomic resolution at the femtosecond time scale. However, critical problems remain to hinder the coupling of femtosecond pulse lasers into the STM in the tunneling regime. We have demonstrated the coupling of photons to the tunneling process via two-photon absorption by using femtosecond laser pulses to irradiate a single-molecule junction in a low temperature STM to induce transfer of an electron to a single Mg-porphine molecule [2]. Compared to the experiments with illumination of continuous wave lasers, the illumination of the STM junction in the tunneling regime with femtosecond laser pulses enables the study of nonlinear optical phenomena at the atomic scale and dynamic processes at the simultaneous spatial and temporal limit. The atomic scale resolution in two-photon induced electron transfer is proven in the variation of the electron transfer efficiency at different positions inside the single molecule (Figure 2). In addition, preliminary results show the potential of the approach in revealing possible coherent coupling to molecular vibrations as the electron is transferred to a single molecule (Figure 3). The signal-to-noise ratio needs to be higher to unambiguously show the dynamics of electron-nuclear coupling. Our approach and the results are important for understanding photo-induced charge transfer in nanoscale inorganic-organic interface, which is pivotal to the development of solar cells and molecular electronics, as well as providing new insights into the ubiquitous electron transfer processes in chemistry, biology, and condensed matter.

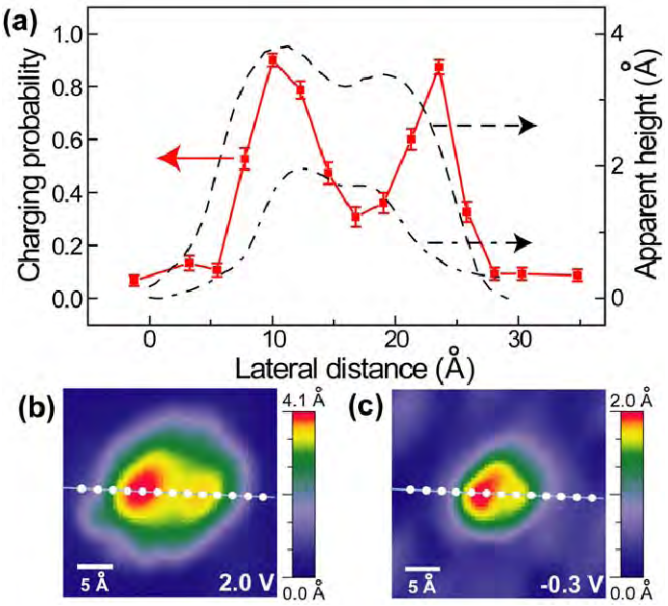

Figure 2. Atomic-scale spatial variation of photo-induced charging probability inside a single Mg-porphine molecule. (a) The charging probabilities were measured along a line through the two-lobe structure of the molecule, shown as red line-connected filled squares. The junction was illuminated by a femtosecond laser at P = 84 μW, and the sample bias voltage V_c was set at 0.3 V. The apparent heights cut along the same line from STM images (b) and (c) are also shown in black dashed curve for V_b = 2.0 V and in black dot-dashed curve for V_b = –0.3 V.

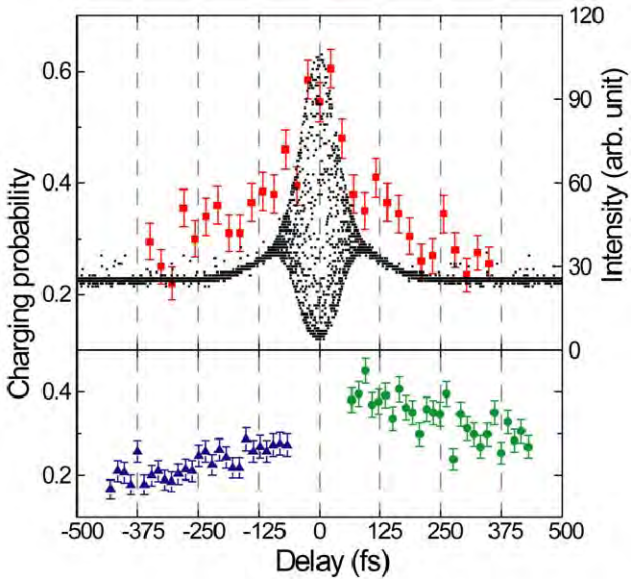

Figure 3. Charging probability as a function of time delay in two-pulse correlation measurement. Three sets of data measured with tip positioned on the bigger lobe of the molecule are shown here in red squares (1.8 pJ/pulse), green circles (1.2 pJ/pulse) and blue triangles (1.2 pJ/pulse). The second-order autocorrelation data in a collinear setup are also shown in black dots.

Future Plans:

The ability to probe changes in real time with sub-Ångström spatial resolution would open a new window for viewing the inner machinery of matter. The plan for the future aims at reaching an additional goal in the time domain by pushing spectroscopic imaging toward the simultaneous limits of sub-Ångström and <30 femtoseconds. Four focused activities have been identified, and all are designed to probe and image the dynamic properties in the interior of single molecules and artificially created nanostructures: 1. Spatially, spectroscopically, and temporally resolved photon imaging, 2. Direct measurement of photo-induced tunneling current, 3. Photo-induced electron tunneling in the time domain, and 4. Two-electron induced light emission. These experiments are expected to provide a fundamental understanding of matter by revealing them in previously unattainable regimes of space and time. Furthermore, knowledge of the coupling of light to nanoscale objects bring us one step closer toward the realization of efficient conversion of sun light to energy, a broad range of optoelectronics and plasmonics, and economically competitive photocatalysis.

References to Publications of DOE Sponsored Research:

[1] "Viewing the Interior of a Single Molecule: Vibronically Resolved Photon Imaging at Submolecular Resolution", Phys. Rev. Lett. **105**, 217402 (2010), with C. Chen, P. Chu, C.A. Bobisch, and D.L. Mills. Selected for a Viewpoint in Physics, "Mapping the Luminescence of a Single Molecule", by Marina Pivetta; "Lighting Up the Inside of a Single Molecule", by Yvonne Carts-Powell, Optics & Photonics News of Optical Society of America; "A Peek at a Molecule's Guts", Research Highlights, Nature, Dec. 2, 2010; "The Ultimate Resolution", by Brad Deutsch, Optics & Photonics Focus, Vol. 12, Story 5, Feb. 16, 2011.

[2] "Two-Photon-Induced Hot-Electron Transfer to a Single Molecule in a Scanning Tunneling Microscope", S.W. Wu and W. Ho, Phys. Rev. B **82**, 085444 (2010).

THEORY OF THE REACTION DYNAMICS OF SMALL MOLECULES ON METAL SURFACES

Bret E. Jackson

Department of Chemistry
701 LGRT
710 North Pleasant Street
University of Massachusetts
Amherst, MA 01003
jackson@chem.umass.edu

Program Scope

Our objective is to develop realistic theoretical models for molecule-metal interactions important in catalysis and other surface processes. The dissociative adsorption of molecules on metals, Eley-Rideal and Langmuir-Hinshelwood reactions, recombinative desorption and sticking are all of interest. To help elucidate the experiments that study these processes, we examine how they depend upon the nature of the molecule-metal interaction, and experimental variables such as substrate temperature, beam energy, angle of impact, and the internal states of the molecules. Electronic structure methods based on Density Functional Theory (DFT) are used to compute the molecule-metal potential energy surfaces. Both time-dependent quantum scattering techniques and quasi-classical methods are used to examine the reaction dynamics. Effort is directed towards developing improved quantum methods that can accurately describe reactions, as well as include the effects of temperature (lattice vibration) and electronic excitations.

Recent Progress

The dissociative chemisorption of methane on a Ni catalyst is the rate-limiting step in the chief industrial process for H_2 production. However, even on this catalyst the reaction probability is very small, and the dynamics are not fully understood. Most of our efforts these past few years have focused on the dissociative chemisorption of methane on metals, in an attempt to understand how methane reactivity varies with the temperature of the metal, the translational and vibrational energy in the molecule, and the properties of the metal surface. Initial studies of methane dissociation on Ni(111) used DFT to compute the barrier height and explore the potential energy surface (PES) for this reaction, with an emphasis on how it changes due to lattice motion. We found that at the transition state for dissociation, the Ni atom over which the molecule dissociates would prefer to pucker out of the surface by a few tenths of an Å. Put another way, when this Ni atom vibrates in and out of the plane of the surface, the barrier to dissociation increases and decreases, respectively, which should lead to a strong variation in the reactivity with temperature. High dimensional quantum scattering calculations were implemented to explore these issues. These calculations allowed for the inclusion of several key methane degrees of freedom (DOF), as well as the motion of the metal atom over which the reaction occurs. The reactivity was found to be significantly larger than that computed for the case of a static lattice, even at 0 K, and strongly increased with temperature.

Recent experiments by the Beck group (EPFL) showed that the reactivity of methane on Pt(111) was significantly larger than on Ni(111), with an apparent difference in activation energy of 0.29 eV. Using DFT, we examined the pathways to dissociation on both of these surfaces and found that the static surface barrier to reaction was only 0.13 eV lower on the Pt(111) surface than on the Ni(111) [1]. We then constructed DFT-based PESs for both metal surfaces, much

improved over our previous work, and high-dimensional quantum scattering studies were implemented. While the forces for lattice puckering are similar on the two metals, the heavier Pt is much less able to move during the reaction. While we were able to explain the Ni(111) reactivity reasonably well, our model underestimated the reactivity on Pt(111), particularly at lower energies [1]. We believe this is due to the fact that our quantum model ignores the motion of the methyl group during the dissociation. On Pt surfaces, the methyl group prefers to be on the top site during and after the dissociation, while on Ni surfaces it prefers to move towards the hollow site. This should increase the reactivity of Pt relative to Ni. Errors in the DFT energies may also contribute to the discrepancy.

In an attempt to better understand the role of lattice motion on methane dissociation, we implemented a variety of mixed quantum-classical models [2,4]. We found that treating only the lattice classically did not work well, and that the best approach was to treat both the lattice motion and the molecular center of mass motion classically, and the remaining molecular DOF quantum mechanically. While this model did lose some tunneling contributions from motion normal to the surface, it did allow us to directly observe the motion of the lattice at a given collision energy. We found that the majority of the reaction probability came from collisions between a methane molecule and a lattice atom that was at or near its outer turning point, where the barrier is lowest, at the time of impact. Moreover, most of the reactions occurred for lattice atoms that were "hot"; i. e., on the high-energy tail of the Boltzmann distribution. In addition, there was only minor recoil of the metal atom. This led to the development of a sudden model, where quantum calculations were implemented for several frozen lattice configurations, Monte Carlo sampled at the substrate temperature. Because the heavy metal atom was not explicitly included in the evolution, this model required two orders of magnitude less computer time, and was shown to reproduce our quantum studies on Ni(111) reasonably well [2]. More detailed studies led to a further improvement of this model. In particular, the change in both the energy and the location of the barrier to dissociation, with lattice motion, were included. This was shown to give excellent agreement with the quantum studies of methane dissociation on both Ni(111) and Pt(111) [4].

We spent over two years using DFT to examine the energetics of methane dissociation in great detail on Ni(100), Ni(111), Pt(100), Pt(111) and the stepped Pt(110)-(1x2) surface. The data we collected was eventually published, compared and contrasted in a single rather large paper [3]. For all 5 surfaces we examined product binding energies at all high-symmetry sites, and then mapped out the lowest energy transition states (24 in all). Zero point energy corrections were computed for all 24 transition states, and these various pathways to reaction were compared with each other and with experiment. We also examined how the heights and the locations of these barriers changed with lattice motion, which we refer to as the electronic and mechanical components, respectively, of the lattice (phonon) coupling. While these metals share many characteristics, there are interesting surface-to-surface variations in both the barrier height and the phonon coupling. A simple model was developed, based on our sudden approximation, for a temperature-dependent "activation energy", using only data from our DFT studies of the transition state [3]. This activation energy can be several tenths of an eV lower than the static surface barrier height. This variation in the apparent barrier height with substrate temperature has been observed in recent experiments on Pt(110).

It has long been known that exciting the various vibrational modes of methane can increase reactivity. The increase in reactivity relative to putting the same amount of energy into translation, the so-called efficacy, is different for different vibrational modes, as well as for the same mode on different metal surfaces. The nature of this mode-selective chemistry has never been understood. Over the past year and a half we have made significant progress on this

problem, using a formulation based on the Reaction Path Hamiltonian. In this approach, one locates (using DFT, in our case) the reaction path (RP) or minimum energy path for reaction, and implements a normal mode analysis at several points along this RP. This leads to a PES that includes all 15 molecular DOF, and that accurately describes the normal vibrational modes. In a first study, we computed the RP Hamiltonian for methane dissociation on Ni(100), including computation of all the vibrationally nonadiabatic couplings. We then recast this Hamiltonian into a close-coupled wave packet form by expanding the wavefunction in the adiabatic vibrational states of the molecule. Time-dependent quantum dynamics on this 15-DOF Hamiltonian showed that the ν_1 mode (symmetric stretch) significantly softens at the transition state, and is strongly coupled to the reaction coordinate. As a result there is a large vibrational efficacy for this mode, which has been observed by two experimental groups. We have demonstrated how these large efficacies for vibrational enhancement are related to transitions from higher to lower energy vibrationally adiabatic states, or to the ground state, with the excess energy going into motion along the reaction path, increasing the tunneling (reaction) probability [5].

In recent years we have studied H-graphite reactions, important in the formation of molecular Hydrogen on graphitic dust grains in interstellar space, the etching of graphite walls in fusion reactors, and the modification of the electronic properties of graphene. Our DFT studies demonstrated that an H atom could chemisorb onto a graphite terrace carbon, with the C atom puckering out of the surface plane by several tenths of an Å. We computed the PES for the Eley-Rideal reaction of a gas phase H atom with this chemisorbed H, and our scattering calculations showed that the reaction cross sections should be very large, a prediction that was later confirmed experimentally. However, in interstellar space any adsorbed H is likely to be physisorbed. To estimate the rates for H_2 formation via this pathway, one must know the sticking probability of H into the physisorption well. We have developed a powerful approach to these types of problems based on the reduced density matrix, which allows us to evolve a quantum system weakly coupled to a bath over relatively long times. Thus, we can not only compute, quantum mechanically, the scattering into free and bound states, we can observe the relaxation and/or desorption from these states over long times. In a study of H physisorption on graphite, we demonstrated that sticking is enhanced at low energies due to diffraction mediated trapping states that relax into the substrate vibrations. Last year, in a collaboration with a group in Toulouse, we examined the adsorption and subsequent desorption of H on graphite in even greater detail. In particular, we made extensive comparisons between our reduced density approach and more traditional wavefunction-based approaches. We demonstrated the utility and accuracy of the reduced density approach, and corrected some minor problems with our initial formulation. [6].

Future Plans

Over the past 6 months we have extended our RP approach to compute full-dimensional reaction probabilities for methane dissociation on metal surfaces. All 15 DOF of the methane are now included, and the coordinates corresponding to surface impact site are correctly averaged over, to give a proper reaction probability. The effects of lattice motion have also been included, using our sudden model. These are the first calculations, based entirely on *ab intio* data, which can be compared directly with experiment. A detailed study of methane dissociation on Ni(100) is being prepared for publication. Agreement with experiment is good, in terms of both the magnitude of the reactivity over a broad range of incident energy, and the efficacies of the different vibrational modes for promoting reaction. More importantly, it is possible to follow the flow of energy within the molecule as it dissociates, providing a detailed understanding of how translational, vibrational and lattice energy effect reactivity.

In a second study, we are revisiting our comparison of methane chemisorption on Ni(111) and Pt(111). On both metals, the transition state is over the top site. However, on Ni, the methyl group moves towards a hollow site during the reaction, while on Pt the methyl remains at the top site. In the mass-weighted coordinates of our RP, this leads to a broadening of the barrier and a lowering of the reactivity for Ni relative to Pt, as the heavy methyl group does not tunnel as effectively as the H. We have been computing the RP Hamiltonian for both of these surfaces, which requires computation of the normal mode frequencies and eigenfunctions at enough points along the path to converge the non-adiabatic couplings. We have completed this on Ni(111), and the overall ground state reactivity is in good agreement with experiment. We hope to complete this task for Pt(111) by the end of summer, compare probabilities for dissociative chemisorption on the two metals, and examine the vibrational efficacy, which is very different on the two metals.

The development of our sudden model for lattice motion allows us to significantly extend our other quantum scattering approaches by including more molecular DOF. In particular, we are looking at ways to average over impact sites and better describe vibrational motion. We should be able to accurately model CD_3H and CH_2D_2 reactions by treating the C-D bonds as unreactive. About a year ago we began to map out a PES for CD_3H chemisorption on Ni(111), treating the molecule as a pseudo-diatomic by having the CD_3 group evolve adiabatically, and correctly including the zero point energy effects in the 6-dimensional Hamiltonian. This study should allow us to elucidate the CD_3H/Ni(111) experiments of the Utz group (Tufts), using a scattering approach complementary to our RP formulation.

About two years ago we derived a fully quantum model for the time evolution of a reacting, scattering, or adsorbed molecule coupled to the electronic excitations of a metal substrate, using reduced density matrix methodologies. We have yet to compute the electronically non-adiabatic couplings, and hope to do so soon, initially for the case of H and H_2 sticking.

References

[1]. S. Nave and B. Jackson," Methane dissociation on Ni(111) and Pt(111): Energetic and dynamical studies," J. Chem. Phys. 130, 054701 (2009).

[2]. A. K. Tiwari, S. Nave and B. Jackson," Methane dissociation on Ni(111): A new understanding of the lattice effect," Phys. Rev. Lett. 103, 253201 (2009).

[3]. S. Nave, A. K. Tiwari and B. Jackson," Methane dissociation on Ni(111), Pt(111), Ni(100), Pt(100) and Pt(110)-(1x2): Energetic study," J. Chem. Phys. 132, 054705 (2010).

[4]. A. K. Tiwari, S. Nave and B. Jackson," The temperature dependence of methane dissociation on Ni(111) and Pt(111): Mixed quantum-classical studies of the lattice response," J. Chem. Phys. 132, 134702 (2010).

[5]. S. Nave and B. Jackson," Vibrational mode-selective chemistry: Methane dissociation on Ni(100)" Phys. Rev. B 81, 233408 (2010).

[6]. Bruno Lepetit, Didier Lemoine, Zuleika Medina, and Bret Jackson, "Sticking and desorption of hydrogen on graphite: a comparative study of different models," J. Chem. Phys. 134, 114705 (2011).

Probing catalytic activity in defect sites in transition metal oxides and sulfides using cluster models: A combined experimental and theoretical approach

DE-FG02-07ER15889

Caroline Chick Jarrold and Krishnan Raghavachari
Indiana University, Department of Chemistry, 800 East Kirkwood Ave.
Bloomington, IN 47405
cjarrold@indiana.edu, kraghava@indiana.edu

I. Program Scope

The highly complex nature of applied heterogeneous catalytic systems can confound attempts to identify the critical electronic and structure features that result in desirable catalytic properties, which is necessary for system optimization. Our research program combines experimental and computational methods to study well-defined cluster models of heterogeneous catalytic materials. The focus of our studies has been transition metal oxide and sulfide clusters in non-traditional oxidation states (surface defect models) and their chemical and physical interactions with water and CO_2. The applications that are being modeled are H_2 production from photocatalyic decomposition of water, and photocatalytic CO_2 reduction using Group 6 (Mo and W) oxides and sulfides. The experiments and calculations are designed to probe fundamental, cluster-substrate molecular-scale interactions that are governed by charge state, peculiar oxidation states, and unique physical structures.

The general strategy of our multipronged studies is as follows: (1) Determine how the molecular and electronic structures of transition metal suboxide and subsulfide clusters evolve as a function of oxidation state by reconciling anion photoelectron spectra of the bare clusters with high-level DFT calculations. Anions are of particular interest because of the propensity of metal oxide and sulfides to accumulate electrons in applied systems. (2) Measure and kinetically analyze cluster reactivity with water or CO_2. (3) Dissect possible reaction mechanisms computationally, to determine whether catalytically relevant interactions are involved. (4) Verify these challenging computational studies by spectroscopic investigation of observed reactive intermediates. (5) Probe the effect of local electronic excitation on bare clusters and cluster complexes, to evaluate photocatalytic processes.

The overarching goal of this project is to identify particular defect structures that balance structural stability with electronic activity, both of which are necessary for a site to be simultaneously robust and catalytically active, and to find trends and patterns in activity that can lead to improvement of existing applied catalytic systems, or the discovery of new systems.

II. Recent Progress

A. Resonant two-photon detachment (R2PD) spectroscopy of WO_2^-

R2PD is an experimental technique that has been newly implemented in our laboratory. Given that transition metal oxides and sulfides accumulate negative charge in applied environments, the electronic absorption spectrum of *anionic* systems is relevant to understanding photocatalytic activation in applied systems. While the number density of the mass-separated clusters in our anion beam are too low for conventional absorption spectroscopy, the R2PD

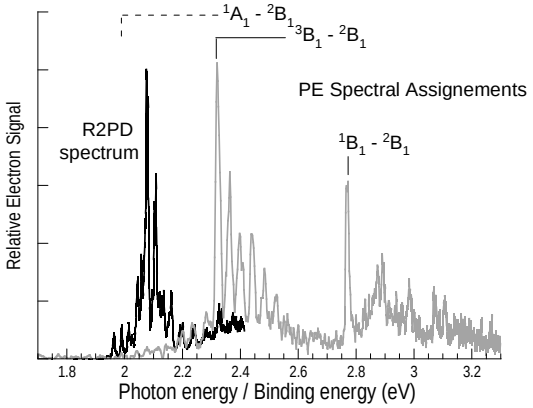

Fig. 1 R2PD spectrum of WO_2^- (black trace) superimposed on the PE spectrum of WO_2^- (gray trace) .

technique is analogous to resonant two-photon ionization, in which the absorption at a particular wavelength is indicated by the appearance of a charged particle. In the case of R2PD, electrons are produced at photon energies resonant with electronic transitions in the anionic cluster.

The simple suboxide WO_2^- anion has a well understood photoelectron spectrum [Lineberger et al., J. Phys. Chem. A **103**, 6167 (1999)], and because the highest several occupied and lowest unoccupied orbitals can be described as nearly-degenerate W-local 5*d*-orbitals, it was anticipated to have fairly low-energy (e.g., visible) excitations below, but in the vicinity of the detachment threshold. Indeed, at least two distinct electronic transitions were observed just below and above the detachment continuum, one of which was nominally spin-forbidden doublet to quartet transition, which was observed because of significant relativistic effects. The R2PD spectrum of WO_2^- is shown in Figure 1, superimposed on the direct detachment spectrum. In the final analysis, it was determined that this simple cluster has a rich, visible absorption spectrum (560 – 620 nm) involving local excitations, enhanced by relativistic effects, and coupled at the high energy end to electrostatically-bound anion states. [Ref. 1]

B. Computational studies of molybdenum sulfide versus molybdenum oxide clusters

Molybdenum sulfide is an interesting lamellar material used that has shown an activating effect in photocatalytic production of H_2 from water decomposition. Much of our computational and experimental work to date has involved molybdenum suboxide clusters, and given that the most stable bulk stoichiometry of molybdenum sulfide is MoS_2, in which the Group 6 metal is in a +4 oxidation state, the comparison between the suboxide and sulfide species is of some interest.

A comparative computational study of the $Mo_3X_y^-$ series (X = O, S; y = 6, 9) was targeted because the trimetallic-oxo clusters can form fairly high symmetry ring structures in which each metal center shares a single oxo bridge bond with its two neighbors. For $Mo_3X_6^-$ (X = O or S), the lowest energy C_{3v} structures were similar, in spite of the fact that sulfur atoms are much more electronically bulky than oxygen atoms. However, as the value of y was increased, the $Mo_3S_y^-$ species evolved toward elongated disulfide bridged structures, while $Mo_3O_y^-$ clusters maintained single bridge-bound cyclic structures. Furthermore, investigations into the adsorption of water on the oxides and sulfides suggest thermodynamic control for the sulfides, and kinetic control by the oxides. [Ref. 2]

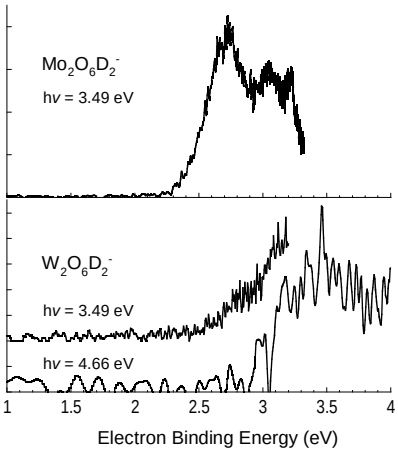

Fig. 2 Comparison of the PE spectra of $Mo_2O_6D_2^-$ and $W_2O_6D_2^-$.

C. Spectroscopic investigation of molybdenum oxo-hydroxy reactive intermediates

In past kinetics studies of the $Mo_xO_y^-$ + H_2O (or D_2O) [Ref. 4] and $W_xO_y^-$ + H_2O (or D_2O) [Ref. 7], we observed evidence of sequential oxidation accompanied by H_2 (or D_2) evolution via $M_xO_y^-$ + $H_2O \rightarrow M_xO_{y+1}^-$ + H_2, with eventual termination of the sequential reaction with the $M_xO_{y+1}H_2^-$ product ion. Rate constants determined for reactions with D_2O were identical to those with H_2O. An extensive computational study of the $W_2O_y^-$ (y = 4, 5 and 6) + H_2O reaction mechanism suggested the lowest energy pathways for the reactions to take place, and also that the $W_2O_6H_2^-$ complex observed in the reactivity studies was in fact a trapped intermediate [Ref. 8]. This was subsequently supported by spectroscopic investigation of the $W_2O_6H_2^-$ complex [Ref. 9].

The $Mo_2O_6H_2^-$ complex was also observed in molybdenum oxide reactivity studies, but the rate constants associated with the sequence of reactions leading to $Mo_2O_6H^-$ formation followed strikingly different trends. Furthermore, in the trimetallic metal oxide cluster reactions with water, $Mo_3O_y^-$ and $W_3O_y^-$ form the $M_xO_{y+1}H_2^-$ complexes at different values of *y*. In order to better understand the cause of disparate reactivities in molybdenum and tungsten oxide clusters, we have obtained the PE spectra of the $Mo_2O_6D_2^-$ and $Mo_3O_6D_2^-$. Figure 2 shows the spectrum obtained for $Mo_2O_6D_2^-$ and how distinctly it differs from the $W_2O_6D_2^-$ spectrum. While the source of this disparity is currently under computational investigation [manuscript in preparation] these cluster studies are evocative of possibly different (photo)-catalytic properties of oxygen vacancies on tungsten and molybdenum oxides.

D. Comparing the Structures of $Mo_3O_y^-$ and $W_3O_y^-$ suboxide clusters

One possible cause of disparate patterns of reactivity observed in $Mo_xO_y^-$ and $W_xO_y^-$ analogs may simply be different molecular structures. While different trends in sequential rate constants were determined for the bimetallic oxide clusters in both water reactions [Refs. 4 and 7] and CO_2 reactions [Ref. 5], completely different product patterns were observed for the trimetallic oxide clusters.

Using PE spectroscopic studies combined with DFT calculations, we have evaluated the structural trends in sequential oxidation of $Mo_3O_y^-$ and $W_3O_y^-$ for $y = 3–6$. In general the results suggest that from a molecular structural standpoint, the clusters are very similar. However, the electronic structure of the similarly structured clusters can be quite different, as reflected in striking differences observed in the PE spectra. The results therefore suggest that in the case of differences in $Mo_3O_y^-$ and $W_3O_y^-$ reactivities toward water and CO_2, electronic structure is the more important factor. [manuscript in preparation] This will become a notable effect in future experiments on photodissociation of the reaction products observed in the reactivity studies.

E. Computational study of OH migration via proton hop on trimetallic oxo-hydroxide clusters

From computational studies of the $W_2O_y^-$ + H_2O sequential oxidation reaction mechanism for y = 4, 5 and 6, the barrier between dihydroxide complexes and the requisite hydride-hydroxide structures emerged as a determining factor in whether the reaction would go to completion with H_2 production, or get trapped. This barrier is associated with the ability of a hydroxyl group to bend toward a metal center to allow hydroxide to hydride conversion. This same consideration was applied to $Mo_3O_6H_2^-$ and $W_3O_6H_2^-$ complexes to determine how barriers to hydrogen mobility compared between the two species. Interesting fluxionality of the metal oxide structures emerged from the studies, as illustrated in Figure 3. Barriers to the hydroxide migration that accompanies conversion of *M*–O–*M* bridge bonds to *M*=O terminal bonds, were calculated to be higher for *M* = Mo than for *M* = W, suggesting that this may be an underlying source of the unique trapped species observed in $Mo_3O_y^-$ reactivity studies.

Fig. 3 Proton hop intermediate calculated for $M_3O_6H_2^-$

III. Future Plans

A strength of the research program is the synergistic interplay between theory and experiment. Another manifestation of this interplay will be new temperature-dependence studies of reaction kinetics, which will allow a direct benchmarking of calculated reaction barriers. The temperature controlled reactivity channel has been designed, and construction should be completed by mid-May, 2011. Metal sulfide cluster structure and reactivity studies will also be initiated. A further extension of current reactivity studies will be the introduction if independently controlled two-reagent reactivity studies (e.g., $Mo_xO_y^-$ + CO_2 + H_2), which will be done in an effort to model full-cycle processes. $Mo_xO_y^-$ clusters

show both sequential oxidation by CO_2 as well as dissociative adsorption to a subset of clusters, though preliminary computational results and past spectroscopic measurements on molybdenum oxo-carbonyls suggests that the CO group is vulnerable to photodissociation and has more C=O double-bond character, suggesting that subsequent H_2 addition may result in value addition to the CO group.

We will continue to apply the R2PD technique to larger metal oxide species as well as metal sulfides with high electron affinities. These studies will be combined with photodissociation studies on reaction complexes observed in the reactivity studies. Specific targets include $Mo_2O_6D_2^-$, $Mo_3O_6D_2^-$, and a number of the molybdenum-oxo carbonyls formed in reactions between the clusters and CO_2, and results will be correlated to possible photocatalytic properties of bulk-defect analogs of these complexes.

Furthering our recent observation of reactivity associated fluxionality in the transition metal oxides, the scope of fluxionality when hydrogen sulfide, ammonia and phosphine react with the transition metal oxides will be extensively probed. Each of these small molecule reactants presents unique and different opportunities for possible hydrogen liberation. Further, these studies could possibly also lead to alternate ways of capturing poisonous hydrogen sulfide and phosphine.

The reactivity of methanol with $Mo_xO_y^-$ and $W_xO_y^-$ will be investigated carefully. The presence of three unique kinds of bonds in methanol presents a great opportunity to study the interesting reactivity patterns of $Mo_xO_y^-$ and $W_xO_y^-$ with different functionalities. This could potentially be of aid in relevant energy related processes such as methanol oxidation and hydrogen liberation.

IV. References to publications of DOE sponsored research that have appeared in 2009–present or that have been accepted for publication

1. "Molybdenum Oxides versus Molybdenum Sulfides: Geometric and Electronic Structures of $Mo_3X_y^-$ (X = O, S and y = 6, 9) Clusters," N.J. Mayhall, E.L. Becher, A. Chowdhury, and K. Raghavachari, J. Phys. Chem A, **115**, 2291-2296 (2011).

2. "Resonant two-photon detachment of WO_2^-," J.E. Mann, S.E. Waller, D.W. Rothgeb and C.C. Jarrold, Chem. Phys. Lett. **506**, 31-36 (2011).

3. "Proton Hop Paving the Way for Hydroxyl Migration: Theoretical Elucidation of Fluxionality in Transition-Metal Oxide Clusters," R.O. Ramabhadran, N.J. Mayhall, and K. Raghavachari, J. Phys. Chem. Lett. **1,** 3066-3071 (2010).

4. "H_2 production from reactions between water and small molybdenum suboxide cluster anions," D.W. Rothgeb, J.E. Mann, and C.C. Jarrold, J. Chem. Phys. **133**, Article 054305 (2010).

5. "CO_2 reduction by group 6 transition metal suboxide cluster anions," E. Hossain, D.W. Rothgeb, and C.C. Jarrold, J. Chem. Phys. **133**, Article 024305 (2010).

6. "Electronic structure of coordinatively unsaturated molybdenum and molybdenum oxide carbonyls," Ekram Hossain and Caroline Chick Jarrold, J. Chem. Phys. **130** 064301 (2009).

7. "Unusual products observed in gas-phase $W_xO_y^- + H_2O$ and D_2O reactions," David W. Rothgeb, Ekram Hossain, Angela T. Kuo, Jennifer L. Troyer, Caroline Chick Jarrold, Nicholas J. Mayhall, and Krishnan Raghavachari, J. Chem. Phys. **130**, 124314 (2009).

8. "Water reactivity with tungsten oxides: H_2 production and kinetic traps," Nicholas J. Mayhall, David W. Rothgeb, Ekram Hossain, Caroline Chick Jarrold and Krishnan Raghavachari, J. Chem. Phys. **131**, Article 144302 (2009).

9. "Termination of the $W_2O_y^- + H_2O/D_2O \rightarrow W_2O_{y+1}^- H_2/D_2$ reaction: Kinetic versus thermodynamic effects," David. W. Rothgeb, Ekram Hossain, Nicholas J. Mayhall, Krishnan Raghavachari, and Caroline Chick Jarrold, J. Chem. Phys. **131**, Article 144306 (2009).

Coordinating experiment and theory to understand how excess electrons are accommodated by water networks through model studies in the cluster regime
RE: DE-FG02-00ER15066 and DE-FG02-06ER15800

K. D. Jordan (jordan@pitt.edu), Dept. of Chemistry, University of Pittsburgh, Pittsburgh, PA 15260
and M. A. Johnson (mark.johnson@yale.edu), Dept. of Chemistry, Yale University, New Haven, CT 06520

Our program exploits size-selected clusters as a medium with which to unravel molecular level pictures of key transient species in aqueous chemistry that mediate radiation damage in chemical and biological systems. Primary among these processes is the nature of the excess electron (hydrated electron) and elementary steps by which the water network mediates electron capture onto secondary scavengers such as O_2 and CO_2. Our role in the large community working on the hydrated electron was highlighted in our *Perspective*[1] in *Science* in which we were requested to comment on a recent paper by Schwartz describing a possible paradigm shift away from the traditional cavity model. Two subsequent *Comments* on the Schwartz paper validate our call for caution before adopting the new point of view. In our own work, much of our early effort has been directed at understanding how the shape of the water network controls the excess electron binding properties, and in the past year we have completed a long-standing goal of experimentally isolating how individual sites contribute to the overall binding, with the results presented in *J. Phys. Chem. Lett.*[2] This was accomplished by randomly incorporating a single, intact, D_2O molecule into a network of six water molecules, and then using two IR lasers and three stages of mass-selection to extract the site-specific spectral signatures of D_2O in each site. That work provided a rigorous test of the theoretical predictions for the structures and dramatically validated our earlier hypothesis that the excess

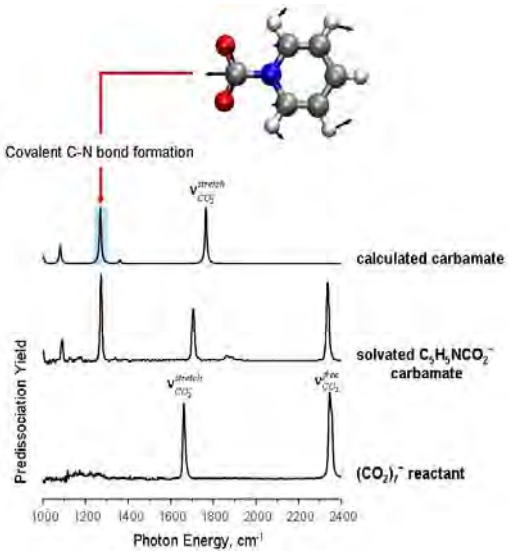

Figure 1: Probing the formation of the carbamate ion (structure at top) from the reaction of pyridine with negatively charged CO_2 clusters using vibrational spectroscopy. The vibrational band highlighted by the red arrow indicates the appearance of the C-N stretching transition associated with formation of the covalent bond to the CO_2 group. The top trace shows the theoretical spectrum (B3LYP/6-311G++(d,p)) for the product species. The calculated displacement vectors of the new band are shown in the inset.

electron trapped preferentially onto a single water molecule held to the network in a double H-bond acceptor motif.

The expertise we have built up in understanding charge accommodation is not limited to the excess electron systems of primary focus for our DOE program. In fact, we collaborated using our multidimensional spectroscopic tools and theoretical analysis capabilities to unravel how water network shape critically controls proton-coupled covalent bond formation in the water-mediated conversion of nitrosonium (NO^+) to nitrous acid in the ionosphere. That work appeared in *Science* this past year, and although not nominally funded by our DOE program, it marks a harbinger for new directions in our DOE sponsored work, where we expand the scope of the program to focus on fundamental chemistry needed for the conversion of solar energy to fuel. As a first step, we have engaged a fundamental issue involved in the photoelectrochemical reduction of CO_2 in the scheme recently announced by Bocarsly and co-workers. [*J. Am. Chem. Soc*., **132**, 11539, 2010] A key feature of their approach invokes activation of CO_2 molecules by formation of the carbamate radical anion shown in Fig. 1. We were able to exploit our extensive expertise on excess electron reactions to isolate the critical carbamate and characterize it using Ar-predissociation spectroscopy, a workhorse of our DOE program. The resulting spectra are included in the lower two traces of Fig. 1, unambiguously establishing the formation of the C-N covalent linkage through its characteristic vibrational transition at 1250 cm^{-1}. This work appeared as a *Communication* in *J. Am. Chem. Soc.* in the fall of 2010. This project is continuing as we characterize other intermediates in the proposed reaction mechanism and determine how a water network shape controls formation of a covalent bond between carbon atoms in the $C_2O_4^-$ radical ion.

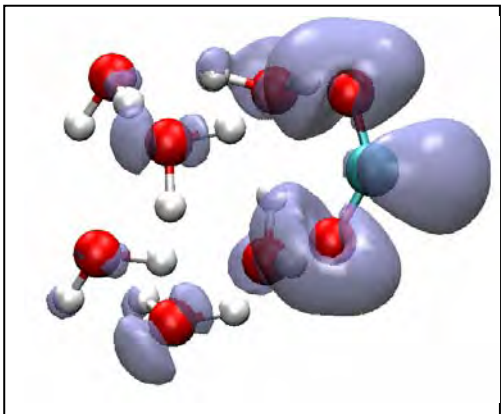

Figure 2: Snapshot from the direct dynamics simulation of photoinduced, intracluster reduction of CO_2 mediated by a thermally activated water network.

Cluster studies are also extremely valuable in the elucidation of the molecular-level mechanics of the elementary chemical events at play in photoelectrochemical catalysis in an aqueous environment. Specifically, we have capitalized on our extensive experience with Ar-cluster mediated chemistry to capture the key reaction intermediate in the reduction of CO_2:

$$CO_2 + (H_2O)_n^-\cdot Ar_q \rightarrow CO_2\cdot(H_2O)_n^-\cdot Ar + (q\text{-}1)\ Ar, \qquad [1]$$

where neutral CO_2 resides in a remote location relative to the diffuse excess electron trapped on the water cluster. The reduction reaction is then triggered through photoexcitation of either the electron itself or through vibrational excitations on all constituents of the aggregate:

$$CO_2\cdot(H_2O)_6^-\cdot Ar + h\nu \rightarrow [CO_2^-\cdot(H_2O)_6]^*\cdot Ar \rightarrow CO_2^-\cdot(H_2O)_5 + H_2O + Ar. \qquad [2]$$

The mechanics of this network-mediated reduction are then followed by carrying out direct dynamics calculations, which allows us to follow how the diffuse electron cloud responds to fluctuations of the network that facilitate electron capture on the CO_2 reactant. A snapshot of the product from the simulation is included in Fig. 2. This activity integrates the experimental and theoretical machinery we have been developing for many years into a powerful technology to reveal how complex, solvent-mediated reactions occur in a thermally activated process.

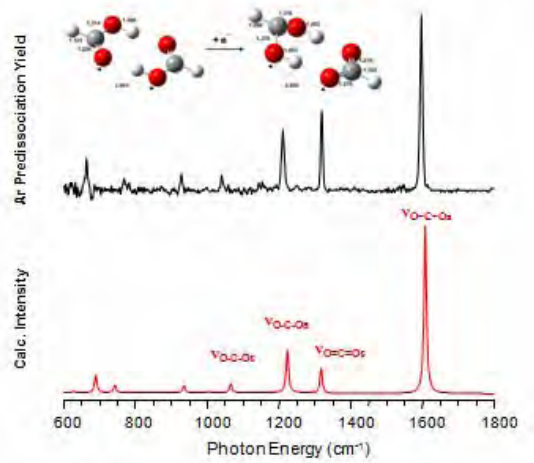

Figure 3: Examining proton transfer induced by excess electron attachment to formic acid dimer (as depicted above) with vibrational spectroscopy. The product radical features an H-bonded, formate-like anion tethered to a neutral dihydroxymethyl radical. The Ar predissociation spectrum of the perdeutero isotopologue is displayed in the upper trace, while the calculated harmonic spectrum for the structure in the upper right is included in the lower trace.

The CO_2 activation study described above is an example where we transition from fundamental study of network-dependent charge accommodation to the next step of using these systems as a vehicle to engage important problems encountered in photoelectrochemical activation of CO_2. Another example where we are in process of leveraging our knowledge to branch out is in the characterization of DNA damage by low-energy electrons. In this case, it is thought that the double and triple H-bond bridges are sites where an excess electron drives an internal transfer of one proton across the bridge in a so-called "electron-driven proton transfer" event. To explore the basic physics of this process, we have prepared and spectroscopically characterized the species formed when the neutral formic acid dimer (FAD) accepts a free electron, with preliminary data presented in Fig. 3. Analysis of these spectra reveals that the ion consists of a largely intact formate ion tethered to the dihydroxymethyl radical as indicated by the calculated structure in the top in Fig. 3. As in many of our studies that capture the first qualitative look at a new binding paradigm, this analysis required careful consideration of anharmonic effects arising from strong vibrational coupling between high frequency bonds and soft mode displacements that induce large changes in the high energy oscillators. Here the calculations of the cubic force constants and anharmonic spectra by the Pittsburgh portion of the team proved crucial. With the success of this initial study, we now foresee forging ahead to spectroscopically characterize motifs involved in proton-coupled electron transfer (PCET), a dominate motif in covalent bond formation and charge translocation in biomimetic water splitting schemes.

Looking to the future, we have very recently dramatically expanded the scope of our work by incorporating electrospray ionization and cryogenic ion processing techniques for

preparing and spectroscopically characterizing reaction intermediates. Under our DOE program, we are interfacing this methodology with a 7 Tesla Ion Cyclotron Resonance mass spectrometer (Bruker) in a configuration that uses D_2 as the active messenger species to carry out predissociation spectroscopy. We expect this new instrument to be on line by the end of summer 2011. Initial scientific targets for this instrument include the characterization of proton-coupled covalent bond formation in organometallic catalysts designed to carry out CO_2 activation in both homogeneous and heterogeneous regimes. On the theory side we anticipate that *ab initio* dynamics simulations, such as those that we recently completed for $CO_2 \cdot (H_2O)_6^-$, will play an increasingly important role in our efforts to unravel the mechanisms involved in electron-driven chemistry.

References (* indicates papers published under this grant)

1. "**Downsizing the Hydrated Electron's Lair**," K. D. Jordan and M. A. Johnson, *Science*, **329**, 42-43, 2010.*

2. "**Isolating the spectral signatures of individual sites in water networks using vibrational double-resonance spectroscopy of cluster isotopomers**," T. L. Guasco, B. M. Elliott, M. A. Johnson, J. Ding and K. D. Jordan, *J. Phys. Chem. Lett.*, **1**, 2396-2401, 2010.*

3. "**How the shape of an H-bonded network controls proton-coupled water activation in HONO formation**," R. A. Relph, T. L. Guasco, B. M. Elliott, M. Z. Kamrath, A. B. McCoy, R. P. Steele, D. P. Schofield, K. D. Jordan, A. A. Viggiano, E. E. Ferguson and M. A. Johnson, *Science*, **327**, 308-312, 2010.

4. "**Vibrational predissociation spectrum of the carbamate radical anion, $C_5H_5N\text{-}CO_2^-$, generated by reaction of pyridine with $(CO_2)_m^-$**," M. Z. Kamrath, R. A. Relph and M. A. Johnson, *J. Am. Chem. Soc.* (Communication), **132**, 15508-15511, 2010.*

5. "**Unraveling structural aspects of 'electron-induced proton transfer' in the formic acid dimer anion, $(HCOOH)_2^-$, with vibrational photoelectron spectroscopies**" H. K. Gerardi, C. M. Leavitt, A. F. DeBlase, M. A. Johnson, A. B. McCoy, X. Su, and K. D. Jordan, *in preparation**

6. "**Structural Evolution of the $[(CO_2)_n(H_2O)]^-$ Cluster Anions: Quantifying the Effect of Hydration on the Excess Charge Accommodation Motif** ", A. Muraoka, Y. Inokuchi, N. I. Hammer, J.-W. Shin, T. Nagata, and M. A. Johnson, J. Phys. Chem. A, **113**, 8942–8948, 2009.*

7. "**Potential Energy Landscape of the $(H_2O)_6^-$ Cluster**", T.-H. Choi and K. D. Jordan, Chem. Phys. Lett. **475**, 293-297, 2009.*

8. "**Survey of Ar-tagged predissociation and vibrationally mediated photodetachment spectroscopies of the vinylidene anion, $C_2H_2^-$**", H. K. Gerardi, K. J. Breen, T. L. Guasco, G. H. Weddle, G. H. Gardenier, J. E. Laaser, and M. A. Johnson, J. Phys. Chem. A, **114**, 1592-1601, 2010.*

Nucleation: From Vapor Phase Clusters to Crystals in Solution

Shawn M. Kathmann
Chemical and Material Sciences Division
Pacific Northwest National Laboratory
902 Battelle Blvd.
Mail Stop K1-83
Richland, WA 99352
shawn.kathmann@pnl.gov

Program Scope

The objective of this work is to develop an understanding of the chemical physics governing nucleation. The thermodynamics and kinetics of the embryos of the nucleating phase are important because they have a strong dependence on size, shape and composition and differ significantly from bulk or isolated molecules. The technological need in these areas is to control chemical transformations to produce specific atomic or molecular products without generating undesired byproducts, or nanoparticles with specific properties. Computing reaction barriers and understanding condensed phase mechanisms is much more complicated than those in the gas phase because the reactants are surrounded by solvent molecules and the configurations, energy flow, and electronic structure of the entire statistical assembly must be considered.

Recent Progress

Ab initio Electric Potentials at the Interface of Water

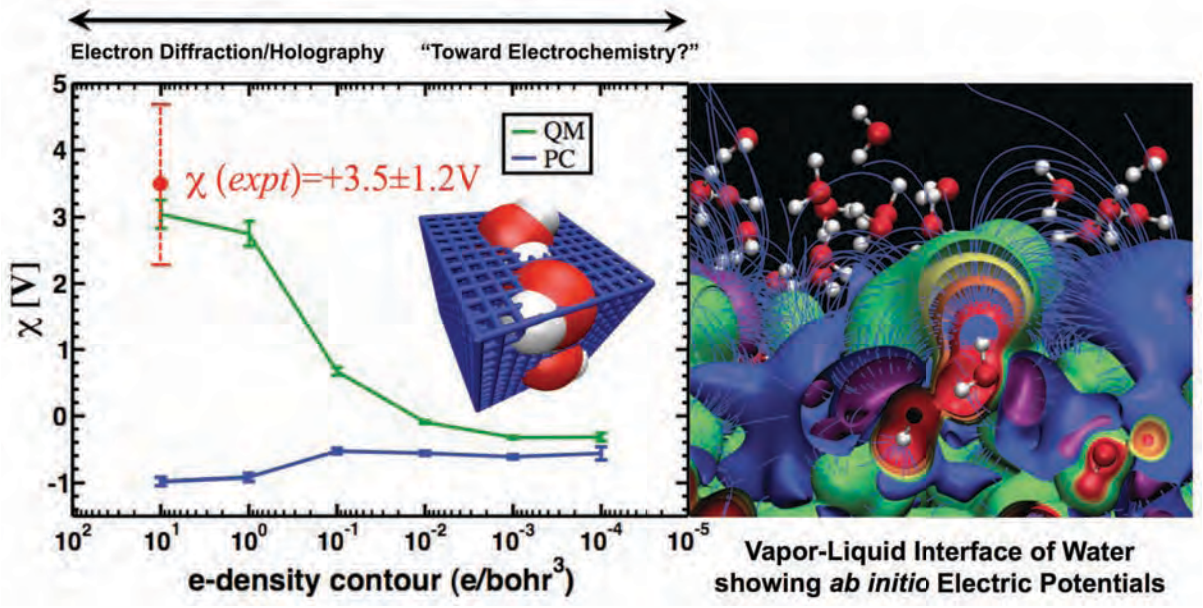

Figure 1. (Left) Computational results of the surface potentials for the QM and PC models with standard deviations as error bars and the electron holography measurement on vitrified ice for comparison. The computed surface potentials for both QM and PC models are very sensitive to the e-density isocontours, i.e., where one probes the electric potential "between the molecules" – clearly the QM is in excellent agreement with experiment. (Right) Plot of the QM electric potential isocontours at the vapor-liquid interface of water – red is positive potential, green is zero potential, and purple is negative potential. The positive potential arises from the protons in the nuclei and the negative potential arises from the electrons.

The surface potential, χ, of the vapor-liquid interface of pure water is relevant to electrochemistry, solvation thermodynamics of ions, and interfacial reactivity. We have resolved the inconsistency in quantifying the surface potential at the liquid-vapor interface when using explicit quantum mechanical (QM) electronic charge density and effective atomic partial charge (PC) models of liquid water. This is related, in part, to the fact that the resulting electric potentials from partial-charge models and *ab initio* charge distributions are quite different except for those regions of space between the molecules. We find excellent agreement with electron holography measurements of vitrified ice using *ab initio* molecular dynamics – see Figure 1. We suggest that certain regions of space be excluded when comparing computed surface potentials with electrochemical measurements. From this, the electric potentials in the low e-density region can be correlated with the degree of electronic overlap and, thus, provide a measure of the enrichment or depletion of electronic charge as a function of electrolyte concentration occurring in electrochemical measurements of the surface potential differences and estimates of the surface potential for pure water. This analysis highlights the possibility that previous calculations of the interfacial electric potentials obtained by averaging over all computational mesh points may require reinterpretation and reevaluation if they are to be compared with the results from electrochemical measurements. Additional *ab initio* molecular dynamics studies are necessary to better understand the connection between the electrochemical surface potential measurements and computation. Future studies will address the roles of using H_3O^+ as an electrochemical probe, quantum nuclear degrees of freedom, finite size effects for small water clusters, surface enrichment/depletion of various ions as a function of concentration on the surface potential.

Photoelectron Spectroscopy of Cationic Interactions with Dicarboxylate Dianions

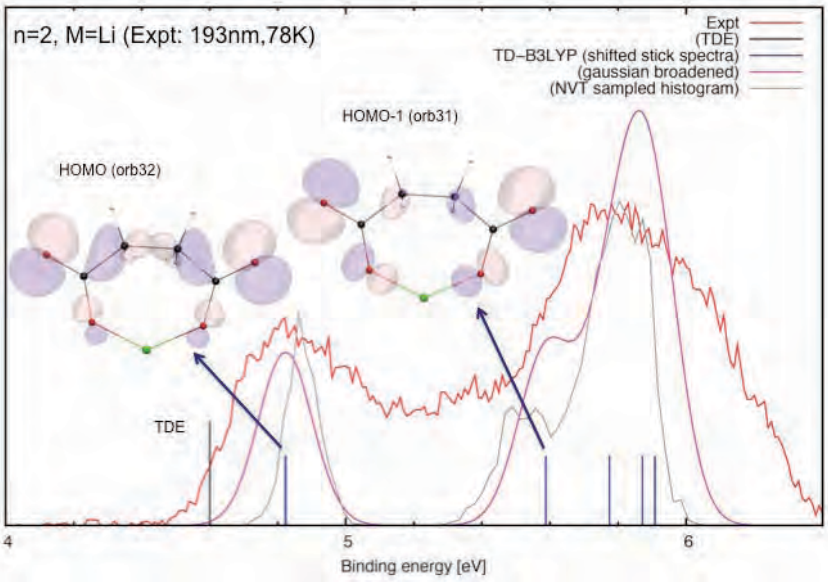

Figure 2. UV photoelectron spectroscopy for electron detachment of the Li^+ cation complexed with the dicarboxylate $^-O_2C(CH_2)_2CO_2^-$ transforming the complex from a singlet to a doublet state. The measured electron binding energy spectrum is shown in red. We see two broad peaks, roughly centered at 4.8 and 5.8 eV. To understand the effects of anharmonicity, we performed *ab initio* NVT dynamics at 78K and find good agreement with the harmonic results and experiment.

Alkali metal cations often show pronounced ion specific interactions and selections with macromolecules in biological processes, colloid, and interface sciences. A number of theoretical modeling and solution / interface experiments have been recently conducted to rationalize such ion specificity, but a fundamental understanding about the underlying microscopic mechanism is still very limited. We have performed synergetic photoelectron spectroscopy and *ab initio* electronic structure calculations on nine complexes of alkali metal cation (M^+) (M = Li, Na, K) and dicarboxylate dianions, $^-O_2C(CH_2)_nCO_2^-$ (D_n^{2-}) (n = 2,4,6), which are used as models to

probe direct ion-macromolecule interactions – see Figure 2 for the case of Li^{+}–D_2^{2-}. Photoelectron spectra show distinct spectral characteristics among these clusters dependent on both cations and the number of –CH_2– groups, *n* in the backbone. Theoretical modeling suggests that the cation prefers to interact with both ends of –COO^{-} groups by bending the flexible aliphatic backbone. In addition, the local binding environments are found to dependent upon the ring size, i.e., the number of –CH_2– groups, *n*.

Future Plans

Concentration Effects, Charge Transfer, and Crystalloluminescence

To understand and accurately quantify the mechanisms underlying crystallization several challenging aspects of condensed phase chemical physics must be confronted: concentration effects, charge transfer, and electronic transitions. Concentrated aqueous solutions have varying degrees of solvation, slowed diffusion, as well as interesting interfacial properties. *Ab initio* calculations have shown that charge transfer occurs between the solvated ions and the surrounding water molecules. It has also been observed that during crystallization of alkali- and metal-halide salts from solution a burst of some photons of visible light is emitted. Figure 3a shows the water O-O RDFs as a function of concentration using simple point charges as well as a polarizable model. These RDFs show a dramatic restructuring of water surprising consistent with experiments for pure water under high pressure (~7700 atm). Figure 3b shows the charge transfer as a function of concentration via *ab initio* re-sampling the classical trajectories and using Bader analysis to partition the electronic density into charges. For the configurations sampled, the Cl^{-} and H_2O charges show the greatest changes. Figure 3c shows the CHelpG partial charges for a NaCl crystallite compared to the true *ab initio* Hartree potential. For this NaCl configuration some of the Na^{+} atoms have been reduced to Na^{0} metal using the electrons from the Cl^{-} atom on the other end of the crystallite. These types of configurations may play a role in forming the excitonic states that recombine during subsequent crystallization dynamics responsible for the luminescence. Furthermore, this analysis helps to understand and quantify the limitations of modeling atoms in condensed phases with partial point charges.

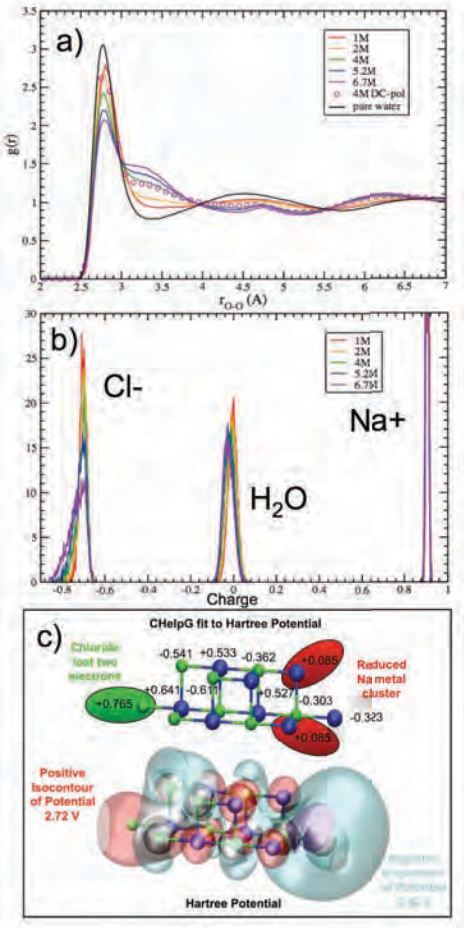

Figure 3. a) RDFs for (NaCl)aq at various concentrations. b) Charge transfer between H_2O, Cl-, and Na+ for various concentrations. c) Comparison of the partial charges for a NaCl crystallite with the *ab initio* Hartree electrostatic potential.

Future work will include: (1) performing *ab initio* MD instead of simply using *ab initio* methods to resample the classical potential to study charge transfer, (2) using hydrid DFT functionals to obtain quantitative excitonic state energies, (3) to use the Hartree potential analysis to compute

the surface potentials of various aqueous electrolytes as functions of concentration as well as investigate the electrical properties of the crystal-aqueous phase interfaces to compare with available experiments, and (4) computing potentials of mean force for ions in solutions from the *ab initio* MD to use in accelerated dynamics to model crystallization kinetics.

Direct collaborators on this project include G.K. Schenter, C.J. Mundy, Xuebin Wang, and Marat Valiev.

Acknowledgement: This research was performed in part using the Molecular Science Computing Facility in the Environmental Molecular Sciences Laboratory located at PNNL and the BES NERSC facility. Battelle operates PNNL for DOE.

Publications of DOE Sponsored Research (2009-present)

1. Implementation of Dynamical Nucleation Theory with Quantum Potentials, L.D. Crosby, S.M. Kathmann, and T.L. Windus, *Journal of Computational Chemistry*, **30**, 743 (2009).
2. **Invited Cover Article** – Thermodynamics and Kinetics of Nanoclusters Controlling Gas-to-Particle Nucleation, S. M. Kathmann, G.K. Schenter, B.C. Garrett, B. Chen, and J.I. Siepmann, *Journal of Physical Chemistry C*, **113**, 10354 (2009).
3. Fulton JL, SM Kathmann, GK Schenter, and M Balasubramanian, "Hydrated structure of Ag(I) ion from symmetry-dependent, K- and L-edge XAFS multiple scattering and molecular dynamics simulations." *Journal of Physical Chemistry A* **113**, 13976-13984 (2009).
4. Kathmann SM, I-FW Kuo, and CJ Mundy, "Electronic effects on the surface potential at the vapor-liquid interface of water." *Journal of the American Chemical Society* **131**, 17522-17522 (2009).
5. **Invited Cover Article** – S.M. Kathmann, GK Schenter, BC Garrett, B Chen, and JI Siepmann, "Thermodynamics and kinetics of nanoclusters controlling gas-to-particle nucleation." *Journal of Physical Chemistry C* **113**, 10354-10370 (2009).
6. **Invited** - C.J. Mundy, S. M. Kathmann, R. Rousseau, G. K. Schenter, J. Vande Vondele, and J. Hutter, "Scalable Molecular Simulation: Toward and Understanding of Complex Chemical Systems," *SciDAC Review*, 17, 10, (2010).
7. **Cover Article** – S.M. Kathmann, I-FW. Kuo, C.J. Mundy, and G.K. Schenter, "Understanding the Surface Potential of Water." *Journal of Physical Chemistry B*, **115**, 4369 (2011).

Chemical Kinetics and Dynamics at Interfaces

Structure and Reactivity of Ices, Oxides, and Amorphous Materials

Bruce D. Kay (PI), R. Scott Smith, and Zdenek Dohnálek

Chemical and Materials Sciences Division
Pacific Northwest National Laboratory
P.O. Box 999, Mail Stop K8-88
Richland, Washington 99352
bruce.kay@pnl.gov

Additional collaborators include P. Ayotte, G. A. Kimmel, J. Knox, J. Matthiesen, C. J. Mundy, G. S. Parkinson, and N. G. Petrik

Program Scope

The objective of this program is to examine physiochemical phenomena occurring at the surface and within the bulk of ices, oxides, and amorphous materials. The microscopic details of physisorption, chemisorption, and reactivity of these materials are important to unravel the kinetics and dynamic mechanisms involved in heterogeneous (i.e., gas/liquid) processes. This fundamental research is relevant to solvation and liquid solutions, glasses and deeply supercooled liquids, heterogeneous catalysis, environmental chemistry, and astrochemistry. Our research provides a quantitative understanding of elementary kinetic processes in these complex systems. For example, the reactivity and solvation of polar molecules on ice surfaces play an important role in complicated reaction processes that occur in the environment. These same molecular processes are germane to understanding dissolution, precipitation, and crystallization kinetics in multiphase, multicomponent, complex systems. Amorphous solid water (ASW) is of special importance for many reasons, including the open question over its applicability as a model for liquid water, and fundamental interest in the properties of glassy materials. In addition to the properties of ASW itself, understanding the intermolecular interactions between ASW and an adsorbate is important in such diverse areas as solvation in aqueous solutions, cryobiology, and desorption phenomena in cometary and interstellar ices. Metal oxides are often used as catalysts or as supports for catalysts, making the interaction of adsorbates with their surfaces of much interest. Additionally, oxide interfaces are important in the subsurface environment; specifically, molecular-level interactions at mineral surfaces are responsible for the transport and reactivity of subsurface contaminants. Thus, detailed molecular-level studies are germane to DOE programs in environmental restoration, waste processing, and contaminant fate and transport.

Our approach is to use molecular beams to synthesize "chemically tailored" nanoscale films as model systems to study ices, amorphous materials, supercooled liquids, and metal oxides. In addition to their utility as a synthetic tool, molecular beams are ideally suited for investigating the heterogeneous chemical properties of these novel films. Modulated molecular beam techniques enable us to determine the adsorption, diffusion, sequestration, reaction, and desorption kinetics in real-time. In support of the experimental studies, kinetic modeling and simulation techniques are used to analyze and interpret the experimental data.

Recent Progress and Future Directions

Measuring diffusivity in supercooled liquid nanoscale films using inert gas permeation

Amorphous materials are important in nature and have numerous technological applications. Despite their importance, understanding and controlling the properties of amorphous materials remains a scientific challenge. In particular, understanding the physics related to the formation of an amorphous solid, or glass, from its supercooled liquid is difficult because of their inherent metastability toward crystallization. Deeply supercooled liquids and amorphous materials (glasses) are thermodynamically metastable and typically have extremely low diffusivities. These properties make studies of these fundamental materials difficult at temperatures approaching the glass transition temperature (T_g).

Our previous approach to this problem has been to use molecular beam techniques to create the amorphous solid by vapor deposition onto a low-temperature substrate and thereby avoid the

crystallization that occurs when cooling from the liquid phase. We then heat the amorphous solid above its T_g, at which time it transforms into a supercooled liquid prior to crystallization. An advantage of this approach is that the viscosity of the supercooled liquid just above its T_g is typically orders of magnitude larger than the viscosity of a supercooled liquid just below the melting temperature. As a result, the crystallization rate can be dramatically reduced, and hence the lifetime of the highly viscous metastable liquid will be longer.

While measuring the desorption rate from the outer layer of an isotopically labeled or binary composite film works well for some systems, the approach has limitations. Specifically, the species of interest must have an experimentally measurable desorption rate that reflects the kinetic process (intermixing, crystallization, etc.) being studied. For example, crystallization of the pure components and diffusive intermixing of layered methanol/ethanol films occurs prior to the onset of detectable desorption of either component thus limiting the utility of the desorption method. We have developed a technique where the permeation of inert gases through initially amorphous overlayers is used to study the diffusivity of the supercooled liquid created when the film is heated above its T_g. The main idea of the technique is that as the amorphous film is heated to temperatures near its T_g, it transforms into a supercooled liquid and the inert gas can begin to diffuse through the overlayer. The hypothesis is that the transport of the inert gas is directly related to the diffusivity of the supercooled liquid overlayer itself. We have demonstrated the utility of this approach by depositing one monolayer of Kr underneath various overlayer thicknesses of amorphous methanol and desorbing the Kr at various heating rates. The desorption spectra shift to higher temperatures with increasing overlayer thickness and ramp rate which is consistent with diffusive-like transport. Numerical simulations using a one-dimensional kinetic model in which the Kr diffusion was represented by a series of discrete hops between potential minima between adjacent overlayers are in excellent agreement with the experimental results.

We have shown that the diffusivity can be extracted from permeation experiments using simulations or simply using the overlayer thickness, the heating rate, and the desorption peak temperature. The assumption that the transport of the rare gas through the supercooled liquid overlayer is directly and quantitatively correlated to the diffusivity of the supercooled liquid itself has been confirmed by measuring the intermixing of isotopically labeled methanol layers using reflection absorption infrared spectroscopy. The diffusivity for supercooled liquid methanol near its T_g obtained using the Kr permeation technique along with higher temperature supercooled liquid and liquid diffusivities are well-fit by a single Vogel-Fulcher-Tamman equation, $D = D_o exp(-B/(T-T_o))$, where D_o, B, and T_o are fit parameters. The Vogel-Fulcher-Tamman fit and the unusually large prefactors and activation energies of the diffusivity near T_g suggest that methanol is a *fragile* liquid. Non-Arrhenius behavior at temperatures approaching T_g is characteristic of fragile liquids where diffusion is occurring as part of a complex collective motion on a rugged energy landscape. Conversely, Arrhenius behavior is indicative of "strong" liquids where the diffusion mechanism is due to the physical crossing of a single barrier.

The above results show that inert gas atoms permeating through a nanoscale supercooled liquid film provide an excellent method to probe mobility near the glass transition. Such transport data are requisite to address many of the questions related to supercooled liquids and amorphous materials. The conceptual simplicity of the permeation approach and its potential applicability to a wide range of systems will make it a valuable tool for acquiring transport data at temperatures previously unattainable and provide valuable insights into the complex dynamics of supercooled liquids near the glass transition. Future work will involve applying this technique to other supercooled liquids – alcohols, alkanes, glass formers and exploring diffusion in supercooled liquid solutions and mixtures (salts, acids, bases).

Crystallization kinetics and excess free energy of H_2O and D_2O nanoscale films of amorphous solid water The relationship between liquid, supercooled liquid, and amorphous forms of water is of great interest driven by the importance of water in nearly all fields of science and because of the puzzling and apparently anomalous behavior of this relatively simple molecule. One such topic is whether there is thermodynamic continuity between ASW and normal supercooled liquid water. The difficulty in resolving this issue is that water can only be supercooled to ~231 K whereas the melt of ASW is purported to exist just above 136 K until crystallization, which occurs rapidly at ~150 K. The intervening temperature regime, from 150 to 231 K, is often referred to as *no man's land*. ASW is a metastable form

of water created by vapor deposition on a cold substrate (T < 130 K). Our group has used ASW films heated above their glass transition to probe the physical and thermodynamic properties of "liquid" water into the temperature range of no man's land. In addition to providing insight into the behavior of liquid water, ASW films can be used as models for studying the crystallization mechanisms in amorphous solids and for the growth and characterization of highly porous materials.

The metastability of the amorphous phase results in a discernable *bump* in the desorption rate which arises because of the decrease in the desorption rate (vapor pressure) that occurs with the conversion from the amorphous phase to the lower free energy crystalline phase. With increased heating rates, the crystallization bump shifts to higher temperature and becomes less pronounced. The TPD spectra show that by varying the heating rate from 0.001 to 3.0 K/s, the crystallization temperatures span a range of ~20 K. A coupled desorption-crystallization kinetic model was able to accurately simulate the crystallization kinetics for the entire set of ramp rate experiments. This approach offers several advantages over traditional isothermal measurements and enables the crystallization process to be studied over a broader temperature range (140-160 K).

There has been a long-standing question as to whether or not there is continuity between the liquid melt of ASW above its glass transition and supercooled liquid water. The question arises because many of the thermodynamic properties of supercooled liquid water appear to diverge at a temperature (227 K) well above the reported glass transition (~136 K) for water. In 1996, we published a paper where we used the desorption rates from the amorphous and crystalline phases of water to determine the excess free energy and entropy of ASW near 150 K. We have repeated these measurements with improved experimental sensitivity to acquire data over a broader temperature range (125-150 K). The H_2O excess free energy calculated from these improved measurements along with tabulated values of the free energy of supercooled liquid water near the melting point (236-273 K) demonstrate that both the excess free energy and entropy meet the thermodynamic criteria for there being continuity between ASW and normal supercooled liquid water. This work demonstrates the utility of using ASW films to gain insight into the physical properties of liquid water and as a model system for studying crystallization in metastable amorphous solids. In the future we plan to explore additional ASW properties such as transport and reactions of ASW and other metastable materials.

Measuring Diffusion in Supercooled Liquid Solutions of Methanol and Ethanol at Temperatures near the Glass Transition Our group has previously studied supercooled liquid solutions of ethanol and methanol using the desorption kinetics from the composite films. In that work, initially separated amorphous layers of methanol and ethanol were deposited at 20 K and then heated above T_g, where upon the two layers formed a homogeneous solution. These experiments found that the intermixing of methanol and ethanol acts to inhibit crystallization that would have otherwise rapidly occurred in either of the pure components. Further, the desorption kinetics from the supercooled liquid mixtures were quantitatively described by a kinetic model for desorption from an ideal solution. However, because the layers intermixed at temperatures (<110 K) where the desorption rate was below the detection limit of the experiment (~10^{-4} ML/s), it was not possible to study the diffusive intermixing kinetics using this approach. This makes this system an ideal candidate for the inert gas permeation technique to investigate the temperature and composition dependence of the diffusivity of supercooled liquid mixtures of methanol and ethanol.

The permeation spectra of Kr through methanol and ethanol mixtures of various overlayer thicknesses all have a Gaussian-like shape that broadens as the capping layer gets thicker. This is the expected behavior for diffusion through a homogeneous overlayer. In contrast, for the pure methanol and ethanol films, the desorption spectra for some of the thicker overlayers are clearly non-Gaussian. These distorted lineshapes are the result of crystallization of the pure supercooled liquids. This is consistent with our previous work that found that the crystallization is suppressed in ethanol/methanol mixtures. Thus, the use of mixtures provides a method to extend the temperature range beyond where information about the pure supercooled liquids can be acquired.

From a series of permeation experiments over a range of overlayer thicknesses, heating rates, and mixture compositions, it is possible to extract the isothermal composition-dependent diffusivities. The diffusivity in binary mixtures is often described as a compositionally weighted average of the diffusivities

of the individual components. In one approach, the binary diffusivity is given by an arithmetic average of the component diffusivities (Darken equation), whereas in the other approach, the binary diffusivity is expressed as a geometrical average of the component diffusivities exponentially weighted by their respective mole fractions (Vignes equation). We find that at temperatures near T_g, the exponentially weighted Vignes equation provides a more accurate description of the composition-dependent diffusivity. In contrast, at room temperature (298 K), the composition-dependent diffusivity can be equally well described by either the Darken equation or the Vignes equation. The reason is that the room temperature methanol and ethanol diffusivities differ by only a factor of ~2. On the other hand, at temperatures approaching Tg, the diffusivities differ by about 2 orders of magnitude, making the low-temperature data far more sensitive to the details of the composition weighted averaging. We have demonstrated the ability to accurately determine the physical properties of supercooled liquid solutions at temperatures near their T_g. Such data are requisite to understanding the complex changes in the molecular dynamics that occur as a supercooled liquid is cooled to temperatures near T_g, whereupon it forms a glass. Future work will focus on other binary systems and on isotope effects to assess the role translational and rotational coupling plays in diffusion near T_g.

References to Publications of DOE sponsored Research (CY 2009- present)

1. G. S. Parkinson, Z. Dohnalek, R. S. Smith, and B. D. Kay, "*Reactivity of Fe^0 Atoms, Clusters, and Nanoparticles with CCl_4 Multilayers on FeO(111)*", Journal of Physical Chemistry C **113**, 1818 (2009).
2. G. S. Parkinson, Y. K. Kim, Z. Dohnalek, R. S. Smith, and B. D. Kay, "*Reactivity of Fe^0 Atoms and Clusters with D_2O over FeO(111)*", Journal of Physical Chemistry C **113**, 4960 (2009).
3. F. Cholette, T. Zubkov, R. S. Smith, Z. Dohnalek, B. D. Kay, and P. Ayotte, "*Infrared Spectroscopy and Optical Constants of Porous Amorphous Solid Water*", Journal of Physical Chemistry B **113**, 4131 (2009).
4. R. S. Smith, T. Zubkov, Z. Dohnalek, and B. D. Kay, "*The Effect of the Incident Collision Energy on the Porosity of Vapor-Deposited Amorphous Solid Water Films*", Journal of Physical Chemistry B **113**, 4000 (2009).
5. G. S. Parkinson, Z. Dohnalek, R. S. Smith, and B. D. Kay, "*Reactivity of C_2Cl_6 and C_2Cl_4 Multilayers with Fe^0 Atoms over FeO(111)*", Journal of Physical Chemistry C **113**, 10233 (2009).
6. G. A. Kimmel, J. Matthiesen, M. Baer, C. J. Mundy, N. G. Petrik, R. S. Smith, Z. Dohnalek, and B. D. Kay, "*No Confinement Needed: Observation of a Metastable Hydrophobic Wetting Two-Layer Ice on Graphene*", Journal of the American Chemical Society **131**, 12838 (2009).
7. J. Matthiesen, R. S. Smith, and B. D. Kay, "*Using Rare Gas Permeation to Probe Methanol Diffusion near the Glass Transition Temperature*", Physical Review Letters **103**, 245902 (2009).
8. R. S. Smith, J. Matthiesen, and B. D. Kay, "*Breaking through the glass ceiling: The correlation between the self-diffusivity in and krypton permeation through deeply supercooled liquid nanoscale methanol films*", Journal of Chemical Physics **132**, 124502 (2010).
9. G. S. Parkinson, Z. Dohnalek, R. S. Smith, and B. D. Kay, "*Reactivity of Fe^0 Atoms with Mixed CCl_4 and D_2O Films over FeO(111)*", Journal of Physical Chemistry C **114**, 17136 (2010).
10. R. S. Smith, J. Matthiesen, and B. D. Kay, "*Measuring diffusivity in supercooled liquid nanoscale films using inert gas permeation. I. Kinetic model and scaling methods*", Journal of Chemical Physics **133**, 174504 (2010).
11. J. Matthiesen, R. S. Smith, and B. D. Kay, "*Measuring diffusivity in supercooled liquid nanoscale films using inert gas permeation. II. Diffusion of Ar, Kr, Xe, and CH_4 through Methanol*", Journal of Chemical Physics **133**, 174505 (2010).
12. J. Matthiesen, R. S. Smith, and B. D. Kay, "*Mixing It Up: Measuring Diffusion in Supercooled Liquid Solutions of Methanol and Ethanol at Temperatures near the Glass Transition*", Journal of Physical Chemistry Letters **2**, 557 (2011).
13. R. S. Smith, J. Matthiesen, J. Knox, and B. D. Kay, "*Crystallization Kinetics and Excess Free Energy of H_2O and D_2O Nanoscale Films of Amorphous Solid Water*", Journal of Physical Chemistry A, dx.doi.org/10.1021/jp110297q (2011).
14. P. Ayotte, P. Marchand, J. Daschbach, R. S. Smith, and B. Kay, "*HCl Adsorption and Ionization on Amorphous and Crystalline H_2O Films below 50 K*", Journal of Physical Chemistry A, Accepted (2011).

Correlating electronic and nuclear motions during photoinduced charge transfer processes using multidimensional femtosecond spectroscopies and ultrafast x-ray absorption spectroscopy

Munira Khalil
University of Washington, Department of Chemistry, Box 351700, Seattle, WA 98115
Email: mkhalil@chem.washington.edu

The goal of this research program is to measure coupled electronic and nuclear motions during photoinduced charge transfer processes in transition metal complexes by developing and using novel femtosecond spectroscopies. In this program, we will use a unique two-pronged experimental approach to relate commonly measured kinetic parameters in transient photochemical experiments to the time-evolving distributions of molecular and electronic structures of the reactants and products and their interactions with the solvent bath. One part of the research program will focus on the development of novel three-dimensional visible-infrared experiments employing a sequence of visible and infrared fields to directly correlate electronic and vibrational motion during ultrafast photochemical reactions. These experiments will measure time-dependent anharmonic vibrational couplings of the high-frequency solute vibrations with the low-frequency solvent and solute degrees of freedom, time-dependent vibronic couplings, and elucidate the role of incoherent and coherent vibrational relaxation and transfer pathways during electron transfer.

Over the past one and a half years, our work has focused on the following areas: (i) understanding photoinduced linkage isomerism in Fe(II) complexes (ii) 2D IR spectroscopy of mixed valence complexes to measure vibrational couplings between terminal and bridging cyanide ligands (iii) Elucidating the role of high frequency vibrations during ultrafast back electron transfer (iv) Developing fifth-order spectroscopies to measure the non-equilibrium spectral density of metal-cyanide stretching frequencies during a photoinduced electron transfer process (v) Using DFT based methods to model Fe K-edge transient x-ray experiments probing ultrafast photoinduced spin crossover in Fe(II) complexes and (vi) Using the Ru L-edge x-ray spectrum as a probe of electronic changes during intramolecular charge transfer processes.

Photoinduced linkage isomerism in metal – nitrosyl compounds is a rich field of study in which irradiation of the sample by light causes the nitrosyl ligand to bond to the metal center in multiple ways. To date, photoinduced linkage isomerism has been documented in several transition metal – nitrosyl species, and there is great interest in understanding how the M – NO coordination of these species relates to the overall photochemistry of the compound including NO radical release pathways. We studied photoinduced metal – nitrosyl linkage isomerism in sodium nitroprusside ($Na_2[Fe^{II}(CN)_5NO]\cdot 2H_2O$, SNP) dissolved in methanol using picosecond transient infrared (IR) spectroscopy. The high sensitivity of this technique allowed the simultaneous observation of two known metastable (MS) iron – nitrosyl linkage isomers of SNP, $[Fe^{II}(CN)_5(\eta^1\text{-ON})]^{2-}$ (MS1) and $[Fe^{II}(CN)_5(\eta^2\text{-NO})]^{2-}$ (MS2) at room temperature. The transient population of free nitrosyl radicals (NO·) is also measured in the sample solution. These three transient species are detected using their distinct

nitrosyl stretching frequencies at 1794 cm^{-1} (MS1), 1652 cm^{-1} (MS2) and 1851 cm^{-1} (NO·). The metastable isomers and NO· are formed on a sub-picosecond time scale and have lifetimes greater than 100 ns. A UV (400 nm)−pump power dependence study reveals that MS1 can be formed with one photon, while MS2 requires two photons to be populated at room temperature in solution. Other photodissociation products including cyanide ion, Prussian blue (PB) and $[Fe^{III}(CN)_5(CH_3OH)]^{2-}$ are observed. We developed a photochemical kinetic scheme to model our data and the analysis revealed that photoisomerization and photodissociation of the metal – NO moiety are competing photochemical pathways for SNP dissolved in methanol at room temperature. Based on the analysis, the solvent-associated Fe(III) species and Prussian blue form on a 130 ps and 320 ps time scale, respectively. The simultaneous detection and characterization of photoinduced linkage isomerism (MS1 and MS2) and photodissociation of the metal−NO bond in SNP highlights the importance of understanding the role played by metastable metal – NO linkage isomers in the photochemistry of metal – nitrosyl compounds in chemistry and biology. We are currently improving our set-up to measure femtosecond transient IR spectra of SNP dissolved in solution to directly monitor the formation of the nitrosyl radical and the metastable linkage isomers.

To decipher the role of vibrational phase and energy relaxation in ultrafast photoinduced charge transfer processes, we have performed several experiments on a trinuclear cyano-bridged mixed valence complex of the form $[(CN)_5Fe^{II}–CN–Pt^{IV}(NH_3)_4–NC–Fe^{II}(CN)_5]^{4-}$ (herein denoted as $Fe^{II}Pt^{IV}Fe^{II}$) in aqueous solution. This complex has a strong metal−metal charge transfer (MMCT) band centered at 424 nm that induces the forward-electron transfer (FET) from Fe^{II} to Pt^{IV} to generate a transient $Fe^{III}Pt^{III}Fe^{II}$ (or equivalently $Fe^{II}Pt^{III}Fe^{III}$) species. From this intermediate state, the system can relax back to the ground state via back-electron transfer (BET; Φ_{BET} ~ 99%) or undergo a thermal FET to afford $Fe^{III}Pt^{II}Fe^{III}$ (Φ_{FET} ~ 1%). The photoinduced FET between iron and platinum is strongly coupled to both intermolecular solvent and intramolecular solute nuclear motions. This produces large displacements of the coordinates of the coupled modes, which will govern the dynamics of BET and subsequent vibrational relaxation. Our experiments seek to understand how inter- and/or intramolecular interactions are controlling the rate of BET and, once back in the ground electronic state, how the excess vibrational energy is dissipated into the solvent bath.

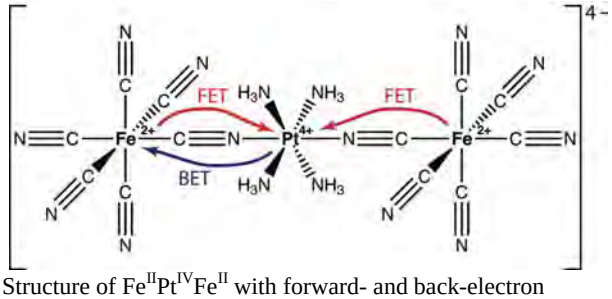

Structure of $Fe^{II}Pt^{IV}Fe^{II}$ with forward- and back-electron transfer shown in red and blue, respectively.

Our approach in understanding coupling of electronic and nuclear motions in $Fe^{II}Pt^{IV}Fe^{II}$ is to directly probe the CN ligands via their unique CN stretching frequencies as a function of an electron transfer reaction. Thus, it is important to understand the CN vibrational modes within the electronic ground state before inducing the electron transfer. We have collected polarization-selective 2D IR spectra of $Fe^{II}Pt^{IV}Fe^{II}$ in D_2O in order to (1) assign the broad resonances in the FTIR spectrum in terms of a bridging CN stretch and three CN stretches involving the terminal ligands, (2) determine the diagonal anharmonicities of the four vibrational modes (~20 cm^{-1}) , (3) measure maximum

anharmonic couplings of ~20 cm^{-1} between the terminal and bridging CN ligands, (4) characterize timescales of ~ 2 ps for intramolecular vibrational relaxation (IVR) among the various modes and vibrational lifetimes of ~19 ps for the cyanide stretching modes, and (5) extract the characteristic solvation time scales present in the system via frequency-frequency auto- and cross-correlation functions (FFCF).

The ultrafast electron transfer kinetics of FET, BET, and IVR in $Fe^{II}Pt^{IV}Fe^{II}$ are known to occur within ~3.5 ps, but it had not been possible to deconvolve each of these contributions with previous transient absorption experiments. We performed sub-100 fs transient infrared spectroscopy in an attempt to systematically characterize each contribution to the photochemical dynamics. The use of an IR probe allows this technique to characterize vibrational relaxation in a mode-selective way. We have formulated a target model describing both BET and mode-specific vibrational relaxation and globally fit our spectro-temporal data to this model. The results show that back-electron transfer occurs on a ~120 fs time scale and highly excited vibrational modes (ν>5) along the MMCT axis are the first to accept the excess energy upon back-electron transfer. This energy is then either transferred to orthogonal (i.e., radial) modes and/or climbs down the vibrational ladder of vibrational modes parallel to the MMCT axis. All of the vibrational modes subsequently return to the ground state (υ_i = 0) on a 16−20 ps time scale. These results have implications on the use and design of transition metal mixed-valence complexes as energy harvesting materials, as it emphasizes the importance of vibrational relaxation in electron transfer processes.

It is of interest to understand non-equilibrium solvation dynamics on electronic excited states during a photochemical process. We have developed a technique known as transient heterodyned dispersed vibrational echo (tHDVE) spectroscopy that allows the simultaneous detection of dynamics occurring on both the electronic ground and excited states. This approach combines optical spectroscopy with 3rd-order nonlinear infrared spectroscopies such that vibrational relaxation, dephasing times, and solvation dynamics can be measured as a function of the photochemical electron transfer process. This information is extracted by simultaneously collecting transient grating (TG), dispersed vibrational echo (DVE), and vibrational echo peak shift (PS) signals, following charge transfer on a 0.1 – 5 ps timescale. The ability to monitor a time-evolving spectral density of low-frequency modes coupled to specific high-frequency modes as a function of a photochemical reaction will provide microscopic insight into the coupling of intramolecular degrees of freedom to the electronic motion.

Time-resolved X-ray absorption spectroscopy is a sensitive probe of time evolving nuclear and electronic structure in molecules. Our work investigates the photochemistry of transition metal complexes including Fe(II) spin crossover, Fe and Ru mixed valence metals, and Ru-based solar cell dye molecules. Our joint experimental-theoretical approach combines performing ultrafast time-resolved X-ray absorption measurements at the Advanced Light Source in collaboration with Dr. Robert Schoenlein's group and developing the computational tools necessary to interpret these experiments.

We have investigated the photoinduced spin crossover event in the Fe(II) complex $[Fe(tren(py)_3]^{2+}$ using density functional methods. Previous experimental work has demonstrated that excitation of this Fe complex dissolved in solution with 400 nm light converts the low-spin singlet ground state into a high-spin quintet species. The transition

to high-spin is accompanied by a large geometric change that is indicated by the transient X-ray absorption spectrum. We have subsequently focused on identifying signatures of the changing electronic structure in these spectra. Our work has extended the transition potential (TP) DFT method that has been widely used for first row elements to simulate the k-edge X-ray absorption near edge spectra of iron. Our results show that one can use the TP methodology to simulate a 40 eV range of the X-ray spectrum. These simulations reproduce changes in the Fe K-edge XAS that accompany photo-excitation with visible light. Consequently, this method can be used to correlate changes in molecular and electronic structure with changes in the experimentally observed spectrum. We have also used time-dependent (TD) DFT calculations to simulate the pre-edge features in the XAS spectrum. We find that these peaks report directly on the Fe 3d orbitals providing information about the metal-ligand bonding. Analysis of the pre-edge features has allowed us to map out the 3d orbitals of the low- and high-spin moieties. From this analysis, we have extracted ligand field parameters and information about excited state electron distributions.

Finally, we have performed static Ru L-edge X-ray absorption measurements on the mixed valence metal dimers $Na[(NC)_5M^{II}\text{-}CN\text{-}Ru^{III}(NH_3)_5]$ where M = Fe and Ru. Ru L-edge spectroscopy is a direct probe of valence Ru 4d orbitals. By comparing the spectra of the mixed valence compounds with that of the model complexes $K_4Ru^{II}(CN)_6$ and $Ru^{III}(NH_3)_6Cl_3$, we can accurately assess many of the properties of the metals including oxidation states, ligand field splitting, and magnitudes of spin-orbit effects. In particular, we have directly identified the presence of both Ru^{II} and Ru^{III} in the Ru-Ru dimer. Further analysis employing charge transfer multiplet calculations will allow us to determine the degree of electron delocalization in the mixed valence species.

DOE Supported Publications (Oct 2009 - Present)

1. M. S. Lynch, M. Cheng, B. E. Van Kuiken, and M. Khalil, J. Am. Chem. Soc. 133, 5255 (2011).
2. M. S. Lynch, B. E. Van Kuiken, M. Cheng, S. Daifuku, and M. Khalil, In Ultrafast Phenomena XVII, Oxford University Press, 346, (2011) (346-348).
3. N. Huse, T. K. Kim, M. Khalil, L. Jamula, J. K. McCusker, and R. W. Schoenlein, Springer Series in Chemical Physics 92, 125 (2009).
4. N. Huse, M. Khalil, T. K. Kim, A. L. Smeigh, L. Jamula, J. K. McCusker, and R. W. Schoenlein, J. Phys.: Conf. Ser.148, 012043 (2009).

Chemical Kinetics and Dynamics at Interfaces

Non-Thermal Reactions at Surfaces and Interfaces

Greg A. Kimmel (PI) and Nikolay G. Petrik

Chemical and Materials Sciences Division
Pacific Northwest National Laboratory
P.O. Box 999, Mail Stop K8-88
Richland, WA 99352
gregory.kimmel@pnl.gov

Program Scope

The objectives of this program are to investigate 1) the thermal and non-thermal reactions at surfaces and interfaces, and 2) the structure of thin adsorbate films and how this influences the thermal and non-thermal chemistry. Energetic processes at surfaces and interfaces are important in fields such as photocatalysis, radiation chemistry, radiation biology, waste processing, and advanced materials synthesis. Low-energy excitations (e.g. excitons, electrons, and holes) frequently play a dominant role in these energetic processes. For example, in radiation-induced processes, the high energy primary particles produce numerous, chemically active, secondary electrons with energies that are typically less than ~100 eV. In photocatalysis, non-thermal reactions are often initiated by holes or (conduction band) electrons produced by the absorption of visible and/or UV photons in the substrate. In addition, the presence of surfaces or interfaces modifies the physics and chemistry compared to what occurs in the bulk.

We use quadrupole mass spectroscopy, reflection-absorption infrared spectroscopy (RAIRS), and other ultra-high vacuum (UHV) surface science techniques to investigate thermal, electron-stimulated, and photon-stimulated reactions at surfaces and interfaces, in nanoscale materials, and in thin molecular solids. Since the structure of water near interface plays a crucial role in the thermal and non-thermal chemistry occurring there, a significant component of our work involves investigating the structure of aqueous interfaces. A key element of our approach is the use of well-characterized model systems to unravel the complex non-thermal chemistry occurring at surfaces and interfaces. This work addresses several important issues, including understanding how the various types of low-energy excitations initiate reactions at interfaces, the relationship between the water structure near an interface and the non-thermal reactions, energy transfer at surfaces and interfaces, and new reaction pathways at surfaces.

Recent Progress

Electron- and hole-mediated reactions in UV-irradiated O_2 adsorbed on reduced rutile TiO_2(110)

Oxygen plays an important, but often poorly understood, role in many photocatalytic processes. We have investigated the adsorption and photochemistry of O_2 on TiO_2(110). Our results indicate that no more than 15% of the chemisorbed O_2 has dissociated after adsorption at 28 K followed by annealing to 100 K. However, typically less than half of the adsorbed O_2 photodesorbs. The oxygen remaining on the surface after UV irradiation is in at least two forms: a molecular form that is inactive for photodesorption and photo-dissociated O_2. Our results indicate that the photodesorption depends on the charge state of the chemisorbed O_2, and that reactions between the chemisorbed O_2 and conduction band electrons are responsible for the both the dissociated and non-dissociated O_2 remaining after UV irradiation.

Figure 1 (left panel) shows the integrated O_2 PSD and TPD signals versus $\theta(O_2)$. In this experiment, $^{18}O_2$ was adsorbed at 28 K and the sample was subsequently heated to 100 K while the $^{18}O_2$ thermal desorption was monitored (Fig. 1, left panel, squares). The sample was then irradiated for 300 s at 28 K to obtain the integrated $^{18}O_2$ PSD (Fig. 1, left panel, triangles). In contrast to the O_2 TPD signal, O_2 PSD is readily observed even at very low coverages. The slope of the integrated O_2 PSD versus $\theta(O_2)$ gives the O_2 PSD yield per chemisorbed O_2. The data can be fit with two straight lines for $\theta(O_2) < 0.09$ ML, and for $0.09 < \theta(O_2) \leq 0.18$ ML. An important observation is that less than 50% of the chemisorbed

O_2 desorbs. To explain the observations, we proposed that the photodesorption probability depends on the charge state of the chemisorbed O_2. Specifically, more negatively charged oxygen molecules have a lower hole-mediated photodesorption probability than less negatively charged molecules. Since each vacancy nominally has a charge of -2*e*, a single O_2 chemisorbed in a vacancy should adsorb as O_2^{2-} while two O_2 chemisorbed at or near a vacancy should adsorb as O_2^-. Thus for $\theta(O_2) < \theta(V_O)$, the photodesorption yield should be lower (as observed). Although not shown here, other experiments showed that some of the oxygen that remained on the surface after irradiation was dissociated and some was left in a molecular state that was inactive for hole-mediated photodesorption.

We also found that *physisorption* of O_2 on TiO_2(110) dramatically changes the photodesorption of *chemisorbed* O_2. The right panel in Fig. 1 shows the results of an experiment in which $^{18}O_2$ is first chemisorbed (by adsorption at 28 K followed by annealing to 100 K) on the TiO_2(110). Next, the sample is exposed to large dose of $^{16}O_2$ at 28 K such that any remaining chemisorption sites are filled with $^{16}O_2$ plus the surface is covered with ~1.4 ML of physisorbed $^{16}O_2$. The sample was then irradiated for 300 s. Compared to the experiments without physisorbed $^{16}O_2$ (Fig. 1, left panel), the $^{18}O_2$ PSD yield increased substantially. Surprisingly, we also observed reactions between the chemisorbed $^{18}O_2$ and physisorbed $^{16}O_2$ leading to the production of $^{16}O^{18}O$. The figure shows the integrated $^{18}O_2$, $^{16}O^{18}O$, and "total" $^{18}O_2$ PSD signals versus the initial $^{18}O_2$ coverage. (The total amount of the initial $^{18}O_2$ that desorbs as either $^{18}O_2$ or $^{16}O^{18}O$ is given by $^{18}O_2$ yield plus half the $^{16}O^{18}O$ yield.) All the PSD yields increase monotonically for $\theta(^{18}O_2) < \theta_{sat}$, and are approximately constant once the chemisorption sites are saturated with $^{18}O_2$. For $\theta(^{18}O_2) < \theta_{sat}$, the $^{18}O_2$ PSD yield increases linearly with a slope of ~0.70 ML/ML, and the total $^{18}O_2$ yield initially increases with a slope of ~1. The results showed that at least 85% of O_2 had not dissociated after adsorption at 28 K and annealing to 100 K.

These results show that the photochemistry of O_2 on TiO_2(110) is more complicated than previously appreciated. In particular, the reactions of chemisorbed O_2 with both the holes and electrons produced by the absorption of UV photons in the TiO_2 need to be considered.

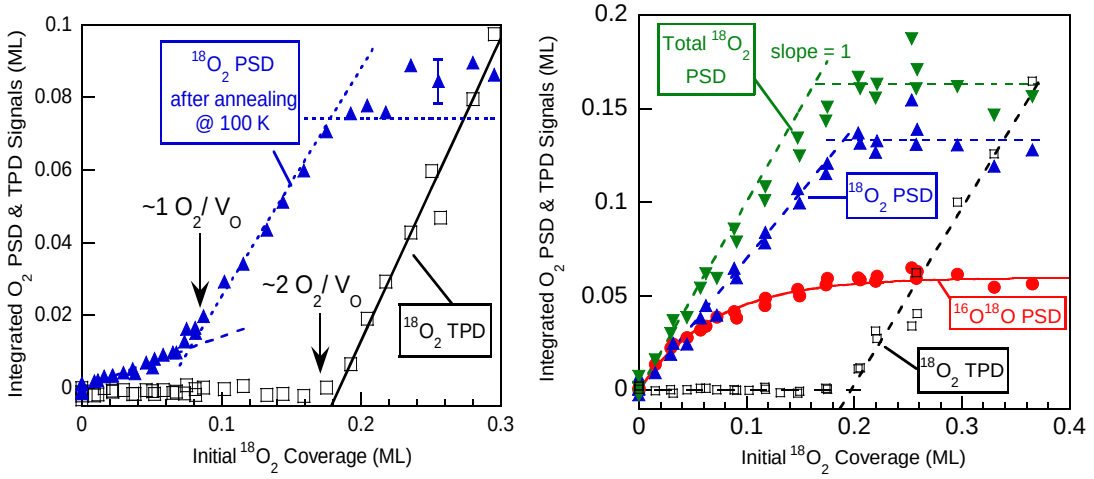

Figure 1: Integrated O_2 PSD and TPD yields with (right panel) and without (left panel) physisorbed $^{16}O_2$. $^{18}O_2$ PSD (blue triangles) and TPD (squares) versus $^{18}O_2$ coverage. While no thermal desorption is observed for $\theta(O_2) < 0.19$ ML, photon-stimulated desorption increases linearly over two different coverage ranges corresponding to $\theta(O_2) < \theta(V_O)$ and $\theta(V_O) < \theta(O_2) < 2\theta(V_O)$.

A Unique Vibrational Signature of Rotated Water Monolayers on Pt(111) – Predicted and Observed

The structure of water at interfaces influences the physical, chemical and biological processes relevant to a large number of natural and man-made systems. As a result, the structure of water at surfaces has been

extensively studied. Still, even the simplest and arguably most experimentally accessible issue – the ground-state arrangement of the first water layer on a solid surface – has been hard to resolve. For water on Pt(111), helium atom scattering (HAS) and low-energy electron diffraction (LEED) have revealed two ordered structures that grow at temperatures above ~120 K. At submonolayer coverages, the water forms a $(\sqrt{37}\times\sqrt{37})R25.3^{\circ}$ (or "$\sqrt{37}$") layer, while for a slowly grown water monolayer, a $(\sqrt{39}\times\sqrt{39})R16.1^{\circ}$ (or "$\sqrt{39}$") structure is observed. Originally, both ordered layers were interpreted as arising from strained and rotated "ice-like" monolayers. However, new structures were recently proposed based scanning tunneling microscopy (STM) results. In the proposed structures, the central motif consists of hexagons of flat-lying water molecules, surrounded by pentagons and heptagons of water molecules. DFT predicts six short O – O bonds per unit cell (with lengths of ~2.5 – 2.6 Å) for both structures. According to a broadly obeyed correlation between O – O bond length and OH-stretch frequency, the proposed structures should have an infrared absorption band that is red-shifted by more than 1000 cm^{-1} from the normal OH-stretch band of ice.

In collaboration with Peter Feibelman, Bruce Kay, Scott Smith, and Tyhkon Zubkov, we have investigated the structure of thin water films on Pt(111) using RAIRS and density functional theory (DFT). We have observed the signature, red-shifted OH-stretch modes in infrared absorption measurements for both the "$\sqrt{37}$" and "$\sqrt{39}$" wetting layers on Pt(111). For water films grown at 45 K, the signature modes are largely absent. However, these modes develop for films that are subsequently annealed to higher temperatures. DFT calculations of the vibrational densities of states of the "$\sqrt{37}$" and "$\sqrt{39}$" wetting layers on Pt(111) also predict the red-shifted stretch frequencies.

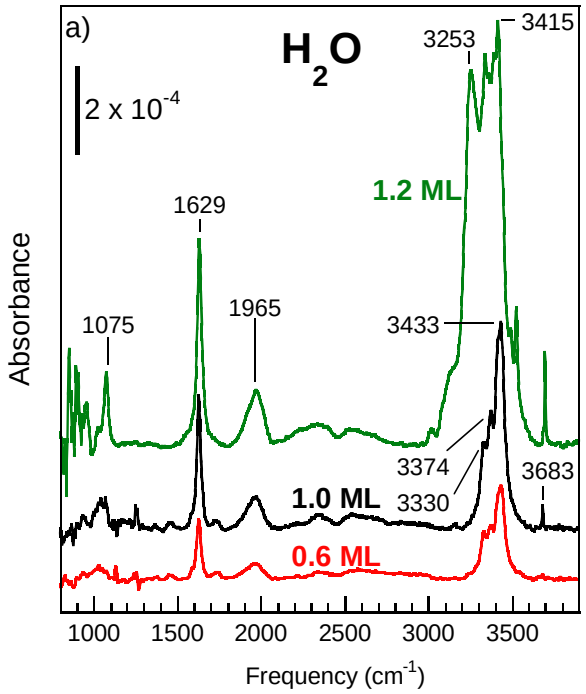

Figure 2. RAIRS spectra of thin water films grown on Pt(111). The absorption peak at 1965 cm^{-1} is due to short O – O bonds in the water films.

Figure 2 shows RAIRS spectra for three water films on Pt(111). The red and black lines show spectra for $\sqrt{37}$ films with coverages of 0.6 and 1.0 ML deposited at 152 K. For these films there are three closely spaced peaks in the OH-stretch region at 3330, 3374 and 3433 cm^{-1}, and a relatively narrow peak at 1965 cm^{-1} in between the OH-stretch and the bending mode. For 1.2 ML of H_2O deposited at 159 K (Fig. 2, green line), the film has the $\sqrt{39}$ wetting layer along with a small amount of non-wetting crystalline ice. In this case, the structure in the OH-stretch region is different, but the film also shows a peak at 1965 cm^{-1} similar to the peak observed for the $\sqrt{37}$ films. The absorption peak at 1965 cm^{-1} is due to six short O – O bonds that are present in both the $\sqrt{37}$ and $\sqrt{39}$ layers for water on Pt(111). DFT calculations (not shown) also predict absorptions at ~2100 cm^{-1} for the $\sqrt{37}$ and $\sqrt{39}$ layers. The results provide valuable evidence supporting the proposed structures of water on Pt(111).

Future Directions:

Important questions remain concerning the factors that determine the structure of thin water films on various substrates. We plan to continue investigating the structure of thin water films on non-metal surfaces, such as oxides, and on metals where the first layer of water does not wet the substrate. For the non-thermal reactions in water films, we will use RAIRS to characterize the electron-stimulated reaction products and precursors. We will also continue our investigations into the photochemistry of small molecules on TiO_2(110).

References to publications of DOE sponsored research (FY 2009 – present)

[1] Zhenrong Zhang, Yingge Du, Nikolay G. Petrik, Greg A. Kimmel, Igor Lyubinetsky, and Zdenek Dohnálek, "Water as a Catalyst: Imaging Reactions of O_2 with Partially and Fully Hydroxylated TiO_2(110)," *J. Phys. Chem. (C)* **113**, 1908 (2009).

[2] Nikolay G. Petrik and Greg A. Kimmel, "Non-thermal water splitting on Rutile TiO_2: Electron-stimulated production of H_2 and O_2 in Amorphous Solid Water films on TiO_2(110)," *J. Phys. Chem. (C)* **113**, 4451 (2009).

[3] Minta C. Akin, Nikolay G. Petrik and Greg A. Kimmel, "Electron-Stimulated Reactions and O_2 production in Methanol-Covered Amorphous Solid Water Films," *J. Chem. Phys.* **130**, 104710 (2009).

[4] Nikolay G. Petrik, Zhenrong Zhang, Yingge Du, Zdenek Dohnálek, Igor Lyubinetsky, and Greg A. Kimmel, "The Chemical Reactivity of Reduced TiO_2(110): The dominant role of surface defects in oxygen chemisorption," *J. Phys. Chem. (C)* **113**, 12407 (2009).

[5] Greg A. Kimmel, Jesper Matthiesen, Marcel Baer, Christopher J. Mundy, Nikolay G. Petrik, R. Scott Smith, Zdenek Dohnálek, and Bruce D. Kay, "No Confinement Needed: Observation of a Metastable Hydrophobic Wetting Two-Layer Ice on Graphene," *J. Am. Chem. Soc.* **131**, 12838 (2009).

[6] Nikolay G. Petrik and Greg A. Kimmel, "Photoinduced Dissociation of O_2 on Rutile TiO_2(110)," *J. Phys. Chem. Lett.* **1**, 1758 (2010).

[7] Nikolay G. Petrik and Greg A. Kimmel, "Off-Normal CO_2 Desorption from the Photooxidation of CO on Reduced TiO_2(110)," *J. Phys. Chem. Lett.* **1**, 2508 (2010).

[8] Nikolay G. Petrik and Greg A. Kimmel, "Electron- and hole-mediated reactions in UV-irradiated O_2 adsorbed on reduced rutile TiO_2(110)," *J. Phys. Chem. (C)*, **115**, 152 (2011).

Radiation Effects in Heterogeneous Systems and at Interfaces

Jay A. LaVerne, laverne.1@nd.edu

Daniel M. Chipman, Ian Carmichael, Dan Meisel, Sylwia Ptasinska

Notre Dame Radiation Laboratory, University of Notre Dame, Notre Dame, IN 46556

chipman.1@nd.edu, carmichael.1@nd.edu, dani@nd.edu, ptasinska.1@nd.edu

Program Scope

The nature and mechanism of the formation of the primary species in the radiolysis of multi-phase systems consisting of water and aqueous solutions in association with ceramic oxide or metallic particles under ambient conditions are elucidated. Research is focused on the radiolysis of water and how it is affected by the presence of the liquid – solid interface. Radiation induced reactions at the water – solid interface and the transport of energy, charge, and matter through the interface are examined. One approach examines ceramic oxides in association with a relatively small number of adsorbed water layers. Emphasis is placed on the role of the solid phase on water radiolysis and species formed at the interface are directly probed using techniques developed in the surface sciences. A second approach primarily examines suspensions of ceramic oxide particles where the solid phase is essentially a solute that participates in the water radiolysis via redox reactions. The suspended particles may act as a sink or source of electrons or holes. Both directions contain significant theoretical components to facilitate interpretation of the observed results.

Recent Progress

This project has focused on the radiolysis of liquid-solid heterogeneous systems in order to understand the role of interfaces in the transfer of energy, mass, and charge. The main liquid of interest has been water because of its wide use in nuclear reactors, in separation systems, and in waste storage. Most of the work in the last fiscal period concerned the radiolysis of adsorbed water, which are systems consisting predominantly of the solid phase. Energy in these systems is initially deposited mainly in the solid and then migrates to or through the interface to decompose water.

A great amount of progress has been made in the last period on examination the radiolysis of water adsorbed on ceramic oxides. Part of this project has focused on the spectroscopic examination of ceramic oxides following their irradiation with 3 MeV electrons. The samples are sealed in a temperature controlled device suitable for irradiation followed by examination using diffuse reflectance infrared Fourier transform (DRIFT) techniques without exposing the sample to the atmosphere. Selected gaseous atmospheres can be chosen to influence the chemistry or the samples can be evacuated. Temperature variation is important to strip off the various physisorbed and chemisorbed water layers in order to probe their contribution to the overall radiolysis process. At temperatures of 400°C and above only the hydroxyl groups due to dissociated chemisorbed water are observed on the ceramic oxide surface. This interfacial layer of hydroxyl groups is found to be invariant to extreme fluences of fast electrons. Energy deposited within the solid oxide is passing through this layer to decompose water overlayers with little effect to the surface hydroxyl group. Alternatively this entity is being reformed on the time scales of these experiments. Raman spectroscopic studies have been performed post irradiation

of the samples. The lack of variation in the Raman spectra confirms the robustness of the water-solid interface under radiolysis. Previous low temperature electron paramagnetic resonance (EPR) studies found the signature of H atoms in these systems following radiolysis, which combined with this more recent work suggests that decomposition involves the water layers slightly displaced from the oxide surface. Very preliminary X-ray photoelectron spectroscopic (XPS) studies find that the radiolysis of ZrO_2 results in a very small enhancement in the percentage of OH bonds. Not only are the surface hydroxyl groups radiation inert, they may even be formed in radiolysis by reactions with holes. Clearly, the ceramic oxide is being modified by radiolysis, but the effects are difficult to observe using normal optical spectroscopic techniques.

The production of H_2 was examined in the fast electron radiolysis of water adsorbed on several ceramic oxides. Special interest was given to ZrO_2 because it is known to greatly enhance the production of H_2 over that of pure water. The relative amount of H_2 production was found to increase by a factor of 4 from room temperature to 200°C. A further increase in temperature leads to a decrease in the amount of H_2 production. This result agrees with the above spectroscopic result showing the relative radiation inertness of the surface layer of water on the ceramic oxide. The hydroxyl layer at the surface does not seem to be responsible for the direct production of excess H_2 even though energy is probably passing through it. The chemisorbed water layers that exist up to about 200°C are responsible for most of the H_2 formation. These results explain where the source of the excess H_2, but not the mechanism for its enhanced yields with ZrO_2. The amount of water on these oxides has an obvious effect on H_2 production as does the oxide type. A wide series of oxides is currently being investigated to determine what oxide characteristics are most responsible for water decomposition.

The *in situ* examination of the radiolysis of compounds frozen on a clean substrate has been performed in this past period to further observe radiation effects occurring at water – ceramic oxide interfaces. The purpose of this work is to examine the radiolytic modification of a few well defined layers of a material on a particular substrate. Water and other compounds are frozen onto a clean Al_2O_3 substrate, irradiated with low energy electrons and examined *in situ* using infrared reflectance spectroscopy. IR spectra are taken of the samples immediately after deposition and following irradiations to selected energy deposition. Electron energies are about 1000 eV, which is sufficient to penetrate the condensates and deposit most of the energy in the substrate. Condensing water with added substrates has proven to be difficult with the present experimental configuration so neat alcohols have been examined in this period. The radiolysis of methanol and isopropanol ices shows their conversion to aldehydes and other higher molecular weight compounds. For instance, the figure shows the formation of formaldehyde, methyl formate and acetone at 1490 cm^{-1}. These products suggest a simple rearrangement from methanol to formaldehyde that probably occurs following the breaking of a C-H bond. However, the data also suggests the breaking of the C-O bond. The resulting methyl group adds to a medium molecule to give methyl formate or acetone following rearrangement. The OH group abstracts H atoms from medium molecules to form water as evidenced by the broadening of the OH stretch at 3260 cm^{-1}. The formation of CO_2 is also apparent by the peaks at 660, and 2340 cm^{-1}, which suggests the breaking of a C-C bond. Binary systems will be made with selected scavengers to positively identify precursors.

Gold nanoparticles containing no foreign stabilizer are obtained upon reduction of Au_2O_3 by molecular hydrogen. Ambient temperature and H_2 pressure control particle size, which was characterized by a range of techniques. The particles were shown to be highly active redox catalysts in the conversion of strongly reducing radicals to hydrogen from water in basic

solution. Surface-enhanced Raman scattering, SERS, spectra of a probe molecule, p-aminothiphenol, adsorbed on the particle surface was determined and the effects of pH, electron injection, and added Au(III) ions on the SERS spectra were measured producing results in line with those observed previously on similarly-prepared silver particles.

The adsorption geometry of the thymidine on Au(111) and Cu(110) surfaces has been determined from experimental results of soft X-ray photoelectron spectroscopy (XPS) and near-edge X-ray absorption fine structure (NEXAFS) spectroscopy. The XPS of C, N, and O 1s as well as the absorption spectra at the N and O K-edges were measured for monolayer thymidine films, and the nature of the bonding with the two metal surfaces has been determined. The NEXAFS data at the N and O K-edge show a strong angular dependence of the π^*/σ^* intensity ratios. The thymine moiety is lying nearly parallel to the Au(111) surface, while on the Cu(110) surface, it adsorbs at a steep angle.

Minimum energy paths linking the various locally-stable structures for water absorption onto the α-Al_2O_3(0001) surface have been elucidated and the kinetically accessible transformations characterized.

Future Plans

A 3 MeV electron accelerator and a 10 MeV heavy ion accelerator will be used to irradiate powders in a controlled atmosphere chamber configured for inclusion in a spectrometer for DRIFT measurements. Samples will be evacuated or purged with selected gases while undergoing controlled heating to remove adsorbed water overlayers so surface species can be observed. This device can also be used for the simultaneous measurement of evolved gases. The purpose of this approach is to remove excess water layers by raising the sample temperature while spectroscopic and chromatographic measurements are made under the same conditions. Much work has been expended to examine zirconia because of the relatively large amount of literature information characterizing the surface of this system. Future efforts will focus on transition metals because of their extensive use as construction materials and in various components in the nuclear industry. Experiments have begun using two of the iron oxides, FeO and Fe_2O_3. The chemistry at the surface of at least FeO is expected to be different than that of ZrO_2 because of the ability to oxidize the iron. Fenton reactions or something similar may oxidize the iron whereas the zirconium cannot be oxidized further. This additional reaction pathway may facilitate certain water decomposition mechanisms.

Extensive use will be made of XPS to examine the oxide surface following radiolysis. This powerful technique directly measures electron binding energies to determine the oxidation environment of the component elements. Various studies strongly suggest that holes remain on the surface of the solid oxides in the radiolysis of heterogeneous water systems. These holes lead to the oxidation of surface elements that should readily be observed by XPS. Particular attention will be given to examination of iron oxides and other transition metal oxides. New oxidation states or even a variation in the makeup of the surface components should be observed following radiolysis.

The second technique to examine surfaces following radiolysis will make use high vacuum chamber with integrated infrared spectrometer and an electron gun of a few keV energy. This device will allow for preparation of samples with controlled amounts of adsorbed water followed by radiolysis and then infrared probing. Reasonable progress has been made on examination of alcohol systems and work will continue on these systems while techniques for looking at pure water are being refined. Optical variations of the ceramic oxide surfaces will be

coupled with stable product formation such as H_2 and theoretical predictions of interfacial species in order to elucidate the radiation induced reactions at interfaces.

As of November 2010, elements of this project will be combined with part of another reported elsewhere in these proceedings (Bartels, *et al.*; Carmichael, *et al.*) in new initiatives pursuing the basic science underpinning fundamental radiation chemistry.

Publications Sponsored by this DOE Program, 2009-2011

O. Roth, A. Hiroki and J. A. LaVerne **(2011)** "Effect of Al_2O_3 Nanoparticles on Radiolytic H_2O_2 Production in Water ", **J Phys Chem C** *115*, 8144-8149.

O. Roth and J. A. LaVerne **(2011)** "Effect of pH on H_2O_2 Production in the Radiolysis of Water", **J Phys Chem A** *115*, 700-709.

J. A. LaVerne (2011). *Radiation Chemistry of Water with Ceramic Oxides*. In Charged Particle and Photon Interactions with Matter. Y. Hatano, Y. Katsumura and A. Mozumder, Eds. Boca Raton, Taylor & Francis.

O. Plekan, V. Feyer, S. Ptasinska, N. Tsud, V. Chab, V. Matolin, K. C. Prince **(2011)** "Cyclic dipeptide immobilization on Au (111) and Cu (110)" **J Chem Phys** in press

O. Plekan, V. Feyer, S. Ptasinska, N. Tsud, V. Chab, V. Matolin, K. C. Prince **(2010)** "Photo-emission Study of Thymidine Adsorbed on Au(111) and Cu(110)", **J Phys Chem C** *114*, 15036-15041.

L. Lefticariu, L. A. Pratt, J. A. LaVerne and A. Schimmelmann **(2010)** "Anoxic Pyrite Oxidation by water Radiolysis Products - A Potential Source of Biosustaining Energy", **Earth and Planet Sci Lett** *292*, 57-67.

A. Baidak and J. A. LaVerne **(2010)** "Radiation-Induced Decomposition of Anion Exchange Resins", **J Nucl Mater** *407*, 211-219.

G. Merga, N. Saucedo, L. C. Cass, J. Puhussery, and D. Meisel **(2010)** ""Naked" Gold Nanoparticles: Synthesis, Characterization, Catalytic Hydrogen Evolution, and SERS" **J Phys Chem C** *114*, 14811-14818.

Ranea, V.A., I. Carmichael, and W.F. Schneider **(2009)** "A DFT investigation of intermediate steps in the hydrolysis of α-Al_2O_3(0001)" **J Phys Chem C** *113*, 2149-2158.

Single-Molecule Interfacial Electron Transfer

H. Peter Lu
Bowling Green State University
Department of Chemistry and Center for Photochemical Sciences
Bowling Green, OH 43403
hplu@bgsu.edu

Program Scope

Our research is focused on the use of single-molecule high spatial and temporal resolved techniques to understand molecular dynamics in condensed phase and at interfaces, especially, the complex reaction dynamics associated with electron and energy transfer rate processes. The complexity and inhomogeneity of the interfacial ET dynamics often present a major challenge for a molecular level comprehension of the intrinsically complex systems, which calls for both higher spatial and temporal resolutions at ultimate single-molecule and single-particle sensitivities. Single-molecule approaches are unique for heterogeneous and complex systems because the static and dynamic inhomogeneities can be identified, characterized, and/or removed by studying one molecule at a time. Single-molecule spectroscopy reveals statistical distributions correlated with microscopic parameters and their fluctuations, which are often hidden in ensemble-averaged measurements. Single molecules are observed in real time as they traverse a range of energy states, and the effect of this ever-changing "system configuration" on chemical reactions and other dynamical processes can be mapped. In our research, we have been integrating two complementary methodologies; single-molecule spectroscopy and near-field scanning probe microscopy (modified STM and AFM) to study interfacial electron transfer dynamics in solar energy conversion, environmental redox reactions, and photocatalysis. The goal of our project is to integrate and apply these techniques to measure the energy flow and electron flow between molecules and substrate surfaces as a function of surface site geometry and molecular structure. We have been primarily focusing on studying electron transfer under ambient condition and electrolyte solution involving both single crystal and colloidal TiO_2 and related substrates. The resulting molecular level understanding of the fundamental interfacial electron transfer processes will be important for developing efficient light harvesting systems and broadly applicable to problems in interface chemistry and physics.

Recent Progress

Combined Single-Molecule Photon-Stamping Spectroscopy and Femtosecond Transient Absorption Spectroscopy Studies of Interfacial Electron Transfer Dynamics. Inhomogeneous interfacial electron transfer (IET) dynamics of 9-phenyl-2,3,7-trihydroxy-6-fluorone (PF) sensitized TiO_2 nanoparticles (NPs) has been probed by single-molecule photon-stamping technique and by ensemble-averaged femtosecond transient absorption spectroscopy. Single-molecule photon-stamping technique and ensemble-averaged transient absorption spectroscopy provide efficient “zoom in” and “zoom out” approaches in probing the interfacial ET dynamics. The physical nature of the observed multi-exponential or stretched-exponential ET dynamics in the ensemble-averaged experiments, often associated with dynamic and static inhomogeneous ET dynamics, can be identified and analyzed by the single-molecule spectroscopy measurements.

The forward ET time shows a broad distribution at the single-molecule level, indicating the inhomogeneous interactions and ET reactivity of the PF/TiO_2 NP system. The broad distribution of the forward ET time is measured to be 0.4±0.1 ps in the transient absorption and picoseconds to nanoseconds in the photon-stamping measurements. The charge recombination time, having a broad distribution at the single molecule level, clearly shows a biexponential dynamic behavior in the

transient absorption: a fast component of 3.0±0.1 ps and a slow component of 11.5±0.5 ns. We suggest that both strong and weak interactions between PF and TiO_2 coexist, and we have proposed two mechanisms to interpret the observed interfacial ET dynamics. The inhomogeneous electron transfer rate due to the interaction between a dye molecule and the semiconductor surface depends on the chemical and physical nature of both dye molecule and the semiconductor.

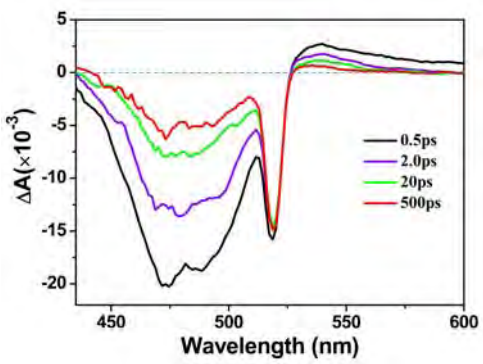

Figure 1. Transient absorption spectra of PF in TiO_2 NP aqueous solution at 0.5 ps, 2.0 ps, 20 ps and 500 ps delay times, with the pulse excitation at 518 nm. The spectrum at each time delay consists of a broad ground-state bleaching from 420 nm to 520 nm, and a positive broad charge separation band with a maximum at 540 nm. The group velocity dispersion of the probe light and spectral signal was already considered when constructing the time-resolved spectra.

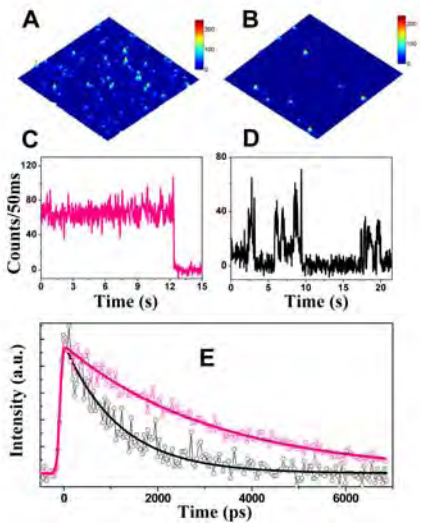

Figure 2. (A) and **(B).** Single molecule images of PF on a glass cover slip and on a TiO_2 NPs coated surface (size: 20×20 μm), respectively, obtained under the same experimental imaging condition. **(C)** and **(D)** are typical fluorescence trajectories of single-molecule PF on a cover slip and a TiO_2 NPs covered surface, respectively, with the binning time of 50 ms. **(E)** Typical fluorescence emission traces of single molecule PF on a cover slip (pink) and a TiO_2 NPs coated surface (black), using single photon stamping recording with the pulse laser excitation at 528 nm and 200 fs. Single exponential decay is observed with a 3.2±0.1 ns lifetime of PF on the cover slip and 1.2±0.1 ns on the TiO_2 NPs covered surface.

Probing Ground-State Single-Electron Self-Exchange Across a Molecule-Metal Interface. We have probed single-molecule redox reaction dynamics of Hemin (Chloride) adsorbed on Ag nanoparticle surfaces by single-molecule surface-enhanced Raman spectroscopy (SMSERS) combined with spectroelectrochemistry. Redox reaction at the molecule/Ag interface is identified and probed by the prominent fluctuations of the Raman frequency of a specific vibrational mode ν_4, which is a typical marker of the redox state of the Iron center in a Hemin molecule. Based on the autocorrelation and crosscorrelation analysis of the single-molecule Raman spectral trajectories and the control measurements of single-molecule spectroelectochemistry and electrochemical STM, we suggest that single-molecule redox reaction dynamics at the Hemin/Ag interface is primarily driven by thermal fluctuations. The spontaneous fluctuation dynamics of the single-molecule redox reaction is measured under no external potential across the molecule-metal interfaces, which provides a novel and unique approach to characterize the interfacial electron transfer at the molecule-metal interfaces. Our demonstrated approaches are powerful for obtaining molecular coupling and dynamics involving

in interfacial electron transfer processes. The new information obtained is critical for a further understanding, design and manipulation of the charge transfer processes at the molecule-metal interface or metal-molecule-metal junctions, which are fundamental elements in single-molecule electronics, catalysis, and solar energy conversion.

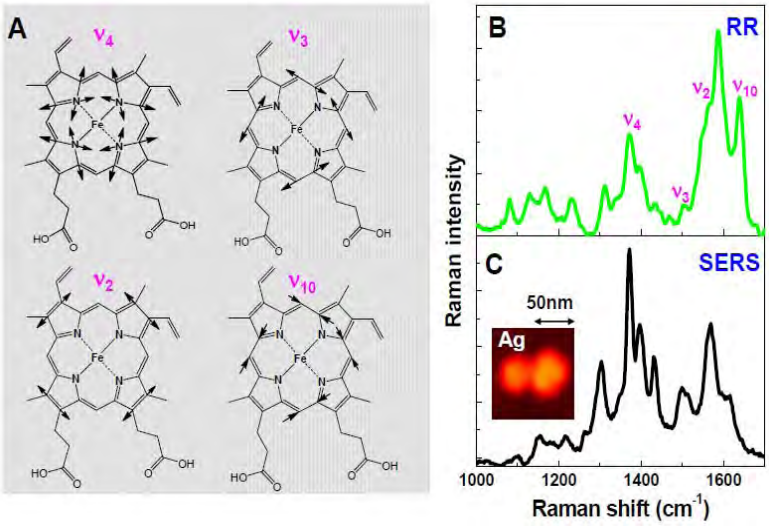

Figure 3. Typical vibrational modes and Raman spectra of Hemin. **(A)** Diagram illustrating four characteristic vibrational modes of the porphyrin skeletal structures of Hemin (or Heme). **(B)** and **(C)** show the typical Resonance Raman spectrum and single-molecule SERS of Hemin, respectively. A SEM image of a Raman-active dimmer of Ag NPs is shown as inset in (C).

As a high-spin five-coordinate Fe(III) compound, Hemin is a model molecule to probe the redox reaction at the molecule-metal interfaces by using SERS. So far, the redox reaction at the Hemin/metal interface has been observed at both ensemble and single molecule level. However, the detailed charge-transfer dynamics as well as the inherent nature of the mechanism of the redox reaction have not been revealed yet. Several vibrational modes of Hemin such as ν_4, ν_3, ν_2 and ν_{10} are typical markers of the porphyrin core size and the Iron electronic structure. A schematic description of these four vibrational modes is shown in Fig. 3A. The ν_4 mode is the marker of Iron oxidation state and its vibrational frequency is in a range of ~1368-1377 cm^{-1} for ferric (Fe^{III}) state and ~ 1344-1364 cm^{-1} for ferrous (Fe^{II}) state. For the ν_3 mode, it is sensitive to the coordination and spin state. Fig.3B and 3C show the resonance Raman (RR) and a typical SMSERS of Hemin. Apparently, the two spectra have similar profile, and the typical vibrational modes such as ν_4, ν_3, ν_2 and ν_{10} are all well resolved. As the Iron oxidation state marker, ν_4 peaks at 1373 and 1372 cm^{-1} in the RR and SMSERS spectra, respectively, which indicates that Hemin is in the oxidized state. In the SMSERS measurements of Hemin of 1.4×10^{-9} M or 4.8×10^{-11} M, we observed spectral fluctuations, blinking, and final quantized single-step photobleaches of the Raman spectra, the typical signatures of the measurements at the single-molecule detection limit.

To probe the single-molecule charge transfer dynamics at the Hemin/Ag interface, we have analyzed the fluctuation trajectories of vibrational mode ν_4 and ν_3 by calculating autocorrelation function (ACF) from the Raman spectral mean trajectories. We also carried out a 2D regional crosscorrelation analysis between ν_4 and ν_3, and we observed that, with ν_4 fluctuating between two redox states, ν_3 shows correlation or anticorrelation with the ν_4 fluctuations from time to time. The correlation or anticorrelation analyses reveal more detailed information such as rate of the redox reaction. The correlation or anticorrelation of two specific modes, which are the oxidation state marker and the spin state (and coordination) marker, most likely reflect the real rate of the redox reaction. From the reaction rate, we estimate that a single self-exchange charge-transfer event rate constant is about 0.01 s^{-1}. Taking the pre-exponential factor with a normal range (10^{10}-10^{13} s^{-1}), we get the activation energy

in a range of 68.2-85.3 KJ/mol, i.e., 0.7 to 0.8 eV for the redox reaction at the Hemin/Ag interface. This value is close to the reported 0.3 to 0.5 eV for one electron transfer from Fermi level of Aluminum surface to the adsorbed Oxygen molecule.

Future Research Plans

Intermittent interfacial ET dynamics of individual molecules, beyond the conventional kinetic scope, could be a characteristic of the surface chemical reactions strongly involved with and regulated by molecule-surface interactions. The fluorescence fluctuation dynamics were found to be inhomogeneous from molecule to molecule and from time to time, showing significant static and dynamic disorders in the interfacial ET reaction dynamics. The intermittent interfacial reaction dynamics that likely occur among single molecules in other interfacial and surface chemical processes can typically be observed by single-molecule studies, but not by conventional ensemble-averaged experiments. To decipher the underlying mechanism of the intermittent interfacial electron transfer dynamics, we plan to study interfacial electron transfer on single crystal TiO_2 surfaces by using pump-probe ultrafast single-molecule spectroscopy and near-field scanning microscopy. Our study will focus on understanding the interfacial electron transfer dynamics at specific crystal sites (kinks, planes, lattices, and corners) with high-spatially and temporally resolved topographic/spectroscopic characterization at individual molecule basis, characetrizing single-molecule rate processes, reaction driving force, and molecule-substrate electronic coupling.

Publications of DOE sponsored research (FY2008-2011)

1. Yuanmin Wang, Papatya C. Sevinc, Yufan He, H. Peter Lu, " Probing Ground-State Single-Electron Self-Exchange Across a Molecule-Metal Interface," *J. Am. Chem. Soc.*, **133**, 6989-6996 (2011).
2. Sevinc, Papatya; Wang, Xiao; Wang, Yuanmin; Zhang, Dai; Meixner, Alfred; Lu, H. Peter, "Simultaneous Spectroscopic and Topographic Near-Field Imaging of TiO_2 Single Surface States and Interfacial Electronic Coupling," *Nano Letter*, **11**, 1490-1494 (2011).
3. H. Peter Lu, "Acquiring a Nano-View of Single Molecules in Actions," *Nano Reviews* **1**, 6-7 (2010).
4. Guo, Lijun; Wang, Yuanmin; Lu, H. Peter, "Combined Single-Molecule Photon-Stamping Spectroscopy and Femtosecond Transient Absorption Spectroscopy Studies of Interfacial Electron Transfer Dynamics," *J. Am. Chem. Soc.* **132**, 1999-2004 (2010) (Cover page).
5. Yufan He, Xiaohua Zeng, Saptarshi Mukherjee, Suneth Rajapaksha, Samuel Kaplan, H. Peter Lu, "Revealing Linear Aggregates of Light Harvesting Antenna Proteins in Photosynthetic Membranes," *Langmuir* **26**, 307-313 (2010) (Cover page).
6. Yuanmin Wang, Xuefei Wang, and H. Peter Lu, "Probing single-molecule interfacial geminate electron-cation recombination dynamics," *J. Am. Chem. Soc.* **131**, 9020–9025 (2009).
7. Yuanmin Wang, Xuefei Wang, Sujit Kumar Ghosh, H. Peter Lu, "Probing single-molecule interfacial electron transfer dynamics of porphyrin on TiO_2 nanoparticles," *J. Am. Chem. Soc.* **131**, 1479-1487 (2009).
8. Xuefei Wang, and H. Peter Lu, "2D Regional Correlation Analysis of Single-Molecule Time Trajectories," *J. Phys. Chem. B.* **112**, 1492--14926 (2008).

Solution Reactivity and Mechanisms through Pulse Radiolysis

Sergei V. Lymar
Chemistry Department, Brookhaven National Laboratory, Upton, NY 11973-5000
e-mail: lymar@bnl.gov

Scope

This program applies pulse radiolysis for investigating reactive intermediates and inorganic reaction mechanisms. The specific systems are selected based on their fundamental significance or importance in energy and environmental problems. Two such projects are described here.

The first project investigates physical chemistry of nitrogen oxides and their congeneric oxoacids and oxoanions, which play an essential role in biology, environmental chemistry and are central to the radiation-induced reactions that occur in nuclear fuel processing and within attendant nuclear waste. Over 60 million gallons of this highly radioactive, nitrate/nitrite-rich waste is currently in the DOE custody. Redox and radical chemistry of the nitrate/nitrite system mediates the most of radiation-induced transformations in these environments. This research program focuses on the prospective reactions in terms of their thermodynamics, rates and mechanisms, focusing on the positive nitrogen oxidation states, whose chemistry is of the greatest current interest.

The goal of the second project is to gain mechanistic insight into water oxidation catalysis through characterization of the catalyst transients involved in the catalytic cycle. Development of catalysts to carry out the four-electron water oxidation remains the greatest challenge in the solar energy utilization. Of all catalysts that have been examined, the dimeric μ-oxo-bridged ruthenium ion ($[(bpy)_2(H_2O)Ru\text{-}O\text{-}Ru(OH_2)(bpy)_2]^{4+}$, aka *the blue dimer*, shown to the left) has been the most extensively studied. Although important features have been discerned, the reaction mechanisms remain to be established. The major impediment in unraveling these and other water oxidation catalysts has been the difficulties in identification and characterization of the reaction intermediates; pulse radiolysis can help.

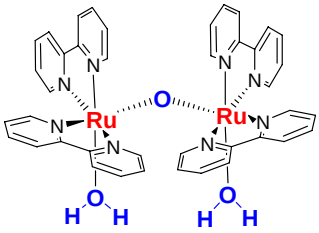

Progress

Pulse radiolysis studies have shown that one-electron reduction of aqueous NO results in the formation of nitroxyl (HNO/NO^-) that rapidly concatenates two more NO, sequentially producing the hyponitrite radical ($N_2O_2^-$) and nitrosyl hyponitrite ($N_3O_3^-$), scheme to the right.[1-3] The latter then decays ($\tau \approx 3$ ms) to the final products: $N_2O + NO_2^-$. In terms of the nitrogen oxidation states, both $N_2O_2^-$ and $N_3O_3^-$ lie between NO and N_2O and are, thus, important intermediates in biological and environmental reductive chemistries of NO. At the same time, major disagreements on the properties and reactivity of these intermediates exist in the literature because the spectral assignments for $N_2O_2^-$ and $N_3O_3^-$ differ significantly.[1-5] Other unexplored questions include: (a) What isomer (*cis* or *trans*) of $N_2O_2^-$ is produced? (b) Do they exhibit different UV spectra? (c) If

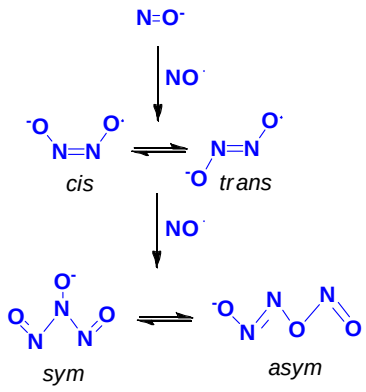

so, what is the rate of *cis-trans* isomerization? Similarly, to which [1]isomer of $N_3O_3^-$ does the experimentally observed spectrum belong? These questions bear on the NO reduction mechanism, but the answers are practically impossible to obtain experimentally. Theoretical modeling is routinely used for structural interpretation of IR spectra, but these are generally experimentally inaccessible for aqueous transients. However, we have succeeded in using the combined quantum mechanical/molecular mechanics approach for theoretical modeling and attribution of the UV spectra of the hydrated $N_2O_2^-$ radical and $N_3O_3^-$ anion.[6]

Comparison of the calculated spectra and energetics with the experimental data reveals that: (a) our recent spectrum assignment[1,4] is correct and that *trans*-$ONNO^-$ is the dominant isomer of $N_2O_2^-$, (b) the earlier spectrum[2,3] has been misinterpreted, (c) the barrier for the *trans-cis* isomerization is prohibitively high.

Turning to $N_3O_3^-$ and comparing spectra to the right, we note that the calculated spectrum of the symmetric $N_3O_3^-$ isomer much better reproduces the shape and band positions of the experimental spectrum than the asymmetric isomer. Analysis of the intensity mismatch has allowed to suggest the $N_2O_2^-$ + NO reaction mechanism (scheme below) where the combination reaction between $ONNO^-$ and NO branches to produce both symmetric and asymmetric $N_3O_3^-$ isomers. This mechanism is consistent with all experimental facts, and has important implications for interpreting experimental data. First, it is difficult to imagine how symmetric $N_3O_3^-$ can break up into the observed N_2O and NO_2^- products; in contrast, asymmetric $N_3O_3^-$ has the proper structure for this decomposition. Second, isotopic product analysis experiments[7] in which $O^{14}N^{15}NO^-$ was allowed to react with large excess of ^{15}NO gave the product ratios $^{14}N^{15}NO/^{15}N^{15}NO$ = 4.1 and $^{14}NO/^{15}N^{15}NO$ = 1.2, in good agreement with the the predicted ratios of 4.0 and 1.0, respectively, for α = ½. Given the apparent symmetry of $ONNO^-$ and that the overall $ONNO^-$ + NO combination is diffusion-controlled,[1,4,5] it is not at all surprising that α should be close to ½. Third, the experimental rate constants for overall $N_3O_3^-$ formation, k_{form}, and decay, k_{decay}, are related to the equilibrium constant for homolysis of the symmetric $N_3O_3^-$ isomer as $K_{hom} = k_{hom}/k_{sym} = k_{decay}/\alpha^2 k_{form}$. With α = ½ and k_{decay} = 300 s^{-1} and k_{form} = 5.4 × 10^9 M^{-1} s^{-1} determined previously,[4,5] K_{hom} is 2.2 × 10^{-7} M, which is consistent with the our prior estimate for the K_{hom} upper limit of 5 × 10^{-7} M.[5] Forth, when both formation and heterolysis reactions are rapid, the experimentally observable spectrum belongs to symmetric $N_3O_3^-$ only.

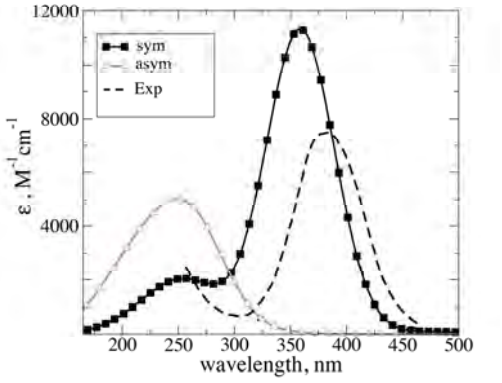

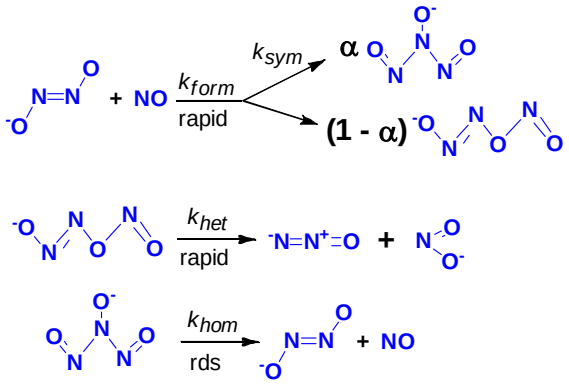

Research from several laboratories have established that water oxidation catalysis by the *blue dimer* involves its progressive oxidation above the Ru^{III},Ru^{III} state (denoted as **{3,3}**) with the attendant loss of protons to the ruthenyl **{5,5}** dimer (scheme below). However, only the **{3,3}** and **{3,4}** states could be characterized over a broad pH range. We began with the assessments of the reactivity of the **{3,3}** and **{3,4}** states toward the radiolytically-generated

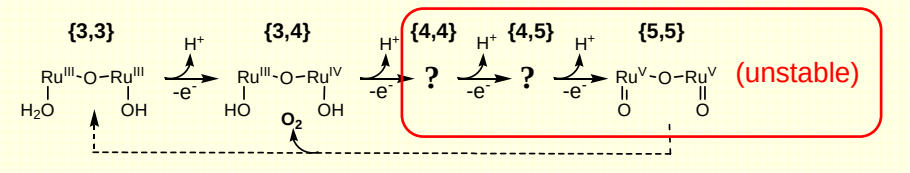

radicals focusing on obtaining and characterization of the **{4,4}** state.[8] Of several tested, two convenient systems have been identified. In the t-BuOH/$S_2O_8^{2-}$ system, the hydrated electrons are converted into the $SO_4^{\bullet-}$ radical (E^o = 2.43 V), which rapidly (k = 1.5 ×10^{10} $M^{-1}s^{-1}$) oxidizes **{3,4}** to **{4,4}**. The kinetic analysis yields the first unambiguous **{4,4}** spectrum shown to the right. Essentially the same spectrum is obtained by the oxidation of **{3,4}** by the $CO_3^{\bullet-}$ radical (E^o = 1.57 V) in the N_2O/CO_3^{2-} system; these results make the spectrum assignment definitive. The oxidation by $CO_3^{\bullet-}$ occurs much slower (k = 4 × 10^8 $M^{-1}s^{-1}$) possibly indicating the approach to the **{3,4}** reduction potential. The **{4,4}** complex is found to be unstable in neutral solution and undergoes further reaction(s) on the time scale of milliseconds to minutes leading to regeneration of **{3,4}** (kinetics below). Although these processes are not yet fully understood, it appears that a disproportionation of **{4,4}** is the major contributor. Other pertinent observations can be summarized as follows: (1) the H atom cleanly reduces **{3,4}** to **{3,3}**, (2) the $OH^{\bullet}$ radical oxidizes **{3,3}** to **{3,4}**, (3) in contrast and unexpectedly, $OH^{\bullet}$ attack on **{3,4}** results in its reduction to **{3,3}** probably via a bpy-ring adduct, indicating that the catalyst in **{4,4}** and higher states may be susceptible to nucleophilic attack by H_2O or OH^-, (4) the comproportionation reaction **{3,3}** + **{4,4}** → **{3,4}** + **{3,4}** has been detected, suggesting E(**{3,4}**) > E(**{3,3}**) for the reduction potentials, (5) the reaction between **{4,4}** and the C-centered t-BuOH radical has been observed, suggesting a radical-like nature of the **{4,4}** state; if confirmed, this finding will have important mechanistic implications.

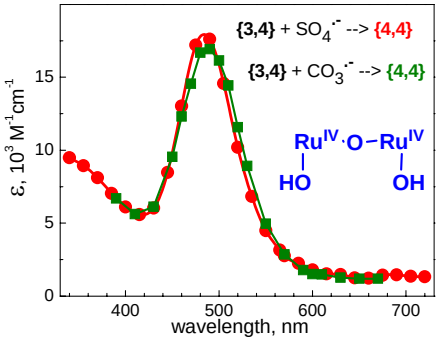

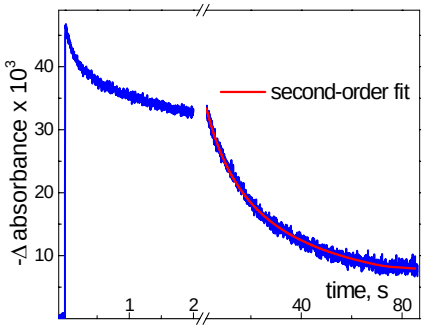

Plans

Pathways and energetics of NO reduction will be investigated with the purposes to develop new methods of generating nitroxyl and to establish its thermochemistry. With respect to the former, reduction of NO by the CO_2^- radical is of interest. All present estimates for the reduction potentials for NO and pK_a for HNO involve significant assumptions spreading a range of ~0.2 V and ~4 pK_a units; we will attempt determination of nitroxyl thermochemistry by measuring its redox equilibria.

Spin-forbidden bond breaking/making reactions involving nitroxyl will be investigated. The first is protonation of $^3NO^-$ by Brønsted acids. The second spin-forbidden reaction of interest is the addition of $^3O_2$ to ^{1}HNO, which could directly lead to peroxynitrite, $ONOO^-$, and is potentially very significant because it replaces mildly reducing HNO by strongly oxidizing $ONOO^-$.

Energetics of $NO_3^{\bullet 2-}$ radical will be studied through examining its equilibrium $NO_3^{\bullet 2-}$ + H_2O = $NO_2^{\bullet}$ + $2OH^-$ at high alkalinities, which should yield the reduction potential provided it is not

below about -1.1 V. If it is, we will attempt obtaining or bracketing the potential from equilibrating $NO_3^-/NO_3^{\bullet 2-}$ couple with the reference redox couples.

Dimerization/hydrolysis of $NO_2^\bullet$ radical will be explored. It is widely held that the hydrolysis of occurs through the intermediacy of its symmetric N-N bonded dimer. We question this mechanism and conjecture that the hydrolysis involves the higher-energy N-O bonded asymmetric dimer, while the N-N bonded dimer is an unreactive bystander.

The nature of catalyst transients formed during water oxidation will be further clarified: (1) we will continue characterization of the **{4,4}** state of "blue dimer" focusing on identification of its protonation state and understanding the decomposition pathways; a set of time-resolved spectra over a range of pH will be obtained and analyzed to unravel the decay mechanism. Analogous study will be attempted for the **{4,5}** state, (2) it is generally agreed, that **{5,5}** is the catalytically active form, but it has been difficult to reach this state in a non-rate-determining manner. Radiolysis with large pulses generating sufficient excess of $SO_4^{\bullet -}$ or $CO_3^{\bullet -}$ over **{3,4}** should allow us to rapidly produce the **{5,5}** state, thus opening a possibility to observe the details of the O_2-forming step, (3) a set of "blue dimer" congeners with electron-donating and withdrawing ligand substitutions that can modulate reduction potentials and catalytic activities will be included in this study.

Collaborators on these projects include M. Valiev (PNNL), V. Shafirovich (NYU), J. Hurst (WSU), and H. Schwarz (BNL, emeritus).[9]

References (DOE sponsored publications in 2009-present are marked with asterisk)

(1) Lymar, S. V.; Shafirovich, V.; Poskrebyshev, G. A. *Inorg. Chem.* **2005**, *44*, 5212-5221.
(2) Grätzel, M.; Taniguchi, S.; Henglein, A. *Ber. Bunsen-Ges. Phys. Chem.* **1970**, *74*, 1003-1010.
(3) Seddon, W. A.; Fletcher, J. W.; Sopchyshyn, F. C. *Can. J. Chem.* **1973**, *51*, 1123-1130.
(4) Poskrebyshev, G. A.; Shafirovich, V.; Lymar, S. V. *J. Am. Chem. Soc.* **2004**, *126*, 891-899.
(5) Poskrebyshev, G. A.; Shafirovich, V.; Lymar, S. V. *J. Phys. Chem. A* **2008**, *112*, 8295-8302.
(6*) Valiev, M.; Lymar, S. V. *J. Chem. Phys. A* **2011**, accepted.
(7) Bazylinski, D. A.; Hollocher, T. C. *Inorg. Chem.* **1985**, *24*, 4285-4288.
(8*) Cape, J. L.; Lymar, S. V.; Lightbody, T.; Hurst, J. K. *Inorg. Chem.* **2009**, *48*, 4400-4410.
(9*) Lymar, S. V.; Schwarz, H. A. *J. Phys. Chem. A* **2011**, submitted.

Spectroscopy of organometallic radicals

Michael D. Morse, Principal Investigator
Department of Chemistry, University of Utah, Salt Lake City, UT 84112
Email: morse@chem.utah.edu

Overall research goals: The objective of this project is to provide detailed and highly accurate spectroscopic and thermochemical data concerning organometallic radicals and actinide-containing species, concentrating on thorium and uranium compounds that can be safely handled in a university environment.

Significant achievements during 2009-20011: Major efforts during the 2009-2011 period have concentrated on the construction of a cryogenically cooled ion trap photodissociation spectrometer. A schematic diagram of the instrument is shown below, along with a photograph of one of the two-dimensional turning quadrupoles.

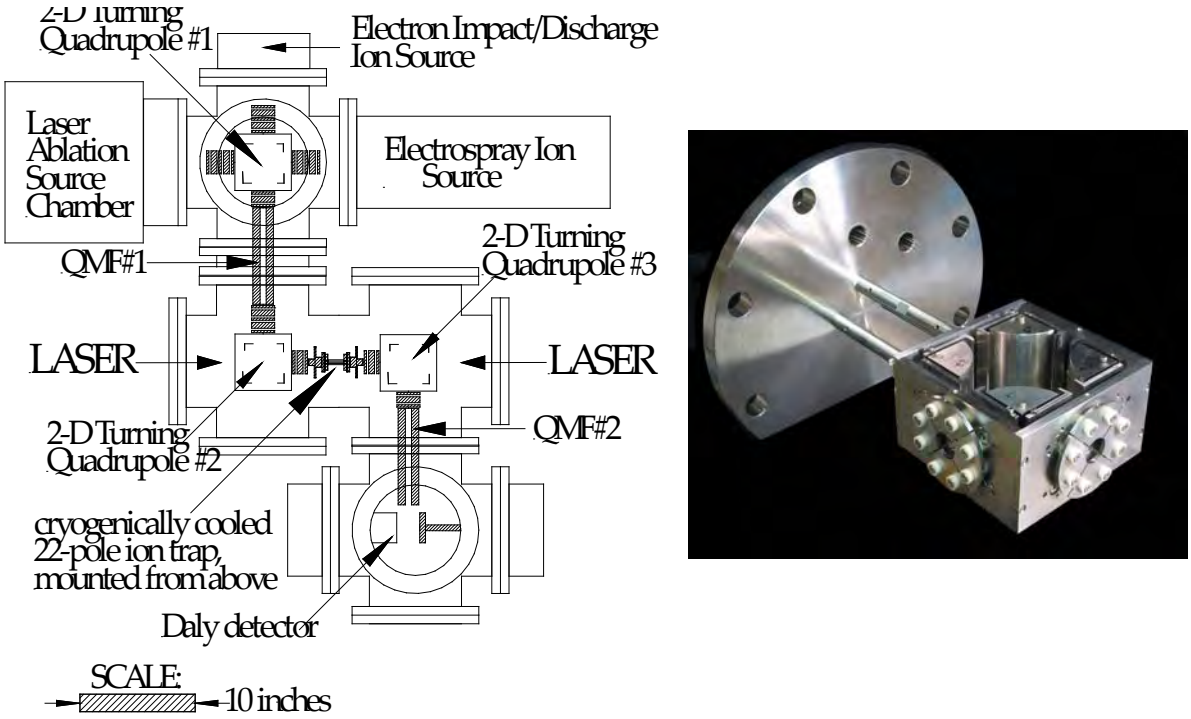

Figure 1. Scheme of the cryo-cooled ion photodissociation spectrometer (left); one of the three turning quadrupoles (right).

During the 2009-2011 time frame, the electron impact ion source, first quadrupole mass filter, two of the turning quadrupoles, and the Daly ion detector have been built and tested. Although much of the ion trap itself has been built, the pieces have not yet been assembled and tested; currently the machine shop is making the heat shield and flanges needed to support the cryostat that will cool the trap to temperatures below 10K. In addition to turbomolecular pumping, a cryogenic pumping facility will be placed under the second turning quadrupole assembly, just upstream of the ion trap, in order to trap condensable gases before they impinge onto the cold surfaces of the trap. This project is the primary responsibility of my postdoctoral researcher, Sergei Aksyonov.

Other significant achievements during this time frame are the analysis and publication of the spectrum of diatomic CrC (a $^3\Sigma^- \leftarrow X\ ^3\Sigma^-$ band system) and TaC (for which several $^2\Pi_{1/2} \leftarrow X\ ^2\Sigma^+$ transitions were observed and analyzed). These studies represent the first spectroscopic investigations of any kind on these molecules, and provide experimental verification of the ground

state electronic symmetries that have been computationally predicted, along with precise measurements of the ground state bond lengths (1.6188 and 1.7490 Å, respectively). Additional achievements are the measurement and analysis of spectra of ZrF and OsN, which will be submitted for publication shortly. Experimental work on the spectrum of CuCCH is nearly complete, as is the analysis of the 1-0 band of the $\tilde{A}\,^6\Sigma^+ \leftarrow \tilde{X}\,^6\Sigma^+$ band system of CrCCH.

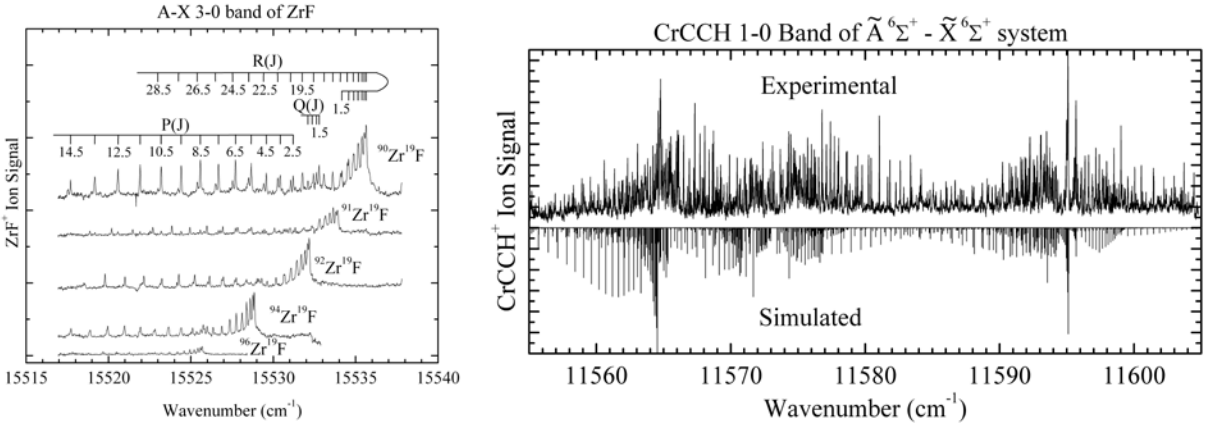

Figure 2. Rotationally resolved spectra of the isotopes of ZrF (left) and of the 1-0 band of the $\tilde{A}\,^6\Sigma^+ \leftarrow \tilde{X}\,^6\Sigma^+$ system of CrCCH (right).

Science objectives for 20011-2013:

- Complete the construction of the 22-pole trap, the second quadrupole mass filter, and the software needed to trap and photodissociate ions. Test and completely debug the system using the electron impact ion source. Collect spectra of simple species that can be generated with this source, particularly those that are fragments of volatile organometallic complexes such as $Fe(CO)_5$, $Co(CO)_3NO$, $Ni(CO)_4$, and $Cr(CO)_6$.
- Integrate the 22-pole ion trap instrument with the laser ablation source, and begin experiments using laser-ablated ion sources, including uranium and thorium. Important goals here are to collect spectra of UO_2^+ and its solvated analogs.
- Design and begin construction of the electrospray ion source, so that multiply-charged ions such as UO_2^{2+} can be investigated, both as a bare ion and as a solvated system.
- Obtain resonant two-photon ionization spectra of ThO_2 and other small thorium and uranium species. The electronic and geometric structure of ThO_2 will be compared to the known isovalent species TiO_2, ZrO_2, and HfO_2.

Publications supported by this project 2009-2011

1. D. J. Brugh, M. D. Morse, A. Kalemos and A. Mavridis, "Electronic spectroscopy and electronic structure of diatomic CrC," J. Chem. Phys. **133**, 034303/1-034303/8 (2010).
2. O. Krechkivska and M. D. Morse, "Resonant two-photon ionization spectroscopy of jet-cooled tantalum carbide, TaC," J. Chem. Phys. **133**, 054309/1-054309/8 (2010).
3. A. Martinez and M. D. Morse, "Spectroscopic studies of jet-cooled ZrF," (in preparation for the Journal of Chemical Physics).
4. M. Garcia and M. D. Morse, " Resonant two-photon ionization spectroscopy of jet-cooled OsN," (in preparation for the Journal of Chemical Physics).
5. D. J. Brugh and M. D. Morse, "Rotational analysis 1-0 band of the $\tilde{A}\,^6\Sigma^+$ $\tilde{X}\,^6\Sigma^+$ system of CrCCH," (in preparation for the Journal of Chemical Physics).

Ab initio approach to interfacial processes in hydrogen bonded fluids

Christopher J. Mundy
Chemical and Materials Sciences Division
Pacific Northwest National Laboratory
902 Battelle Blvd, Mail Stop K1-83
Richland, WA 99352
chris.mundy@pnl.gov

Program Scope

The long-term objective of this research is to develop a fundamental understanding of processes, such as transport mechanisms and chemical transformations, at interfaces of hydrogen-bonded liquids. Liquid surfaces and interfaces play a central role in many chemical, physical, and biological processes. Many important processes occur at the interface between water and a hydrophobic liquid. Separation techniques are possible because of the hydrophobic/hydrophilic properties of liquid/liquid interfaces. Reactions that proceed at interfaces are also highly dependent on the interactions between the interfacial solvent and solute molecules. The interfacial structure and properties of molecules at interfaces are generally very different from those in the bulk liquid. Therefore, an understanding of the chemical and physical properties of these systems is dependent on an understanding of the interfacial molecular structure. The adsorption and distribution of ions at aqueous liquid interfaces are fundamental processes encountered in a wide range of physical systems. In particular, the manner in which solvent molecules solvate ions at the interface is relevant to problems in a variety of areas. Another major focus lies in the development of models of molecular interaction of water and ions that can be parameterized from high-level first principles electronic structure calculations and benchmarked by experimental measurements. *The aforementioned studies are performed using novel algorithms based in density functional theory (DFT) in conjunction with high performance computing through a **2008-2010 INCITE award***. These models will be used with appropriate simulation techniques for sampling statistical mechanical ensembles to obtain the desired properties.

Progress Report

Elucidating structure and reactivity ions in bulk and at the air-water interface: Although DFT holds tremendous promise as an efficient electronic structure theory; applications of DFT to aqueous systems have produced mixed results when attempting to reproduce experimentally determined benchmarks. Although there is no molecular model that can reproduce the full phase diagram of water, the shortcomings of popular exchange-correlation functionals based on the generalized gradient approximation (GGA), *e.g.* BLYP and PBE, are known to underestimate the liquid density and yield a more structured liquid then classical empirical potentials. Although there could be many reasons for these deficiencies in DFT, one major shortcoming is the lack of dispersion interactions in current implementations. Correcting the liquid density at ambient conditions has far reaching implications for use of DFT in studying systems with open boundary conditions, such as liquid-vapor interfaces. Previously we have implemented the correction due to Grimme[1] that amounts to an empirical damped dispersion interaction that is parameterized to used with both BLYP and PBE.[4] Our results have shown that the addition of the empirical correction due to Grimme[1] yields the correct density for liquid water at ambient conditions for

both PBE and BLYP. This work has also been extended by my co-workers to the calculation of the melting point of liquid water using dispersion corrected DFT [**see abstract of Sotiris Xantheas**] Moreover, we have used this methodology to weigh in on the critical debate on the propensity of the hydroxide anion at the air-water interface. Our results, indicate that hydroxide ion has a slight propensity to the liquid-vapor interface on the order of k_BT.[6]

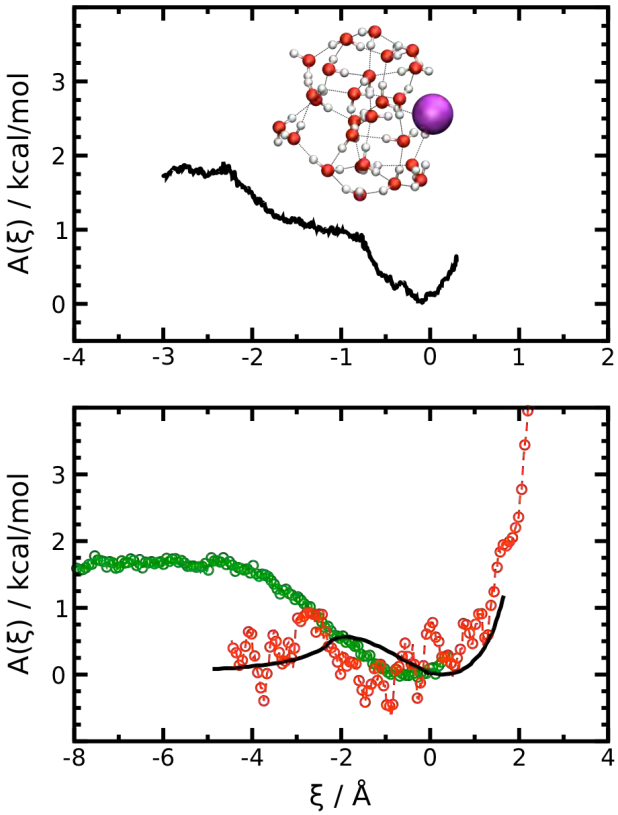

Figure 1: The DFT-D PMF of adsorption of iodide to the air-water interface of a water cluster (*n*=27) [black curve in top panel] and extended interface [red curve in bottom panel]. The reaction coordinate x is the radial distance from the center of mass of the cluster, and the *distance, z to* the air-water interface, respectively. The green and black curves in the bottom panel represent the PMF of iodide using the empirical polarizable potential due to Dang and co-workers, and that obtained by dielectric continuum theory due to Levin and co-workers [12].

The aforementioned work has focused our research efforts into benchmarking the role of DFT regarding the propensity of anions at interfaces. The only indisputable experimental evidence relating to surface adsorption is surface tension, in conjunction with the Gibb's Adsorption Isotherm (GAI). Other pioneering surface sensitive experimental techniques can measure anions at the air-water interface, but open questions still remain regarding the precise potential of mean force (PMF) for anions to the air-water interface[2].

Recent literature has pointed to the specific ion effect as being a ***local*** effect, as opposed to an ions long-range effect on water's structure[3]. This opens up the opportunity to study the first solvation shell of iodide using the extended x-ray absorption fine structure (EXAFS) technique. EXAFS in conjunction with molecular dynamics (MD) was pioneered at PNNL. To this end, we studied the first shell solvation structure using a multi-edge EXAFS to benchmark the performance of DFT and the empirical polarizable model due to Dang and co-workers. The results of this study indicated that both models gave good agreement with experiment. On closer examination of the data it was revealed that the DFT-D produced a ***less*** structured first solvation shell that the empirical polarizable interaction potential in better agreement with EXAFS[12]. This over structuring of the empirical polarizable potential can be traced to a larger induced dipole moment of iodide, namely 2.6 Debye compared to the DFT value of 1.2 Debye. Other independent theoretical studies have also indicated that empirical polarizable models may overestimate the induction effect.

Given that DFT-D produces a first solvation shell that resembles the EXAFS data, we then ask the question of how this will manifest itself in the anion propensity for the air-water interface. To this end we performed extensive DFT-D in the extended interface geometry predict the PMF of iodide at the air-water interface. Using umbrella-sampling techniques, our results produced a picture where the iodide anion has a local minimum ~k_BT. This is in contrast to the empirical polarizable potential that produces a global minimum of ~3 k_BT[13].

Self-Consistent Polarization (SCP)-Neglect of differential diatomic overlap (NDDO) (with G.K. Schenter):

The development of fast, scalable, interaction potentials based in quantum mechanics holds tremendous promise for studying chemical processes in complex fluids. As pointed out in the previous section, the non-perturbative treatment of electrostatics may be important for describing the interactions of some anions. Semi-empirical methods, although approximate, provide a direct route to chemistry and accurate electrostatics via the quantum mechanical wavefunction. Moreover, having an accurate semi-empirical approach to aqueous systems will allow for larger systems and better sampling than current state-of-the-art DFT based interaction potentials can afford. To this end we have extended the previous developed SCP-NDDO theory for water clusters to the condensed phase. SCP-NDDO calculations were run for ice, liquid water, and the air-water interface. Our results display a significant improvement over uncorrected NDDO (for example PM3), and produced a correctly structured liquid, dipole moments consistent with DFT, good diffusive properties, and a liquid density of ~1 g/cc (**see abstract of Greg Schenter)** [12].

Future directions

Complex anions (with G.K. Schenter and J. Fulton): Future research will be extended to elucidation of the solvation and surface properties of more complex anions such as the oxyanions. IO_3^- and ClO_3^- exhibit very interesting behavior in the context of the Hofmeister series where IO_3^- exhibits a more hydrated anion and ClO_3^- displays properties of a cavity former. This is in contrast to the respective halide anion where iodide exhibits properties of being less hydrated than chloride. We are examining the first solvation shell of these fascinating oxyanions to be directly compared to EXAFS experiments. The goal will be to experimentally verify the extent of hydration of each anion.

Acknowledgements. This work benefited greatly from active collaborations with D.J. Tobias (UC-I), M.E. Tuckerman (NYU), and I.-F.W. Kuo (LLNL), Marcel D. Baer (PNNL), Abe Stern (UC-I), Joost VandeVondele (U. Zurich), Greg Kimmel (PNNL), Roger Rousseau (PNNL).

Publications from BES support (2009- present)

1. Goldman N, E Reed, IFW Kuo, L Fried, **CJ Mundy**, and A Curioni. 2009. "Ab initio simulation of the equation of state and kinetics of shocked water." *Journal of Chemical Physics* 130(12):Article no. 124517.
2. Maerzke KA, G Murdachaew, **CJ Mundy**, GK Schenter, and JI Siepmann. 2009. "Self-consistent polarization density functional theory: Application to Argon." *Journal of Physical Chemistry A* 113(10):2075-2085.
3. Kimmel GA, J Matthiesen, M Baer, **CJ Mundy**, NG Petrik, RS Smith, Z Dohnalek, and BD Kay. 2009. "No Confinement Needed: Observation of a Metastable Hydrophobic Wetting Two-Layer Ice on Graphene.". *Journal of the American Chemical Society* **131**,12838 (2009)
4. Schmidt J, J VandeVondele, IFW Kuo, D Sebastiani, JI Siepmann, J. Hutter, and **CJ Mundy**. 2009. "Isobaric-Isothermal Molecular Dynamics Simulations Utilizing Density Functional Theory: An Assessment of the Structure and Density of Water at Near-Ambient Conditions." *Journal of Physical Chemistry B* **113**, 11959 (2009)
5. **Mundy CJ**, KA Maerzke, MJ McGrath, IFW Kuo, G. Tabbachi, and JI Siepmann. 2009. "Vapor-liquid phase equilibria of water modelled by a Kim-Gordon potential." *Chemical Physics Letters* **479**, 60-64 (2010)
6. **Mundy CJ**, IFW Kuo, ME Tuckerman, HS Lee, and DJ Tobias. "Hydroxide Anion at the Air-Water Interface." *Chemical Physics Letters: Frontiers Article*, **481**, 2-8 (2009)
7. Baer M, **Mundy CJ**, Chang TM, et al, "Interpreting Vibrational Sum-Frequency Spectra of Sulfur Dioxide at the Air/Water Interface: A Comprehensive Molecular Dynamics Study," *Journal of Physical Chemistry B* **114**, 7245 (2010)
8. Murdachaew G, **Mundy CJ**, Schenter GK, "Improving the density functional theory description of water with self-consistent polarization," *Journal of Chemical Physics* **132,** 164102 (2010)
9. Fulton JL, Schenter GK, Baer MD, et al. "Probing the Hydration Structure of Polarizable Halides: A Multiedge XAFS and Molecular Dynamics Study of the Iodide Anion," *Journal of Physical Chemistry B* **114,** 12926 (2010)
10. McGrath MJ, Ghogomu JN**, Mundy CJ**, et al. "First principles Monte Carlo simulations of aggregation in the vapor phase of hydrogen fluoride," *Physical Chemistry Chemical Physics* 12, 7678 (2010)
11. S. M. Kathmann, I-F. W. Kuo, **C. J. Mundy**, and G. K. Schenter, "Understanding the Surface Potential of Water," *Journal of Physical Chemistry B* (2011). dx.doi.org/10.1021/jp1116036
12. G. Murdachaew, **C. J. Mundy**, G. K. Schenter, T. Laino, and J. Hutter, "Semiempirical Self-Consistent Polarization Description of Bulk Water, the Liquid-Vapor Interface, and Cubic Ice," *Journal of Physical. Chemistry. A* (2011). dx.doi.org/10.1021/jp110481m
13. Baer M.D. and **Mundy C.J**., "Toward and Understanding fo the Specific Ion Effect Using Density Functional Theory," *Journal of Physical Chemistry Letters*, (2011) doi:10.1021/jz200333b

References

(1) Grimme, S. *Journal of Computational Chemistry 25*, 1463 (2004).

(2) Petersen, P.B. and Saykally, R.J., *Journal of Physical Chemistry B* 110, 14060 (2006)

(3) Tobias D.J. and Hemminger, J.C.; *Science* 319, 1197 (2008).

DYNAMIC STUDIES OF PHOTO- AND ELECTRON-INDUCED REACTIONS ON NANOSTRUCTURED SURFACES

Richard Osgood,
Center for Integrated Science and Engineering, Columbia University, New York, NY 10027, Osgood@columbia.edu

Program Scope or Definition:

Our current research program examines the photon- and electron-initiated reaction mechanisms, half-collision dynamics, and other nonequilibrium-excited dynamics effects, occurring with excitation of adsorbates on well-characterized metal-oxide and nanocrystal surfaces. In order to explore these dynamics, our program has first developed new synthesis methods for uncapped nanocrystals *with specific reconstructions and orientation* in a UHV STM instrument. Our intent is use the tunneling from the tip of our STM or an *in situ* flood UV lamp to excite adsorbate molecules at specific sites of these nanocrystals. The resulting chemistry and surface dynamics will be investigated via imaging of the reaction fragments in the vicinity of the reaction sites. Additional research tools are time-of-flight detection, XPS, standard UHV probes, *in situ* TPD, and molecular computational tools.

Our initial experiments have been directed toward electronic-tunneling reactions in a series of linear aromatics on rutile TiO_2(110) surfaces, as well as determining the conditions needed to form uncapped TiO_2 nanocrystals with a known atomic structure. Our adsorbate molecules have been chosen to enable studies of one monolayer adsorption at room temperature, as determined by *in situ* thermal desorption spectroscopy.

From the perspective of DOE energy needs, photoexcitation has been of continuing interest for its importance in photocatalytic destruction of environmental pollutants, in several methods of solar-energy conversion, and in a variety of applications of nanotechnology. Our recent work in this program has yielded several new research findings regarding the preparation of nanocrystals, the structure of adsorbed aromatics on TiO_2 surfaces and the observation of tip-induced electron bond cleavage within these molecules.

Recent Progress:

Scanning Tunneling Microscopy Study of the Adsorption Geometry of Reaction Target Molecules on a Reconstructed Surface: Planar Aromatics on Single-Crystal, Rutile TiO_2(110) Surfaces

Molecular orientation plays a key role in many surface or interfacial applications such as self-assembly, catalysis, and charge transfer; adhesion and organic-molecular adsorbate interactions with TiO_2 surfaces are also important for such applications as dye-sensitized solar cells and photocatalytic purification of water and air. STM in conjunction with a pristine surface is a powerful tool that allows direct observation of the geometric orientation of the adsorbed molecules and hence can further our understanding of the factors that control orientation.

Recent studies by others have examined the adsorption geometry of organic molecules on a variety of surfaces, particularly noble metals and graphite. These studies have elucidated the comparative role of the intermolecular and substrate-molecule interactions in determining the orientation of adsorbed molecules. A variety of striking cases of uniform long-range order and unanticipated phenomena such as chirality in adsorption have

been shown. In contrast, the understanding of interactions of oxide surfaces such as TiO_2 with relatively large organic molecules is still rudimentary. The structural and chemical complexity of many metal-oxide surfaces makes *in situ* preparation demanding, and studies of molecular adsorption on metal-oxide crystals have been confined to certain well-studied systems, typically with relatively small molecules. Thus while titanium oxide is important for a variety of applications, particularly those in solar-energy-related science, studies of molecular adsorption have been limited, with a few exceptions, to very simple species. Even more limited are direct scanning-probe observations of the adsorption geometry of organic molecules on TiO_2.

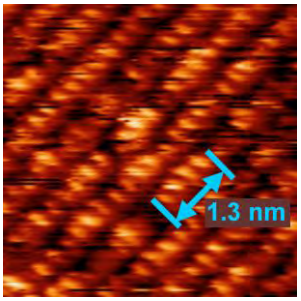

Fig. 1: 5 nm × 5 nm STM image of 4-bromobiphenyl-exposed TiO_2 (110) surface at T=300K. Bright ellipse-like features are due to Ti sites in the TiO_2 substrate.

We have now used STM to examine the adsorbate geometries at ~1 ML coverage of relatively large aromatic molecules, *viz* anthracene and its halogenated derivative chloroanthracene, and the related molecule 4-bromobiphenyl. Our experiments use room temperature (RT) STM imaging in conjunction with UHV methods to allow direct observation of certain features of the resulting geometric orientation of the adsorbed molecules and Temperature-Programmed Desorption (TPD) to evaluate thermal stability of the adsorbed species. The choice of the rutile (110) substrate surface was motivated by its well-understood atomic structure, which has been carefully established through a large number of prior studies. Our choice of model organic molecules is a result of the fact that each is a relatively simple multiring aromatic compound, which is stable on a TiO_2 surface at RT.

Our TPD measurements showed multilayer and single-layer desorption peaks at 270 K and 360 K for anthracene and at 260 K and 360 K for bromobiphenyl, respectively. Our imaging experiments at a series of low temperatures demonstrated that our apparatus could image a single adsorbed molecule and found our surface adsorbates have anisotropic, temperature-dependent mobilities for diffusion across the surface. STM images taken at room temperature show that at high coverage both of molecular species assemble into periodic patterns on the TiO_2 surface with individual molecules aligned along the 5-coordinated Ti atom row of the substrate. Individual molecules of the organic adsorbates were found to be mobile on the surface in the direction parallel to the Ti atomic lattice. The observed lateral alignment of the molecules suggests attractive interactions for anthracene and 2-chloroanthracene and repulsive interactions for 4-bromobiphenyl.

In particular our experiments with anthracene showed that a ~ 1 ML anthracene-covered surface exhibited a surface image periodicity or pattern. This pattern consisted of an array of identical elongated bright features oriented parallel to the [001] direction, i.e. along the bridging oxygen rows on the rutile(110) surface. The spacing between the rows is 0.65 nm, which corresponds to the known bridging-oxygen row separation on this face of TiO_2. This observation correlates well with the conclusion of an earlier NEXAFS study that anthracene molecules are adsorbed on a rutile(110) surface in a planar geometry with the molecules positioned along the troughs between bridging oxygen. Thus elongated bright features are imaged, which are due to anthracene molecules, with the long axis of the anthracene molecule aligned along the [001] direction. A similar set of imag-

ing experiments was conducted with 1ML coverage of 4-bromobiphenyl exposures on the (110) surface in order to understand changes due to well-defined molecular-structure modifications. In general, the adsorption geometry of the brominated hydrocarbon was very similar to that of anthracene: the molecules align themselves along the atomic rows of the rutile(110) surface to form trains of bright spots or protrusions with a spatial period of ~1.3 nm.

However, in the case of the 4-bromobiphenyl layers, the *mutual* arrangement of the molecules in the neighboring rows in **Fig. 1** differs strikingly from the arrangement of anthracene on the same substrate. While there is a substantial disorder in the lateral, i.e. across the Ti rows, alignment of the molecules, on average the arrangement is such that a molecule is situated near a gap between two molecules in the neighboring row, that is a molecular arrangement exhibiting an anti-phase pattern. Such an arrangement can be readily explained through the polarity of 4-bromobiphenyl: the presence of the halogen atom at the extremity of the molecule creates a significant electric dipole moment. This polarity leads to the negatively charged bromine atom being electrostatically attracted to the positively charged aromatic rings of a neighboring molecule.

Finally note that it is crucial to consider artifacts in imaging the layer due to the presence of the substrate surface structure. **Figure 1** displays an atomically resolved image of the TiO_2 surface exposed to 4-bromobiphenyl. In the image a repeating patterning of protrusions or bright ellipse-like dots is seen with a spacing of ~0.3 nm due to the TiO_2 surface lattice spacing for the 5-coordinated Ti atoms. Thus, as is also seen in case of anthracene, the closely spaced bright spots originate from the lattice rather from the atomic structure of the organic molecules themselves.

STM Tip-Induced Dissociation Dynamics on Surfaces.

Scanning tunneling microscopy offers a unique approach to exploration of molecular dissociation dynamics at an atomic scale. Namely, as shown by the W. Ho Group, an STM offers, in principle, the possibility to inject an electron or electrons with a specified energy into a selected molecule in a specific adsorption configuration. This approach, which was examined by the Palmer and Polanyi Groups for reactions on semiconductor surfaces, allows dynamical information to be collected including the charge-transfer threshold electron energy for the reaction, the identity of adsorbate states suitable for dissociation, fragment trajectories across the surface following bond scission, and the nature and adsorption geometry of the products. Note that in the case of photocatalysis, the electron-induced reaction similarly involves charge transfer from the bulk of a substrate to an adsorbed molecule followed by bond cleavage. Such a study thus tries to answer the same fundamental chemical physics questions as in gas phase reaction dynamics except on a surface one must understand the role of surface perturbation on the half-collision event and on the fragment trajectories. Recently we have begun to examine the use of STM tip-induced reaction technique on oxide surfaces. In particular, we have initiated investigation of the technique using single-crystal TiO_2(110) surface as a model substrate.

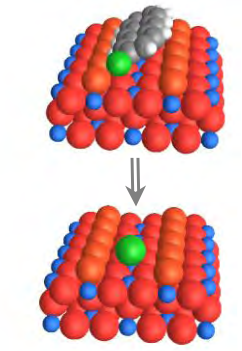

Fig. 2: Cartoon showing the change in 2-chloroanthracene following tip-induced *e* reaction. The green atom is the remaining Cl atom.

An excellent molecule to use for studies of tip-induced reactions is 2-chloro-anthracene since typically such a halogenated species is labile to electron bond cleavage after electron attachment. Our STM imaging studies showed that these molecules are aligned along Ti^{5+} rows. As with anthracene, electrostatic interactions are responsible for the surface adsorption geometry of 2-chloroanthracene, but due to chlorine functionalization the molecules are permanently tilted. To investigate tip-induced reactions, individual molecules were imaged before and after a voltage was applied to the tip placed within tunneling distance to the molecule. It was found that if a voltage greater than 3V was applied to the tip a reaction was seen, where the reaction was seen to be disappearance of the molecule and appearance of a new fragment, chlorine. **Figure 3** shows such a dissociation event; after dissociation it was found that an adatom of Cl was located above a titanium atom in a $Ti^{(5)}$ row. However, the organic fragment of the reaction has not been found on the surface indicating its desorption. Our studies have shown the pattern of fragmentation of this molecule is reproducible. The found threshold electron energy was shown to be related to the alignment of the molecular orbital energies with the substrate.

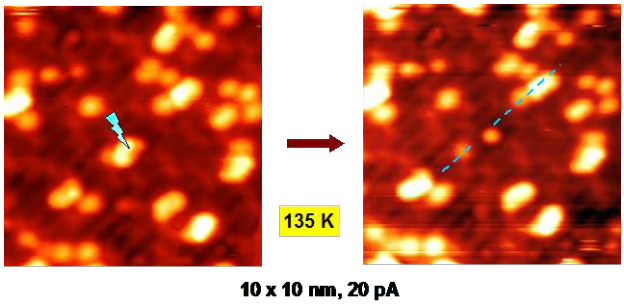

Fig. 3: STM images showing a surface prior to and after tip injection of an electron in an adsorbate molecule.

Future Plans

In summary, our work will focus on dynamical phenomena uncovered via the STM imaging of the spatial distribution of molecular fragments from tip-induced reactions with precise control of current and energy of the tunneling electrons. Our intent is to understand the methods and physics of the tip induced reaction process, first on well prepared single- crystal metal-oxides and, subsequently, on nanocrystals of these same materials. For each type of nanoparticle our research will have the following elements: a) formation and characterization of the nanoparticles; b) determination of adsorbed state, c) investigation of any thermal surface chemistry; and, c) measurement of dynamics following either tip- or UV-induced fragmentation. These experiments have involved establishing new experimental methods and instrumentation in our STM chamber, including a precise evaporator, UV source, and XPS instrumentation

Recent DOE-Sponsored Publications

1. D. Potapenko, J. Hrbek, and R.M. Osgood, Jr., "Scanning Tunneling Microscopy Study of Titanium Oxide Nanocrystals Prepared on Au(111) by Reactive-Layer-Assisted Deposition." ACS Nano 2, 7, 1353-1362 (2008)
2. T.-L. Chen, M.B. Yilmaz, D. Potapenko, A. Kou, N. Stojilovic, R.M. Osgood, Jr., "Chemisorption of Tert-Butanol on Si(100)." Surf. Sci. 602, 21, 3432-3437 (2008)
3. D. Potapenko and R.M. Osgood, Jr., "Preparation of TiO_2 nanocrystallites by oxidation of Ti-Au(111) surface alloy." Nano Lett. 9, 6, 2378-2383 (2009)
4. L. Cao, N.-C. Panoiu, and R.M. Osgood, Jr., "Surface Second Harmonic Generation from Scattering of Surface Plasmon Polaritons by Radially Symmetric Nanostructures" Phys. Rev. B, 79, 235416 (2009)
5. D. Potapenko, N. Choi, and R.M. Osgood, Jr., "Adsorption Geometry of Anthracene and 4-Bromobiphenyl on TiO_2(110) Surfaces." J. Phys. Chem. 114, 19419 (2010)

Optical manipulation of ultrafast electron and nuclear motion on metal surfaces

Hrvoje Petek
Department of Physics and Astronomy
University of Pittsburgh
Pittsburgh, PA 15260
petek@pitt.edu

Program Scope

We study the electronic structure and ultrafast electron induced dynamics of clean and adsorbate covered surfaces by time-resolved-two-photon photoemission (TR-2PP) spectroscopy, scanning tunneling microscopy (STM), and electronic structure theory. Our goal is to understand the electronic structure of the interface between solid (metal or semiconductor) surface and an adsorbate overlayer (atomic or molecular). We are interested in developing a general understanding of how the component materials and their main mode of interaction determine the interfacial electronic properties. We perform the spectroscopy of such interfaces with photon and electron probes. Nonlinear two-photon photoemission reveals the unoccupied electronic states of the interface and the optical excitation pathways. Single molecule level information can be obtained with STM by identifying the tunneling resonances, and performing spectroscopic imaging of single molecules or their 1D or 2D aggregates. Transiently excited resonances decay by resonant charge transfer to the conduction band of the substrate or through electron-electron scattering. If the resonance lifetimes are sufficiently long, the coupling of electron and nuclear degrees can lead to surface femtochemistry. Femtosecond TR-2PP spectroscopy can probe the nuclear motion-induced changes in the surface electronic structure. Lastly, we investigate intermolecular interactions on 1D surfaces. Anisotropic direct and substrate-mediated interactions lead to novel chemisorption structures and molecular self-assembly of significant interest to heterogeneous catalysis.

Recent Progress

Alkali atom chemisorption and femtochemistry.[1-5] We have investigated the electronic structure of clean and alkali atom covered on noble metal [Cu(111), Cu(001), Ag(111)] surfaces.[6, 7] Near a metal surface, *n*s valence electron of an alkali atom experiences a repulsive Coulomb interaction with the image charge of ionic core. Upon chemisorption the *n*s state becomes an unoccupied resonance of the metal-alkali atom interface at approximately 3 eV above the Fermi level. This σ resonance can be detected in TR-2PP experiments as it acts as an intermediate state in the 2PP process. Surprisingly, the σ resonance energy is independent of the alkali atom period, which we showed to be an outcome of the inverse relationship between the atomic size and the *n*s valence electron binding energy. We further investigated the role of the band structure of the substrate. The σ resonance binding energy with respect to the vacuum level is systematically ~0.2 eV lower for Ag(111) then for Cu(111). Our simple theoretical model for the electronic structure of adsorbate covered metal surfaces show that this difference arises from the different positions of projected electronic band gaps on Cu(111) and Ag(111) surfaces.

Photoexcitation of the σ resonance of alkali atoms on noble metal surfaces can occur via direct dipole excitation or the indirect hot-electron mechanism. By angle resolved 2PP measurements of alkali atoms on Ag(111), we demonstrated that the excitation process is a direct one involving the bulk sp-band initial state of the substrate. The excitation can occur from the delocalized bands of the substrate to the localized σ resonance on account of the spatial overlap of the initial and intermediate states within the bulk. All initial states that satisfy energy conservation in the optical transition can participate irrespective of momentum, because momentum is undefined within the intermediate state. Alkali atoms represent an excellent model for developing quantitative models for optical excitation at solid surfaces, and therefore, we plan further studies with tunable excitation and photoelectron momentum imaging.

The lifetime of Cs σ resonance on Ag(111) surface is sufficiently long to observe the nuclear motion associated with frustrated photodesorption. The population of the σ resonance energy excites Cs atom to the neutral, repulsive electronic state surface at the position of the ionic ground state. The repulsion initiates the nuclear wave packet motion, which can be detected by the change of the σ resonance energy as a function of the pump-probe delay in a TR-2PP experiment. We have studied the femtochemistry of Cs/Ag(111) system by measuring the photoemission angle and energy dependent σ resonance dynamics. From these measurements it is clear that the dynamics cannot be simply interpreted in terms of energy and population decay dynamics of the σ resonance energy. In order to gain greater understanding of the origin of the unusual dynamics we went to Max Planck Institute (MPI) for Microstructure Physics in Halle, Germany, to perform momentum-imaging experiments. The TR-2PP apparatus at MPI enables 2π steradian imaging of photoelectron momentum. From these measurements we concluded that: i) the angle resolved femtochemistry measurements can provide information on the wave function evolution during the desorption process; ii) the coherent 2PP processes via the bulk and surface intermediate states interfere so as to distort energy and momentum dependent photoelectron distributions; and iii) the final state in photoemission via σ resonance is a quasibound state, which decays by tunneling into the plane-wave photoemission continuum. These initial experiments provide a wealth of new physical processes to investigate, but will require upgrades in the apparatus in order to disentangle the individual contributions.

Superatom states of hollow molecules.[8-11] In low temperature STM measurements we discovered atom like states of C_{60} molecules. We identified these states from the local density of states images, which have the appearance of spherical harmonic orbitals. DFT calculations using a plane wave basis set confirmed the existence of such orbitals. Our hypothesis was that these orbitals are derived from the image potential states of molecular sheets, and are primarily defined by the molecular geometry rather than the composition of the material. We tested our hypothesis by calculating the image potential (IP) states of graphene, and then we investigated how the IP states of graphene hybridize into the interlayer state (IS) of graphite. Specifically, calculations on bilayer graphene as a function of

interlayer distance show that the IP states hybridize into IS state with essentially the same properties as the lowest s-superatom state of C_{60}.

In addition to graphene, we also calculated the superatom states of carbon (CNT) and boron nitride (BNNT) nanotubes. DFT calculations find atom like states that are infinitely extended along the nanotube axis and have atom-like properties in the cross sectional plane. Interestingly, the s-superatom state has most of its density in the nonnuclear region within the nanotube core, and therefore, would be expected to have interesting transport properties. In all important conducting and semiconducting materials the conduction charge density is localized on the positive ions, where the electron-phonon interaction is expected to be large. Of course, the superatom states of CNTs are above the unoccupied π^* states, and so could not participate in transport. By contrast, the s-superatom states BNNTs are at the conduction minimum, where we would expect to find free electron conduction superior even to common metals. We also investigated different ways of stabilizing the superatom states by internal doping with alkali atoms, and internanotube interactions (parallel and coaxial).

Finally, we investigated the superatom state $Sc_3N@C_{80}$ molecules. Our hypothesis was that superatom states of endohedral fullerenes will be strongly affected by the internal cluster, because its density is maximum in the center of the fullerene cage. The interaction may stabilize or destabilize the superatom state, depending on the electronic structure of the included species. The Sc_3N cluster destabilizes the superatom states because of the high density of electron charge provided by the N atom in the center of the molecule. The result of the included cluster is to destabilize the superatom state thereby increasing its external density. In aggregates of $Sc_3N@C_{80}$ molecules this leads to stronger intermolecular hybridization then we observed for C_{60} molecules.

Molecular self-assembly on 1D surfaces.[12] We investigated the structure of CO molecules on the Cu(110)-(2x1)-O surface. The surface consists of 1D Cu-O chains, with electrons propagating along the chains and essentially no interaction between the chains. Unlike any other surface, CO molecules at maximum coverage (~0.12 ML) self-assemble at 77 K into a nanograting structure consisting of one-molecule wide rows running orthogonal to the Cu-O- chains and with 8-9 unit cells separation between the rows. Moreover, at low coverage single CO molecules appear as two bright spots separated by 0.5 nm. DFT calculations, performed in collaboration with Donostia International Physics Center in San Sebastian, Spain, explain this unusual behavior by the unusual interaction between CO molecule and its host atom. Although the interaction can be explained by the Blyholder model, in order for the Cu atom to form a bond with CO and simultaneously maintain bonding with the Cu-O- chain, it must lift up by 1 Å from the Cu-O- chain. Lifting of the substrate atom allows the Cu-CO unit to tilt as if on a hinge by 45° with respect to the surface normal to optimize dipole-induced dipole interaction with the surface. CO molecules can exist in either of the two equivalent tilted structures that interconvert faster then the STM imaging time scale, explaining the binary single molecule images. Lifting of the Cu atom also induces strain, which poisons CO molecule adsorption on the same Cu-O- chain within several unit cells from an existing molecule. We believe that similar molecule-surface interactions may occur

on other low-dimensional surfaces such as defect sites that are thought to play an important role in catalysis.

Future Plans

In May of 2011, we expect to take the delivery of a 2 MHz optical fiber pumped noncollinear optical parametric amplifier (NOPA) femtosecond laser, purchased with funds from DOE. This laser will enable us for the first time to measure the wavelength dependence of many of the phenomena that we have been observing with 3.1 eV excitation. The ability to tune our excitation source between 1-6 eV and to perform two color pump-probe measurements will enable many experiments that were inaccessible to us thus far.

In addition, we will purchase a 2D imaging photoelectron energy analyzer with support from the University of Pittsburgh. This instrument will enable us to simultaneously image photoemission energy and momentum in one of the orthogonal directions. The data acquisition rate will increase enormously, because we will be able to acquire thousands of data channels simultaneously.

These upgrades will be essential to perform femtochemistry experiments of alkali atom photodesorption. In particular, we hope to be able to perform the wave function imaging experiments with minimal complications from interference multiple pass interference effects. Moreover, the higher photon energy and momentum imaging capability will enable us to study the band formation of superatom states of C_{60} molecules. Finally, we plan to investigate the clean and CO covered Cu(110)-(2x1)-O surface, in order to investigate the 1D properties of its Cu-O- chains and CO rows.

References

1 J. Zhao, et al., *Phys. Rev.* B **78**, 085419 (2008).

2 A. G. Borisov, et al., *Phys. Rev. Lett.* **101**, 266801 (2008).

3 S. Achilli, et al., *Phys. Rev.* B **80**, 245419 (2009).

4 H. Petek, M. Feng, and J. Zhao, in *Current-Driven Phenomena in Nanoelectronics*, edited by T. Seideman, 2010), p. 215.

5 L.-M. Wang, V. Sametoglu, A. Winkelmann, J. Zhao, and H. Petek, *J. Phys. Chem.* A, ASAP (2011).

6 A. Winkelmann, V. Sametoglu, J. Zhao, A. Kubo, and H. Petek, *Phys. Rev.* B **76**, 195428 (2007).

7 A. Winkelmann, W.-C. Lin, F. Bisio, H. Petek, and J. Kirschner, *Phys. Rev. Lett.* **100**, 206601 (2008).

8 M. Feng, J. Zhao, and H. Petek, *Science* **320**, 359 (2008).

9 S. Hu, J. Zhao, Y. Jin, J. Yang, H. Petek, and J. G. Hou, *Nano Lett.* **10**, 4830 (2010).

10 T. Huang, J. Zhao, M. Feng, H. Petek, S. Yang, and L. Dunsch, *Phys. Rev.* B **81**, 085434 (2010).

11 M. Feng, J. Zhao, T. Huang, X. Zhu, and H. Petek, *Acc. Chem. Res.*, ASAP (2011).

12 M. Feng, P. Cabrera-Sanfelix, C. Lin, A. Arnau, D. Sanchez-Portal, J. Zhao, P. M. Echenique, and H. Petek, *Phys. Rev. Lett.* (submitted).

Ultrafast electron transport across nanogaps in nanowire circuits

Eric O. Potma
University of California, Irvine, Natural Sciences II, Department of Chemistry, Irvine, CA 92697.
Tel. 949 824 9942; e-mail: epotma@uci.edu

1. Introduction

The first phase of this Program involved the development of an assay that enables a closer look at electron transfer through single molecules. This assay is based on ultrafast spectroscopic investigations of single molecules that are incorporated into a nanowire circuit. A key aspect of this project is the use of metallic nanowires with an engineered nanogap, in which the probe molecule is positioned. This assay allows for controlled injection of electrons into the probe molecule through excitation of the nanowires with laser light.

Our overall goal for Phase I (first 18 months) of this Program was to develop a method for transferring excitation energy from a focused femtosecond laser beam through a surface plasmon polariton (SPP) over a gold surface to a distant target. The purpose of this method is to decouple the photon radiation flux from the surface electric field used for excitation of the molecular target. This decoupling allows for a reduced photodamaging effects to the nanocircuit due to heating, and enables a clean electronic excitation mechanism by using solely the surface electric field for excitation rather than using freely propagating light. We accomplished all of the specific goals of Phase I by demonstrating the principle of dual-frequency wave-mixing at a nano-particle through remote excitation. Using surface plasmon polariton (SPP) excitation, we achieved a remote excitation distance of more than 40 micrometer.

2. Specific scope of research of Phase I (first 18 months)

In our Program, we aim to achieve the following specific goals for Phase I of the project:

1) Our first goal is to optimize our existing optical microscope for precisely focusing femtosecond laser pulses onto the desired locations in the circuit.
2) Our second goal is to optimize the nanowire circuits such that laser pulses can be successfully used for launching surface plasmon polaritons (SPP). The SPP excitations are crucial in this research as they provide the key mechanism for injecting electrons into the probe molecule in a controlled fashion.

3. Research Accomplishments

Specific goal 1: Build a femtosecond microscope system

We have successfully built a microscope setup suitable for excitation and detection of SPP modes in gold films. The layout is shown in Figure 1a. Briefly, the system is based on an optical microscope equipped with a CCD camera. An optical parametric oscillator (OPO) provides the femtosecond pulse trains need for the wave-mixing experiments. The collinearly aligned beams are focused to micron-sized spot with a high numerical aperture lens at an angle close to the Kretschmann coupling angle for SPP excitation.

We have lithographically fabricated simple test samples composed of a 45 nm thick gold film on a borosilicate coverslip. The edge of the gold film is patterned with

large extensions (10 – 100 μm) of 3 μm width, forming plasmonic waveguides, as shown in Figure 1b.

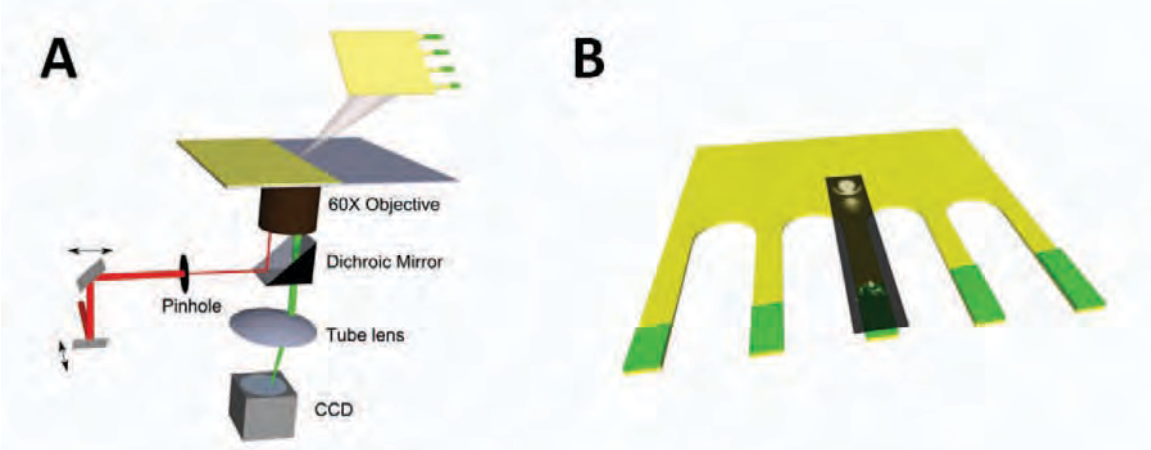

Figure 1. (A) Schematic of the experimental setup. (B) Sketch of the patterned gold film (yellow) with extensions partially covered with CdSe quantum dots (green). The overlaid image represents actual data showing the FWM signals at the laser spot and the TPEF of quantum dots.

Specific goal 2: Launching of SPP modes in the circuit

We have successfully coupled freely propagating femtosecond pulses to propagating SPP modes in the gold waveguides. An example is shown in Figure 2a, where a 240 fs pulse at 730 nm is coupled to a surface polariton mode that propagates into the gold extension. It can be seen through the leakage radiation that the SPP mode travels for more than 40 μm before it partially couples to the radiation field at the tip of the gold extension. These experiments show that femtosecond pulses can be conveniently coupled to SPP modes and transported over distances of more than 40 μm in the gold waveguide.

We have been able to couple a second fs-laser beam of a different color (935 nm) in the film. The presence of two SPP modes allows for wave-mixing experiments at locations far away from the laser spot. For this purpose, we have chosen to use CdSe quantum dots, which exhibit a strong fluorescence reponse, as a probe for the wave-mixing process. In Figure 2b, the four wave-mixing (FWM) signal at the laser spot is shown in addition to the two-photon excited fluorescence (TPEF) of a cluster of CdSe quantum dots, which are positioned near the tip of the waveguide.

Figure 3 shows that the two SPP of different frequency can combine at the target to excite electronic transitions through nonlinear wave-mixing. The time-resolved TPEF signal shows a clear maximum when the two SPP modes overlap in time, indicating that dual-color wave-mixing occurred at the quantum dot. We have verified that the nonlinear signatures exhibit the correct dependence on the coupling angle and input polarization, which firmly confirm that nonlinear mixing of surface fields delivered by SPP wave-packets is responsible for the observed excitation mechanism.[1]

These experiments demonstrate that time-resolved femtosecond experiments can be performed at the distal site of a plasmonic waveguide. This assay decouples the required excitation energy from the residual illuminating photon flux, which is

particularly important for the anticipated experiments involving plasmon controlled electron ejection at nanogaps.

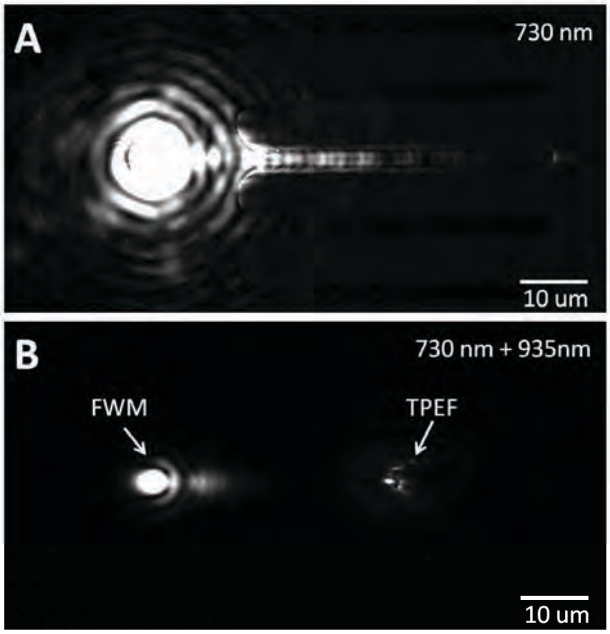

Figure 2. (A) CCD image showing the laser spot and the leakage radiation of the propagating SPP mode excited by 730 nm p-polarized light. Note that the SPP mode propagates into the gold finger. (B) Image showing the FWM signal at the location of the laser spot, the leakage radiation from a SPP mode at $2\omega_1$-ω_2 and the remotely-excited TPEF from the quantum dots positioned on the golf finger.

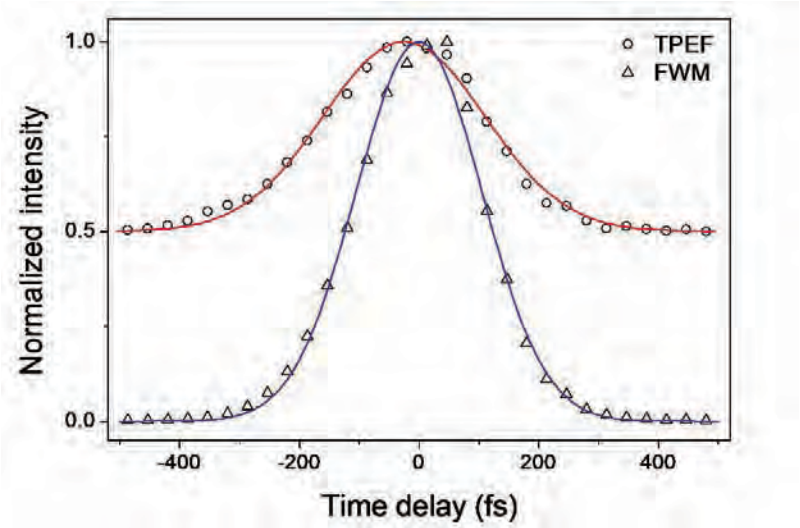

Figure 3. TPEF and FWM signals as a function of the time delay between the signal and idler beams. The red and blue curves show Gaussian estimates of the TPEF and FWM cross correlations, respectively.

We have also devised an alternative scheme based on two counter-propagating surface plasmons. Using this scheme, which is illustrated in Figure 4, we have performed surface-mediated FWM measurements of nanoparticles placed on gold surfaces. This remote excitation scheme enabled us to investigate the ability of surface waves to act as a source for FWM signals in nanotargets in a reproducible and background-free fashion. Our experiments indicate that pure surface wave induced FWM signals in individual nanoparticles can be achieved and that the ensuing radiation from the nanoparticles is coherent.[2] This approach is a promising strategy for future surface-enhanced FWM experiments on molecular structures, including vibrational CARS of surface bound molecules at low copy numbers.

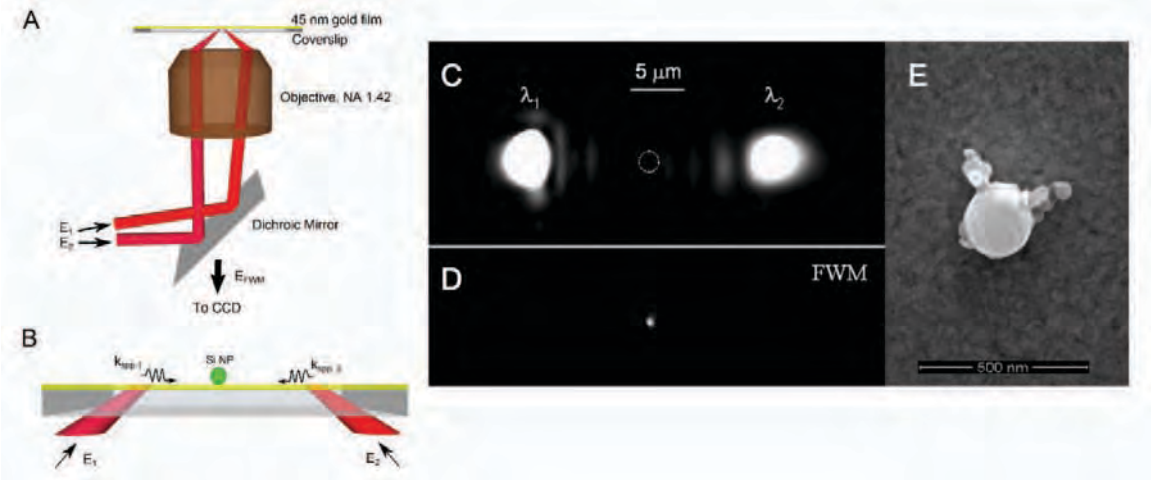

Figure 4. FWM with two counter-propagating surface polaritons. (A) Beam configuration for objective-based focusing of incident fields E_1 and E_2. (B) Excitation configuration. Two counter-propagating surface plasmon polaritons are launched into an Au film. The Si nanotarget is placed onto the gold surface in between the launching spots. (C) CCD image of the focused laser spots on the gold film. Dotted circle indicates the location of the nanoparticle. (D) CCD image of the FWM radiation from the nanoparticle. (E) SEM image of a 200 nm Si nanoparticle.

4. Next steps

Our next efforts will be focused on refining the SPP excitation scheme such that single molecules can be probed. A second goal is to engineer nanogaps in the metallic waveguides for incorporation of a single molecular bridge.

References

1. Y. Wang, X. Liu, D. Whitmore, W. Xing and **E. O. Potma**. "Remote femtosecond wave-mixing using propagating surface plasmon polaritons in gold films", *Opt. Express, submitted*.
2. X. Liu, Y. Wang and **E. O. Potma**. "Remote surface-enhanced four-wave mixing of nanostructures", *Opt. Letters, submitted.*

Project I. Soft X-ray Spectroscopy of Liquids and Solutions

Richard J. Saykally
Department of Chemistry
University of California
and
Chemical Sciences Division
Lawrence Berkeley National Laboratory
Berkeley, CA 94720-1460
saykally@berkeley.edu
http://www.cchem.berkeley.edu/rjsgrp/index.html

Program Scope or Definition

The goal of this project is to explore, develop, and apply novel methodologies for atom-specific characterization of volatile liquids, solutions, and and their surfaces, employing combinations of liquid microjet technology with synchrotron X-ray and Raman spectroscopies and close connection with state-of-the-art theory.

Recent Progress

Towards a Predictive Theory of Core-Level Molecular Spectra [4,5, 11-13]

The development of near edge X-ray absorption fine structure spectroscopy (NEXAFS) of liquid microjets has provided a useful new tool for characterizing the details of solvation for increasingly complex systems. NEXAFS probes the unoccupied molecular orbitals, which are highly sensitive to intermolecular interactions. This new approach to the study of liquids is yielding important insights into the behavior of aqueous systems, but the chemical information that can be extracted from the measurements is currently limited by the reliability of available theoretical methods for computing core-level spectra. The accurate description of an absorption event of several hundreds of eV of energy is an ongoing challenge in theoretical chemistry. In collaboration with LBL scientist David Prendergast, we are using the excited core hole (XCH) method recently developed by Prendergast and Galli to compute the NEXAFS spectra of prototype systems, such as pyrrole[12] –an archtypical aromatic molecule-and compare the results with experimental spectra measured at the ALS. Near edge X-ray absorption fine structure (NEXAFS) spectra of pyrrole measured at the carbon and nitrogen K-edges both in the gas phase and when solvated in water, are compared with spectra simulated using a combination of classical molecular dynamics and first principles density functional theory in the excited state core hole approximation. The excellent agreement enabled detailed spectral assignments. Pyrrole is highly reactive in water and reaction products formed by the autopolymerization of pyrrole in water are identified. The solvated spectra measured at two different temperatures, indicate that the final states remain largely unaffected by both hydration and temperature. This is somewhat unexpected, as the nitrogen in pyrrole can donate a hydrogen bond to water. This study provides a good demonstration of the ability of the XCH method to describe core-level spectra of highly delocalized bonding systems, which are problematic for the methods now commonly used.

As methods of core-level spectroscopy involving X-ray absorption spectroscopy (XAS), near edge X-ray absorption fine structure (NEXAFS), X-ray absorption near edge structure (XANES), or X-ray photoelectron spectroscopy (XPS) mature, they are increasingly being applied to

complex molecular systems, including proteins, DNA, large organic molecules, and polymers. Our recent study[20] indicates that calculations on such systems are extremely sensitive to the molecular geometries; therefore, in addition to an accurate theoretical formalism to describe the electronic excitation, the molecular geometries and their thermal fluctuations must be correctly sampled. We reported[11,13] on the effects of quantized nuclear motion with path integral molecular dynamics PIMD in calculations of the nitrogen K-edge spectra of two isolated organic molecules. S-triazine, a prototypical aromatic molecule occupying primarily its vibrational ground state at room temperature, exhibits substantially improved spectral agreement when nuclear quantum effects are included via PIMD, as compared to the spectra obtained from either a single fixed-nuclei based calculation or from a series of configurations extracted from a classical molecular dynamics trajectory. Nuclear quantum dynamics can accurately explain the intrinsic broadening of certain features. Glycine, the simplest amino acid, is problematic due to large spectral variations associated with multiple energetically accessible conformations at the experimental temperature. This work highlights the sensitivity of near edge X-ray absorption fine structure NEXAFS to quantum nuclear motions in molecules, and the necessity of accurately sampling such quantum motion when simulating their NEXAFS spectra.

Towards a Systematic Atom-Specific Spectroscopic Method for the Study of Hydration in Small Biomolecules(6,7,10)

Using liquid microjets to avoid the often incapacitating problem of radiation damage to fragile solutes has enabled the measurement of pH-dependent NEXAFS spectra of amino acids, including glycine, proline, lysine, and the tripeptide triglycine[7], as well as ATP[6] and peptoid molecules[10]. This, in turn, has permitted the study of the effets of selected salts on polypeptide conformations[7,9], with the aim of elucidating the origins of Hofmeister effects in biology.

Future Plans

1. Complete the XAS study of ionic perturbation of local water structure, such that the entire Hofmeister series is ultimately addressed. We seek a comprehensive picture of the effects of both cations and anions on the local structure of water. Raman spectroscopy measurements will also be performed on these systems, the data from which provide complementary insights and aid in the theoretical modeling.

2. Extend our XAS studies of local hydration to important free radical species of interest in the context of nuclear reactor corrosion and physiology, generated in liquid water microjets by excimer laser photolysis.

3. Extend our studies of amino acid hydration vs. pH to include all natural amino acids. Use the same approach to continue the study of hydration of the peptide bonds in small polypeptides, nucleotide bases, nucleosides, and nucleotides, as well as the novel "peptoid" molecules.

References (DOE supported papers: 2009-present) – 13 total

[available at http://www.cchem.berkeley.edu/rjsgrp/opening/pubs.htm]

1. A.H. England, A. Duffin, C. Schwartz, J. Uejio, D. Prendergast, and R.J. Saykally, "On the Hydration and Hydrolysis of Carbon Dioxide," *Science,* Submitted (2011).

2. A. Duffin, A.H. England, C.P. Schwartz, JS. Uejio, G.C. Dallinger, O. Shih, D. Prendergast, and R.J. Saykally, "Borohydid-Water Interactions Characterized by X-ray Absorption Spectroscopy," *PNAS,* Submitted (2011).
3. A. Duffin, C. Schwartz, A. England, J. Uejio, D. Prendergast, and R.J. Saykally, "pH-Dependent X-ray Absorption Spectra of Aqueous Boron Hydrides," *J. Chem. Phys.* **134 –** In press (2011).
4. C.P. Schwartz, S. Fatehi, R.J. Saykally, and D. Prendergast, "The importance of electronic relaxation for intercoulombic decay in aqueous systems," *Physical Review Letters* **105,** 198102 (2010).
5. C.P. Schwartz, R.J. Saykally, and D. Prendergast, "An analysis of the NEXAFS spectra of molecular crystal: α-glycine," *j. Chem. Phys.* **133,** 044507 (2010).
6. D. Kelly, C.P. Schwartz, J.S. Uejio, A.M. Duffin, A.H. England, and R.J. Saykally, "Near edge x-ray absorption fine structure spectroscopy of aqueous adenosine triphosphate at the carbon and nitrogen K-edges," *J. Chem. Phys.* **133,** 101103-101106 (2010).
7. C.P. Schwartz, J.S. Uejio, A.M. Duffin, A.H. England, D. Kelly, D. Prendergast, and R.J. Saykally, "Investigation of Protein Conformation and Interactions with Salts via X-ray Absorption Sectroscopy," *PNAS* **107,** 14008-14013 (2010).
8. G.N.I. Clark, C.D. Cappa, J.D. Smith, R.J. Saykally, and T. Head-Gordon "The Structure of Ambient Water," *Mol. Phys.* **108,** 1415-1433 (2010).
9. C.P. Schwartz, J.S. Uejio, A.M. Duffin, W.S. Drisdell, J.D. Smith, and R.J. Saykally, "Soft X-ray Absorption spectra of aqueous salt solutions with highly charged cations in liquid microjets," *Chem. Phys. Lett.* **493,** 94-96 (2010). LBNL-3897E
10. J.S. Uejio, C.P. Schwartz, A.M. Duffin, A.H. England, D. Prendergast, And R.J. Saykally, "Monopeptide versus Monopeptoid: Insights on Structure and Hydration of Aqueous Alanine and Sarcosine via X-ray Absorption Spectroscopy," *J. Phys. Chem. B* **114,** 4702-4709 (2010). LBNL-3896E
11. S. Fatehi, C.P. Schwartz, R.J. Saykally, and D. Prendergast, "Nuclear quantum effects in the structure and lineshapes of the N_2 NEXAFS spectrum," *J. Chem. Phys.* **132,** 094302-094309 (2010). LBNL-3895E
12. C.P. Schwartz, J.S. Uejio, A.M. Duffin, A.H. England, D. Prendergast, and R.J. Saykally, "Auto-oligomerization and hydration of pyrrole revealed by x-ray absorption spectroscopy," *J. Chem. Phys.* **131,** 114509-114516 (2009). LBNL-2651E
13. C.P. Schwartz, J.S. Uejio, R.J. Saykally, and D. Prendergast, "On the importance of nuclear quantum motions in near edge x-ray absorption fine structure spectroscopy of molecules," *J. Chem. Phys.* **130,** 184109-184120 (2009). LBNL-1885E

Project II. Characterization of Liquid Electrolyte Interfaces

Program Scope or Definition

The goal of this project is to apply nonlinear optical spectroscopies in close connection with state-of-the-art theory for characterization of electrolyte interfaces, seeking to establish the general principles that govern surface properties and reactivities of liquid-vapor and solid-liquid interfaces and fundamental processes such as evaporation.

Recent Progress

Liquid microjet technology affords the opportunity to study the details of water evaporation, free from the obfuscating effects of condensation that have plagued previous studies. Studying small (diameter < 5 μm) jets with Raman thermometry, we find compelling evidence for the existence of a small but significant energetic barrier to evaporation, in contrast to most current models. Studies of heavy water indicate a similar evaporation coefficient, and thus an energetic barrier similar to that of normal water[. A transition state model developed for this process provides a plausible mechanism for evaporation in which variations in libration and translational frequencies account for the small observed isotope effects. The most important practical result of this work is the quantification of the water evaporation coefficient (0.6), which has been highly controversial, and is a critical parameter in models of climate and cloud dynamics. A molecular-level description of the mechanism for water evaporation is being developed by the Chandler group using their TPS methodology for simulating such rare events.

Most recently, we have measured the effects of ionic solutes on water evaporation rates. Ammonium sulfate, the most common ionic solute in atmospheric aerosols, was shown to have no statistically significant effect on the rate[1], whereas sodium perchlorate effected a 25% reduction[2]. These effects were interpreted in terms of the surface propensities of the respective ionic components, with both cations and the sulfate ion being repelled from the interface, whereas perchlorate is one of the most surface active ions known. Acetic acid was shown toeffect a ca. 30% reduction in the evaporation rate of pure water, in preliminary and ongoing experiments. The reasons for these relatively small effects on the evaporation rates are under consideration.

As a route to clarifying the mechanism that selectively drives ions to and away from the air/water interface, we have measured the temperature dependence of the adsorption free energy of the thiocyanate ion by UV resonant SHG spectroscopy. This study unexpectedly yielded large and negative values for both the enthalpy and entropy, casting doubt on the popular notion that it is the ion polarizability that is most responsible for the interfacial propensities of the species. Instead, the solvation enthalpy and entropy of the ion relative to those properties of bulk water seem to be the important order parameters. Theoretical investigations in the Geissler group support these findings.

Future Plans

1. We plan to continue our exploration of the evaporation of liquid water by Raman thermometry and mass spectrometry, seeking to quantify the effects of salts and surfactants on the evaporation process.
2. Temperature dependences for surface adsorption of some other salts will be measured, as we seek to develop a general understanding of the forces that drive some ions to the surface and repel others.
3. Extension of these measurements to solid/liquid interfaces will be explored.

References (DOE supported papers: 2009-present) – 2 total

[available at http://www.cchem.berkeley.edu/rjsgrp/opening/pubs.htm]

1. W.S. Drisdell, R.J. Saykally, and R.C. Cohen, "Effecto of Surface Active Ions on the Rate of Water Evaporation," *J. Phys. Chem.C* **114,** 11880-11885 (2010).
2. W.S. Drisdell, R.J. Saykally, and R.C. Cohen, "On the evaporation of ammonium sulfate solution," *PNAS* **106,** 18897-18901 (2009). LBNL-2972E

Molecular Theory & Modeling

Development of Statistical Mechanical Techniques for Complex Condensed-Phase Systems

Gregory K. Schenter
Chemical & Materials Sciences Division
Pacific Northwest National Laboratory
902 Battelle Blvd.
Mail Stop K1-83
Richland, WA 99352
greg.schenter@pnl.gov

The long-term objective of this project is to advance the development of molecular simulation techniques to better understand the relation between the details of molecular interaction and the prediction and characterization of macroscopic collective properties. This involves the investigation of representations of molecular interaction as well as statistical mechanical sampling techniques. Molecular simulation has the promise to provide insight and predictive capability of complex physical and chemical processes in condensed phases and interfaces. For example, the transport and reactivity of species in aqueous solutions, at designed surfaces, in clusters and in nanostructured materials play significant roles in a wide variety of problems important to the Department of Energy. This includes the design, control and characterization of catalytic systems for energy storage and conversion.

The focus of the current effort has been to understand the balance between efficiency and accuracy in the description of molecular interaction. The evaluation of intermolecular potential energy needs to be efficient enough to allow for effective statistical mechanical and dynamical sampling. At the same time, enough of the underlying physical chemistry and sufficient parameterization needs to be contained in the models of molecular interaction so that the resulting simulation of collective molecular properties are reliable. Towards these ends we have been exploring the relation between empirical potential descriptions of molecular interaction such as multipole-polarizable empirical potentials, semiempirical NDDO electronic structure, and density functional theory (DFT). We continue to develop a self-consistent polarization (SCP) electronic structure method that supplements efficient electronic structure such as NDDO and DFT with an atom-site multipole-polarizability that enhances molecular polarizability and accounts for dispersion interactions. This approach may be understood in terms of the enhancement of the base energy functional, $E_0[\rho_0]$, by an auxiliary SCP charge density and functional $E_{SCP}[\rho_{SCP}]$, to give $E[\rho_0,\rho_{SCP}] = E_0[\rho_0] + E_{SCP}[\rho_{SCP}] + E^{Coul}[\rho_0,\rho_{SCP}]$, where the cross interaction terms, $E^{Coul}[\rho_0,\rho_{SCP}]$, are entirely described by Coulomb interaction. The energy functional associated with SCP, $E_{SCP}[\rho_{SCP}]$, is based on linear response and requires effective multipole polarizabilities. The associated multipole dispersion interaction is introduced in a "Casimir-Polder" form as $E^{disp} = -\frac{1}{2\pi}\int_0^\infty d\omega \sum_{\alpha<\beta}\sum_{\bar{\alpha}<\bar{\beta}} a_{\alpha,\bar{\alpha}}(i\omega)a_{\beta,\bar{\beta}}(i\omega)(\alpha|\beta)(\bar{\alpha}|\bar{\beta})$, where $a_{\alpha,\bar{\alpha}}(\omega)$ are dynamic multipole polarizabilities (associated with $E_{SCP}[\rho_{SCP}]$) and $(\alpha|\beta)$ are Coulomb integrals over an appropriate basis.

Initial implementations of this approach were used to describe water clusters with NDDO theory.[a] The dispersion-dominated system of the gas, liquid and solid phases of Argon were described with SCP-DFT [Ref. 3] Here, the base DFT is purely repulsive and all of the cohesive

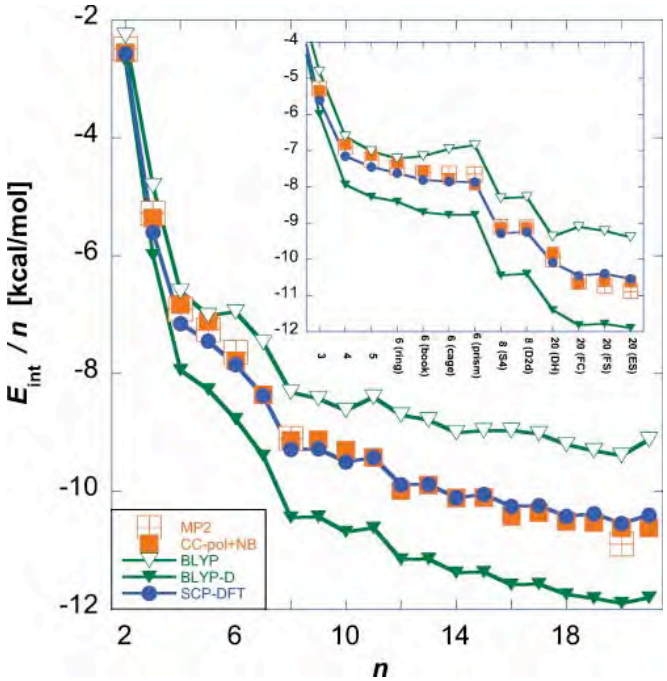

Figure 1. $(H_2O)_n$ Cluster Formation Energy

interaction is due to dispersion. The SCP-DFT and SCP-NDDO approaches for both cluster and periodic systems have been successfully implemented in the molecular simulation package, CP2K.[b] Work continues to enhance the efficiency of the SCP-NDDO periodic electronic structure in order to effectively treat increasingly larger systems. SCP-DFT method was parameterized to describe water clusters. [Ref. 6] In Figure 1 we compare the formation energy of water clusters versus size (n) using SCP-DFT (blue dots) compared to benchmark calculations (red squares). Uncorrected DFT (BLYP, green triangles) tend to underbind the clusters. The enhanced polarization and dispersion attraction stabilizes the clusters to be consistent with benchmark results. It is interesting to note that the recent empirical dispersion correction developed by Grimme (BLYP-D, solid green triangles) tends to overbind the water system.

With efficient implementation in the CP2K package, we have successfully applied the SCP-NDDO model to investigate properties of bulk water the liquid-vapor interface, and cubic ice. [Ref. 11] In Figure 2 we compare the radial distribution functions from the SCP-NDDO approach to experimental measurement as well as other semiempirical parameterizations (PM3 and PM6). Significant improvement in the water structure is recovered by adding SCP.

Future plans will include expanding the numerical efficiency of both approaches by improving preconditioning of the combined SCP and orbital optimization procedure. With efficient implementations of our SCP approach, we plan to explore complex solvation in more complex environments. Future efforts will extend the parameterization to aqueous solvation of more complex ions. We are exploring more systematic techniques for parameterizing the model based on detailed electronic response from converged electronic structure calculations as well as features in the Hartree potential. We are also

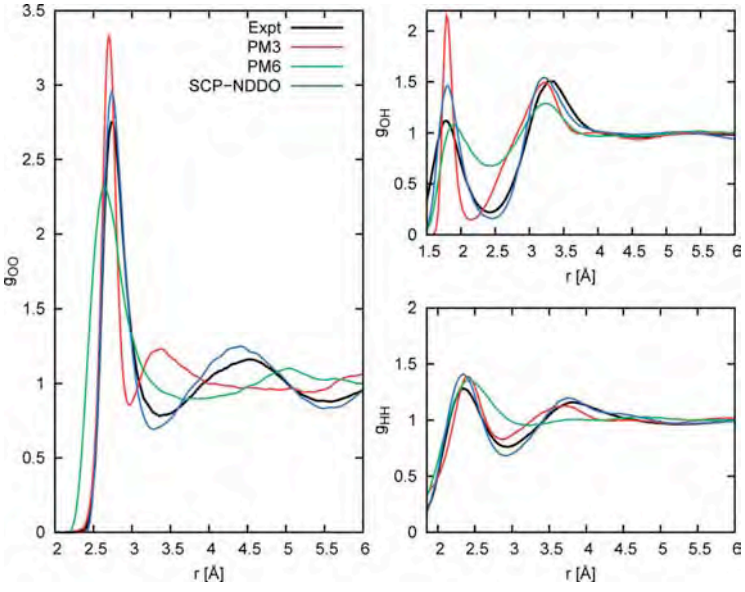

Figure 2. Water radial distribution functions.

exploring more effective screening terms for the SCP interaction.

Another focus of our effort is to make direct connection to experimental measurement. In particular, we have investigated the solvation structure of aqueous ions as measured through x-ray absorption spectroscopies. Recently we have considered the aqueous solvation of Ag^{+} [Ref. 5], Zn^{2+} [Ref. 7], I^{-} [Ref. 9], and Cm^{3+} [Ref. 12]. In these cases we test the ability of a DFT describe the solvation structure of the aqueous ion as compared to empirical potentials. From our representation of molecular interaction we generate ensembles of configurations. From this ensemble, a series of electron multiple scattering calculations are performed using the FEFF8 code[c] to generate a configuration averaged EXAFS spectra.

In our investigation of the solvation structure of iodide from EXAFS, we compared the polarizable Dang-Chang (DC) empirical model to DFT calculations. O-I-O and H-I-O angular distributions revealed differences between the DFT and DC models. The DC model shows more ordering of H around the I^{-}, and the DFT shows less structure in the H-O-I angular distribution. The DFT shows a peak of the O-I-O distribution at 142° that is absent in the DC model. When we compare calculations of simulated multi-edge EXAFS signal, we find that DFT provides a better agreement with measured features in the spectra. (See Figure 3) We find that the DC interaction potential is over structured due to a strong iodide dipole moment. (2.6 Debye for DC and 1.1 Debye for DFT) These results have profound implications o n the partitioning of iodide to the liquid/vapor interface. (See contributions by C. J. Mundy.)

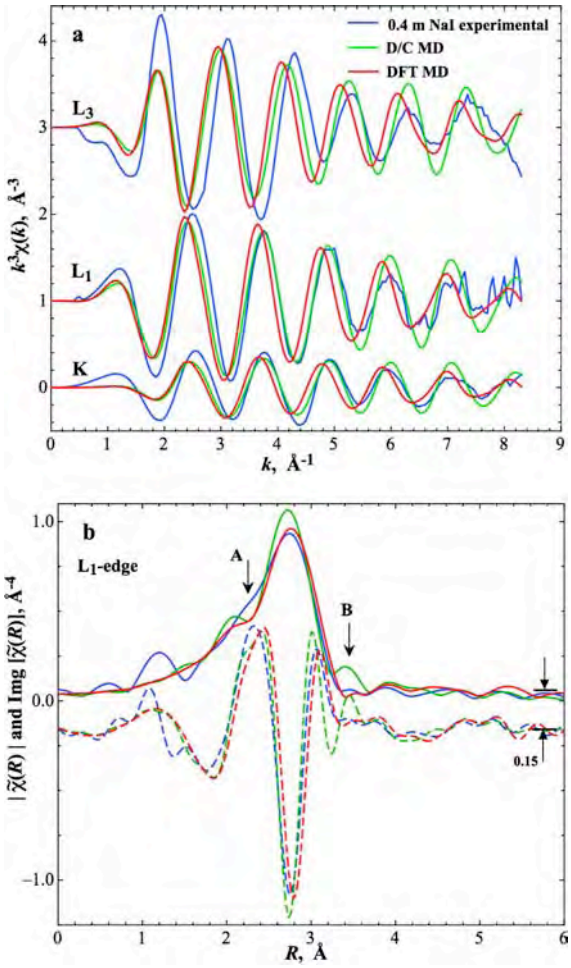

Figure 3. DC and DFT MD-EXAFS comparison to measurement.

In future studies we will consider the influence of molecular interaction between ion-pairs. Our challenge is to be able to account for changes in features in EXAFS measurement as a function of solute concentration. We will continue to use EXAFS to benchmark descriptions of molecular interaction, understand the strengths and limitations of empirical potentials, DFT, QM/MM techniques and pseudopotentials used in DFT. We have initiated studies that explore the hydration structure for the first row metal ions (Ca^{2+}, Cr^{3+}, Mn^{2+}, Fe^{3+}, Co^{2+}, Ni^{2+}, Cu^{2+}, and Zn^{2+}) evaluating DFT descriptions of interaction. In addition, we have started to explore the hydration of complex oxyanion series: IO_3^{-}, BrO_3^{-}, ClO_3^{-}, and ClO^{-}.

Acknowledgements: Direct collaborators on this project include C. J. Mundy, G. Murdachaew and J. Fulton. Interactions with S. S. Xantheas, L. X. Dang and S. M. Kathmann have significantly influenced the course of this work. This research was performed in part using the computational resources in the National Energy Research Supercomputing Center (NERSC) at

Lawrence Livermore National Laboratory. Battelle operates Pacific Northwest National Laboratory for the US Department of Energy.

References

a. D. T. Chang, G. K. Schenter, and B. C. Garrett "Self-consistent polarization neglect of diatomic differential overlap: Application to water clusters," J. Chem. Phys. **128** (16), 164111 (2008).
b. The CP2K developers group, http://cp2k.berlios.de/ (2008) J. VandeVondele, M. Krack, F. Mohamed, M. Parrinello, T. Chassaing and J. Hutter, Comp. Phys. Comm. **167**, 103 (2005).
c. J. J. Rehr, R. C. Albers, S. I. Zabinsky, Phys. Rev. Lett. **69**, 3397 (1992); M. Newville, B. Ravel, D. Haskel, J. J. Rehr, E. A. Stern, and Y. Yacoby, Physica B, **208-209**, 154 (1995); A. L. Ankudinov, C. Bouldin, J. J. Rehr, H. Sims, and H. Hung, Phys Rev. B **65**, 104107 (2002).

References to publications of DOE sponsored research (2009-present)

1. R. C. Bell, K. Wu, M. J. Iedema, G. K. Schenter, and J. P. Cowin, "The Oil-Water Interface: Mapping the Solvation Potential," J. Am. Chem. Soc. **131** (3), 1037-1042 (2009).
2. S. M. Kathmann, G. K. Schenter, B. C. Garrett, B. Chen, and J. I. Siepmann, "Thermodynamics and Kinetics of Nanoclusters Controlling Gas-to-Particle Nucleation," J. Phys. Chem. C **113** (24), 10354-10370 (2009).
3. K. A. Maerzke, G. Murdachaew, C. J. Mundy, G. K. Schenter, and J. I. Siepmann, "Self-Consistent Polarization Density Functional Theory: Application to Argon," J. Phys. Chem. A **113** (10), 2075-2085 (2009).
4. D. Shiyu, J. S. Francisco, G. K. Schenter, and B. C. Garrett, "Interaction of ClO Radical with Liquid Water," J. Am. Chem. Soc. **131**, 14778 (2009).
5. J. L. Fulton, S. M. Kathmann, G. K. Schenter, and M. Balasubramanian, "Hydrated Structure of Ag(I) Ion from Symmetry-Dependent, K- and L-Edge XAFS Multipole Scattering and Molecular Dynamics Simulations," J. Phys. Chem. A **113** (50), 13976-13984 (2009).
6. G. Murdachaew, C. J. Mundy, and G. K. Schenter, "Improving density functional theory description of water with self-consistent polarization," J. Chem. Phys. **132**, 164102 (2010).
7. E. Cauet, S. Bogatko, J. H. Weare, G. K. Schenter, and E. J. Bylaska, "Structure and dynamics of the hydration shells of the Zn^{2+} ion from *ab initio* molecular dynamics and combined *ab initio* and classical molecular dyamics simulations," J. Chem. Phys. **132**, 194502 (2010).
8. C. J. Mundy, S. M. Kathmann, R. Rousseau, G. K. Schenter, J. Vande Vondele, and J. Hutter, "Scalable Molecular Simulation: Toward and Understanding of Complex Chemical Systems," SciDAC Review, **17**, 10 (2010).
9. J. L. Fulton, G. K. Schenter, M. D. Baer, C. J. Mundy, L. X. Dang, and M. Balasubramanian, "Probing the Hydration Structure of Polarizable Halides: A Multiedge XAFS and Molecular Dynamics Study of the Iodide Anion," J. Phys. Chem. B, **114** (40), 12926-12937 (2010).
10. S. M. Kathmann, I-F. W. Kuo, C. J. Mundy, and G. K. Schenter, "Understanding the Surface Potential of Water," J. Phys. Chem. B (2011). dx.doi.org/10.1021/jp1116036
11. G. Murdachaew, C. J. Mundy, G. K. Schenter, T. Laino, and J. Hutter, "Semiempirical Self-Consistent Polarization Description of Bulk Water, the Liquid-Vapor Interface, and Cubic Ice," J. Phys. Chem. A (2011). dx.doi.org/10.1021/jp110481m
12. R. Atta-Fynn, E. J. Bylaska, G. K. Schenter, and W. A. DeJong, "Hydration Shell Structure and Dynamics of Curium(III) in Aqueous Solution: First Principles and Empirical Studies," J. Phys. Chem. A (2011). dx.doi.org/10.1021/jp201043f

Seventh Annual CPIMS Meeting Abstract for DE-SC0002583

Chemical Imaging and Dynamical Studies of Reactivity and Emergent Behavior in Complex Interfacial Systems

Report Date April 29, 2011

Steven J. Sibener
The James Franck Institute and Department of Chemistry; GCIS E-215
The University of Chicago, 929 East 57th St., Chicago, IL 60637
Email: s-sibener@uchicago.edu

Program Scope

This new program is exploring the efficacy of using molecular-level manipulation, imaging and scanning tunneling spectroscopy in conjunction with supersonic molecular beam gas-surface scattering to significantly enhance our understanding of chemical processes occurring on well-characterized interfaces including structurally-dynamic nanoscale catalytic substrates. One program focus is on the spatially-resolved emergent behavior of complex reaction systems as a function of the local geometry and density of adsorbate-substrate systems under reaction conditions. Another focus is on elucidating the emergent electronic and related reactivity characteristics of intentionally constructed single and multicomponent atom- and nanoparticle-based materials. We are also examining emergent chirality and self-organization in adsorbed molecular systems where collective interactions between adsorbates and the supporting interface lead to spatial symmetry breaking. In many of these studies we are combining the advantages of scanning tunneling (STM) and atomic force (AFM) imaging, scanning tunneling local electronic spectroscopy (STS), and reactive supersonic molecular beams to elucidate precise details of interfacial reactivity that have not been observed by more traditional surface science methods. Using these methods, it will be possible to examine, for example, the differential reactivity of molecules adsorbed at different bonding sites in conjunction with how reactivity is modified by the local configuration of nearby adsorbates. At the core of this proposal resides the goal of significantly extending our understanding of interfacial atomic-scale interactions to create, with intent, molecular assemblies and materials with advanced chemical and physical properties. This ambitious program addresses several key topics in DOE Grand Challenge Science, including emergent chemical and physical properties in condensed phase systems, novel uses of chemical imaging, and the development of advanced reactivity concepts in combustion and catalysis including carbon management. These activities directly benefit national science objectives in the areas of chemical energy production and advanced materials development.

Overview

This new DOE-BES program was initiated in Fall 2009 (September 15, 2009). Since program launch we have successfully recruited several talented postdoctoral scholars and graduate students to this effort. Moreover, our scientific program in emergent materials properties involving molecular and nanoscale systems is now underway, with details on progress during the past grant period given below. New variable-temperature UHV-STM/AFM capabilities (20K to >1000K) coupled with molecular beam dosing is presently coming on-line, giving us improved approaches for conducting studies with real-time/real-space resolution.

Personnel

We have recruited several excellent participants to this new effort. [Note: *denotes primary support and effort from this DOE grant.] Dr. Christopher Fleming* has been recruited to our STM effort in emergent materials; he arrived in Chicago after receiving his doctoral degree in Scotland. Graduate student Gaby Avila-Bront* (under-represented minority) is a key participant who is examining emergent chiral films; she has recently been awarded an NSF pre-doctoral fellowship. Graduate students Miki Nakayama and

Tuo Wang* are working on emergent materials involving nanoparticles. Finally, grad students Jim Becker, Ryan Brown & Q.Q. Tong and Senior Scientist Dr. Kevin Gibson* are assisting with molecular beam and STM/AFM instrumentation development for our effort in interfacial molecular reactivity.

Recent Progress Activity and Future Plans

1. Nanoparticle Assembled Clusters and Materials

In this theme we are using local probes to interrogate and intentionally assemble atom and nanoparticle-based clusters to form extended ensembles that exhibit emergent electronic and chemical behavior. Using our first generation cryogenically cooled STM we have assessed the electronic structure of quantum dots (semiconductor nanoparticles), and are presently extending these experiments to include nanoparticle structures adsorbed in different local ensembles. During the past year we have used the STM to locate thermodynamically-formed nanoparticle assemblies spanning single dots, few dot clusters, and monolayer films. The four panels shown in **Figure 1** are illustrative of our results on 9.5nm PbSe quantum dot assemblies. (We gratefully acknowledge the synthetic efforts of graduate student Sara Rupich and Prof. Dmitri Talapin, who have worked with us to produce the designer nanoparticles needed for this project.)

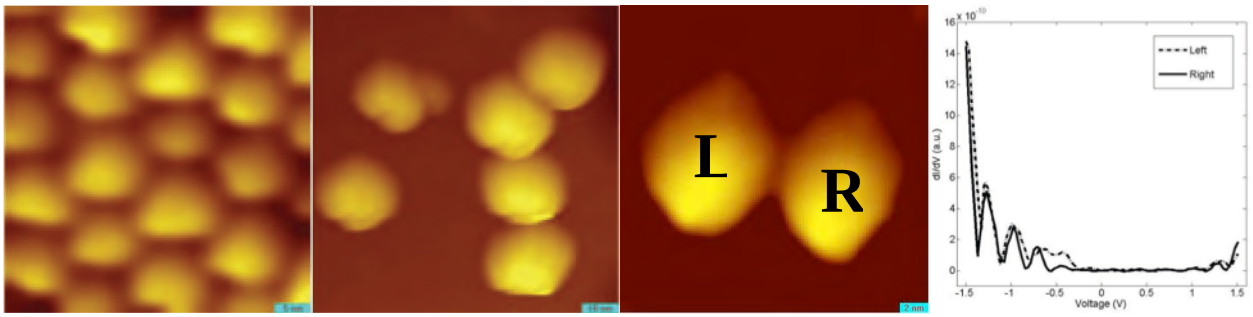

Figure 1: Topographic and spectroscopic images PbSe quantum dots (diameter: 9.5nm) on Au(111). Left: PbSe QD array at room temperature; image size 42nm×42nm, set-point current 22.2pA, sample bias 2.57 V. Mid-left: PbSe QD oligomer at room temperature; image size 83nm×83nm, set-point current 21.2pA, sample bias 2.24 V. Mid-right: PbSe QD dimer at 90K; image size 22nm×22nm, set-point current 50.2pA, sample bias 1.74 V. Right: Tunneling spectra (dI/dV) of the QD dimer shown in the mid-right image. Solid line: spectrum of the right dot; dashed line: spectrum of the left dot.

A key goal of these studies is to elucidate the local electronic spectra of nanoparticle assembled materials, and to see how variation in nanoparticle cores and ligand structure influence inter-nanoparticle electronic coupling. The right-most image in **Figure 1** shows Scanning Tunneling Spectroscopy (STS) measurements of the 9.5 nm PbSe dimer, with composite band gap and confined states clearly evident. Work is continuing on refining the electronics and experimental procedures for collecting such spectra. The recent addition of a new DSP-based lock-in amplifier has significantly improved the signal-to-noise characteristics for these measurements. Interference effects from ligands hoping to the STM tip are, apparently, pervasive. We are now going to explore using conductive AFM to obtain the desired local electronic spectra. Our new combo STM-AFM is now under vacuum and has passed the required imaging and spectroscopic tests on Si (7x7).

Going forward (using STS or conductive AFM measurements) we will examine supported nanoparticle arrays to see how these systems function as mesoscale electronic systems and catalysts, and especially local cluster arrangements influence electronic structure and inter-dot communication. On the more chemical side, we intend to explore how size modification influences reaction energetics. Moreover, issues pertaining to adsorption and reaction energetics on nanoparticles are largely unexplored. Tremendous effort has been expended to understand activated chemisorption on single crystal surfaces – at this time one cannot address the shape of adsorption barriers, or the precise active site location, for nanocatalysts; we seek to address such questions involving emergent reactivity in nanosystems.

2. Emergent Chirality and Self-Organizing Molecular Materials

In this research theme we are examining emergent chirality and self-organization in molecularly adsorbed films. Ever since Pasteur first uncovered the direct correlation between the structure of a crystal and the handedness of its component molecules, researchers have been intrigued by the mechanisms of chiral separation. STM provides the ultimate technique for determination of the exact structure and chirality of adlayers on a substrate. The structure of an adlayer is the result of a delicate balance of lateral molecule-molecule interactions and adsorbate-substrate forces. The strength of the adsorbate-substrate interaction must be balanced such that adsorbed molecules are mobile enough to self-assemble into an organized array but greater than the adsorbate-adsorbate energy to allow two-dimensional crystallization. We are working with metalloporphyrin adlayers on Au(111) as such systems meet these criteria perfectly. They form well-ordered arrays on a variety of surfaces and are highly stable. These porphyrin arrays are especially interesting because they self-assemble at room temperature without the need for annealing, making them a likely candidate for technological applications. Our initial focus is on NiTPP (nickel-2,3,7,8,12,13,17,18-octaethyl-21H,23H-porphine) and NiOEP (nickel-5,10,15,20-tetraphenyl-21H,23H-porphine) on Au(111), as well as C_{60} decoration of these systems. These molecules are achiral when isolated in the gas phase but we find that symmetry is broken when the molecules adsorb onto a surface in small clusters, where they form local chiral ensembles. Such racemic mixtures contain left- and right-handed domains for both porphyrins, indicating that the interplay of surface-adsorbate and intermolecular interactions induces chirality for the substrate-adsorbate system as a whole. We are pursuing not only general rules for the formation of racemic mixtures, but also methods of forcing (guiding) the system to form only one of the two mirror image structures. This might be achieved by the introduction of a "seed" chiral entity or, as shown below from our newest publication, by the use of a high index crystal face.

We have recently succeeded in using kinked and stepped surfaces to guide the formation of only one chiral structure of NiTPP on gold. Here, we use a locally kinked step as a symmetry-breaking template to lift the structural equivalence of the right- and left-handed racemic packing structures of NiTPP (**Figure 2**). In an effort to extend these initial findings to macroscopic dimensions, we have fabricated a bulk chiral gold crystal with extended defects and kinks (STM image shown in the right panel of this figure).

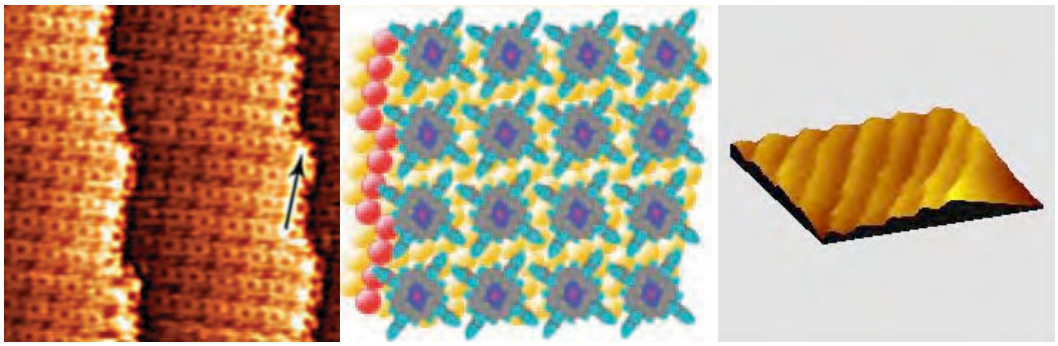

Figure 2. Left: STM image of a NiTPP adlayer on a Au(111) surface that locally contains kinked and stepped features of only one chirality that approximate a (336 316 315) surface plane. This structure successfully guides the chiral assembly of the porphyrin molecules into single-handed domains on three adjacent steps, image acquired at 1.0 nA and 1.5 V (16.7x16.7 nm^2). This image demonstrates that such kinks can act as nucleation sites for domains of only one particular enantiomer. Center: Schematic of a kinked step edge, shown in red, guiding the assembly of an array of NiTPP molecules. Right: STM image of our stepped and kinked single crystal with surface Au(336 316 315) having ca. 15 nm terraces.

It is our plan to use our new macroscopically stepped crystal to guide the self-assembly of a homochiral crystal. Such experiments are now underway. A surface structure whose chirality can be precisely controlled at the molecular level is immensely attractive to industrial techniques that fabricate enantiospecific reaction products or optically active materials.

Another aspect of this program has also gotten underway during the past year that focuses on the self-assembly of complex systems using mixtures SAMs as well as 11-phenoxy undecanethiol monolayers on Au(111) as the foundation for functional multicomponent thin films. Our most recent studies have examined with STM the influence of the phenoxy group on the striped-structure of the SAM itself, **Figure 3**. Future work will focus on the ability of this functionalized SAM to template C_{60} structures of interest for their charge transfer characteristics in molecular-level systems.

Figure 3. STM images of a striped phenoxy SAM monolayer (10 x 10 nm^2, left) and of C_{60} adsorbed on the templating SAM underlayer (20 x 20 nm^2, right). Sample preparation methods being used include drop-casting and spin coating. The right image shows that C_{60} can be templated by the SAM into linear structures of single and double row thickness.

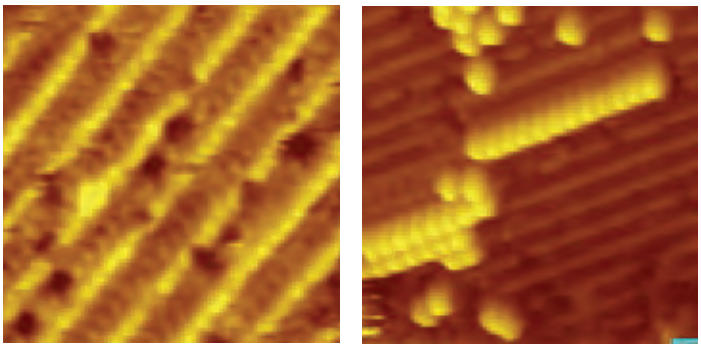

3. Reaction Dynamics

This part of our program focuses on emergent chemical reactivity at interfaces. Recent exploratory measurements from our group have examined the partial oxidation of condensed phase arenes and unsaturated hydrocarbons on non-catalytic support substrates, and found substantial changes in the reactive potential energy barriers and the product distributions as compared with isolated molecule energetics. This raises a classic issue in the chemical sciences: how does molecular reactivity evolve when going from the single molecule level to the condensed state? Profound changes in electronic structure and energy relaxation pathways as a function of the local molecular environment lead to such emergent changes in reaction rates and mechanism. In these studies we have seen, for example, markedly different oxidative reaction pathways, activation energies, and product channels for several small hydrocarbons as compared to known gas-phase behavior. These preliminary studies have been done on "thermodynamic ensemble averages", that is, where we have measured reaction rates using molecular beam techniques while varying coverages and temperature without the benefit of local imaging or local electronic spectroscopy. In essence, there remains a remarkably incomplete understanding of molecular reactivity at interfaces as a function of local adsorbate density (coverage), i.e., *local ensemble structure*. We seek to change this situation. We are setting up to use scanning probe methods in conjunction with scattering, to directly correlate reactivity with local adsorbate and substrate geometry, and electronic structure. This will allow us to develop a more comprehensive understanding of emergent molecular reactivity with respect to the precise geometry of locally-adsorbed reactants.

References to Publications

• Mixing Up Surface Properties, Seth B. Darling and S. J. Sibener, *Physics Today*, 62, 88 (2009).

• Chiral Domains Achieved by Surface Adsorption of Achiral Nickel Tetraphenyl- or Octaethylporphyrin on Smooth and Locally Kinked Au(111), Lieve G. Teugels, L. Gaby Avila-Bront, and S.J. Sibener, *J. Phys. Chem. C* 115, 2826-2834 (2011).

• Rough Waters (First Place, AAAS Science/NSF Intl. Science & Engineering Visualization Challenge – Photography Category), Seth B. Darling and Steven J. Sibener, *Science* (Cover Story) 331, 852 (2011).

Publication with DOE-BES support in conjunction with the Center for Nanoscale Materials at Argonne National Laboratory (DE-AC02-06CH11357):

• Improved Hybrid Solar Cells via *In Situ* UV-Polymerization, Sanja Tepavcevic, Seth B. Darling, Nada Dimitrijevic, Tijana Rajh, and S. J. Sibener, *Small* 5, 1776-1783 (2009).

Water dynamics in heterogeneous and confined environments: Salt solutions, reverse micelles, and lipid multi-bilayers

James L. Skinner
Department of Chemistry
University of Wisconsin
Madison, WI 53706
skinner@chem.wisc.edu

Project Scope

Our goal is to understand the structure and dynamics of water, in its different phases, at the interfaces between these phases, and in confined and heterogeneous environments. To this end, linear and nonlinear vibrational spectroscopy is playing a very important role. We are developing techniques for calculating spectroscopic observables, and then using our results to analyze and interpret experiment.

Recent Progress

A. Bulk water

We have continued our studies of nonlinear vibrational spectroscopy for isotopic mixtures of bulk water, particularly dilute HOD in H_2O. In this system, the OD stretch is an isolated vibrational chromophore, and thus can report cleanly on the structure and dynamics of H_2O. We have calculated 2DIR spectra as a function of temperature, in collaboration with Tokmakoff and coworkers.[11] Together with experiment, our results determine the activation energy for hydrogen-bonding rearrangement dynamics. We have also shown how different levels of theory affect the calculation of anisotropic frequency-resolved pump-probe signals.[4] For neat H_2O, intramolecular and intermolecular vibrational coupling produce modest effects on the linear spectra,[3] but dramatic effects on the anisotropic pump-probe signals.[6] In particular, for neat H_2O vibrational energy transfer causes the anisotropic pump-probe signal to decay 25 times faster than for HOD in H_2O, which is direct and convincing evidence for the importance of intermolecular vibrational coupling in neat H_2O.

B. Ice Ih

As is well known, there are at least 15 thermodynamically stable phases of ice, with ice Ih being the stable phase at one atmosphere pressure between 72 and 273 K. Ice Ih is a most interesting crystal indeed, as the hydrogen nuclei are disordered. We have been interested in using vibrational spectroscopy to assess the nature of this proton disorder. For the HOD/H_2O system, the proton disorder leads to inhomogeneous broadening of the OD spectrum.[5] The vibrational spectroscopy of neat H_2O is very rich, manifesting the competing effects of vibrational coupling and proton and thermal disorder. Our recent

work provides what we believe in the first assignment of the five different peaks in the IR and Raman spectra for single crystal ice Ih.[7]

C. Water liquid/vapor interface

Sum-frequency generation (SFG) spectroscopy has been used for nearly twenty years to probe the structure of the water liquid/vapor interface. Interpretation of experiment has been difficult for two reasons. First, studies on neat H_2O suffer from the effects of intramolecular and intermolecular vibrational coupling, as described above. Second, the sum-frequency intensity has contributions from the real and imaginary parts of the resonant and nonresonant susceptibilities. The first issue is alleviated by considering HOD in H_2O (or D_2O), while recent phase-sensitive detection techniques have allowed for direct measurement of the imaginary part of the resonant susceptibility. Experiments by Tian and Shen show the existence of a positive peak at low OH stretch frequency (for HOD in D_2O), and interpret this peak as arising from ice-like ordering at the liquid surface.

We had previously used the SPC/E simulation model to calculate the imaginary part of the susceptibility, and we did not find this positive low-frequency peak. We began to think that this resulted from a limitation of this and other two-body water simulation models. To this end, we developed a new model with explicit three-body interactions,[13] and used this model to recalculate the imaginary part of the susceptibility, this time finding good agreement with experiment (as shown).[12,14] We find that the positive low-frequency peak arises from cancelling positive and negative contributions from water molecules in different hydrogen-bonding environments, and does not reflect any ice-like ordering at the surface.

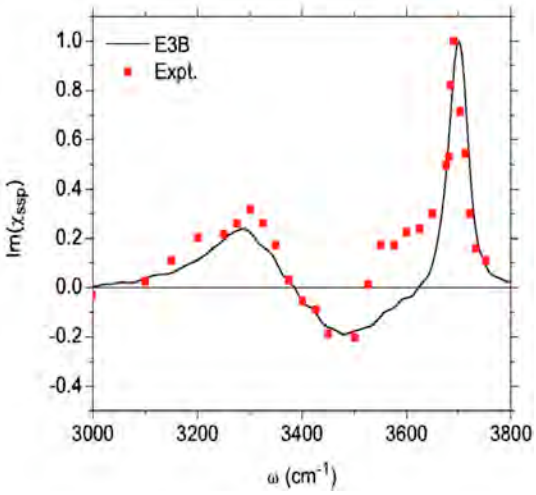

We have also collaborated with Benderskii and coworkers on understanding the peak frequencies of the free OD peak, for HOD in H_2O and for neat D_2O. Experimentally, the peak shifts to the blue by 17 cm^{-1} for the latter. We interpret this as arising from intramolecular coupling. We estimate that the frequency, of the other (hydrogen-bonded) OD group of the D_2O molecule with the free OD, is close to that of bulk water, providing experimental evidence for a very sharp liquid/vapor interface.[10]

D. Salt solutions

It is of great interest to understand how the dynamics of water is perturbed by anions and cations. To this end, we were interested in recent ultrafast spectroscopy experiments performed by Fayer and coworkers on sodium bromide solutions. They found that water

dynamics in 6M solution slows down by a factor of 3 or 4. Our calculations on this system were in reasonable agreement with experiment.[1] Moreover, we found that water structure and dynamics is hardly perturbed outside an ion's first solvation shell. We conclude, in agreement with recent sentiment, that the Hoffmeister series reflects only local ordering of water molecules. The situation with divalent ions may be somewhat different.[8]

E. Reverse micelles

AOT reverse micelles provide beautiful model systems for studying nano-confined water. Depending on the ratio of water to surfactant concentrations, reasonably mono-disperse water nano-pools containing between 25 and several hundred thousand molecules can be created. FTIR experiments by Fayer and coworkers on the HOD/H_2O system show a red-shift of the absorption spectrum as micelle size decreases, and pump-probe experiments show a concomitant slow-down of the water rotational dynamics. We can qualitatively reproduce these effects with our models.[2] We interpret the slower rotational dynamics as resulting from "curvature-induced frustration".

F. Lipid multi-bilayers

A related system, for studying water near planar interfaces with headgroups, involves aligned hydrated lipid multi-bilayers. Experiments with DLPC lipids have been performed by Fayer and coworkers. FTIR line shapes now shift to the blue with decreasing hydration, because of stronger hydrogen bonding to lipid phosphate moieties. Rotational dynamics is also slowed down considerably with decreasing hydration level. We have reproduced these effects qualitatively with our models.[15] In doing so, we provide for a consistent calculation of all experimental observables within a unified theoretical framework.

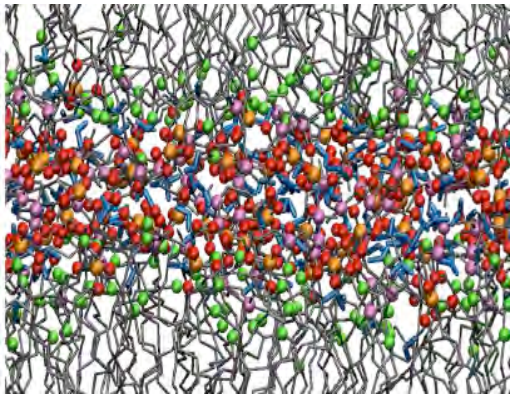

Future Plans

In addition to continuing on in the above areas, we plan to expand our scope to several news topics, including Raman spectroscopy of supercritical water, pump-probe and 2DIR spectroscopy of ice Ih, 2DSFG spectroscopy of the water liquid/vapor interface, SFG spectroscopy of water near the headgroups of lipid monolayers, and the vibrational spectroscopy of urea/water mixtures.

Publications acknowledging DOE support (2009-2011)

1. Water structure, dynamics, and vibrational spectroscopy in sodium bromide solutions, Y.-S. Lin, B. M. Auer, and J. L. Skinner, J. Chem. Phys. **131**, 144511 (2009).
2. Vibrational spectroscopy and dynamics of water confined inside reverse micelles, P. A. Pieniazek, Y.-S. Lin, J. Chowdhary, B. M. Ladanyi, and J. L. Skinner, J. Phys. Chem. **113**, 15017 (2009).
3. Signatures of coherent vibrational energy transfer in IR and Raman line shapes for liquid water, M. Yang and J. L. Skinner, Phys. Chem. Chem. Phys. **12**, 982 (2010).
4. On the calculation of rotational anisotropy decay, as measured by ultrafast polarization-resolved vibrational pump-probe experiments, Y.-S. Lin, P. A. Pieniazek, M. Yang, and J. L. Skinner, J. Chem. Phys. **132**, 174505 (2010).
5. IR and Raman line shapes for ice Ih. I. Dilute HOD in H_2O and D_2O, F. Li and J. L. Skinner, J. Chem. Phys. **132**, 204505 (2010).
6. Two-dimensional infrared spectroscopy and ultrafast anisotropy decay of water, T. l. C. Jansen, B. M. Auer, M. Yang, and J. L. Skinner, J. Chem. Phys. **132**, 224503 (2010).
7. IR and Raman line shapes for ice Ih. II. H_2O and D_2O, F. Li and J. L. Skinner, J. Chem. Phys. **133**, 244504 (2010); erratum J. Chem. Phys. **134**, 099901 (2011).
8. Following the motions of water molecules in aqueous solutions, J. L. Skinner, Science **328**, 985 (2010).
9. Vibrational energy relaxation of small molecules and ions in liquids, J. L. Skinner, Theor. Chem. Acc. **128**, 147 (2011).
10. Vibrational coupling and hydrogen bonding at the water surface revealed by isotopic dilution spectroscopy, I. V. Stiopkin, C. Weeraman, P. A. Pieniazek, J. L. Skinner, and A. V. Benderskii, Nature (in press).
11. Collective hydrogen bond reorganization in water studied with temperature-dependent ultrafast infrared spectroscopy, R. A. Nicodemus, S. A. Corcelli, J. L. Skinner, and A. Tokmakoff, J. Phys. Chem. (in press).
12. Surface of liquid water: Three-body interactions and vibrational sum-frequency spectroscopy, P. A. Pieniazek, C. J. Tainter, and J. L. Skinner, J. Am. Chem. Soc. (submitted).
13. Robust three-body water simulation model, C. J. Tainter, P. A. Pieniazek, Y.-S. Lin, and J. L. Skinner, J. Chem. Phys. (in press).
14. Interpretation of the water surface vibrational sum-frequency spectrum, P. A. Pieniazek, C. J. Tainter, and J. L. Skinner, J. Chem. Phys. (submitted).
15. Vibrational spectroscopy of water in hydrated lipid multi-bilayers. I. FTIR spectra and ultrafast pump-probe observables, S. M Gruenbaum and J. L. Skinner, J. Chem. Phys. (submitted).
16. Vibrational spectroscopy of water at interfaces, J. L. Skinner, P.A. Pieniazek, and S. M. Gruenbaum, Accounts of Chemical Research (submitted).

Generation, Detection and Characterization of Gas-Phase Transition Metal Containing Molecules

Timothy C. Steimle
Department of Chemistry and Biochemistry
Arizona State University
Tempe, Arizona 85287-1604
E-mail: tsteimle@asu.edu

I. Program Scope

Experimental determination of the properties of small transition metal (TM) containing molecules is the objective of this project. These radical molecules represent bound regions of the complex potential energy surface used to describe metal activation chemistries. Geometric and electronic structure for both ground and low-lying excited states are determined from the analysis of high resolution electronic spectra. The sensitivity required for probing these ephemeral molecules is realized by use of laser induced fluorescence (LIF) detection. The high spectral resolution garnered from molecular beam generation assures extraction of the maximum information content. The determined properties include electronic state energies, bond lengths and angles, vibrational frequencies, permanent electric dipole moments, $\vec{\mu}_{el}$, magnetic dipole moments, $\vec{\mu}_{m}$, magnetic hyperfine interactions and radiative lifetimes. The $\vec{\mu}_{el}$ and $\vec{\mu}_{m}$ values are derived from the analysis of the spectral shifts and splittings induced by the application of either an external static electric (i.e. Stark effect) or magnetic (i.e. Zeeman effect) field. $\vec{\mu}_{el}$ gives insight into the polarity of the chemical bonds and $\vec{\mu}_{m}$ into the number of unpaired electrons. A knowledge of $\vec{\mu}_{el}$ and $\vec{\mu}_{m}$ is essential for developing schemes for kinetic energy manipulation (i.e. trapping) and enters into the description of numerous physical phenomena. The spatial distribution and nature of the chemically relevant valence electrons is garnered from analysis of the magnetic hyperfine interactions. Electronic state energies, bond lengths and angles, vibrational frequencies, and $\vec{\mu}_{el}$ values are routinely predicted and a comparison of our measured values with predictions is the most efficient method of assessing the reliability of numerous computational methodologies being developed to model TM chemistry. The established synergism between experiments and theory for these simple molecules guides computations, particularly those based on density functional theory, for more extended chemical systems (e.g. clusters, nanoparticles and surfaces).

II. Recent progress

A. Gas-Phase Metal Dioxides: TiO_2, ZrO_2, HfO_2 and NiO_2

Although of considerable interest as models for catalysis, gas-phase transition metal dioxides are very poorly characterized [Gong, Y.; Zhou, Andrews, L. *Chem.Rev*.(2009), 109, 6765)]. During this funding period we recorded and analyzed the $\tilde{A}^1B_2 \leftarrow \tilde{X}^1A_1$ band system of TiO_2 (publications # 1 and 7) generated in a supersonic expansion of laser ablated titanium with an Ar/O_2 mixture. Our experience with TiO_2 has identified the experimental conditions necessary for efficient production and detection of metal dioxides while at same time suppressing the production and detection of monoxides. Recently we recorder the low-resolution LIF spectra of molecules generated in the reaction of ablated

zirconium (Zr), hafnium (Hf) and nickel (Ni) with an Ar/O_2 mixture and have tentatively assigned the observed spectra to ZrO_2, HfO_2 and NiO_2. The LIF spectrum of the ablated Zr products in the 16800 cm^{-1} to 18900 cm^{-1} region is shown in Figure 1. The mass selected, resonance enhance multi-phonon ionization (MS-REMPI) spectrum, recorded in collaboration with Prof. John Maier at the University of Basel is also shown. Based upon the results for isovalent TiO_2, and a recent high-level EOM-CCSD calculation (Li, S.; Dixon, D. A.. *J. Phys. Chem. A* (2010), 114, 2665), the spectrum has been assigned to progressions in the $\tilde{A}^1B_2$ (ν_1,ν_2, ν_3)$\leftarrow \tilde{X}^1A_1$ (0,0,0) band system. Like TiO_2, the ground state of ZrO_2 has a large apex angle (108.1º) [Brugh, D. J.; Suenram, R. D.; Stevens, W. *J. Chem. Phys* (1999), 111 3526]. The observed excitation transitions wavenumbers were fit to determine the origin and harmonic frequency for the $\tilde{A}^1B_2$ state: T_E= 16308.14 cm^{-1}, ω_1=817(4)cm^{-1} ω_2=149(4) cm^{-1}, and ω_3=519(7) cm^{-1}. A comparison of the excitation spectrum for ZrO_2 (Fig.1) with that for TiO_2 reveals that strong progressions in the non-symmetric mode (e.g. $\tilde{A}^1B_2$ (0,0, ν_3) $\leftarrow \tilde{X}^1A_1$ (0,0,0)) are present in ZrO_2 but absent in TiO_2. Evidently vibronic coupling is much larger in the excited state of ZrO_2 than TiO_2.

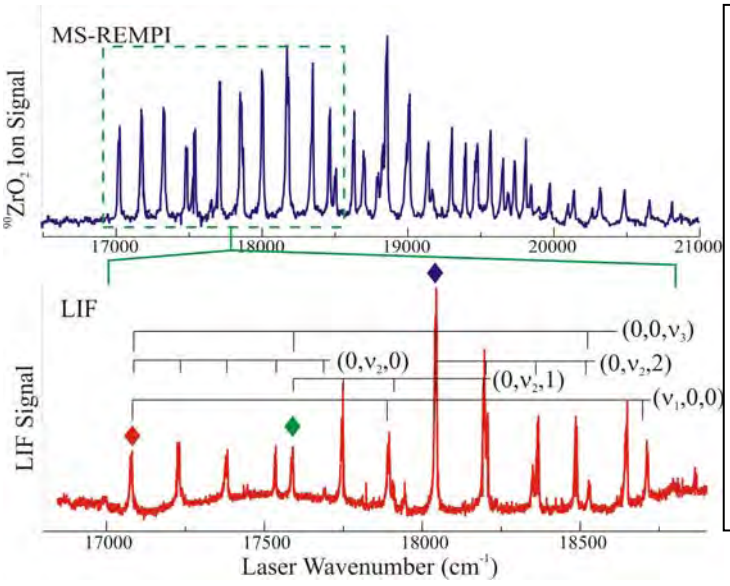

Figure 1. The low-resolution LIF and MS-REMPI spectra of the $\tilde{A}^1B_2 \leftarrow \tilde{X}^1A_1$ band system of ZrO_2. The MS–REMPI spectrum was recorded a Basel University. The appearance of strong progression in the ν_3, the non-symmetric stretch, is in sharp contrast to that observed for isovalent TiO_2 (Publ #7). Dispersed fluorescence spectra for the bands indicate by "♦" are presented in Figure 2.

Dispersed LIF resulting from excitation of three bands (marked as "♦") are shown in Figure 2. A comparison of dispersed fluorescence spectra for ZrO_2 (Fig.2) and TiO_2 reveals that, similar to the excitation spectra, strong progressions in the non-symmetric mode (e.g. $\tilde{A}^1B_2$ (0,1,0) $\rightarrow \tilde{X}^1A_1$ (0,0,3)) are present for ZrO_2 but absent for TiO_2. The observed transitions in the dispersed LIF were fit to determine the harmonic frequency for the $\tilde{X}^1A_1$ state: ω_1=898(1)cm^{-1} ω_2=287(2)cm^{-1}, and ω_3=808(3) cm^{-1}, which are in reasonable agreement with the predicted (*J. Phys. Chem. A* **109**, 11521 (2005) values of 887 cm^{-1}, 281 cm^{-1} and 835 cm^{-1}. The determined harmonic frequencies are consistent

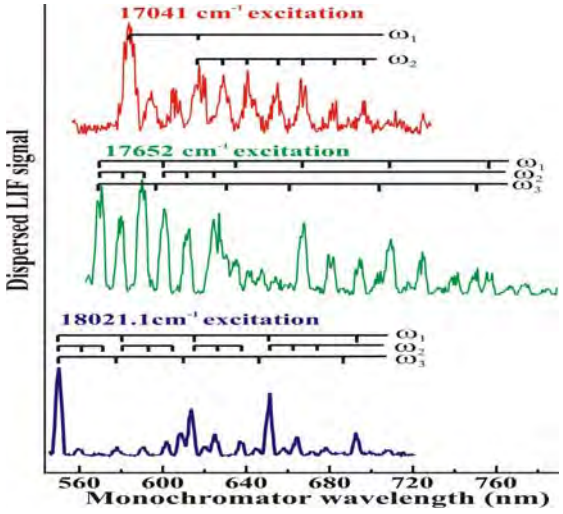

Figure 2. The $\tilde{A}^1B_2 \rightarrow \tilde{X}^1A_1$ dispersed fluorescence of the three bands indicated by "♦" observed in the excitation spectrum of ZrO_2 presented in Figure 1.

with ω_1 (=887(40) cm^{-1}) derived from the analysis of the photodetachment spectrum [Zheng, W. et al *J. Phys. Chem. A* (2005), 109(50), 1152; Mok, et al *Chem.Phys.Lett.* (2008), 458(1-3), 11] and ω_1 and ω_3 of 884.3cm^{-1} and 818. 0 cm^{-1} derived from the matrix isolation studies (Chertihin, G.V.; Andrews, L. *J. Phys. Chem.* **97**, 6356 **(**1995). We are now in the process of modeling the spectra using multi-dimensional Franck-Condon predictions. As expected, the excitation spectrum for HfO_2 exhibits similarities to those of isovalent TiO_2 and ZrO_2. High resolution LIF studies ZrO_2 and HfO_2 are underway. Spectroscopic studies of ZrO_2 and HfO_2 are more challenging due to the presence of numerous isotopes.

B. Iridium containing molecules

Iridium, one of the rarest transition metal elements in the earth's crust, is of great technological importance. It is a key component of automobile catalytic converters. Recently, there has been an intense effort to use DFT to model the mechanism and kinetics for the C-H and C-halogen activation catalyzed by newly developed Ir-complexes. Correctly modeling the properties of simple diatomic Ir-halides, such as IrF, is an essential test of the various functionals and basis sets used in these DFT predictions. During this funding period we recorded and analyzed the $A^3\Phi_4 \leftarrow X^3\Phi_4$ (1,0) band near 628.2 nm of a molecular beam of iridium monofluoride, ^{193}IrF, field free and in the presence of a static electric field. The permanent electric dipole moment, $\vec{\mu}_{el}$, for the $A^3\Phi_4$ (υ=1) and $X^3\Phi_4$ (υ=0) states were determined to be 1.88(5) D and 2.82(6) D, respectively. The most fundamental electrostatic property $\vec{\mu}_{el}$, for IrF, IrC, IrN, and CoF has now been accurately determined. The ordering of the ground state $\vec{\mu}_{el}$ values for IrC (=1.60(7) D), IrN(=1.67(7) D) [*J. Chem. Phys.* **104**, 8183(1996)], IrF(=2.82(6) D), and CoF(4.51(5)[*J. Chem. Phys.* **113**, 114315(2009)] is consistent with the difference in electronegativity (Pauling scale) of C (=2.55), N (=3.04), F (=3.98), Ir (=2.20), and Co (=1.88). The challenge for the electronic structure calculations is to quantitatively predict both ground and excited state values of $\vec{\mu}_{el}$ for this set of molecules using a consistent level of theory. We recently recorded the electronic spectrum of iridium monohydrides, IrH.

III. Future Plans

A. Metal dioxides

We have tentatively assigned low-resolution LIF spectra observed in the ablation of Hf and Ni in the presence of an O_2/Ar mixture to HfO_2 and NiO_2. High-resolution LIF

spectra of these two molecules will be recorded. An analysis of the observed rotational fine structure will be used to confirm the assignment. Optical Stark spectroscopy will be performed to extract $\vec{\mu}_{el}$. Little is known about other TM dioxides. The experimental photoelectron studies Prof. Lai-Sheng Wang (Brown University and Pacific Northwest Laboratories) of ScO_2 , VO_2 ,CrO_2, MnO_2, FeO_2, NiO_2 and CuO_2 anions demonstrate that such species are chemically stable. Unfortunately, in many cases the energy used for photodetachment was no sufficient to probe excited electronic states of the neutral. A systematic search for these species will be performed using the MS-REMPI spectrometer under construction.

B. Construction of a MS-REMPI spectrometer.

The most unambiguous assignment of an electronic transition comes from mass selected REMPI spectra such as that in Figure 1. We have intimated the construction of a REMPI spectrometer similar to that of Prof. John Maier (U. of Basel). The primary purpose is for identification of bands that will be examined at high resolution via LIF. Accordingly, a relatively low spectral resolution pulsed dye laser system will be used for the resonant excitation. The F_2 ionization laser that will be used has a photon energy of 6.36 eV and the dye laser produce photon energies up to 3.0 eV giving a combined maximum energy of 9.36 eV, which more than sufficient to ionization most metal containing molecules. For example the adiabatic ionization potentials of TiO, ZrO, NbO, and MoO have been determined to be 6.8197(7) eV, 6.812(2) eV, 7.154(1) eV, and 7.4504(5) eV, respectively.

Publications of DOE sponsored research - 2008-present:

1. "Characterization of the $X^1A_1 - A^1B_2$ electronic state of titanium dioxide, TiO_2" Hailing Wang, T. C. Steimle, C. Apetrei and J. P. Maier, Phys. Chem. Chem. Phys. **11** 2649-2656 (2009).
2. "The Permanent Electric Dipole Moments and Magnetic ge-Factors of Praseodymium Monoxide (PrO)" Hailing Wang, Colan Linton Tongmei Ma, and Timothy C. Steimle Journal of Physical Chemistry A (2009), 113(47), 13372-13378.
3. "Permanent Electric Dipole Moment of Cerium Monoxide." Colan Linton, Jinhai Chen Timothy C. Steimle Journal of Physical Chemistry A (2009), 113(47) 13379-13382.
4. "The permanent electric dipole moment of vanadium monosulfide" Xiujuan Zhuang and Timothy C. Steimle Journal of Chemical Physics (2010), 132(23), 234304/1-234304.
5. "Permanent electric dipole moment of copper monoxide, CuO" Xiujuan Zhuang, Sarah E. Frey and Timothy C. Steimle, Journal of Chemical Physics (2010), 132(23), 234312/1-234312/6.
6. "Visible Spectrum of Titanium Dioxide" Xiujuan Zhuang, Anh Le, Timothy C. Steimle Ramya Nagarajan, Varun Gupta and John P. Maier Phys. Chem. Chem. Phys. (2010), 12(45), 15018-15028.
7. "The permanent electric dipole moment in iridium monofluoride " Xiujuan Zhuang Colan Linton and Timothy C. Steimle J. Chem. Phys. (2010), 133(16), 164310/1-164310/6

A Single-Molecule Approach for Understanding and Utilizing Surface and Subsurface Adsorption to Control Chemical Reactivity and Selectivity

E. Charles H. Sykes (charles.sykes@tufts.edu)
Department of Chemistry, Tufts University, 62 Talbot Ave, Medford, MA 02155

The first year research has been focused in two main areas: 1) single palladium atom surface chemistry[1] and 2) cobalt nanoparticle growth. These well-defined Pd and Co systems are being designed so as to be amenable to high resolution scanning probe studies, X-ray photoelectron spectroscopy, and chemical analysis of adsorbate binding, diffusion and reaction. Thioether and phosphine adsorption has also been studied on metals in an effort to understand their self-assembly and lay a base for chirally modified versions of these molecules to be used for enantioselective hydrogenation chemistry.[2-4] In terms of equipment, a state of the art temperature programmed reaction system has just come on line and will be used in years two-four to study the activity and selectivity of hydrogenation reactions on these model systems. This approach will allow atomic scale alloy arrangement and adsorbate binding to be directly related to chemical reactivity.

Atomic-scale Palladium Alloy Surface Structure

Palladium and its alloys play a central role in a wide variety of industrially-important applications such as hydrogen reactions, separations, storage devices, and fuel cell components. Alloy compositions are very complex as they are often heterogeneous at the atomic-scale and the exact mechanisms by which many of these processes operate have yet to be discovered. The two alloy systems of most relevance to this project are Pd/Cu(111) and Pd/Au(111).[5,6] Pd/Cu alloys are an important class of materials used for hydrogen purification membranes, and also serve as the active metals in many heterogeneous catalysts. The choice of supporting metal allowed the study of Pd particles as a function of size; from individual atoms in and under the surface to islands >30 nm in diameter.

We have shown that ultra high vacuum surface preparation methods can be used to yield a range of Pd-based surface and subsurface alloys.[5] High-resolution STM allowed us to interrogate the atomic-scale geometry of these alloys and crucially revealed that for both Cu and Au substrate metals, Pd tends to surround itself with host metal atoms and bury itself in subsurface sites. This can be rationalized in the case of Pd/Cu (figure 1) by steric repulsion of nearest neighbor Pd atoms as well as Pd's higher surface free energy and the formation of stronger hetero-element bonds in both cases.

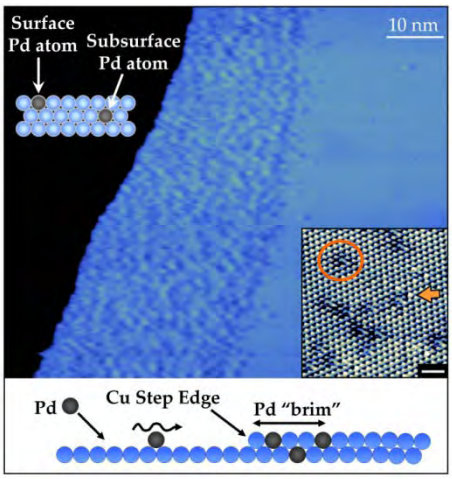

Figure 1. *STM images and schematics of the Pd/Cu(111) alloy. The schematic at the bottom shows the mechanism for Pd alloying into ascending step edges via place exchange to form a Pd-rich brim. The large STM image of an alloy prepared at 435 K shows a Pd-rich brim on a Cu step edge. Imaging conditions: -0.4 V, 0.5 nA, 80 K. The atomically-resolved STM image inset of a Pd/Cu alloy prepared at 460 K shows a Cu(111) lattice with subsurface (circle) and surface (arrow) Pd atoms. Imaging conditions: 0.04 V, 1 nA, 80 K, scale bar = 1 nm. The schematic in the upper left hand corner shows a side-view of the alloy.*

Depending on surface temperature during the alloying procedure a range of metastable states of Pd can be formed including Pd atoms in the surface layer and Pd islands on Au(111) (figure 2). These well-defined systems allowed us to interrogate the active sites for H_2 dissociation. We discovered that individual, isolated Pd atoms were active for the dissociation and spillover of H atoms onto Cu but not Au.[1,6] This can be understood by the thermodynamic stability of H atoms on Cu(111) but not Au(111). In order to get significant uptake of H on Pd/Au, larger ensembles of Pd were required. We found that major restructuring of the Pd/Au system occurred after exposure to H that could be explained by strong Pd-H bonds reversing Pd's tendency to segregate into the bulk. We discovered a previously unreported form of PdH in regularly-spaced rows that we postulate form via H-induced ejection of Pd atoms from the surface. This work reveals some of the rich structural diversity of bimetallic alloys that occurs in the presence of reactants and raises the question of how these atomic-scale structures affect hydrogenation chemistry. These will be the next focus areas for the project.

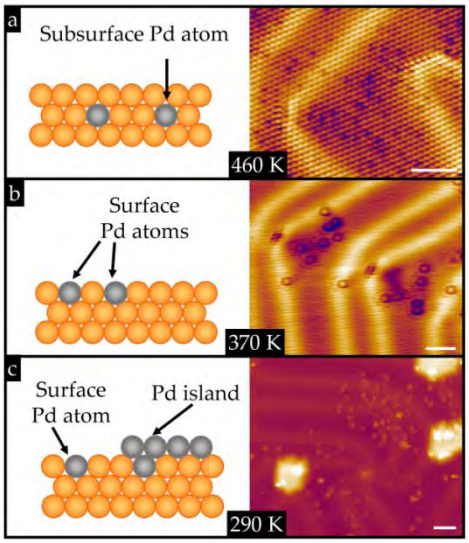

Figure 2. *STM images and corresponding side-view schematics of the deposition temperature dependence on Pd/Au alloy composition. A) Pd alloying occurs in the subsurface region of the Au(111) (atomic resolution) when the sample temperature is 460 K. Imaging conditions: -0.3 V, 2 nA, 7 K. B) Atomically-resolved surface Pd is seen near edge dislocations after a deposition at 370 K. Imaging conditions: -0.5 V, 1 nA, 5 K. C) Surface Pd and Pd-rich islands are present after Pd is deposited at 290 K. Imaging conditions: 0.3 V, 0.3 nA, 80 K. All scale bars = 2 nm.*

Cobalt Nanoparticle Surface Chemistry

Fischer-Tropsch synthesis (FTS) involves the formation of hydrocarbons via the catalytic conversion of syngas (CO and H), which can be derived from biomass, and is itself a renewable energy resource. Currently, it accounts for the production of 200,000 barrels per day of synthetic fuel. This strategic, heterogeneous catalytic process is usually performed using cobalt-based catalysts that are greatly affected by the adsorption state of reactants, as well as nanoparticle shape and size. Previously, there has been very little surface science research on cobalt model catalysts because of difficulties in preparing atomically clean surfaces. We have utilized a new method for preparing model cobalt catalysts by depositing cobalt onto copper single crystals (an inert metal for FTS), yielding well-defined cobalt nanoparticles. Using ultra high vacuum, low-temperature scanning tunneling microscopy we have studied these model nanoparticles and the interaction of syngas with their surfaces on the molecular scale.

We have shown for the first time that the two adsorbates segregate on the cobalt surfaces at 80 K, and we propose that atomic H blocks CO adsorption, preventing complete overlayer formation and causing the build-up of CO at the cobalt nanoparticle step edges. Figure 3 shows that CO and H atoms form phase separated domains on cobalt multilayer islands. This reveals that the available interface for reaction between the two adsorbed reactants will strongly depends on cobalt particle size. In other words the FT

reactivity must be subject to unforeseen kinetic restraints as a function of particle size. This phenomenon is still under investigation in our labs. In addition we are studying the effect of H in its different forms on CO dissociation, a crucial step in FT synthesis.

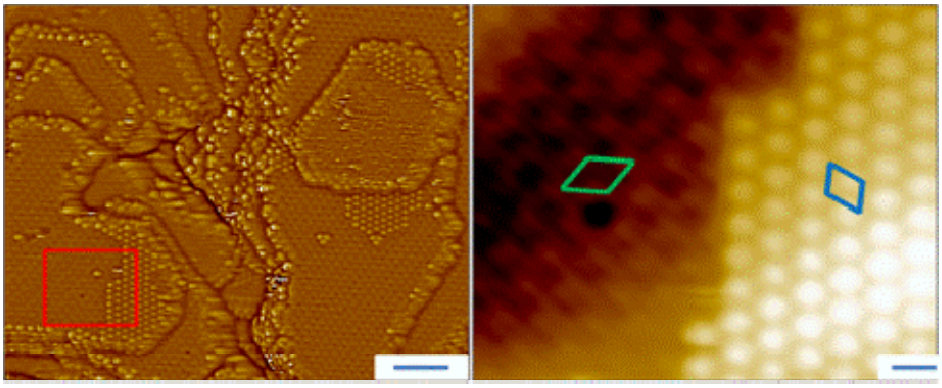

Figure 3. *(a) CO (0.1 ML) and H_2 (0.9 ML) co-adsorbed on cobalt islands deposited on Cu(111). H adatoms occupy predominately cobalt island terraces while the majority of the CO molecules segregate at the step edges. Detailed investigation of high resolution images shows that terrace CO develops around defects present on the surface of the islands. (Imaging conditions: 100 pA, 100 mV, scale bar 3 nm).* ***(b)*** *High-resolution image of the area marked in red. The H 2x2 unit cell is highlighted by a green parallelogram and the CO √3x√3 R30° unit cell appears in blue color (Imaging conditions: Sample temperature = 80 K, 100 pA, 100 mV, scale bar 0.5 nm).*

Our findings reveal that increased CO coverage, results in a disordered CO phase and in a two-dimensional phase compression of H (figure 4). To the best of our knowledge this is *the first direct nanoscale* demonstration of this long proposed phenomenon in a *catalytically relevant* system. The effect is understood by a spillover mechanism in which the CO, that is physisorbed on the copper surface, migrates to the reactive cobalt nanoparticles. This spillover of CO causes H atoms and CO molecules to compete for cobalt surface adsorption sites and ultimately leads to a H phase compression. We are further investigating this effect by means of both theory (Talat Rahman) and experiment (Charles Sykes).

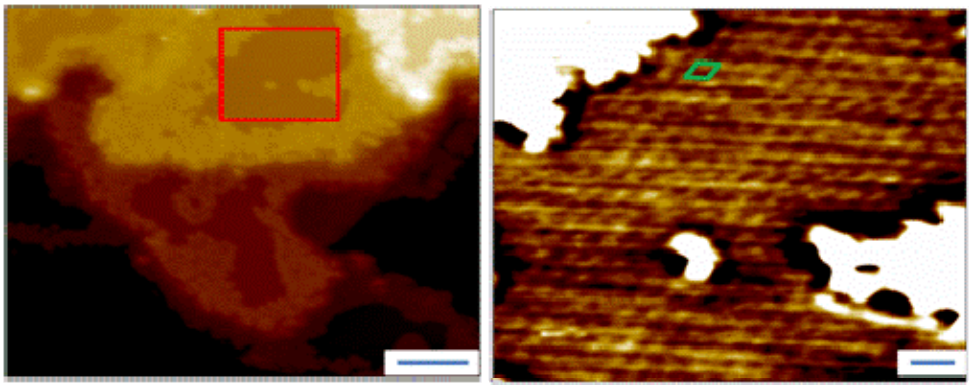

Figure 4. (a) *The H- and CO-covered Co/Cu(111) sample has been further exposed to 121 L of CO at 80 K. CO still resides at the cobalt island step-edges; however, the √3x√3R30° unit cell has compressed, and the CO is entirely disordered. (Imaging conditions: 200 pA, 200 mV, scale bar 3 nm). (b) Zoom of red marked area of figure 3(a) showing that the H-phase has been compressed to a 1x1 unit cell. This observation supports a CO spillover mechanism (unit cell indicated by green box). (Imaging conditions: Sample temperature = 80 K, 500 pA, 100 mV, scale bar 0.5 nm)*

New Ultra high Vacuum system for Temperature Programmed Desorption studies

A new ultra high vacuum system (shown below) for Auger Electron Spectroscopy (AES), Low Energy Electron Diffraction (LEED) and Temperature Programmed Reaction (TPR) has very recently been installed in the Sykes lab. The system includes facilities for sample cleaning via a cold cathode ion source and metal deposition via an electron-beam evaporator. This instrument allows the sample temperature to be controlled between 100 and 1200 K. A Hiden 3F 300AMU mass spectrometer is mounted so as to approach within ~1mm of the sample face and a feedback-controlled power supply offers linear heating ramps for high-quality TPR spectra. The instrument is currently used to investigate the effect of surface and subsurface in hydrogenation reactions on Cu/Pd and Au/Pd alloy surfaces.

References:

1) "An Atomic-scale View of Palladium Alloys and their Ability to Dissociate Molecular Hydrogen" A. E. Baber, H. L. Tierney, T. J. Lawton and E. C. H. Sykes - *ChemCatChem* **2011**, *3*, 607-614

2) "Gently Lifting Gold's Herringbone Reconstruction: Trimethylphosphine on Au(111)" A. D. Jewell, H. L. Tierney and E. C. H. Sykes - *Physical Review B* **2010**, *82*, 205401

3) "Dynamics of Molecular Adsorption at Non-Equilibrium Sites" H. L. Tierney, A. D. Jewell, A. E. Baber, E. V. Iski and E. C. H. Sykes *Langmuir* **2010**, *26*, 15350-15355

4) "Adsorption, Assembly, and Dynamics of Dibutyl Sulfide on Au{111}" D. O. Bellisario, A. D. Jewell, H. L. Tierney, A. E. Baber and E. C. H. Sykes *Journal of Physical Chemistry C* **2010**, *114*, 14583-14589

5) "Atomic-Scale Geometry and Electronic Structure of Catalytically Important Pd/Au Alloys" A. E. Baber, H. L. Tierney and E. C. H. Sykes *ACS Nano* **2010**, 4, 1637-1645.

6) "Hydrogen Dissociation and Spillover on Individual Isolated Palladium Atoms" H. L. Tierney, A. E. Baber, J. R. Kitchin and E. C. H. Sykes *Physical Review Letters* **2009**, 103, 2461021-2461024.

Understanding Nanoscale Confinement Effects in Solvent-Driven Chemical Reactions

Ward H. Thompson
Department of Chemistry, University of Kansas, Lawrence, KS 66045
Email: *wthompson@ku.edu*

Program Scope

It is now possible to synthesize nanostructured porous materials with a tremendous variety of properties including sol-gels, zeolites, organic and inorganic supramolecular assemblies, reverse micelles, vesicles, and even proteins. The interest in these materials derives from their potential for carrying out useful chemistry (*e.g.*, as microporous and mesoporous catalysts with critical specificity, fuel cell electrodes and membranes, molecular sieves, and chemical sensors) and for understanding the chemistry in similar systems found in nature. Despite the advances in synthetic techniques, our understanding of chemistry in solvents confined in nanoscale cavities and pores is still relatively limited. Ultimately, one would like to design nanostructured materials adapted for specific chemical purposes, *e.g.*, catalysis or sensing, by controlling the cavity/pore size, geometry, and surface chemistry. To develop guidelines for this design, we must first understand how the characteristics of the confining framework affect the chemistry. Thus, the overarching question addressed by our work is *How does a chemical reaction occur differently in a nano-confined solvent than in a bulk solvent?*

Solvent-driven reactions, typically those involving charge transfer, should be most affected by confinement of the solvent. The limited number of solvent molecules, geometric constraints of the nanoscale confinement, and solvent-wall interactions can have dramatic effects on both the reaction energetics and dynamics. Our primary focus is thus on proton transfer, time-dependent fluorescence, and other processes strongly influenced by the solvent. A fundamental understanding of such solvent-driven processes in nano-confined solvents will impact many areas of chemistry and biology. The diversity among nanoscale cavities and pores (*e.g.*, in their size, shape, flexibility, and interactions with the solvent and/or reactants) makes it difficult to translate studies of one system into predictions for another.[1] Thus, we are focusing on developing a unified understanding of chemical dynamics in the diverse set of confinement frameworks, including nanoscale silica pores of varying surface chemistry.[2,3]

Recent Progress & Future Plans

Solvation Dynamics in Nanoconfined Solvents.

Solvation dynamics in nanoconfined solvents are generally marked by dramatic changes relative to the corresponding bulk solvent. In particular, long time scales not seen in the bulk solvent – often as long as hundreds of picoseconds or several nanoseconds – are observed in the time-dependent fluorescence signal. A number of models have been proposed to explain the origin of this multi-exponential, long-time decay. However, to this point these models have been derived from simulations using atomic or diatomic model dye molecules and/or simplistic confining frameworks. Thus, a direct comparison of theoretical predictions with experimental measurements is lacking as

is, by extension, a rigorous test of the models.[1] We are taking two approaches to address this issue.

First, we are carrying out simulations of the time-dependent fluorescence confined within ~ 2.4 diameter hydrophilic and hydrophobic amorphous silica pores,[2,3] beginning with the C153 dye molecule, based on a model developed by Maroncelli and co-workers,[4] in ethanol. This system is similar to those used in measurements by Baummann *et al.* on C153 in ethanol confined within 2.5 and 5.0 nm sol-gel pores.[5] Our simulations to this point do show significantly longer solvation dynamics compared to the bulk liquid, but improved statistical sampling is required due to the heterogeneous environment and large planar structure of the C153 model and those simulations are in progress.

Second, we have developed alternative models for both the dye molecule and the confining framework. These models are designed to allow for more general exploration of the phenomena and driving forces involved in TDF experiments in nanoconfined solvents. Specifically, we are investigating four models based on two dye and two pore representations. For the dye, these are the atomistic C153 force-field of Maroncelli and co-workers,[4] and a Stockmayer-type model which consists of a single Lennard-Jones site in which a dipole is embedded (both the size of the sphere and the magnitude of the dipole can be varied). For the pore, these are the atomistic silica pore models we have previously developed[2,3] and atomistic, but smooth cylindrical pores. In both cases the radii and surface interactions can be modulated to examine the driving forces for different phenomena. Together these four models, one of which is that described in the first approach above, allow us to examine the effects of dye size and shape, pore roughness, surface chemistry, pore heterogeneity, and symmetry.

For the Stockmayer-type solute in atomistic silica pores, we have calculations of the free energy, using thermodynamics integration, as a function of solute position for different solute dipole moments. We are in the process of understanding the molecular origins of the features of these free energy curves based on solvent densities and decomposition of the forces involved. In addition to providing a first look at the free energy landscapes relevant to TDF measurements, these calculations will further give us insight into entropic contributions.[6]

A number of open questions remain regarding solvation dynamics in nanoconfined solvents. For example, we are continuing to investigate these systems as potential examples of linear response violations.[7,8] While simple, model confining frameworks exhibit TDF that is well approximated by equilibrium correlation functions,[8] it is not clear that the same will be true for realistic systems, *e.g.*, silica pores, and we plan to examine that.

Proton Transfer (PT).

We have been continuing our work on proton transfer reactions in nanoconfined solvents[1,9–12] by investigating approaches to more generally sample the reaction coordinate, both to identify transition state configurations and simulate infrared spectra. Specifically, we have used an umbrella sampling approach based on the proton vibrational energy gap. This exploits the fact that for a PT reaction the energy gap between the vibrational ground and excited states of the transferring proton reaches a minimum at the transition state. We have implemented this umbrella sampling within mixed quantum-classical simulations to identify the transition state configurations and explore the reaction free energy curve and vibrationally nonadiabatic coupling. We have tested this approach on a model phenol-amine proton transfer reaction complex in a solvent confined within

a hydrophobic nanoscale cavity (and a manuscript is currently in preparation). The results from sampling according to the vibrational energy gap are consistent with those obtained from previous umbrella sampling calculations based on a collective solvent coordinate.[12] This sampling approach further provides insight into the vibrationally nonadiabatic coupling for the proton transfer reaction. Specifically, the coupling is found to be directly correlated to the vibrational energy gap, depending on the inverse square of this gap . It also has potential in the simulation of vibrational spectra of PT reaction complexes in solution. We previously showed that the vibrational spectrum of a PT system can, in the slow exchange limit, be expressed in terms of the reaction equilibrium constant and equilibrium properties of the reactants and products.[11] This sampling approach provides a direct and efficient way to calculate these quantities; the standard method for calculating the spectrum would involve extremely long trajectories that exhibit multiple crossings from reactants to products.

The free energy curves we are calculating for realistic dye molecules in confined solvents will provide insight into the position-dependent properties of PT reaction complexes as well. One connection we are pursuing is the use of Smoluchowski equation models,[13,14] developed from the calculated free energy curves, for describing PT reaction dynamics. This should allow for rapid exploration of the effects of confining framework properties on PT reaction rate constants and spectroscopic observables.

Reorientational Dynamics of Nanoconfined Hydrogen-bonded Liquids.

Both solvation dynamics and proton transfer reactions are governed by the reorientational motion of the solvent molecules. Thus, it is important to understand how liquid molecules rotate when confined within nanoscale frameworks. We have examined this question by examining the reorientational dynamics of water, methanol, and ethanol in identical model silica pores. We have collaborated with Damien Laage, École Normale Supérieure in Paris, who has studied water reorientation extensively, in this work. Using the equilibrium densities obtained from grand canonical Monte Carlo calculations, we have carried out molecular dynamics simulations for these three liquids in nanoscale silica pores of diameter $\sim$ 2.4 nm and varying surface chemistry (hydrophilic and hydrophobic). The results are generally expressed in terms of a reorientational correlation function, $C_2(t) = \langle P_2[\mathbf{e}(t) \cdot \mathbf{e}(t)]\rangle$ with $\mathbf{e}$ the OH unit vector, which provides a measure of the rotational times of the OH bonds in the liquid. A particularly interesting result for these systems is that the long-time decay of $C_2(t)$ for water confined in hydrophilic pores appears to follow a power law, *i.e.*, $C_2(t) \sim (t/\tau)^{\alpha}$. This is related to the hydrophilic surface chemistry since when the pore charges are "turned off," this long-time decay vanishes. In methanol and ethanol, the long-time decay does not show the same time-dependence, but rather follows a stretched-exponential decay, $C_2(t) \sim \exp(-(t/\tau)^{\beta})$, a feature that does *not* disappear when the pore charges are turned off. These results point to the differences in the fundamental reorientational dynamics of water and alcohols, suggesting that the methyl groups in the alcohols introduce steric effects that can alter the qualitative nature of the reorientation.

This idea has led us to consider the origin of the differences in reorientational times in the bulk liquids water, methanol, and ethanol, which are found to be 2.5, 5, and 15 ps, respectively, in MD simulations (in reasonable agreement with experimental measurements). Our initial hypothesis is that the slowdown is due to the greater excluded volume as the hydrocarbon moiety in the alcohol

increases in size. This is based on the molecular jump mechanism,[15] which predicts that the OH reorientation is governed by the switching of hydrogen bonding partners, which cannot take place when volume is excluded by a hydrophobic group.[16] Our studies indicate that this is at least a significant part of the story and we are currently preparing a manuscript on this subject.

There are a number of issues we are continuing to explore in the reorientational dynamics of bulk and nanoconfined hydrogen-bonding liquids. These range from the rotational dynamics of longer-chain chain alcohols in their bulk liquids to the effect of confining geometry, surface chemistry, and pore roughness on the reorientation of liquid molecules in confining frameworks.

References

[1] †W.H. Thompson, *Annu. Rev. Phys. Chem.* **62**, 599-619 (2011). "Solvation Dynamics and Proton Transfer in Nanoconfined Liquids"

[2] T.S. Gulmen and W.H. Thompson, in *Dynamics in Small Confining Systems VIII*, edited by J.T. Fourkas, P. Levitz, R. Overney, M. Urbakh (Mater. Res. Soc. Symp. Proc. **899E**, Warrendale, PA, 2005), 0899-N06-05.

[3] T.S. Gulmen and W.H. Thompson, *Langmuir* **22**, 10919-10923 (2006).

[4] N. Kometani, S. Arzhantsev, and M. Maroncelli, *J. Phys. Chem. A* **110**, 3405-3413 (2006).

[5] R. Baumann, C. Ferrante, E. Kneuper, F.-W. Deeg, and C. Bräuchle, *J. Phys. Chem. A* **107**, 2422-2430 (2003).

[6] K.R. Mitchell-Koch and W.H. Thompson, *J. Phys. Chem. C* **111**, 11991-12001 (2007).

[7] B.B. Laird and W.H. Thompson, *J. Chem. Phys.* **126**, 211104 (2007).

[8] B.B. Laird and W.H. Thompson, *J. Chem. Phys.* (submitted). "Time-Dependent Fluorescence in Nanoconfined Solvents: Linear Response Approximations and Gaussian Statistics"

[9] S. Li and W.H. Thompson, *J. Phys. Chem. B* **109**, 4941-4946 (2005).

[10] W.H. Thompson, *J. Phys. Chem. B* **109**, 18201-18208 (2005).

[11] K.R. Mitchell-Koch and W.H. Thompson, *J. Phys. Chem. B* **112**, 7448-7459 (2008).

[12] †B.J. Ka and W.H. Thompson, *J. Phys. Chem. B* **114**, 7535-7542 (2010). "Nonadiabatic Effects on Proton Transfer Rate Constants in a Nanoconfined Solvent"

[13] X. Feng and W.H. Thompson, *J. Phys. Chem. C* **111**, 18060-18072 (2007).

[14] †X. Feng and W.H. Thompson, *J. Phys. Chem. C* **114**, 4279-4290 (2010). "Time-dependent Fluorescence in Nanoconfined Solvents. A Smoluchowski Equation Model Study"

[15] D. Laage and J.T. Hynes, *Science* **311**, 832-835 (2006).

[16] D. Laage, G. Stirnemann, and J.T. Hynes, *J. Phys. Chem. B* **113**, 2428-2435 (2009).

†DOE-sponsored publication 2009-present.

Structural Dynamics in Complex Liquids Studied with Multidimensional Vibrational Spectroscopy

Andrei Tokmakoff

Department of Chemistry, Massachusetts Institute of Technology, Cambridge, MA 02139
E-mail: tokmakof@MIT.edu

Water is a unique liquid due to the fact that it can form up to four hydrogen bonds, creating a structured tetrahedral network of molecules that evolves on ultrafast time-scales as hydrogen bonds interconvert. It is the fluctuations of this network that allow water to rapidly solvate nascent charge and to participate in chemical reactions. Moreover, it is predicted that the breakage and rearrangement of hydrogen bonds plays a major role in charge transport in water and is an intrinsic element of proton and hydroxide transport. The goal of our research is to develop ultrafast spectroscopic probes of the hydrogen bonding network of water and to use these probes to obtain a mechanistic understanding of how water dynamics influence aqueous charge transport and reactivity.

We use of ultrafast two-dimensional infrared spectroscopy (2D IR) of the OH stretch of a solution of dilute HOD in D_2O and of the OD stretch of dilute HOD in H_2O to probe the structure of water. These isotopic combinations are well suited for studies investigating the fluctuations of the hydrogen bonding network of water since the OH (or OD) absorption lineshape is broadened due to distribution of hydrogen bonding environments present in the liquid. Molecules that participate in strong hydrogen bonds absorb at lower frequencies than molecules in strained or broken hydrogen bonds. Thus, if we excite a water molecule at an initial frequency and follow the frequency in time we gain direct information on the time dependent structure. 2D IR spectroscopy provides the ability to track how different hydrogen bonding environments interconvert over time. A 2D spectrum correlates how a molecule excited at an initial frequency evolves to a final frequency after a given waiting time. By varying the waiting time, we can follow how molecules initially in strong or weak hydrogen bonds exchange environments.

Our work during the past year can be divided into three topics: (1) Reorientational dynamics of hydrogen bonds in water, (2) Temperature-dependent hydrogen bond dynamics in water, and (3) the dynamics of aqueous hydroxide ion transport in water.

Our previous work has suggested that hydrogen bonds in water rearrange in concerted switching events that include large angle excursions in hydrogen bond alignment and a transition state that has bifurcated hydrogen bond character. To test the predictions of the orientational dynamics during switching we are performing polarization sensitive nonlinear experiments. We have recently measured 2D IR spectra of HOD in H_2O/D_2O in different polarization geometries to determine the two dimensional anisotropy. This measurement is analogous to the anisotropy decay from 1D pump-probe techniques that report on the reorientation of molecules as a function of time. In pump-probe measurements, we find a 70 fs decay from inertial librations, or hindered rotations, and a 2.5 ps decay from collective reorientation. There is a probe-frequency dependent decay in pump-probe anisotropy, with larger amplitude sub-100 fs decay at higher probe frequencies, suggesting that molecules in weaker hydrogen bonds sample a wider range of angles during the inertial part of reorientation compared to molecules in more constrained, strongly hydrogen bonded configurations. The advantage of measuring 2D anisotropy over 1D is the ability to correlate both the initial and final frequencies with the degree of rotation of the HOD molecule. Thus, we can determine if a molecule initially at high frequency (weak hydrogen bonding) that moves to lower frequency (strong hydrogen bonding) undergoes a different degree of reorientation than a molecule that remains on either side of the lineshape. Preliminary results of 2D IR anisotropy of HOD in D_2O suggests that molecules initially in strained or broken

hydrogen bonds undergo ~ 15° rotation within 250 fs whereas molecules that remain in strong hydrogen bonds retain memory of their initial orientation but lose this memory if they move toward high frequency. These results are qualitatively similar to those obtained from molecular dynamics simulations and support the conclusion that the exchange of molecules from one side of the OH lineshape to the other involves molecular reorientation. At waiting times on the order of spectral diffusion timescales (~1 ps), we observe a frequency-independent uniform decay in anisotropy across the lineshape, since the OH stretch loses memory of its initial frequency.

In addition, our studies of concerted hydrogen bond rearrangements make certain predictions about the temperature-dependence of hydrogen bond rearrangement dynamics in the liquid. We have performed temperature-dependent experiments on HOD in H_2O to investigate these dynamics: 2D IR lineshape measurements of the OD frequency dynamics, pump-probe anisotropy measurements of reorientational motions, and magic angle pump-probe measurements of vibrational lifetime. The time scale for hydrogen bond rearrangement, found by the decay of the phase line slope in a 2D IR waiting time series, decreases from roughly 2 ps at 278 K to 0.5 ps at 345 K and we find the barrier to dephasing to be $E_{a,\omega} = 3.4 \pm 0.5$ kcal/mol. The spectrally dispersed pump-probe anisotropy decay decreases from 6.8 ps at 278 K to 2.6 fs at 345 K and appears to be non-Arrhenius. The trend is somewhat more linear for temperatures less than 323 K and a fit gives the barrier $E_{a,rot} = 4.0$ kcal/mol. The similar barrier height indicates that the mechanism of vibrational dephasing, reorientational motion, and hydrogen bond rearrangement are all strongly correlated. Finally, we find a similar vibrational lifetime for temperatures at and below room temperature but a slight increase at higher temperatures. This suggests the relaxation pathway may not simply be through the fundamental of the HOD bend as previously suggested. We are currently performing a self-consistent analysis of all experiments to unravel the underlying dynamics

Over the course of the last year, we have also performed studies to reveal how water participates in the dynamics of hydroxide ion transport. This ion undergoes anomalously fast diffusion due to the ability to accept a proton from neighboring water molecules leading to the translocation of the ion. Simulations have suggested that hydrogen bond rearrangements play a strong role in guiding proton transfer processes involving these ions. However, experimental work that is able to directly capture proton motion is lacking due in large part to the difficulty of finding probes that can measure the timescales predicted for the transfer, which range from tens of femtoseconds to picoseconds.

We measured 2D IR surfaces of solutions of dilute HOD in concentrated NaOD: D_2O solution. Upon the addition of NaOD to HOD:D_2O solution, two new spectral features appear in a linear FTIR spectrum – a new peak at high frequency due to the OH^- stretch and a broad shoulder that extends to very low frequency due to HOD molecules hydrogen bonded to OD^- ions. Pump probe measurements in the OH stretch region find that as the NaOD concentration increases, a second vibrational relaxation component appears with an extremely fast timescale of 115 fs. Interestingly, the a large off-diagonal intensity is observed on the low frequency side of the 2D IR lineshape that disappears on a ~100 fs timescale, matching the fast decay timescale observed in the pump probe measurements. For better understanding of this feature, we modeled our experiments using an EVB (empirical valence bond) molecular dynamics simulation model of aqueous sodium hydroxide developed by Todd Martinez's group at Stanford University. In order to calculate spectra, we have developed a DFT based electrostatic frequency map which we can use to determine the "instantaneous" OH frequency of a given OH bond for a static configuration of the simulation. We find that in configurations where a proton is significantly shared between two water molecules, all of the transitions within the proton stretching potential undergo significant red shifts, and in particular the OH stretch overtone ($\nu = 2 \leftarrow \nu = 0$) tunes into our experimentally accessible bandwidth. Thus, the rapid loss of intensity in the 2D and pump probe measurements is due to direct excitation of the overtone transition for configurations corresponding to nearly shared protons. As the proton moves to one side of the complex,

stabilizing a water molecule, the overtone will blue shift out of our bandwidth, leading to the relaxation we see in the 2D and pump probe spectra.

We extended these experiments to time scales >1 ps, for which 2D IR spectra reveal chemical exchange processes between the OH^- and HOD molecules. To quantify exchange timescales, we applied a exchange kinetic model for these chemical exchange processes. The growth of these features is best reproduced when a time constant of 3 ps is used for the exchange rate between a OH^- like stretch and a HOD molecule hydrogen bonded to D_2O. This corresponds to the activated rate of deuteron transfer in these solutions.

During this year DOE support has also contributed to our work to develop structure based spectroscopic models for peptide and protein 2D IR spectroscopy, which draws from MD simulation.

DOE Supported Publications (2006-2010)

1. DeCamp, M. F.; Tokmakoff, A., Single-shot two-dimensional spectrometer. *Opt. Lett.* **2006,** *31* (1), 113-115.
2. Ganim, Z.; Tokmakoff, A., Spectral Signatures of Heterogeneous Protein Ensembles Revealed by MD Simulations of 2DIR Spectra. *Biophys. J.* **2006,** *91*, 2636-2646.
3. Loparo, J. J.; Roberts, S. T.; Tokmakoff, A., Multidimensional infrared spectroscopy of water. I. Vibrational dynamics in two-dimensional IR line shapes. *J. Chem. Phys.* **2006,** *125*, 194521.
4. Loparo, J. J.; Roberts, S. T.; Tokmakoff, A., Multidimensional infrared spectroscopy of water. II. Hydrogen bond switching dynamics. *J. Chem. Phys.* **2006,** *125*, 194522.
5. Roberts, S. T.; Loparo, J. J.; Tokmakoff, A., Characterization of spectral diffusion from two-dimensional line shapes. *J. Chem. Phys.* **2006,** *125*, 084502.
6. Loparo, J. J.; Roberts, S. T.; Tokmakoff, A., 2D IR spectroscopy of hydrogen bond switching in liquid water. In *Ultrafast Phenomena XV*, Corkum, P.; Jonas, D.; Miller, R. J. D.; Weiner, A. M., Eds. 2007; Vol. 88, pp 341-343.
7. DeCamp, M. F.; DeFlores, L. P.; Jones, K. C.; Tokmakoff, A., Single-shot two-dimensional infrared spectroscopy. *Optics Express* **2007,** *15* (1), 233-241.
8. Schmidt, J. R.; Roberts, S. T.; Loparo, J. J.; Tokmakoff, A.; Fayer, M. D.; Skinner, J. L., Are water simulation models consistent with steady-state and ultrafast vibrational spectroscopy experiments? *Chem. Phys.* **2007,** *341* (1-3), 143-157.
9. Chung, H. S.; Ganim, Z.; Jones, K. C.; Tokmakoff, A., Transient 2D IR spectroscopy of ubiquitin unfolding dynamics. *PNAS* **2007**, *104*, 14237.
10. Loparo, J. J.; Roberts, S. T.; Nicodemus, R. A.; Tokmakoff, A., Variation of the transition dipole moment across the OH stretching band of water. *Chem. Phys.* **2007,** *341* (1-3), 218-229.
11. Nicodemus, R. A.; Tokmakoff, A., Infrared spectroscopy of tritiated water. *Chem. Phys. Lett.* **2007,** *449* (1-3), 130-134.
12. Tokmakoff, A., Shining Light on the Rapidly Evolving Structure of Water. *Science* **2007,** *317* (5834), 54-55.
13. DeFlores, L. P.; Nicodemus, R. A.; Tokmakoff, A., Two-dimensional Fourier transform spectroscopy in the pump-probe geometry. *Optics Letters* **2007,** *32* (20), 2966-2968.
14. Ganim, Z.; Chung, H. S.; Smith, A. W.; DeFlores, L. P.; Jones, K. C.; Tokmakoff, A., Amide I Two-Dimensional Infrared Spectroscopy of Proteins. *Acc. Chem. Res.* **2008,**

15. Roberts, S. T.; Petersen, P. B.; Ramasesha, K.; Tokmakoff, A., The dynamics of aqueous hydroxide ion transport probed via ultrafast vibrational echo experiments. In *Ultrafast Phenomena XVI*, Corkum, P.; Silvestri, S. D.; Nelson, K. A.; Riedle, E.; Schoenlein, R. W., Eds. Springer: Berlin, 2009; pp 481-483.

16. Petersen, P. B.; Roberts, S. T.; Ramasesha, K.; Nocera, D. G.; Tokmakoff, A., Ultrafast N-H Vibrational Dynamics of Cyclic Doubly Hydrogen-Bonded Homo- and Heterodimers. *J. Phys. Chem. B* **2008,** *112* (42), 13167-13171.

17. DeFlores, L. P.; Ganim, Z.; Nicodemus, R. A.; Tokmakoff, A., Amide I '-II ' 2D IR Spectroscopy Provides Enhanced Protein Secondary Structural Sensitivity. *J. Am. Chem. Soc.* **2009,** *131* (9), 3385-3391.

18. Roberts, S. T.; Petersen, P. B.; Ramasesha, K.; Tokmakoff, A.; Ufimtsev, I. S.; Martinez, T. J., Observation of a Zundel-like transition state during proton transfer in aqueous hydroxide solutions. *PNAS* **2009,** *106* (36), 15154-15159.

19. Roberts, S. T.; Ramasesha, K.; Tokmakoff, A., Structural rearrangements in water viewed through two-dimensional infrared spectroscopy. *Acc. Chem. Res.* **2009,** *42* (9), 1239-1249.

20. Nicodemus, R. A.; Ramasesha, K.; Roberts, S. T.; Tokmakoff, A., Hydrogen Bond Rearrangements in Water Probed with Temperature-Dependent 2D IR. *J. Phys. Chem. Letters* **2010**, *1*, 1068-1072.

21. Ramasesha, K.; Nicodemus, R. A.; Mandal, A.; Tokmakoff, A., Orientational Dynamics of Water Probed with 2D-IR Anisotropy Measurements. In *Ultrafast Phenomena XVII*, Jonas, D.; Riedle, E.; Schoenlein, R.; Chergui, M.; Taylor, A., Eds. Springer: Berlin, 2010; (accepted).

22. "A Source for Ultrafast Continuum Infrared and Terahertz Radiation," Poul B. Petersen and Andrei Tokmakoff, *Optics Letters*, **35** (2010) 1962–1964.

23. "Feature Article: Melting of a β-hairpin peptide using isotope-edited 2D IR spectroscopy and simulations," Adam W. Smith, Joshua Lessing, Ziad Ganim, Chunte Sam Peng, Andrei Tokmakoff, Santanu Roy, Thomas L. C. Jansen, and Jasper Knoester, *Journal of Physical Chemistry B*, in press.

The Role of Electronic Excitations on Chemical Reaction Dynamics at Metal, Semiconductor and Nanoparticle Surfaces

John C. Tully
Department of Chemistry, Yale University, 225 Prospect Street, P. O. Box 208107, New Haven, CT, 06520-8107 USA
john.tully@yale.edu

Program Scope

Achieving enhanced control of the rates and molecular pathways of chemical reactions at the surfaces of metals, semiconductors and nanoparticles will have impact in many fields of science and engineering, including heterogeneous catalysis, photocatalysis, materials processing, corrosion, solar energy conversion and nanoscience. However, our current atomic-level understanding of chemical reactions at surfaces is incomplete and flawed. Conventional theories of chemical dynamics are based on the Born-Oppenheimer separation of electronic and nuclear motion. Even when describing dynamics at metal surfaces where it has long been recognized that the Born-Oppenheimer approximation is not valid, the conventional approach is still used, perhaps patched up by introducing friction to account for electron-hole pair excitations or curve crossings to account for electron transfer. There is growing experimental evidence that this is not adequate. We are examining the influence of electronic transitions on chemical reaction dynamics at metal and semiconductor surfaces. Our program includes the development of new theoretical and computational methods for nonadiabatic dynamics at surfaces, as well as the application of these methods to specific chemical systems of experimental attention. Our objective is not only to advance our ability to simulate experiments quantitatively, but also to construct the theoretical framework for understanding the underlying factors that govern molecular motion at surfaces and to aid in the conception of new experiments that most directly probe the critical issues.

Recent Progress

Independent Electron Surface Hopping

In the previous two years of this grant, we developed the Independent Electron Surface Hopping (IESH) approach to nonadiabatic dynamics at metal surfaces, using the NO/Au system as a benchmark. In the year just completed, we improved the method by incorporating a more accurate method for computing the response of the atomic motions to "surface hops"; i.e., the changes in momenta that must be introduced when a non-resonant electronic transition occurs. This improvement did not change any of the major results reported in our previous publications, but it did have a significant effect on the vibrational excitation simulations described below. The IESH computer code is now sufficiently efficient (at least for the NO/Au system) to allow routine sampling of hundreds of thousands of trajectories in overnight runs, thereby providing predictions with low statistical uncertainties.

Dynamics of scattering of NO from Au(111)

We have completed an extensive series of IESH simulations of the scattering of vibrationally excited NO molecules from the 111 face of a gold crystal. Our simulations, based on a diabatic Hamiltonian constructed *a priori* from density functional theory (DFT), are in remarkable agreement with a host of experiments carried out by the research group of Alec Wodtke (Göttingen). Not only are major findings concerning multi-quantum vibrational transitions reproduced with reasonable accuracy, but unexpected trends in incident energy dependence and rotational excitation are also reproduced. We find that a major factor underlying the observed behavior is "rotational steering"; i.e., the molecule experiences a torque that can pull it into regions of strong nonadiabatic coupling.

More recently (unpublished), we have collaborated directly with the Wodtke group to explore vibrational *excitation* in the scattering of NO molecules from a gold surface. Wodtke and coworkers have carried out molecular beam experiments that, remarkably, reveal not only relative but also absolute probabilities for excitation of NO(v=0) to NO(v=1) and NO(v=2). We have taken advantage of this unusual opportunity for comparison between theory and experiment by carrying out IESH simulations, using the same NO/Au diabatic Hamiltonian as used previously, of vibrational excitation as a function of incident energy and surface temperature. Once again, our results are in good accord with experiment. An example is given in Fig. 1. Overall, the agreement between experiments and simulations for so many different features of the NO/Au system provides confidence that the IESH methodology we have developed is an accurate and practical way to explore nonadiabatic chemical dynamics at metal surfaces, subject to the availability of required molecule-surface interaction potentials and nonadiabatic couplings.

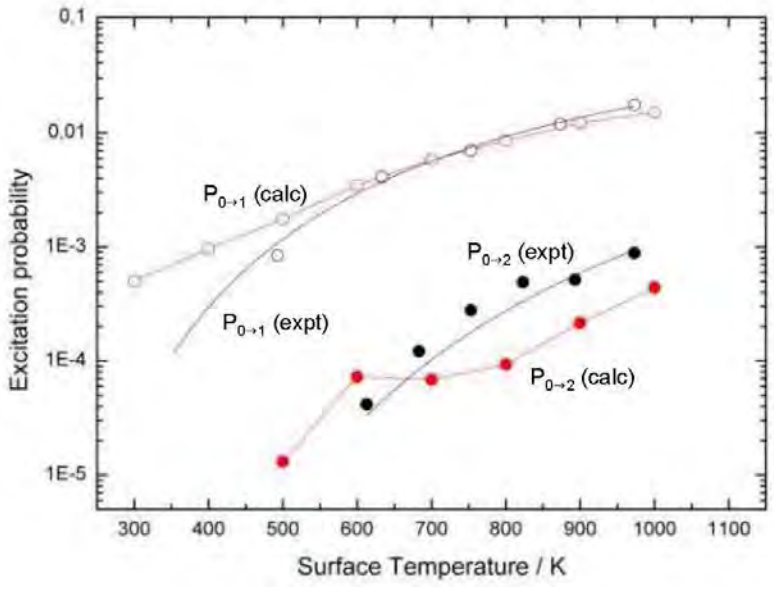

Figure 1. Absolute probabilities as a function of surface temperature for vibrational excitation of NO molecules initially in the v=0 state upon scattered from an Au(111) surface with an incident translational energy of 0.62 eV. Experiments are from Wodtke et al (unpublished). Calculations are IESH simulations (unpublished).

Future Plans

The goals of our research program include completing our studies of the NO-Au system and more general investigations of nonadiabatic behavior at metal and semiconductor surfaces, described below.

1. Carry out a systematic comparison of 3 methods for simulating nonadiabatic dynamics at metal surfaces: electronic friction dynamics, Ehrenfest (self-consistent field) dynamics, and IESH dynamics. We will carry out this comparison using the NO/Au Hamiltonian we have employed for our comparisons with the Wodtke experiments. We also plan to repeat this systematic comparison for hydrogen atom scattering from metal surfaces as described below. The electronic friction model is basically the weak-coupling limit of the Ehrenfest theory. Ehrenfest invokes nuclear motion on an effective potential energy surface that is a weighted average of potential surfaces corresponding to different electronic configurations. IESH is a surface hopping model that invokes stochastic hops between individual potential energy surfaces, with hopping probabilities determined by electronic transition probabilities. The widespread use of the electronic friction model justifies documenting its accuracy in a well-defined comparison, and the extent to which it may be improved by not making the weak coupling assumption, i.e., by carrying out Ehrenfest dynamics exactly, is an unsettled question.

2. Develop methods for computing "diabatic" potential energy surfaces and their off-diagonal couplings for molecules interacting with surfaces. The IESH method appears capable of accurately simulating nonadiabatic dynamics at metal and semiconductor surfaces, provided the required input is available and reliable. The necessary input is a diabatic Hamiltonian matrix that accurately represents the charge and excited states of the molecule embedded in the continuum of conduction band levels, and does so for all relevant molecule and surface atom positions. For NO interacting with the gold surface, we were able to construct a satisfactory diabatic Hamiltonian using density functional theory with the application of fictitious electric fields to modulate the energies of ionic states. This procedure is not applicable to most systems of experimental interest, however. The most critical challenge to further progress is to develop more generally applicable ab initio procedures for computing the necessary diabatic Hamiltonians. We propose to further develop and apply Constrained Density Functional Theory (CDFT) for this purpose. CDFT is conceptually simple; a DFT calculation is carried out with an imposed constraint, such as constraining the net local charge on a molecule to be minus one. This will produce the lowest energy potential energy surface consistent with this charge constraint. This can be repeated with different constraints to produce diagonal elements of the desired diabatic Hamiltonian. However, there are unsolved issues with computing the off-diagonal elements, including the absence of a proper wave function in DFT and non-orthogonality of Kohn-Sham determinants corresponding to different constraints. We will address these issues. As we overcome these obstacles, we will apply this approach to hydrogen atom scattering from metals, as described below. We will also apply CDFT with spin constraints to oxygen atoms and oxygen molecules interacting with metals surfaces. For both of these cases, transitions between the ground state triplet and low-lying singlet states may occur without spin-orbit interactions via a

two-electron exchange with the conduction band, possibly with major implications to chemical reactivity.

3. Inelastic scattering of hydrogen atoms from silver and gold surfaces. The hydrogen atom is the simplest example of an open shell species. While the interaction of an H atom with a metal surface does not exhibit all of the complexities of more complicated systems, because of its simplicity it affords an excellent opportunity to develop and test computational approaches for simulating atom-surface dynamical events. Equally importantly, the experimental group of Alec Wodtke (Göttingen) is planning an extensive molecular-beam study of this system, with the objective of producing detailed and quantitative data about angular distributions, inelasticity, temperature dependence, etc. We will carry out extensive calculations of the potential energy surfaces and nonadiabatic couplings for these systems, using both DFT and quantum chemical methods. Note that since DFT is in practice based on a density arising from a single-determinant Kohn-Sham wavefunction, it may not correctly portray the open-shell nature of the hydrogen atom which requires the intermixing of at least two electronic configurations (spin up and spin down), and perhaps three if the hydrogen negative ion plays a significant role. As mentioned above, we will simulate scattering dynamics with electronic friction, Ehrenfest and IESH methods, and compare each to the Wodtke experiments. This will be the most complete study to date of the role of nonadiabaticity in atom-metal interactions and the accuracy of current theories of nonadiabatic dynamics.

References to Publications of DOE-Sponsored Research: 2009-2011

1. N. Shenvi, "Phase-space surface hopping: Nonadiabatic dynamics in a superadiabatic basis", *J. Chem. Phys*. **130**, 124117 (2009).
2. N. Mateljevic, J. Kerwin, S. Roy, J. R. Schmidt and J. C. Tully, "Accommodation of Gases at Rough Surfaces", *J. Phys. Chem*. **113**, 2360-2367 (2009) (partial DOE support).
3. S. Roy, N. Shenvi and J. C. Tully, "Model Hamiltonian for the interaction of NO with the Au(111) surface", *J. Chem. Phys.* **130**, 174716 (2009).
4. N. Shenvi, S. Roy and J. C. Tully, "Nonadiabatic dynamics at metal surfaces: Independent-electron surface hopping", *J. Chem. Phys*. **130**, 174107 (2009).
5. J. E. Subotnik, R. J. Cave, R. P. Steele and N. Shenvi, "The initial and final states of electron and energy transfer processes: Diabatization as motivated by system-solvent interactions", *J. Chem. Phys*. **130**, 234102 (2009) (partial DOE support).
6. S. Roy, N. Shenvi and J. C. Tully, "The Dynamics of Open-Shell Species at Metal Surfaces", *J. Phys. Chem*. **113**, 16311-16320 (2009).
7. N. Shenvi, S. Roy and J. C. Tully, "Dynamical Steering and Electronic Excitation in NO Scattering from a Gold Surface", *Science* **326**, 829-832 (2009).

Reaction Processes in Complex Environments.

Marat Valiev[1] and Bruce C. Garrett[2]
[1]Environmental Molecular Sciences Laboratory and
[2]Chemical & Materials Sciences Division
Pacific Northwest National Laboratory
902 Battelle Blvd.
Mail Stop K9-90
Richland, WA 99352
marat.valiev@pnl.gov, bruce.garrett@pnl.gov

The major objective of this project is to gain fundamental understanding of the factors controlling reaction processes in condensed-phase environments through the development of advanced computational methods for accurate description of large-scale molecular systems. Chemical reactions in condensed phase environments play crucial roles in a wide variety of problems important to the Department of Energy (DOE), (e.g., catalysis for efficient energy use, corrosion in nuclear reactors promoted by reactive radical species such as OH, release of hydrogen from hydrogen storage materials, and contaminant degradation in the environment by natural and remedial processes). The need in all of these areas is to control chemical reactions to eliminate unwanted reactions and/or to produce desired products. The control of reactivity in these complex systems demands knowledge of the factors that control the chemical reactions and requires understanding how these factors can be manipulated to affect the reaction rates. Our specific interests are reaction mechanisms and free energy activation barriers, analysis of solvation structure around reactive solute species, and spectroscopic (UV absorption and photoelectron) signatures for "chemical imaging".

The main challenge for molecular simulation methods in this area is to balance the electronic structure accuracy requirements with large-scale solvent representations. Our strategy consists of utilizing multi-scale, multi-physics methods that present a natural evolution of conventional computational chemistry applications. These methods recognize natural decomposition of the chemical system into distinct regions (multi-scale) and the advantages, both computational and conceptual, of the integrated approach that uses different theoretical models (multi-physics). The latter descriptions could be associated with different parts of the overall chemical system and/or can coexist in a layered fashion. Such a layered approach is a key component in our methodology for the structural and free energy analysis of various reaction processes in aqueous environments. For the potential of mean force, our approach begins with the standard separation of the condensed phase system into a reactive part, which is treated quantum mechanically (QM), and the rest of the system, which is treated by a classical molecular mechanics (MM) model. We use a thermodynamic cycle to take advantage of the state function property of the potential of mean force (PMF), W, and combine simulations of free energy differences with pure MM models that allow sampling to be performed over ensembles, which are sufficiently large to converge statistical averages, with high-level electronic structure calculations for the QM region to accurately predict energetics. This approach takes advantage of MM, DFT, and coupled cluster (CC) methods in the QM regions to accelerate convergence of accurate energetics.

Similar methodology can also greatly improve the description of processes involving excited states where the accuracy of the electronic structure calculations becomes especially problematic. This is particularly relevant for the analysis of UV absorption spectroscopy data. It

is a powerful technique to probe the structure of reacting solute species in liquid phase, but the interpretation could be uncertain if the absorption signature of individual solute molecules is not known a priori. Theoretical modeling has the capacity to fill this gap provided that both electronic structure effects and the solvent environment are described properly. Compared to IR spectra, the electronic structure side of the problem involves calculations of excited state, which could present a challenge for standard ab-initio methods such as the time-dependent variant of density functional theory (TDDFT). In addition, reasonably accurate description of the solvent environment is needed to capture solute-solvent interactions in sufficient detail. Our methodology has the potential to resolve both these issues. This is the area of research that we have been pursuing with the experimental group of Sergei Lymar (BNL), which involves mechanistic analysis of UV spectra of solvated NO based radical species. In our recent work, we focused of hyponitrite radical ($N_2O_2^-$) and nitrosyl hyponitrite ($N_3O_3^-$) species in aqueous solution, which are important intermediates in biological and environmental reductive chemistries of NO. Major disagreements on the properties and reactivity of these intermediates exist in the literature. The main reason for this situation is that a proper interpretation of the observed transient kinetics hinges on knowing correct UV spectra of $N_2O_2^-$ and $N_3O_3^-$, but the spectral assignments given to these species by different research groups disagree significantly. Based on accurate characterization of excited states within the framework of the coupled cluster molecular mechanics approach, we were able to confirm that the earlier experimental assignment of the UV signature of $N_2O_2^-$ radical needed to be revised as was suggested by Lymar and co-workers. Based on correlation between experimental and computed spectrum, we also showed that the observed $N_2O_2^-$ radical species are predominantly of the *trans*-form (see Figure 1). Similarly for aqueous $N_3O_3^-$, the computational analysis of UV spectrum allowed us to establish that the experimentally observed form of $N_3O_3^-$ is *cis-symmetric* produced along with linear *trans-asymmetric* form of $N_3O_3^-$ with the branching ratio of ½.

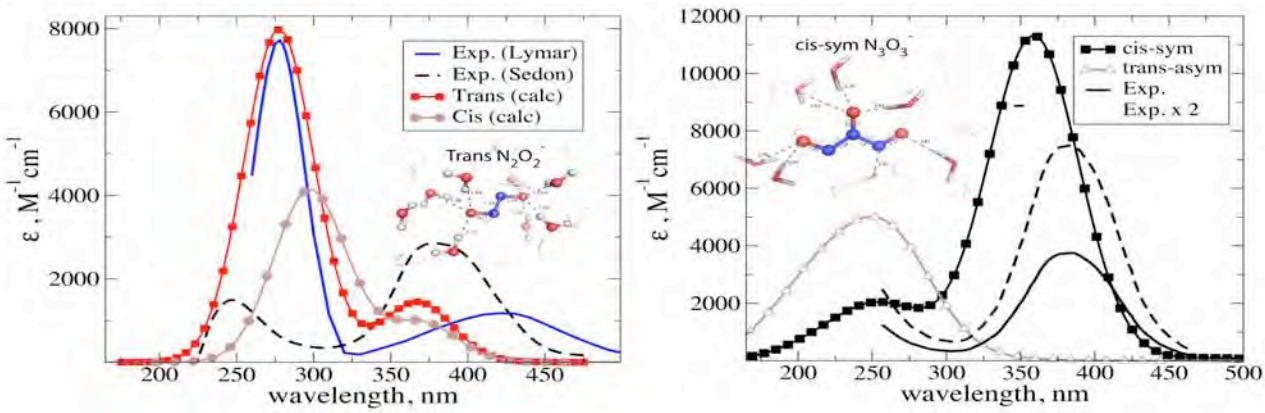

Figure 1: Experimental and computed spectra of hyponitrite radical ($N_2O_2^-$) and nitrosyl hyponitrite ($N_3O_3^-$) species in aqueous solution. Inserts show optimized structures in aqueous solution.

Collaborators on this project include G. K. Schenter, M. Dupuis, S. S. Xantheas, and Sergei Lymar. Some of the work was performed using the Molecular Science Computing Facility in the Environmental Molecular Sciences Laboratory, a national scientific user facility sponsored by the Department of Energy's Office of Biological and Environmental Research, located at Pacific Northwest National Laboratory (PNNL). Battelle operates PNNL for DOE.

References to publications of DOE sponsored research (2009-present)

1. Kathmann SM, GK Schenter, BC Garrett, B Chen, and JI Siepmann. 2009. "Thermodynamics and Kinetics of Nanoclusters Controlling Gas-to-Particle Nucleation." *Journal of Physical Chemistry C* 113(24):10354-10370.
2. Mielke SL, D Schwenke, GC Schatz, BC Garrett, and KA Peterson. 2009. "Functional Representation for the Born-Oppenheimer Diagonal Correction and Born-Huang Adiabatic Potential Energy Surfaces for Isotopomers of H_3." *Journal of Physical Chemistry A* 113(16):4479-4488.
3. Valiev M, R D'Auria, DJ Tobias, and BC Garrett. 2009. "Interactions of Cl^- and OH Radical in Aqueous Solution." *Journal of Physical Chemistry A* 113(31):8823-8825.
4. Arseneau DJ, DG Fleming, O Sukhorukov, JH Brewer, BC Garrett, and DG Truhlar. 2009. "The Muonic He atom and a Preliminary Study of the $^4He\mu + H_2$ Reaction." *Physica B Condensed Matter* 404(5-7):946-949.
5. Du S, JS Francisco, GK Schenter, and BC Garrett. 2009. "Interaction of C1O Radical with Liquid Water." *Journal of the American Chemical Society* 131(41):14778-14785..
6. Wang D, M Valiev, and BC Garrett. 2011. "CH_2Cl_2 and OH^- Reaction in Aqueous Solution: A Combined Quantum Mechanical and Molecular Mechanics Study." *Journal of Physical Chemistry A* 115(8):1380-1384
7. Kolb CE, RA Cox, JPD Abbatt, M Ammann, EJ Davis, DJ Donaldson, BC Garrett, C George, T Griffiths, DR Hanson, M Kulmala, G McFiggans, U Poschl, I Riipinen, M Rossi, Y Rudich, PE Wagner, PJ Winkler, DR Worsnop, and CD O'Dowd. 2010. "An Overview of Current Issues in the Uptake of Atmospheric Trace Gasses by Aerosols and Clouds." *Atmospheric Chemistry and Physics* 10(21):10561-10605.
8. M. Valiev, E. J. Bylaska, N. Govind, K. Kowalski, T. P. Straatsma, H. J. J. Van Dam, D. Wang, J. Nieplocha, E. Apra, T. L. Windus and W. de Jong, 2010. "NWChem: A comprehensive and scalable open-source solution for large scale molecular simulations", *Computer Physics Communications* **181** (9), 1477-1489.
9. Fleming DG, DJ Arseneau, O Sukhorukov, JH Brewer, SL Mielke, GC Schatz, BC Garrett, KA Peterson, and DG Truhlar. 2011. "Kinetic Isotope Effects for the Reactions of Muonic Helium and Muonium with H_2." *Science* 331(6016):448-450.

This page is intentionally left blank

Chemical Kinetics and Dynamics at Interfaces

Cluster Model Investigation of Condensed Phase Phenomena

Xue-Bin Wang
Chemical & Materials Sciences Division, Pacific Northwest National Laboratory, P.O. Box 999, MS K8-88, Richland, WA 99352, & Department of Physics, Washington State University, 2710 University Drive, Richland, WA, 99354. E-mail: xuebin.wang@pnl.gov

Collaborators include L.S. Wang, S.S. Xantheas, J. Li, J.L.Yang, S. M. Kathmann, M. Kappes, A. I. Boldyrev, O. Boltalina, S. Kass, P. Jungwirth

Program Scope

The broad scope of this program is obtaining a microscopic understanding of solution chemistry and condensed phase phenomena using gas phase clusters as model systems. Our current focus is on the microsolvation of complex anions that are important in solution chemistry and the environment. Our primary experimental technique is photoelectron spectroscopy coupled with electrospray ionization, which is used to produce complex anions, including multiply-charged anions, and solvated clusters from solution samples. Complex anions, in particular multiply charged anions, are ubiquitous in nature and often found in solutions and solids. However, few complex anions have been studied in the gas phase due to difficulty in generating them and their intrinsic instability as a result of strong intramolecular Coulomb repulsion in the case of multiply charged anions. Microscopic information on the solvation and stabilization of these anions is important for understanding solution chemistry and properties of inorganic materials or atmospheric aerosols involving these species. Gas phase studies with controlled solvent numbers and molecular specificity are ideal to provide such microscopic information. We have developed a new experimental technique allowing for the precise control of ion temperatures in the range from 10 K to room temperature. This breakthrough has facilitated not only the enhancement of the photoelectron spectroscopic resolution and precision, but also the investigation of new temperature-dependent phenomena. Experiments and *ab initio* calculations are combined to

- Obtain a molecular-level understanding of the solvation and stabilization of complex singly- and multiply-charged anions important in condensed phases
- Study temperature-dependent conformation changes and isomer populations of complex solvated clusters
- Understand the molecular processes and initial steps of dissolution of salt molecules in polar solvents
- Investigate intrinsic electronic structures of environmentally important species and reactive diradicals.

The central theme of this research program lies at obtaining a fundamental understanding of environmental materials and solution chemistry via synergetic experimental and theoretical studies. These are important to waste storage, subsurface and atmospheric contaminant transport, catalysis, and other primary DOE missions.

Recent Progress

Observation of a Remarkable Temperature Effect in the Hydrated Bonding Structure and Dynamics of the $CN^-(H_2O)$ Cluster. The $CN^-(H_2O)$ cluster represents a model diatomic monohydrate with multiple possible solvation sites. We have reported temperature-dependent PES experiments as well as high-level *ab initio* electronic structure calculations that were used to probe its structure and dynamics. A

remarkable temperature effect was observed, namely that the PES spectrum at T = 12 K exhibited a surprising blue shift of 250 meV in the electron binding energy of the cluster relative to the spectrum observed at T = 300 K, while the overall spectral pattern and width remained largely unchanged. Extensive theoretical analysis of the potential energy function of the cluster at the CCSD(T) level of theory revealed the existence of two almost isoenergetic isomers corresponding to the water molecule forming a hydrogen bond on either the carbon or the nitrogen atoms, respectively. This results in four topologically distinct minima on the potential energy function, namely $CN^-(H_aOH_b)$, $CN^-(H_bOH_a)$, $NC^-(H_aOH_b)$, and $NC^-(H_bOH_a)$. There are two main pathways that interconvert those minima: (i) CN^- tumbling relative to water and (ii) water rocking relative to CN^-. The relative magnitude of the barriers associated with these two motions reverses between low (pathway (i) is preferred) and high (pathway (ii) is preferred) temperatures. As a result, at T = 12 K, the cluster adopts a structure that is close to the minimum energy $CN^-(H_2O)$ configuration, while at room temperature it can effectively access regions of the potential energy function close to the transition states. This results in the sharp electron binding energy difference observed during the experiments performed at the low and high temperatures.

Evidence of Significant Covalent Bonding in $Au(CN)_2^-$. There has been intense recent interest in the homogeneous catalytic chemistry of Au(I) complexes. Among the Au(I) molecules, the $Au(CN)_2^-$ ion is the most stable and has been widely used in gold extraction back to ancient times, but has not been observed and studied in the gas phase. Because of relativistic effects, Au-containing molecules exhibit distinctly different properties among the coinage elements. To probe the nature of the chemical bonding in $Au(CN)_2^-$, we performed a joint low-temperature PES and high-level theoretical study of the three coinage-metal cyanide complexes $M(CN)_2^-$ (M = Cu, Ag, Au). We obtained PES spectra of $Au(CN)_2^-$ at three detachment photon energies (193, 157, and 118 nm), and compared them with those of its lighter congeners, $Cu(CN)_2^-$ and $Ag(CN)_2^-$. The PES spectra of $Au(CN)_2^-$ display well-resolved vibrational progressions due to the Au-C stretching, in sharp contrast to the atomic-like transitions observed for the mainly ionic $Cu(CN)_2^-$ complex, and thus provide direct experimental evidence of the existence of significant covalent bonding character in $Au(CN)_2^-$. Theoretical calculations were carried out to provide insight into the nature of the chemical bonding in $Au(CN)_2^-$ in comparison with that in $Cu(CN)_2^-$ and $Ag(CN)_2^-$. Electron localization functions reflecting the probability of finding electron pairs reveal more vividly the increased covalency in the Au–C bonding stem from the strong relativistic effects in gold.

Microsolvation of the Acetate Anion: A Photoelectron Spectroscopy and Ab Initio Computational Study. A volatile organic acid, acetic acid is the most abundant species among organic compounds in the atmosphere. Detailed knowledge of the dissolution of acetic acid and the solvation behavior of acetate may be valuable to understanding their chemistry in solution and the fate and transport of this environmental pollutant. Unlike simple diatomic salts or acids where charge-dipole and polarization interactions with polar solvents dictate the dissolution processes, acetate consists of a hydrophilic ($-CO_2^-$) and a hydrophobic ($-CH_3$) group, which may induce interesting solvation behavior depending on the competition of hydrophilic and hydrophobic interactions. A combined PES and *ab initio* theoretical study was carried out to investigate the microsolvation of the acetate anion. Photoelectron spectra of cold solvated clusters $CH_3CO_2^-(H_2O)_n$ (n = 1-3) at 12 K were obtained and compared with theoretical calculations. The first water is shown to bind to the $-CO_2^-$ group in a bidentate fashion, whereas both water-water and water-CO_2^- interactions are shown for n = 2 and 3. Significant rearrangement of the solvation structures is observed upon electron detachment, and water-CH_3 interactions are present for all the neutral clusters, $CH_3CO_2(H_2O)_n$ (n = 1-3). The solvated structures for $CH_3CO_2^-(H_2O)_n$ (n = 1-3) are clearly dominated by the hydrophilic interactions between H_2O and the $-CO_2^-$ group, similar to what we observed previously in the hydrated clusters of dicarboxylate dianions. The structures of the hydrated neutral CH_3CO_2 radical are interesting, clearly reflecting the competition between the hydrophobic and hydrophilic interactions. The removal of the negative charge on the carboxylate group significantly reduces the hydrophilic interactions with water, resulting in the rearrangement of the water molecules so that they can also interact with the CH_3 group. The acetyloxyl radical CH_3CO_2 is known to be unstable upon electron detachment of acetate, dissociating into $CH_3 + CO_2$. In the hydrated acetyloxyl radical, the

solvent molecules provide a link between the CH_3 and CO_2 groups and should stabilize the acetyloxyl radical against its dissociation compared to the bare one. The growth pattern revealed from the small solvated clusters can compare directly with the solvation behavior of acetate in aqueous solutions, revealing the preference of H_2O to the hydrophilic–CO_2^-. This solvation pattern is consistent with the behavior of acetate at the solution/vapor interface, where the hydrophobic CH_3 group is exposed.

Probing the Electronic Stability of Multiply Charged Anions: The Sulfonated Pyrene Tri- and Tetra-Anions. The strong intramolecular Coulomb repulsion in multiply-charged anions creates a potential barrier that provides dynamic stability to multiply-charged anions and allows electronically metastable species to be observed. The 1-hydroxy-3,6,8-pyrene-trisulfonate $\{[Py(OH)(SO_3)_3]^{3-}$ or $HPTS^{3-}\}$ was recently observed as a long-lived metastable multiply-charged anion with a large negative electron binding energy of -0.66 eV. To further explore the limitation of the stability of multiply-charged anions, we carried out a combined study on the electronic metastability and lifetimes of a series of triply-charged anions consisting of a central pyrene scaffold and peripheral sulfonate groups as charge carriers. Autodetachment of $HTPS^{3-}$ to $HTPS^{\bullet 2-} + e^-$ was measured in a Fourier transform ion cyclotron resonance cell and was used to measure a half-life of 0.1 s for this metastable trianion, which carries 0.66 eV excess energy. The quadruply-charged $[Py(SO_3)_4]^{4-}$ anion estimated to possess a -2.78 eV negative electron binding energy was shown to be too unstable to be observed experimentally. Instead, its autodetachment product, $[Py(SO_3)_4]^{\bullet 3-}$, as well as ion pairs stabilized by H^+ and Na^+ were observed and studied both experimentally and computationally. The measured electron binding energy/half-life of -0.66 eV/0.1 s for $HTPS^{3-}$, along with those reported previously for $PtCl_4^{2-}$ (-0.25 eV/2.5 s) and $[CuPc(SO_3)_4]^{4-}$ (-0.9 eV/~275 s) provide a series of benchmarks to predict electronic metastability in doubly-, triply-, and quadruply-charged anions. Given the comparatively long lifetimes of these multiply-charged anions, it is conceivable that even higher negative binding energies can be observed in suitably designed doubly-, triply-, or quadruply-charged anions.

Future Directions

The main thrust of our BES program will continue to be on cluster model studies of condensed phase phenomena in the gas phase. The experimental capabilities that we have developed give us the opportunity to attack a broad range of fundamental chemical physics problems pertinent to ionic solvation and solution chemistry. In particular, the temperature control will allow us to study different isomer populations and conformation changes of environmentally important hydrated clusters as a function of temperature. We will also be able to study physisorption of various gas molecules onto negatively-charged anions. The physisorption of H_2 and CO_2 are of particular interest because of relevance to identifying potential H_2 and CO_2 storage materials by providing fundamental energetic and structural information between these two gases and different types of molecules. Another major direction is to use gaseous clusters to model ion-specific interactions in solutions and initial nucleation processes relevant to atmospheric aerosol formation. While we will continue to explore the new capabilities of temperature control, we also plan to initiate new research directions in the coming years to study excited state properties of solvated clusters to model possible aerosol photochemistry and high-energy processes at interfaces.

References to Publications of DOE Sponsored Research (2009-present)

1. XP Xing, XB Wang, and LS Wang, "Photoelectron Angular Distribution and Molecular Structure in Multiply Charged Anions." *Journal of Physical Chemistry A* 113, 945-948 (2009).
2. XB Wang and LS Wang, "Photoelectron Spectroscopy of Multiply Charged Anions." *Annual Review of Physical Chemistry* 60, 105-126 (2009).
3. XP Xing, XB Wang, and LS Wang, "Photoelectron Imaging of Multiply Charged Anions: Effects of Intramolecular Coulomb Repulsion and Photoelectron Kinetic Energies on Photoelectron Angular Distributions." *Journal of Chemical Phys*ics 130(7), 074301 (2009).

4. XB Wang, AP Sergeeva, J Yang, XP Xing, AI Boldyrev, and LS Wang, "Photoelectron Spectroscopy of Cold Hydrated Sulfate Clusters, $SO_4^{2-}(H_2O)_n$ (n = 4-7): Temperature-Dependent Isomer Populations." *Journal of Physical Chemistry A* 113, 5567-5576 (2009).

5. XB Wang, AP Sergeeva, XP Xing, M Massaouti, T Karpuschkin, O Hampe, AI Boldyrev, MM Kappes, and LS Wang, "Probing the Electronic Stability of Multiply Charged Anions: Sulfonated Pyrene Tri- and Tetraanions." *Journal of the American Chemical Society* 131, 9836 (2009).

6. XB Wang, B Jagoda-Cwiklik, C Chi, XP Xing, M Zhou, P Jungwirth, and LS Wang, "Microsolvation of the Acetate Anion $[CH_3CO_2^-(H_2O)_n$, n = 1-3]: A Photoelectron Spectroscopy and Ab Initio Computational Study." *Chemical Physics Letters* 477, 41-44 (2009).

7. XB Wang, JC Werhahn, LS Wang, K Kowalski, A Laubereau, and SS Xantheas, "Observation of a Remarkable Temperature Effect in the Hydrogen Bonding Structure and Dynamics of the $CN^-(H_2O)$ Cluster." *Journal of Physical Chemistry A* 113, 9579-9584 (2009).

8. XB Wang, YL Wang, J Yang, XP Xing, J Li, and LS Wang, "Evidence of Significant Covalent Bonding in $Au(CN)_2^-$." *Journal of the American Chemical Society* 131(45), 16368-16370 (2009).

9. MM Meyer, XB Wang, CA Reed, LS Wang, and SR Kass, "Investigating the Weak to Evaluate the Strong: An Experimental Determination of the Electron Binding Energy of Carborane Anions and the Gas Phase Acidity of Carborane Acids." *Journal of the American Chemical Society* 131, 18050-18051 (2009).

10. XB Wang, C Chi, M Zhou, IV Kuvychko, K Seppelt, AA Popov, SH Strauss, OV Boltalina, and LS Wang, "Photoelectron Spectroscopy of $C_{60}F_n^-$ and $C_{60}F_m^{2-}$ (n = 17, 33, 35, 43, 45, 47; m = 34, 46) in the Gas Phase and the Generation and Characterization of C_1-$C_{60}F_{47}^-$ and D_2-$C_{60}F_{44}$ in Solution." *Journal of Physical Chemistry A* 114, 1756-1765 (2010).

11. XB Wang, K Kowalski, LS Wang, and SS Xantheas, "Stepwise Hydration of the Cyanide Anion: A Temperature-Controlled Photoelectron Spectroscopy and Ab Initio Computational Study of $CN^-(H_2O)_n$, n = 2-5." *Journal of Chemical Physics* 132(12), 124306 (2010).

12. XB Wang, Q Fu, and J Yang, "Electron Affinities and Electronic Structures of *o*-, *m*-, and *p*-hydroxyphenoxyl Radicals: A Combined Low-Temperature Photoelectron Spectroscopic and Ab Initio Calculation Study." *Journal of Physical Chemistry A* 114, 9083-9089 (2010).

13. YL Wang, XB Wang, XP Xing, F Wei, J Li, and LS Wang, "Photoelectron Imaging and Spectroscopy of MI_2^- (M = Cs, Cu, Au): Evolution from Ionic to Covalent Bonding." *Journal of Physical Chemistry A* 114, 11244-11251 (2010).

14. Q Fu, J Yang, and XB Wang, "On the Electronic Structures and Electron Affinities of the m-Benzoquinone (BQ) Diradical and the o-, p-BQ Molecules: A Synergetic Photoelectron Spectroscopic and Theoretical Study" *Journal of Physical Chemistry A* dx.doi.org/10.1021/jp1120542 (2011).

Ionic Liquids: Radiation Chemistry, Solvation Dynamics and Reactivity Patterns

James F. Wishart
Chemistry Department, Brookhaven National Laboratory, Upton, NY 11973-5000
wishart@bnl.gov

Program Definition

Ionic liquids (ILs) are a rapidly expanding family of condensed-phase media with important applications in energy production, nuclear fuel and waste processing, improving the efficiency and safety of industrial chemical processes, and pollution prevention. ILs generally have low volatilities and are combustion-resistant, highly conductive, recyclable and capable of dissolving a wide variety of materials. They are finding new uses in chemical synthesis, catalysis, separations chemistry, electrochemistry and other areas. Ionic liquids have dramatically different properties compared to conventional molecular solvents, and they provide a new and unusual environment to test our theoretical understanding of primary radiation chemistry, charge transfer and other reactions. We are interested in how IL properties influence physical and dynamical processes that determine the stability and lifetimes of reactive intermediates and thereby affect the courses of reactions and product distributions. We study these issues by characterization of primary radiolysis products and measurements of their yields and reactivity, quantification of electron solvation dynamics and scavenging of electrons in different states of solvation. From this knowledge we wish to learn how to predict radiolytic mechanisms and control them or mitigate their effects on the properties of materials used in nuclear fuel processing, for example, and to apply IL radiation chemistry to answer questions about general chemical reactivity in ionic liquids that will aid in the development of applications listed above.

Very early in our radiolysis studies it became evident that the slow solvation dynamics of the excess electron in ILs (which vary over a wide viscosity range) increase the importance of pre-solvated electron reactivity and consequently alter product distributions and subsequent chemistry. This difference from conventional solvents has profound effects on predicting and controlling radiolytic yields, which need to be quantified for the successful use under radiolytic conditions. Electron solvation dynamics in ILs are measured directly when possible and estimated using proxies (e.g. coumarin-153 dynamic emission Stokes shifts or benzophenone anion solvation) in other cases. Electron reactivity is measured using ultrafast kinetics techniques for comparison with the solvation process.

Methods. Picosecond pulse radiolysis studies at BNL's Laser-Electron Accelerator Facility (LEAF) are used to identify reactive species in ionic liquids and measure their solvation and reaction rates. IL solvation and rotational dynamics are measured by TCSPC and fluorescence upconversion measurements in the laboratory of E. W. Castner at Rutgers Univ. Diffusion rates of anions, cations and solutes are obtained by PGSE NMR in S. Greenbaum's lab at Hunter College, CUNY and by Castner's group at Rutgers. Professor Mark Kobrak of CUNY Brooklyn College performs molecular dynamics simulations of solvation processes. In collaboration with J. Davis (U. South Alabama) we are a characterizing the radiolytic and other properties of boronium ionic liquids, which could be used to make fissile material separations processes inherently safe from criticality accidents.

Ionic liquid synthesis and characterization. Our work often involves novel ILs that we design to the requirements of our radiolysis and solvation dynamics studies and are not commercially available. We have developed in-house capabilities and a network of collaborations (particularly with S. Lall-Ramnarine of Queensborough CC and R. Engel of Queens College) to design, prepare and characterize ILs in support of our research objectives. Cation synthesis is done with a CEM microwave reactor, resulting in higher yields of purer products in much shorter time than traditional methods. We have assembled an instrumentation cluster including DSC, TGA, viscometry, AC conductivity, Karl Fischer moisture determination and ESI-mass spec (for purity analysis and radiolytic product identification). The cluster

serves as a resource for our collaborators in the New York Regional Alliance for Ionic Liquid Studies and other institutions (Penn State, ANL). Our efforts are substantially augmented by student internships from the BNL Office of Educational Programs, particularly the FaST program, which brings collaborative faculty members and their students into the lab for ten weeks each summer. Since 2003, a total of 29 undergrads, two graduate students, one pre-service teacher, one high school student and four junior faculty have worked on IL projects in our lab, many of them for more than one summer.

Recent Progress

Electron solvation and pre-solvated reactivity in ionic liquids. The reactivity of excess electrons is of prime importance to the radiation chemistry of virtually all liquids. In ionic liquids, the relatively slow relaxation dynamics bestows particular significance to the reactivity of pre-solvated electron states, which occurs in competition with electron solvation processes. On a practical level it is necessary to quantify these effects in order to predict and effect control over the distributions of radiolysis products. On a fundamental level, not enough is understood about how pre-solvated electron scavenging mechanisms operate, including the nature of pre-solvated electron species and how they vary in different media.

Ionic liquids are well suited for these investigations because their relaxation dynamics at room temperature extends comfortably through the picosecond regime and even into the nanosecond time scale. Thus, pre-solvated electron states can be easily detected using the picosecond pulse radiolysis instrumentation of BNL's Laser-Electron Accelerator Facility. In previous work we have used electron pulse-laser probe time delay transient absorption methods to measure the solvation process of the excess electron in the pyrrolidinium ionic liquid C_4mpyrr NTf_2 and two related ILs. We are now in the process of using the optical fiber single-shot spectroscopy (OFSS) detection developed at LEAF by Andrew Cook to observe the electron scavenging kinetics of a wide variety of solutes in the same C_4mpyrr NTf_2 IL in which we have characterized electron solvation. The solubility characteristics of ionic liquids will permit direct comparison of inorganic and organic scavengers that are not normally soluble in the same solvent system at high enough concentrations to scavenge pre-solvated electrons. The OFSS results show that the various solutes have different reactivity profiles with respect to particular solvated or pre-solvated excess electron species. That much had been inferred a long time ago from extrapolations of nanosecond kinetics to "time zero", but the distinction is that the combination of ionic liquids and OFSS permits us to directly observe the solvation and scavenging processes and thus obtain mechanistic insights.

A case in point is the electron scavenger duroquinone (2,3,5,6-tetramethyl-1,4-benzoquinone, DQ). When DQ is added to C_4mpyrr NTf_2, a rapid (~76 ps) decrease in excess electron absorption at 800 nm is observed. When the DQ concentration is low (~40 mM) the amplitude of that decay process is small, but it becomes a dominant feature as the concentration is increased, although the time constant remains the same. (In the absence of DQ, the absorbance at 800 nm actually increases slightly in this time frame due to solvation-induced blue shift of the electron spectrum.) The observed electron scavenging process coincides with the 74-ps feature associated with electron solvation (see adjacent figure to compare the electron decay at two DQ concentrations with the profile of the solvation process as indicated by the red-edge, 1600 nm absorption trace or the solvation function obtained via SVD analysis). In this case, it appears that the pre-solvated may react with DQ molecules in its proximity, perhaps by tunneling, much more efficiently than fully solvated electrons. Effectively, the solvation process shuts down the scavenging pathway. Other solutes, such as nitrate anion, have different kinetic behavior and do not show the prompt decay feature.

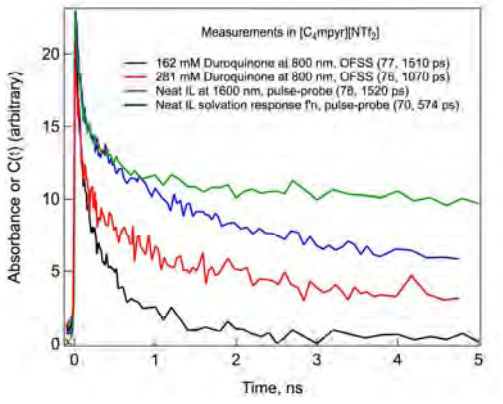

By quantitative measurement of the scavenging profiles of many reactants, we seek to provide a mechanistic basis for understanding excess electron scavenging that can be applied to real-world applications such as predicting radiolytic product distributions during the processing of radioactive materials and guiding the deliberate addition of reactants to reduce radiolytic damage, or conversely, to maximize yields of desired products.

Electron transfer in ionic liquids. **(**In collaboration with Heather Lee and Ed Castner of Rutgers University) Photoinduced electron-transfer reactions in a system comprised of an N,N-dimethyl-1,4-phenylenediamine donor, proline bridge and coumarin 343 acceptor were studied by TCSPC as a function of temperature and viscosity and analyzed using multi-exponential nonlinear least squares fitting (dots and bars) and maximum entropy methods (curves). In two ionic liquids the ET kinetics was broadly distributed, while the distributions were narrow in neutral organic solvents, demonstrating the intrinsic heterogeneity of IL systems.

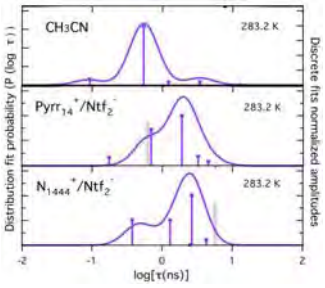

Future Plans

Cage escape and recombination in ILs. Slow dynamics and diffusion in ionic liquids have significant consequences for photoinduced reactions, where product quantum yields often depend on cage escape rates in competition with back reaction. In ILs, cage escape may be slowed by sluggish displacement of the solvent cage, affording greater opportunity for recombination and consequent reduction in quantum yield. In previous work, we observed such effects in the photolysis of *ortho*-chloro-hexaarylbisimidazole (*o*-Cl-HABI, L-L in the adjacent scheme) where quantum yields of the lophyl radical (L•) were much lower in three ILs than in DMSO. We intend to examine the early stages of cage escape of lophyl radical pairs on the picosecond to nanosecond time scale using the OFSS detection (see above). The OFSS system is critical to this effort because the diffusive recombination of lophyl radicals takes many seconds in ILs and in ordinary solvents, making typical repetitive pump-probe experiments completely impractical. In contrast, OFSS provides picosecond-resolution, 5-nanosecond-range transient absorption data using relatively small numbers of shots that can be collected at arbitrarily long delays in-between. With this advantage, we will examine the kinetics of cage escape and recombination in ILs of different viscosities, and the effects of slow IL relaxation dynamics on the planarization of the lophyl radical, which provides the very large reorganization barrier for radical dimerization on longer time scales. (Collaboration with Prof. V. Strehmel (U. of Applied Sci., Krefeld, Germany) and A. Cook and D. Polyanskiy (BNL))

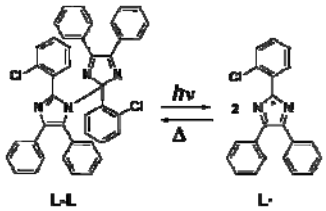

Studies of structure and reaction dynamics in ionic liquids using EXAFS and femtosecond spectroscopy. In a collaboration with R. Crowell, R. Musat and D. Polyanskiy, photoionization of Br^- anion in neat and diluted bromide ionic liquids is being used to probe the dynamics of excess electrons and excited states. Static and time-resolved Br EXAFS is employed to study the structure of the ionic liquid and the dynamics and reactivity of the Br atom formed by the photoionization. The results can be applied to understanding analogous iodide systems of interest in solar photoconversion.

Development of Vibrational Spectroscopies at LEAF. Until recently the detection of short-lived species generated by pulse radiolysis at LEAF has relied primarily upon absorption or emission spectroscopy in the UV-visible-NIR regions. Although these methods afford excellent kinetic information, structural identification of intermediates for the elucidation of reaction pathways can be inconclusive in many cases. Time-resolved vibrational spectroscopic (TRVS) detection methods (both IR

and Raman) offer highly specific molecular and structural characterization. We are therefore in the process of implementing time-resolved infrared (TRIR) and time-resolved resonance Raman (TR^3) detection systems for pulse radiolysis. The successful coupling of these techniques with pulse radiolysis will add a powerful new dimension to our research and enable a wide variety of investigations (in collaboration with D. Grills, J. Preses, A. Cook, D. Polyansky and K. Iwata).

Publications on ionic liquids

1. *Recombination of Photogenerated Lophyl Radicals in Imidazolium-Based Ionic Liquids* V. Strehmel, J. F. Wishart, D. E. Polyansky, and B. Strehmel, *ChemPhysChem* **10**, 3112-3118 (2009).
2. *The radiation chemistry of ionic liquids and its implications for their use in nuclear fuel processing*, J. F. Wishart and I. A. Shkrob in "Ionic Liquids: From Knowledge to Application," Rogers, R. D.; Plechkova, N. V.; Seddon, K. R., Eds. *ACS Symp. Ser.* **1030**, Amer. Chem. Soc.: Washington, (2009) Ch. 8, pp 119-134.
3. *Radiation Chemistry and Photochemistry of Ionic Liquids*, K. Takahashi and J. F. Wishart in "Charged Particle and Photon Interactions with Matter" Y. Hatano, Y. Katsumura and A. Mozumder, Eds. Taylor & Francis, (2010) Ch. 11, pp 265-287.
4. *Heavy Atom Substitution Effects in Non-Aromatic Ionic Liquids: Ultrafast Dynamics and Physical Properties* H. Shirota, H. Fukazawa, T. Fujisawa, and J. F. Wishart, *J. Phys. Chem. B*, **114,** 9400-9412 (2010)
5. *Ionic Liquids and Solids with Paramagnetic Anions*, B. M. Krieger, H. Y. Lee, T. J. Emge, J. F. Wishart, E. W. Castner, Jr., *Phys. Chem. Chem. Phys.*, **12**, 8919-8925 (2010)
6. *Exploring the Effect of Structural Modification on the Physical Properties of Various Ionic Liquids*, S. I. Lall-Ramnarine, J. L. Hatcher, A. Castano, M. F. Thomas, and James F. Wishart in "ECS Transactions - Las Vegas, NV, Vol. 33, Molten Salts and Ionic Liquids 17" Fox, D., *et al.*, Eds.; The Electrochemical Society, Pennington, NJ, (2010) pp. 659 - 665.
7. *Electron solvation dynamics and reactivity in ionic liquids observed by picosecond radiolysis techniques* J. F. Wishart, A. M. Funston, T. Szreder, A. R. Cook and M. Gohdo, *Faraday Discuss.* **154**, submitted.

Publications on other subjects

8. Book: "Recent Trends in Radiation Chemistry," J. F. Wishart and B. S. M. Rao, Eds.; World Scientific, Singapore, (2010). (ISBN 978-981-4282-07-9)
9. *Ultra-fast pulse radiolysis methods*, J. Belloni, R. A. Crowell, Y. Katsumura, M. Lin, J.-L. Marignier, M. Mostafavi, Y. Muroya, A. Saeki, S. Tagawa, Y. Yoshida, V. De Waele, and J. F. Wishart in "Recent Trends in Radiation Chemistry," J. F. Wishart and B. S. M. Rao, Eds. Ch. 5, pp 121-160, World Scientific, Singapore, (2010).
10. *Application of External-Cavity Quantum Cascade IR Lasers to Nanosecond Time-Resolved Infrared Spectroscopy of Condensed-Phase Samples Following Pulse Radiolysis*, D. C. Grills, A. R. Cook, E. Fujita, M. W. George, J. M. Preses, and J. F. Wishart, *Appl. Spect.* **64**, 563-570 (2010), cover publication.

Molecular level understanding of hydrogen bonding environments

Sotiris S. Xantheas
Chemical & Materials Sciences Division, Pacific Northwest National Laboratory
902 Battelle Blvd., Mail Stop K1-83, Richland, WA 99352
sotiris.xantheas@pnl.gov

The objective of this research effort is to develop a comprehensive understanding of the collective phenomena associated with aqueous solvation. The molecular level details of aqueous environments are central in the understanding of important processes such as reaction and solvation in a variety of homogeneous and heterogeneous systems. The fundamental understanding of the structural, thermodynamic and spectral properties of these systems is relevant to the solvation in aqueous solutions, the structure, reactivity and transport properties of clathrate hydrates, in homogeneous catalysis and in atmospheric processes.

The motivation of the present work stems from the desire to establish the key elements that describe the structural and associated spectral features of simple ions in a variety of hydrogen bonded environments such as bulk water, aqueous interfaces and aqueous hydrates. In particular, solid hydrates of salts containing a fixed ratio of water molecules in their crystal structures have attracted special interest due to their importance in geology, chemistry, and physics. The quest for deciphering the properties of hydrogen bonds makes those materials ideal candidates for studying the spectral signatures of water in different, well-defined environments with varying bonding partners and distances.

We obtained the melting temperature (T_m) of water with the Perdew-Burke-Ernzerhof (PBE) and Becke-Lee-Yang-Parr (BLYP) density functionals using a coexisting ice (I_h)-liquid system (Fig. 1) from constant enthalphy (*NPH*) Born-Oppenheimer MD (BOMD) simulations.

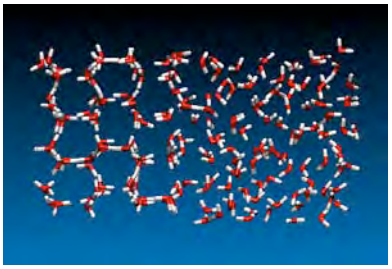

Fig. 1. The ice-liquid coexisting system used in the (*NPH*) ensemble.

Our estimates are T_m = 417 ± 3 K at P = 2,500 bar (PBE) and T_m = 411 ± 4 K at P = 10,000 bar (BLYP) (Fig. 2). The system size effects, investigated with the TIP4P classical potential, suggest that these values are probably a lower limit for T_m. The inclusion of nuclear quantum effects is expected to lower this value by 20-30 K, therefore yielding estimates that are > 100 K larger than the experimental value. Based on this finding, the calculated Oxygen-Oxygen RDFs and MSDs for ρ = 1 g/cm^3 at T = 360 K, 400 K and 440 K furthermore suggested that the liquid phase is supercooled below T_m. These results are consistent with previous reports indicating that both the PBE and BLYP functionals produce an over-structured liquid at room temperature and up to 400 K. The inclusion of *a posteriori* dispersion corrections to BLYP according to the

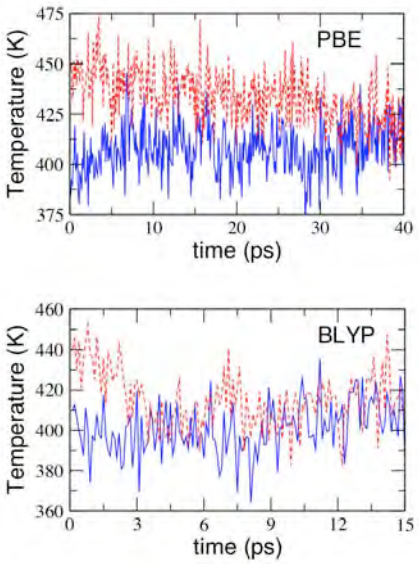

Fig. 2. The coexisting ice-liquid simulation in the (*NPH*) ensemble with the PBE (top) and BLYP (bottom) functionals.

scheme proposed by Grimme (BLYP-D) lowers T_m to about 360 K (Fig. 3), a large improvement over the value of T_m > 400 K previously obtained with the original BLYP functional under the same simulation conditions. For the *ab-initio* based, flexible polarizable classical potential TTM3-F we obtained T_m =248 K from classical molecular dynamics simulations. In order to study the physical, thermodynamic, and structural properties of water with these two functionals and compare with experiment at ambient conditions, simulations at $T > T_m$ need to be performed. Since T_m is probably sensitive to different DFT functionals, it is expected that the phase diagram (including T_m) of water with other popular hybrid and/or meta-DFT functionals (such as B3LYP, TPSS, and M06-2X) could be different from the current results obtained with the PBE and BLYP functionals. The present results can serve as guides in providing the range of conditions that should be used in the simulation of the liquid phase of water with those functionals.

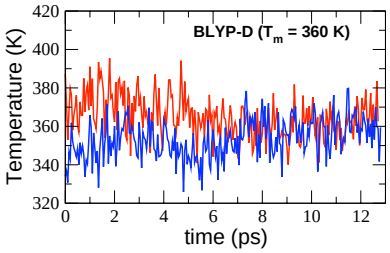

Fig. 3. The (*NPH*) simulation with BLY-D (P = 1 bar, ρ = 1 g/cm^3.

The molecular reorientation associated with the dynamics of the hydrogen-bond network in liquid water is investigated using quantum molecular dynamics simulations performed with the *ab-initio* based, flexible, polarizable TTM3-F interaction potential. The reorientation dynamics calculated at different temperatures are found to be in excellent agreement with the corresponding experimental results obtained from polarization-resolved, femtosecond mid-infrared, pump-probe spectroscopic measurements. A comparison with analogous results obtained from classical molecular dynamics simulations with the same interaction potential clearly indicates that the explicit inclusion of nuclear quantum effects is critical for reproducing the measured time-dependence of the anisotropic signal.

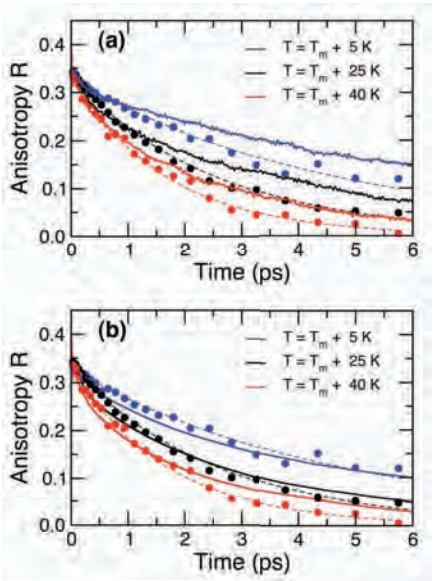

Fig. 4. Comparison (shown on the temperature scale relative to T_m) of the temperature dependence of the experimental anisotropy (filled circles) and the anisotropy (a) calculated from classical MD simulations (solid lines), (b) calculated from quantum CMD simulations with the TTM3-F potential (solid lines). Thin dashed lines are exponential fits of the experimental data.

A preliminary analysis of the underlying mechanism responsible for the cleavage of existing and the formation of new hydrogen bonds within the liquid network indicates the existence of a large number of possible pathways, which also include the "jump mechanism" proposed by Laage and Hynes. Our results, however, do not suggest that the "jump mechanism" is the dominant one among other alternative pathways that break and reform hydrogen bonds. This assertion seems to be invariable on the analysis of either the classical or the quantum trajectories with the TTM3-F potential. Clearly, the overall molecular picture for the hydrogen bond rearrangement will undoubtedly depend upon the underlying potential energy surface that is used to describe the reorientation dynamics.

We plan to perform a more systematic, quantitative analysis of the impact of nuclear quantum effects on the molecular mechanisms that govern the hydrogen bond dynamics in liquid water. We will

specifically analyze the various microstates arising from the different instantaneous conformations and their connectivity via hydrogen bonds for the classical and quantum trajectories with the TTM3-F potential. This analysis largely depends on the underlying definition of whether a hydrogen bond exists by applying either a geometric (Nilsson), a proximity (Buch) or an electronic (Skinner) criterion. The dependence of the results on those different definitions will be assessed. We also plan to introduce an alternative (non geometric) criterion for defining a hydrogen bond between water molecules and use it in conjunction with the analysis of the broad OH stretching band in liquid water.

Acknowledgements: This research was performed in part using the computational resources of the National Energy Research Supercomputing Center (NERSC) at Lawrence Livermore National Laboratory and the Molecular Sciences Computing Facility (MSCF) at the Environmental Molecular Sciences Laboratory, a national scientific user facility sponsored by the Department of Energy's Office of Biological and Environmental Research located at Pacific Northwest National Laboratory. Battelle operates PNNL for the US Department of Energy.

References to publications of DOE sponsored research (2009-present)

1. S. S. Xantheas, "Dances with Hydrogen Cations" *Nature* **457**, 673 (2009). Invited *News & Views* article
2. S. S. Xantheas, G. A. Voth, "Aqueous Solutions and their Interfaces", *Journal of Physical Chemistry B* **113**, 3997 (2009)
3. C. D. Wick and S. S. Xantheas, "Computational Investigation of the First Solvation Shell Structure of Interfacial and Bulk Aqueous Chloride and Iodide Ions", Special Issue on Aqueous solutions and their Interfaces (invited), *Journal of Physical Chemistry B* **113**, 4141 (2009). Journal cover
4. S. Yoo, M. V. Kirov and S. S. Xantheas, "Lowest energy networks of the T-cage $(H_2O)_{24}$ cluster and their use in constructing unit cells of the structure I hydrate lattice", Communication to the Editor, *Journal of the American Chemical Society* **131**, 7564 (2009). Highlighted in the "Science Concentrates" section, Chemical & Engineering News, June 1st (2009). Selected for DOE National Impact feature article
5. S. Yoo, X. C. Zeng and S. S. Xantheas, "On the phase diagram of water with density functional potentials: the melting temperature of ice I_h with the Perdew-Burke-Ernzerhof and Becke–Lee–Yang–Parr functionals", Communication to the Editor, *Journal of Chemical Physics* **130**, 221102 (2009). Featured in the *Virtual Journal of Biological Physics Research*. 3rd most downloaded paper in July 2009
6. X.-B. Wang, J. Werhahn, L.-S. Wang, K. Kowalski, A. Laubereau and S. S. Xantheas, "Observation of a remarkable temperature effect in the hydrogen bonding structure and dynamics of the $CN^-(H_2O)$ cluster", Letter to the Editor, *Journal of Physical Chemistry A* **113**, 9579 (2009). Journal cover
7. F. Paesani, S. S. Xantheas and G. A. Voth, "Infrared Spectroscopy and Hydrogen-Bond Dynamics of Liquid Water from Centroid Molecular Dynamics with an Ab Initio-Based Force Field", *Journal of Physical Chemistry B*, **113**, 13118 (2009)
8. X. Sun, S. Yoo, S. S. Xantheas, L. X. Dang, "The reorientation mechanism of hydroxide ions in water: A molecular dynamics study", Frontiers article (invited), *Chemical Physics Letters*, **481**, 9 (2009)
9. S. Yoo, S. S. Xantheas, X. C. Zeng, "The melting temperature of Bulk Silicon from *Ab initio* Molecular Dynamics Simulations" *Chemical Physics Letters* **481**, 88 (2009)
10. E. Aprà, R. J. Harrison, W. A. deJong, A. P. Rendell, V. Tipparaju, S. S. Xantheas, "Liquid Water: Obtaining the right answer for the right reasons", *SC'09: Proceedings of the Conference on High Performance Computing, Networking, Storage and Analysis*, SESSION: Gordon Bell finalists, article No. 66, Published by ACM, New York, NY USA (2009). ISBN: 978-1-60558-744-8. DOI: http://doi.acm.org/10.1145/1654059.1654127

11. J. R. Hammond, N. Govind, K. Kowalski, J. Autschbah, S. S. Xantheas, "Accurate dipole polarizabilities for water clusters *n*=2-12 at the coupled cluster level of theory and benchmarking of various density functionals" *Journal of Chemical Physics* **131**, 214103 (2009). Featured in the *Virtual Journal of Biological Physics Research*. 11th most downloaded paper in December 2009

12. N. Hontama, Y. Inokuchi, T. Ebata, C. Dedonder-Lardeux, C. Jouvet, and S. S. Xantheas, "Structure of the Calix[4]arene-(H_2O) cluster: The World's Smallest Cup of Water", *Journal of Physical Chemistry A* **114**, 2967 (2010)

13. X.-B. Wang, K. Kowalski, L.-S. Wang and S. S. Xantheas**,** "Stepwise hydration of the cyanide anion: A temperature-controlled photoelectron spectroscopy and *ab-initio* computational study of $CN^-(H_2O)_n$ (n = 2-5)", *Journal of Chemical Physics* **132**, 124306 (2010)

14. R. Kusaka, Y. Inokuchi, S. S. Xantheas and T. Ebata, "Structures and Encapsulation Motifs of Functional Molecules Probed by Laser Spectroscopic and Theoretical Methods", Invited Review article, Special issue on Laser Spectroscopy and Sensing, *Sensors* **10**, 3519 (2010)

15. T. Ebata, N. Hontama, Y. Inokuchi, T. Haino, E. Aprà and S. S. Xantheas, "Encapsulation of Ar_n clusters by Calix[4]arene: *Endo*- vs. *exo*-complexes" *Physical Chemistry Chemical Physics* **12**, 4569 (2010)

16. F. Paesani, S. Yoo, H. J. Bakker and S. S. Xantheas, "Nuclear Quantum Effects in the reorientation of water" *Journal of Physical Chemistry Letters* **1**, 2316 (2010)

17. E. G. Bakalbassis, E. Malamidou-Xenikaki, S. Spyroudis and S. S. Xantheas, "Dimerization of Indanedioneketene to Spiro-oxetanone: A Theoretical Study", *Journal of Organic Chemistry* **75**, 5499 (2010)

18. S. S. Xantheas, M. S. Gordon, "A Tribute to Klaus Ruedenberg", Klaus Ruedenberg special issue, *Journal of Physical Chemistry A* **114**, 8489 (2010)

19. V.-A. Glezakou, S. T. Elbert, S. S. Xantheas and K. Ruedenberg, "Analysis of bonding patterns in the valence isoelectronic series O_3, S_3, SO_2 and OS_2 in terms of oriented quasi-atomic molecular orbitals" Klaus Ruedenberg special issue (invited), *Journal of Physical Chemistry A* **114**, 8923 (2010)

20. S. Pandelov, J. C. Werhahn, B. M. Pilles, S. S. Xantheas, and H. Iglev, "An empirical correlation between the enthalpy of solution of aqueous salts and their ability to form hydrates", *Journal of Physical Chemistry A* **114**, 10454 (2010). Journal cover

21. S. Yoo, E. Aprà, X.-C. Zeng and S. S. Xantheas, "Lowest-Energy Structures of Water Clusters $(H_2O)_{16}$ and $(H_2O)_{17}$ from high-level ab initio calculations", *Journal of Physical Chemistry Letters* **1**, 3122 (2010)

22. J. C. Werhahn, S. Pandelov, S. Yoo, S. S. Xantheas, H. Iglev, "Dynamics of Confined Water Molecules in Aqueous Salt Hydrates", in *Ultrafast Phenomena XVII*, M. Cherqui, D. M. Jonas, E. Riedle, R. W. Schoenlein, A. J. Taylor (Eds.), Oxford University Press, pp. 463-465 (2011)

23. S. Yoo and S. S. Xantheas, "The Effect of Dispersion Corrections on the Melting Temperature of Liquid Water", Communiction to the Editor, *Journal of Chemical Physics* **134**, 121105 (2011). Featured in the *Virtual Journal of Biological Physics Research*

24. S. Yoo and S. S. Xantheas**,** "The role of hydrophobic surfaces in altering the water-mediated peptide-peptide interactions in an aqueous environment" Victoria Buch Memorial Issue (invited), *Journal of Physical Chemistry A in press* (2011) DOI: 10.1021/jp1107137. Publication Date (Web): January 19, 2011 (Article)

25. A. Yoo and S. S. Xantheas, "Structures, Energetics and Spectroscopic Fingerprints of Water Clusters *n*=2-21" Vademecum of Computational Chemistry, Ed. J. Leszczynski. Vol III: "Applications: Solids and nanostructures", Eds. M. Papadopoulos and H. Reis, Springer Verlag, *in press* (2011)

26. T. Ebata, R. Kusaka and S. S. Xantheas, "Laser spectroscopic and theoretical studies of the structures and encapsulation motifs of functional molecules", Proceedings of the Eighth International Conference of Computational Methods in Sciences and Engineering (ICCMSE 2010), American Institute of Physics *in press* (2011)

Ground State Depletion Microscopy: Detection Sensitivity of Single-Molecule Optical Absorption at Room Temperature

X. Sunney Xie
Department of Chemistry and Chemical Biology, Harvard University, Cambridge 02138, MA
Email: xie@chemistry.harvard.edu

Program Definition Optical studies of single molecules in ambient environments, which have led to broad applications, are primarily based on fluorescence detection. Direct detection of optical absorption with single-molecule sensitivity at room temperature is difficult because absorption is not a background-free measurement and is often complicated by sample scattering. Here we report ground state depletion microscopy for ultrasensitive detection of absorption contrast. We image 20 nm gold nanoparticles as an initial demonstration of this microscopy. We then demonstrate the detection of absorption signal by a single chromophore molecule at room temperature. This is accomplished by using two tightly-focused collinear continuous-wave laser beams at different wavelengths both within a molecular absorption band, one of which is intensity modulated at a high frequency (>MHz). The transmission of the other beam is found to be modulated at the same frequency due to ground state depletion. The signal of single chromophore molecules scanned across the common laser foci can be detected with shot-noise limited sensitivity. This measurement represents the ultimate detection sensitivity of nonlinear optical spectroscopy at room temperature.

Recent Progress

Single molecule optical detection, imaging and spectroscopy have made an impact on many disciplines. In particular, room temperature optical detection of single molecules has been applied extensively to biological research. The first single chromophore detection was achieved by optical absorption measurement at 1.6 K with a sophisticated frequency modulation scheme. It was followed by fluorescence detection via excitation at the zero-phonon lines. These methods were limited only to cryogenic temperatures at which zero phonon lines exist. Surface enhanced Raman scattering is capable of detecting single molecules, but it requires close contact of molecules with a metal nanostructure. Other high-sensitivity measurements include interferometry, stimulated emission, photothermal, and direct absorption measurement. The photothermal method has recently reached single molecule sensitivity. However, glycerol has to be used in order to reduce heat conductivity and increase the refractive index change induced by single molecule light absorption. The direct absorption method which recently demonstrated single molecule sensitivity requires careful selection of the sample substrate to avoid the complication of sample scattering. We seek a different approach for detection of single-molecule optical absorption at room temperature.

Nonlinear optical imaging techniques including stimulated Raman scattering microscopy, two-photon absorption microscopy and stimulated emission microscopy have been developed for imaging non-fluorescent species. In these techniques, two pulse laser trains of different wavelengths coincide in the sample. The first beam is intensity modulated at MHz frequency, while the second beam is monitored by a photodetector via phase sensitive detection with a lock-in amplifier. As a result of nonlinear interactions between the two laser beams and the sample, the transmission of the second beam is modulated at the same frequency as the first beam. The high-frequency modulation transfer method effectively circumvents laser intensity fluctuations and the intensity variation of a transmitted laser beam that is scanned across a heterogeneous

sample, both of which occur at low frequencies (DC to kHz). Here we demonstrate ground state depletion microscopy with continuous wave (CW) lasers that offers single-molecule sensitivity for detection of optical absorption.

We employ the modulation transfer detection scheme to measure ground state depletion in a pump-probe experiment (Fig. 1a and 1b). Two CW lasers, a pump beam at frequency ν_1 and a probe beam at frequency ν_2, are both on resonance with the same absorption band of the molecule. The incident power levels of pump and probe beams, P_{pump} and P_{probe}, are adjusted to be near the saturation intensity of the absorption transition. We modulate the incident intensity of the pump beam ν_1 at 1.75 MHz, and keep the incident intensity of the probe beam ν_2 constant (Fig. 1c). The collinearly propagating pump and probe beams are focused to a common spot. The sample is scanned across the fixed laser foci with a piezoelectric scanning stage (Fig. 1b). The transmitted probe beam is detected by a photodiode while the pump beam is blocked by a filter. The photodiode signal is demodulated by a lock-in amplifier to create the ground state depletion contrast. The modulation depth of the transmitted probe beam is

$$\delta\delta P_{probe} = \frac{2k_{relax}\cdot(\sigma^2/S^2\,h\nu)\cdot P_{pump}P_{probe}}{\left(k_{relax}+(\sigma/h\nu S)\cdot P_{probe}\right)\cdot\left(k_{relax}+(\sigma/h\nu S)\cdot(2P_{pump}+P_{probe})\right)} \qquad (1)$$

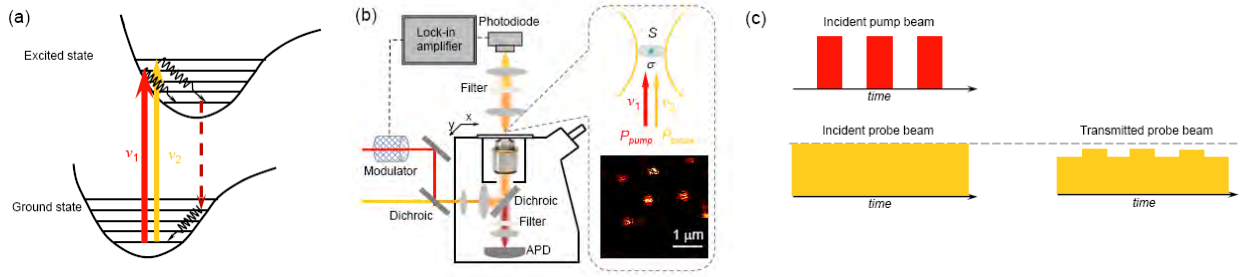

Figure 1. (a) Energy diagram for optical absorption, excited state relaxation and ground state depletion of a molecule. Laser fields ν_1 and ν_2 are both on resonance with the absorption of the molecule. One beam affects the absorption of the other beam by depleting the ground state of the molecule. (b) Experimental setup for the simultaneous ground state depletion and epi-fluorescence detection. The inset indicates single molecule absorption cross section σ and the cross section of a tightly focused laser beam *S*. It also shows a fluorescence image of single molecule Atto647N embedded in PMMA. (c) Schematic diagram of modulation transfer based on ground state depletion. As the intensity of the pump beam is modulated over time, the probe beam is also modulated at the same frequency.

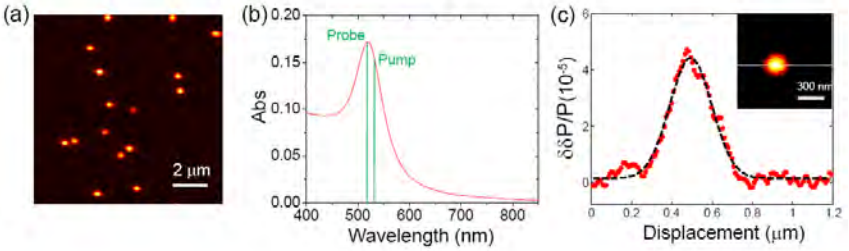

Figure 2. (a) Ground state depletion imaging of single 20 nm gold nanoparticles. (b) Ensemble absorption spectrum of 20 nm gold nanoparticles in aqueous solution. The wavelengths of pump beam (532 nm) and probe beam (520 nm) are indicated. (c) Signal intensity profile of a single nanoparticle. The inset is the ground state depletion image of the nanoparticle whose signal intensity profile is plotted as (c). The lateral position of (c) is indicated. The power level at focus was 450 μW for each beam.

As an initial demonstration of ground state depletion microscopy, we imaged individual 20 nm gold nanoparticles dispersed on a glass surface (Fig. 2a), whose absorption spectrum is

shown in Fig. 2b along with the pump and probe wavelengths. Fig. 2c shows the diffraction-limited intensity profile for a single nanoparticle in the inset image, which reveals a signal of $\delta\delta P/P \sim 0.5\times10^{-4}$, where P refers to the probe beam power at the photodiode. This measured signal is comparable with theoretical estimation $\delta\delta P/P \sim 1\times10^{-4}$.

We detect single molecule absorption of an organic dye Atto647N, whose absorption spectrum is shown in Fig. 3a. Wavelengths for pump and probe are 642nm and 633nm respectively. Epi-fluorescence emitted by the molecule is collected in a confocal mode.

The sensitivity of ground state depletion microscopy was characterized with an aqueous solution of Atto647N in pH 7 phosphate buffer. Fig. 3b shows that the ground state depletion signal depends linearly on the concentration of Atto647N solution. This allows straightforward quantitative analysis. When the power levels for pump and probe beams at the focus are 350 μW each, the detection limit is 15 nM with 1s integration time, which corresponds to 0.3 molecule in the probe volume (~3×10^{-17} liter). The corresponding modulation depth, $\delta\delta P/P$, of a single Atto647N molecule is ~0.9×10^{-7}. This measured result agrees with its theoretical value ~1.2×10^{-7} based on Eq. 1.

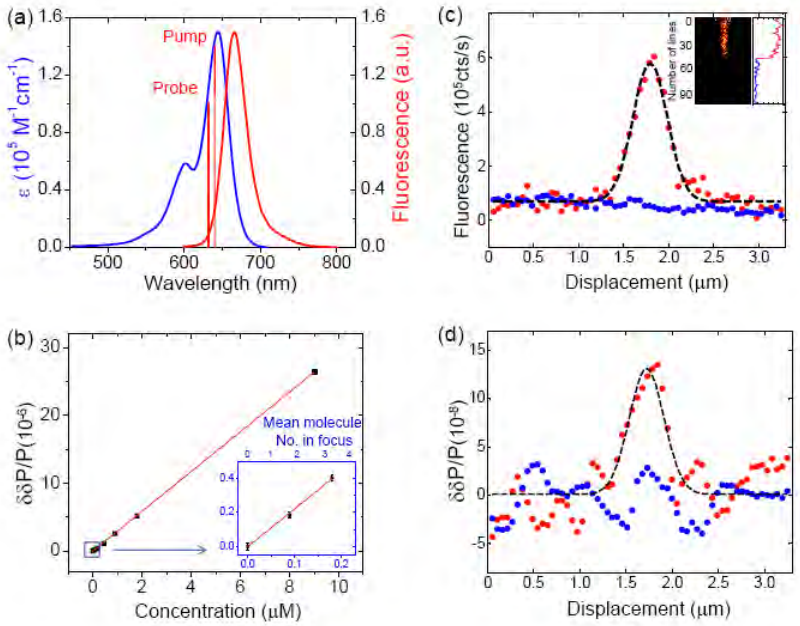

Figure 3. **(**a) Ensemble absorption and emission spectra of Atto647N in pH 7 aqueous solution. The pump and probe wavelengths are indicated. (b) Ground state depletion signal as a function of concentration of aqueous Atto647N solution, with power level 350 μW for each beam. The blue frame indicates the data points at lowest concentrations. The inset is zoom-in of the blue frame of (b), with concentrations labeled at the bottom and estimated mean molecule numbers in the probe volume labeled at the top. Error bars are for 1s integration time. (c) Fluorescence line scans for a single Atto647N molecule, averaged from the inset before (red) and after (blue) photobleaching. The inset is the fluorescence image constructed from repeated line scans across the molecule and the corresponding fluorescence intensity trajectory. (d) Absorption line scans for the same molecule in (c), averaged before (red) and after (blue) photobleaching, simultaneously recorded with (c). The power level is 350 μW for each beam. The time constant of the lock-in amplifier is 30 ms, and the pixel dwell time is 39 ms.

The inset of Fig. 1b depicts a fluorescence image of single-molecule Atto647N embedded in PMMA matrix. The blinking of fluorescence and one-step photobleaching clearly proves that the spot is from a single molecule.

Fig. 3c and 3d show the simultaneous line-scan signals of fluorescence and absorption of a single Atto647N molecule. For this molecule, the fluorescence line scan signal as a function of time is shown in the inset of Fig. 3c. It survived for 45 line scans before photobleaching. The red plots in Fig. 3c and 3d show the average of 45 fluorescence and absorption line-scan signals before it was photobleached. The lateral position of the peak value $\delta\delta P/P \sim 1.4\times10^{-7}$ coincides with the peak position in the single molecule fluorescence line scan. This demonstrates the single-molecule sensitivity of the ground state depletion microscope. The blue plot in Fig. 3d shows that after the molecule was photobleached, the average of 45 absorption line-scan signals vanished. The detection of the absorption signal is shot-noise limited.

We further measured ground state depletion signal from 130 molecules. The single-molecule absorption signals $\delta\delta P/P$ are found to range from 4×10^{-8} to 2.6×10^{-7}, with a mean of 1.1×10^{-7}. This agrees well with the theoretical value expected from Eq. 1.

In conclusion, a high-frequency dual-beam modulation transfer scheme allows the ultimate sensitivity of nonlinear optical microscopy based on saturation spectroscopy: the detection of single-molecule absorption signal at room temperature.

Future Plans

We have employed the phenomena of ground state depletion to provide a contrast mechanism for microscopy and high sensitivity in absorption-like measurements, which is free from the complication of Rayleigh scattering of the sample. The overall quadratic power dependence of the ground state depletion signal under non-saturating conditions would allow three-dimensional sectioning, as in many other multiphoton techniques.

In the future, we aim to apply this ultrasensitive absorption-based microscopy to image non-fluorescent heme proteins in live cells, including cytochromes and hemoglobin. We also plan to study their redox dynamics in nanocrystals.

Publications of DOE sponsored research (2009-present):

1) Min, W.; Freudiger, C. W.; Lu, S.; Xie, X. S. "Coherent nonlinear optical imaging: beyond fluorescence microscopy" *Annu Rev Phys Chem* **62**, 507 (2011).

2) Chong, S.; Min, W.; Xie, X. S. "Ground-State Depletion Microscopy: Detection Sensitivity of Single-Molecule Optical Absorption at Room Temperature" *J. Phys. Chem. Lett.* **1**, 3316 (2010).

3) Lu, S.; Min, W.; Chong, S.; Holtom, G. R.; Xie, X. S. "Label-free imaging of heme proteins with two-photon excited photothermal lens microscopy" *Applied Physics Letters*, **96**, 113701 (2010).

4) Lu, S.; Min, W.; Conchello, J.-A.; Xie, X. S.; Lichtman, J. W. "Super-Resolution Laser Scanning Microscopy through Spatiotemporal Modulation" *Nano Letters*, **9**, 3883 (2009).

5) Min, W.; Lu, S.; Chong, S.; Roy, R.; Holtom, G. R.; Xie, X. S. "Imaging chromophores with undetectable fluorescence by stimulated emission microscopy" *Nature*, **461**, 1105 (2009).

6) Saar, B. G.; Holtom, G. R.; Freudiger, C. W.; Ackermann, C.; Hill, W.; Xie, X. S. "Intracavity wavelength modulation of an optical parametric oscillator for coherent Raman microscopy" *Optics Express*, **17**, 12532 (2009).

7) Min, W.; Lu, S.; Rueckel, M.; Holtom, G. R.; Xie, X. S. "Near-Degenerate Four-Wave-Mixing Microscopy" *Nano Letters*, **9**, 2423 (2009).

8) Min, W.; Lu, S.; Holtom, G. R.; Xie, X. S. "Triple-Resonance Coherent Anti-Stokes Raman Scattering Microspectroscopy," *ChemPhysChem*, **10**, 344 (2009).

DYNAMICS AND KINETICS OF PHOTO-INITIATED CHEMICAL REACTIONS

Hua-Gen Yu (hgy@bnl.gov)
Chemistry Department, Brookhaven National Laboratory, Upton, NY 11973-5000

Program Scope

The purpose of this project is the development and application of computational dynamics and kinetics methods for studying the photochemistry and photophysics processes at liquid and/or solid surfaces. We are interested in developing new dynamics and kinetics models using the molecular and quantum wavepacket dynamics approach, and mathematical graph theory, and in applying these models to specific chemical systems related to solar energy conversion. Particular focus is on the processes at semiconductor and nanoparticle surfaces initiated by ultra-violet (UV) or near UV radiation. Here, we aim to construct a general theoretical framework for understanding the energy and chemical evolution of the photo-initiated processes at those surfaces. This project also carries out electronic structure calculations using modern DFT methods to explore the energetics and optical properties of these systems of interest. The research will be done in collaboration with experimentalists at BNL and elsewhere.

Recent Progress

Optical properties of GaN/ZnO solid solution nanocrystals

In collaboration with Dr. Han at BNL CFN, we have carried out electronic structure calculations to understand the optical properties of GaN/ZnO solid solution nanocrystals, an important solar fuel material. Results show that the solid solutions have an even distribution of (ZnO) units among the (GaN) wurtzite frameworks. The GaN/ZnO nanocrystals have the narrowest band gap of 2.21 eV. The Raman spectra as shown in Fig. 1 strongly imply the existence of oxide states at nanocrystal surfaces. The oxide states could play an important role in the photocatalytic water splitting processes and the mechanism of modifying the band gap in these solid solutions. Further work is required, especially to illustrate the mechanism of band gap narrowing and the stability of nanocrystal surfaces.

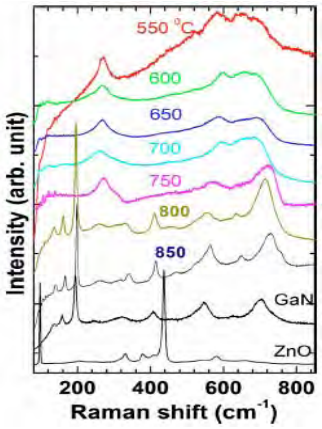

Figure 1 *Raman spectra of GaN/ZnO solid solutions, GaN nanocrystal, and w-ZnO material*

An optimal DFT method for GaN and ZnO

The standard DFT methods using the LDA and/or GGA approach have a typical flaw that often predicts a rather small band gap for semiconductors such as GaN and ZnO. This severely hampers the theoretical study of the properties of GaN/ZnO solid solutions. In order to overcome this drawback, we have developed a hybrid DFT method (bBLYP) optimized for the GaN and ZnO systems. The optimal method can accurately describe the band gaps of both GaN and ZnO bulk materials as well as the properties of some relevant small molecules. The method has successfully been applied for studying the evolution of the band gaps from molecules to bulk materials, and the mixture effect on the band gaps of GaN/ZnO nanoparticles (see figure 2). The results obtained are very promising, and

already show the importance of the appropriate treatments of exchange functional. Therefore, we expect that the optimal bBLYP will probable an accurate and unambiguous method for exploring the mechanism of band gap narrowing, and for understanding the photocatalytic water splitting processes at illuminated aqueous surfaces of GaN/ZnO solid solutions.

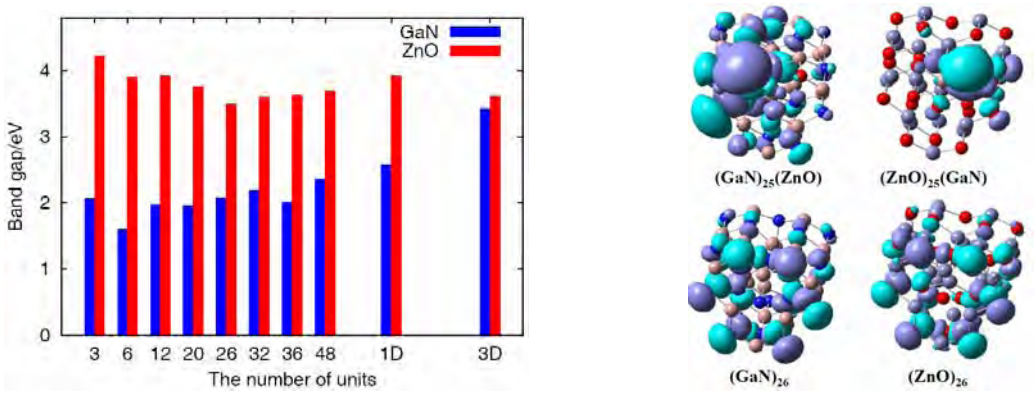

Figure 2 *(***Left***) Calculated band gaps of* $(GaN)_n$ *and* $(ZnO)_n$ *as a function of cluster size or nanowire (1D) and bulk (3D) wurtzite crystals; and (***Right***) Highest occupied molecular orbitals (HOMOs) of four crystal-cut nanoparticles.*

Future Plans

Quantum wavepacket and kinetics studies of photoinduced dynamics of O_2 on TiO_2(110)

One ongoing project is to carry out quantum wavepacket dynamics and kinetics calculation for studying the photoinduced dynamics of the $O_2/TiO_2(110)$ system in collaboration with the BNL Surface Chemical Dynamics Group. This research is an extension of research from our gas-phase molecular dynamics studies toward the gas/solid interface. Here, we will focus on the non-adiabatic effects resulting from the interactions between the photo-excited electrons and the adsorbed molecules on surfaces, and on the electron-hole (e^--h^+) recombination in the TiO_2 case. The non-adiabatic effects will be investigated using a time-dependent wavepacket approach based on the Luntz et al.'s and/or Lara-Castlells and Krause's models. The hot electron dynamics at surfaces will be simulated in a kinetics manner. We have developed a kinetic graph theory (KGT) method for studying the e^--h^+ recombination of TiO_2. Preliminary results show that the photocatalytic efficiency is mainly limited by the fast delocalization of excited electrons and their recombination with holes.

Publications since 2010

W.-Q. Han, Z. Liu and H.-G. Yu, *Synthesis and optical properties of GaN/ZnO solid soulution nanocrystals*, App. Phys. Lett. **96**, 183112 (2010).

H.-G. Yu, *An optimal density functional method for GaN and ZnO*, Chem. Phys. Lett. (accepted, 2011).

Participant List

List of Participants

Dr. Musahid Ahmed
Lawrence Berkeley National Laboratory
mahmed@lbl.gov
http://www.lbl.gov/LBL-Programs/CSD/directory/bio_ahmed_m.html

Professor Scott Anderson
University of Utah
anderson@chem.utah.edu
http://www.chem.utah.edu/directory/faculty/anderson.html

Professor Krishnan Balasubramanian
California State University East Bay
krishnan.balasubramanian@csueastbay.edu
http://www.mcs.csueastbay.edu/~kbalasub/

Dr. David Bartels
Notre Dame Radiation Laboratory
bartels.5@nd.edu
http://www.rad.nd.edu/faculty/bartels.htm

Dr. Nicholas Camillone
Brookhaven National Laboratory
nicholas@bnl.gov
http://www.bnl.gov/chemistry/bio/Camillone%20IIINicholas.asp

Dr. Ian Carmichael
Notre Dame Radiaton Laboratory
carmichael.1@nd.edu
http://www.rad.nd.edu/faculty/carmichael.htm

Professor Emily Carter
Princeton University
eac@princeton.edu
http://www.princeton.edu/mae/people/faculty/carter/homepage/people/

Dr. Michael Casassa
US DOE/Basic Energy Sciences
michael.casassa@science.doe.gov
http://science.energy.gov/bes/csgb/about/staff/dr-michael-p-casassa/

Professor A. Welford Castleman, Jr.
Penn State University
awc@psu.edu
http://research.chem.psu.edu/awcgroup/Castleman%20Homepage.html#

Professor David Chandler
Lawrence Berkeley National Laboratory
chandler@berkeley.edu
http://gold.cchem.berkeley.edu/David/David/David_Chandler.html

Professor Margaret Cheung
University of Houston
mscheung@uh.edu
https://mynsm.uh.edu/groups/cheunggroup//

Dr. Daniel Chipman
Notre Dame Radiation Laboratory
chipman.1@nd.edu
http://www.rad.nd.edu/faculty/chipman.htm

Dr. Andrew Cook
Brookhaven National Laboratory
acook@bnl.gov
http://www.chemistry.bnl.gov/sciandtech/PRC/acook/cook.html

Dr. Robert Crowell
Brookhaven National Laboratory
crowell@bnl.gov
http://www.bnl.gov/chemistry/bio/CrowellRobert.asp

Dr. Liem Dang
Pacific Northwest National Laboratory
liem.dang@pnl.gov
http://www.pnl.gov/science/staff/staff_info.asp?staff_num=5604

Professor Barry Dunietz
University of Michigan
bdunietz@umich.edu
http://www.umich.edu/~bdgroup/

Professor Michael Duncan
University of Georgia
maduncan@uga.edu
http://maduncan.myweb.uga.edu/

Dr. Michel Dupuis
Pacific Northwest National Laboratory
michel.dupuis@pnl.gov
http://www.pnl.gov/cmsd/staff/staff_info.asp?staff_num=5599

Professor Kenneth Eisenthal
Columbia University
kbe1@columbia.edu
http://www.columbia.edu/cu/chemistry/fac-bios/eisenthal/faculty.html

Professor Mostafa El-Sayed
Georgia Institute of Technology
melsayed@gatech.edu
http://www.chemistry.gatech.edu/faculty/El-Sayed/

Professor James Evans
Ames Laboratory
evans@ameslab.gov
http://www.ameslab.gov/cbs/evans

Professor Michael Fayer
Stanford University
fayer@stanford.edu
http://www.stanford.edu/group/fayer/

Dr. Gregory Fiechtner
DOE/Basic Energy Sciences
gregory.fiechtner@science.doe.gov
http://science.energy.gov/bes/csgb/about/staff/dr-gregory-j-fiechtner/

Professor George Flynn
Columbia University
gwf1@columbia.edu
http://www.columbia.edu/cu/chemistry/groups/flynn/

Dr. Bruce Garrett
Pacific Northwest National Laboratory
bruce.garrett@pnl.gov
http://www.pnl.gov/science/staff/staff_info.asp?staff_num=5496

Professor Phillip Geissler
Lawrence Berkeley National Laboratory
geissler@cchem.berkeley.edu
http://www.cchem.berkeley.edu/plggrp/index.html

Professor Mark Gordon
Ames National Laboratory
mark@si.msg.chem.iastate.edu
http://www.ameslab.gov/cbs/mark

Dr. Jeffrey Guest
Argonne National Laboratory
jrguest@anl.gov
http://nano.anl.gov/docs/people/guest.pdf

Dr. Alexander Harris
Brookhaven National Laboratory
alexh@bnl.gov
http://www.bnl.gov/chemistry/bio/HarrisAlex.asp

Professor Mark Hersam
Northwestern University
m-hersam@northwestern.edu
http://www.hersam-group.northwestern.edu/

Dr. Wayne Hess
Pacific Northwest National Laboratory
wayne.hess@pnl.gov
http://www.pnl.gov/science/staff/staff_info.asp?staff_num=5505

Professor Wilson Ho
University of California, Irvine
wilsonho@uci.edu
http://www.physics.uci.edu/~wilsonho/whoghp.htm

Professor Bret Jackson
University of Massachusetts Amherst
jackson@chem.umass.edu
http://www.chem.umass.edu/faculty/jackson.html

Professor Seogjoo Jang
Queens College, City University of New York
seogjoo.jang@qc.cuny.edu
http://chem.qc.cuny.edu/~sjjang/

Dr. Ireneusz Janik
Notre Dame Radiation Laboratory
ijanik@nd.edu
http://www.rad.nd.edu/faculty/Janik.htm

Professor Caroline Jarrold
Indiana University
cjarrold@indiana.edu
http://cjarrold.chem.indiana.edu/

Professor Mark Johnson
Yale University
mark.johnson@yale.edu
http://www.chem.yale.edu/faculty/johnson.html

Dr. Shawn Kathmann
Pacific Northwest National Laboratory
shawn.kathmann@pnl.gov
http://www.pnl.gov/science/staff/staff_info.asp?staff_num=5601

Dr. Bruce Kay
Pacific Northwest National Laboratory
bruce.kay@pnl.gov
http://www.pnl.gov/science/staff/staff_info.asp?staff_num=5530

Professor Munira Khalil
University of Washington
mkhalil@chem.washington.edu
http://depts.washington.edu/chem/people/faculty/mkhalil.html

Professor Shiv Khanna
Virginia Commonwealth University
snkhanna@vcu.edu
http://www.people.vcu.edu/~khanna/

Dr. Greg Kimmel
Pacific Northwest National Laboratory
gregory.kimmel@pnl.gov
http://www.pnl.gov/science/staff/staff_info.asp?staff_num=5527

Dr. Jay LaVerne
Notre Dame Radiation Laboratory
laverne.1@nd.edu
http://www.rad.nd.edu/faculty/laverne.htm

Professor H. Peter Lu
Bowling Green State University
hplu@bgsu.edu
http://www.bgsu.edu/departments/chem/faculty/hplu/peterlu.htm

Professor Alenka Luzar
Virginia Commonwealth University
aluzar@vcu.edu
http://www.people.vcu.edu/~aluzar/al_bio.htm

Dr. Sergei Lymar
Brookhaven National Laboratory
lymar@bnl.gov
http://www.bnl.gov/chemistry/bio/LymarSergei.asp

Diane Marceau
DOE/Basic Energy Sciences
diane.marceau@science.doe.gov
http://science.energy.gov/bes/csgb/about/staff/

Professor Oliver Monti
University of Arizona
monti@u.arizona.edu
http://labmonti.cbc.arizona.edu/

Dr. Christopher Mundy
Pacific Northwest National Laboratory
chris.mundy@pnl.gov
http://www.pnl.gov/science/staff/staff_info.asp?staff_num=5981

Professor Richard Osgood
Columbia University
osgood@columbia.edu
http://www.ee.columbia.edu/fac-bios/osgood/faculty.html

Professor Athanassios Panagiotopoulos
Princeton University
azp@princeton.edu
http://paros.princeton.edu/Panagiotopoulos/index.html

Dr. Mark Pederson
DOE/Basic Energy Sciences
mark.pederson@science.doe.gov
http://science.energy.gov/bes/csgb/about/staff/dr-mark-r-pederson/

Professor Hrvoje Petek
University of Pittsburgh
petek@pitt.edu
http://www.pitt.edu/~toc2/

Professor Eric Potma
University of California, Irvine
epotma@uci.edu
http://chem.ps.uci.edu/~potma/research.htm

Dr. Sylwia Ptasinska
Notre Dame Radiation Laboratory
sptasins@nd.edu
http://www.rad.nd.edu/faculty/ptasinska.htm

Dr. Eric Rohlfing
DOE/Basic Energy Sciences
eric.rohlfing@science.doe.gov
http://science.energy.gov/bes/csgb/about/staff/dr-eric-a-rohlfing/

Professor Richard Saykally
University of California Berkeley
saykally@berkeley.edu
http://www.cchem.berkeley.edu/rjsgrp/

Professor George Schatz
Northwestern University
schatz@chem.northwestern.edu
http://www.theory.northwestern.edu/schatz/

Dr. Gregory Schenter
Pacific Northwest National Laboratory
greg.schenter@pnl.gov
http://www.pnl.gov/science/staff/staff_info.asp?staff_num=5615

Professor Steven Sibener
Univerity of Chicago
s-sibener@uchicago.edu
http://sibener-group.uchicago.edu/

Dr. Wade Sisk
US DOE/Basic Energy Sciences
wade.sisk@science.doe.gov
http://science.energy.gov/bes/csgb/about/staff/dr-wade-sisk/

Professor James Skinner
University of Wisconsin
skinner@chem.wisc.edu
http://www.chem.wisc.edu/~skinner/

Professor Timothy Steimle
Arizona State University
tsteimle@asu.edu
http://www.public.asu.edu/~steimle/

Professor Charles Sykes
Tufts University
charles.sykes@tufts.edu
http://ase.tufts.edu/chemistry/sykes/frameSet.html

Professor Ward Thompson
University of Kansas
wthompson@ku.edu
http://web.ku.edu/~wthompson/Thompson_Group_Home.html

Professor Andrei Tokmakoff
Massachusetts Institute of Technology
tokmakof@mit.edu
http://web.mit.edu/~tokmakofflab/

Professor John Tully
Yale University
john.tully@yale.edu
http://www.chem.yale.edu/~tully/

Dr. Marat Valiev
Pacific Northwest National Laboratory
marat.valiev@pnl.gov
http://emslbios.pnl.gov/bios/biosketch.nsf/bynameinit/valiev_m

Professor Lai-Sheng Wang
Brown University
lai-sheng_wang@brown.edu
http://www.chem.brown.edu/research/LSWang/

Dr. Xue-Bin Wang
Pacific Northwest National Laboratory
xuebin.wang@pnl.gov
http://emslbios.pnl.gov/bios/biosketch.nsf/bynameinit/wang_x

Professor Michael White
Brookhaven National Laboratory
mgwhite@bnl.gov
http://www.bnl.gov/chemistry/bio/WhiteMichael.asp

Dr. James Wishart
Brookhaven National Laboratory
wishart@bnl.gov
http://www.chemistry.bnl.gov/SciandTech/PRC/wishart/wishart.html

Professor X. Sunney Xie
Harvard University
xie@chemistry.harvard.edu
http://bernstein.harvard.edu/

Dr. Sotiris Xantheas
Pacific Northwest National Laboratory
sotiris.xantheas@pnl.gov
http://www.pnl.gov/science/staff/staff_info.asp?staff_num=5610

Dr. Hua-Gen Yu
Brookhaven National Laboratory
hgy@bnl.gov
http://www.bnl.gov/chemistry/bio/YuHua-Gen.asp

Author Index

Author Index

This page is intentionally left blank